1980

RAINDROP-SIZE DISTRIBUTIONS AND THE MEASUREMENT OF PRECIPITATION BY RADAR IN A MARITIME LOCALE

ECCLESTON, ANDREW JOHN

RAINDROP-SIZE DISTRIBUTIONS AND THE MEASUREMENT OF PRECIPITATION BY RADAR IN A MARITIME LOCALE

by

ANDREW JOHN ECCLESTON

BSc (Hons)

Submitted to the Council for National Academic Awards
in partial fulfilment of the requirements for the
degree of Doctor of Philosophy

Faculty of Maritime Studies
Plymouth Polytechnic
Plymouth
Devon
United Kingdom

February 1980

RAINDROP-SIZE DISTRIBUTIONS AND THE MEASUREMENT OF PRECIPITATION BY RADAR IN A MARITIME LOCALE

ERRATA AND ADDENDA

Page 12, line 14	Insert " D" after N_D and "in unit volume of space" after D + D.
Page 62, Table 2.8	Add (mm) to heading of column 2.
Page 165, line 1	Delete 'd' from examined.
Page A 11, line 7	TI 58 not 57.

ACKNOWLEDGEMENTS

Many people have assisted this work either by making material contributions in the form of resources and data, or by offering useful advice and encouragement.

The author is indebted to Plymouth Polytechnic for providing primary resources and in particular to Dr. D. H. Moreby, Dean of the Faculty of Maritime Studies. Fellow members of the Ocean Science Teaching Group provided valuable advice and encouragement throughout. The programme of study and research was completed under the direction of Captain R. H. Motte. The staff of the Learning Resources and Computer Centres also provided help and advice.

Visits to other research establishments produced useful discussion and Dr. K. J. Weston of the Department of Meteorology, Edinburgh University, provided guidance in a supervisory capacity.

This work would not have been possible without the assistance of the Meteorological Office and the author gratefully acknowledges the co-operation of the Radar Research Laboratory at Malvern. Dr. K. A. Browning kindly made the Joss distrometer and the radar data available. The information and advice from Chris Collier, Cyril de Jonckheere, Peter Larke and Bob Smith was invaluable. The siting of the distrometer at St. Mawgan was suggested and organised by Mr. Burton, formerly in charge at the Mountbatten Meteorological Office and his successor, Mr. Hormbury, has continued to give full support to the work. The successful operation at St. Mawgan is due to the excellent co-operation of Mr. Thomson and his staff, whose professional interest and advice were most useful. Brian Roberts, and latterly Brian Christman, explained the operation of the Camborne radar and co-operated in the experiment.

Mr. Duffy of the Constantine Bay Golf and Country Club kindly allowed the siting of the author's gauges alongside his own instruments. In the early stages of this work Denholm Ship Management Ltd. acted as a collaborating establishment.

My wife Sheila has contributed by giving her unswerving support and typing this manuscript.

RAINDROP-SIZE DISTRIBUTIONS AND THE MEASUREMENT OF PRECIPITATION BY RADAR IN A MARITIME LOCALE

by ANDREW JOHN ECCLESTON

ABSTRACT

The relevance of the measurement of raindrop-size distributions is discussed and data collection using a Joss distrometer is described. The most important sources of error in the experiment, due to both instrumental and environmental factors, are discussed. The results are analysed in a conventional manner, providing a relationship between rainfall rate and radar reflectivity factor.

The problems that arise when a fixed relationship is used to estimate rainfall from radar data are discussed. The variations of raindrop-size distributions with respect to time are considered and this leads to a means of varying one of the constants in the relationship, based on a parameter which simply describes the shape of the distribution. The improvement produced by adopting this approach is demonstrated for simulated radar data.

The calibration of actual radar data using this method is attempted, for the first time, using observations from a meteorological radar measuring areal rainfall on an operational basis. The results compare favourably with those obtained by using the conventional gauge calibration technique and some problems of interpretation and analysis are discussed.

The possibility of using the radar data alone as a basis for calibration is explored by considering vertical reflectivity profiles. Recommendations for future work are given.

Symbols and abbreviations are explained as they arise in the text.

References are numbered in parentheses using italics, thus: *(13)*

CONTENTS

INTRODUCTION

The formation of clouds and development of precipitation is a complex physical process which is widely studied by meteorologists. Observation and measurement are vital facets of this study and it is well known that precipitation elements occur in a variety of forms and sizes. This variation is due to the dynamical nature of clouds which are governed by large-scale synoptic features and modified by local effects.

Measurements of the distribution of raindrop concentrations with size have been made with a variety of instruments at locations all over the world since the last century. Some of the earliest results came from WIESNER (*1*) who used dyed filter papers to intercept the falling drops. This simple method has been used by many workers (see for instance *2*, *3*, *4*) and also by the present author (*5*).

Such a technique is easy to perform and cheap to maintain, but requires a great deal of tedious measurement and does not lend itself to rapid reduction by more modern computer interfacing devices. More importantly, it does not easily allow continuous operation during rainfall which results in short-lived, but significant, features remaining undetected. However, SIVARAMAKRISHNAN (*6*) has developed an instrument which made this possible by using a moving tape of filter paper.

A variety of modern techniques are now available for measuring raindrop spectra; these include photoelectric devices (*7*, *8*), Doppler radar (*9*), and impact devices (*10*, *11*). JOSS and WALDVOGEL have described a "distrometer" (*11*) which is available commercially and has been used by other research establishments including, in the UK, the Meteorological Office and the Appleton Laboratory.

Having obtained a spectrum of raindrop sizes, it is possible to compute a number of parameters which have both physical significance and application in a variety of fields of interest. The increased use of microwave frequencies for communications has demanded a consideration of the attenuating nature of hydrometeors. The use of radar as a meteorological tool requires a knowledge of the relationship between the reflective properties of a raindrop population and the information required by users. The raindrop spectra may also be directly useful in meteorology, especially if the temporal variation of the distributions is examined in relation to changes in the mesoscale organisation of the atmosphere. (*12*)

The work presented here is the result of four years' involvement in the measurement of raindrop-size distributions. Initially the object was to collect data and identify fruitful avenues of research, at the same time keeping the observations within a maritime locale for which few data are available. The first data collection exercise was made from ships, on a semi-global scale, using the filter paper method already referred to (*5*). The disadvantages of this technique led to the development of a doppler radar device which worked well in the laboratory but failed to withstand the rigours of field operation.

A Joss distrometer was obtained on loan in 1977 and superseded the earlier techniques by providing reliable and continuous data. The following pages describe how these data were obtained and analysed to provide an understanding of the error which occurs in the measurement of rainfall by radar, through the variation in raindrop sizes. This source of error has been known for some time, but there has apparently been no attempt to quantify it directly from observational evidence. In some operational radar systems it is compensated for by

using a real-time calibration based on telemetering raingauges. The innovative approach presented here may provide a more elegant solution to this problem which is of real significance in the field of radar meteorology.

CHAPTER ONE

GENERAL FEATURES OF RAINDROP-SIZE DISTRIBUTIONS

1.1 THE FORM OF THE SPECTRUM

1.1.1 Histograms

The distribution of raindrops with size is best represented by the relationship between drop diameters and their spatial concentration. Measuring techniques typically involve intercepting raindrops near the surface and allocating them to specified size intervals. This method leads to the construction of a histogram where the area of the rectangles represents the frequency of the raindrops in each size interval.

Such a histogram appears in Figure 1.1. Since the numbers of drops vary from very few to thousands, the scale on the vertical axis is logarithmic. The units on this axis are: number of drops per cubic metre per unit size interval, which in this case is 0.25 mm.

If the size intervals are not equal (as in the Joss distrometer), care must be taken to erect the rectangles to conform to the units. Throughout this work the spectra will be represented on axes of diameter (D) in millimetres and number (N_D) per cubic metre per millimetre. A spectrum from the distrometer is shown in Figure 1.2.

A simpler method of representing a histogram with equal class intervals is by the use of a frequency polygon, obtained by plotting each frequency against the mid-point of its range. For ease of illustration, most of the spectra will be represented in this manner although it must be realised that this frequency polygon is for a distribution with unequal class intervals. Calculations on the spectra are performed on the basis of the distribution as represented by the full histogram. Hence Figure 1.2 may be represented by Figure 1.3.

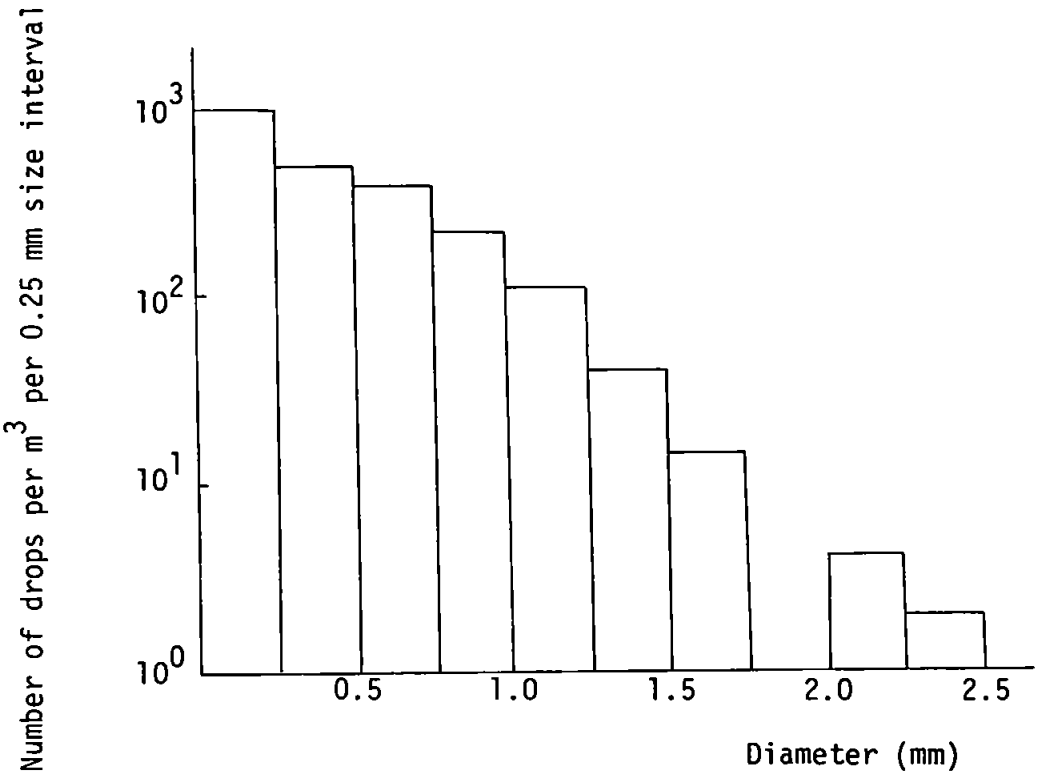

Figure 1.1 Drop-size spectrum represented by a histogram with equal class intervals. After MASON and ANDREWS (*4*).

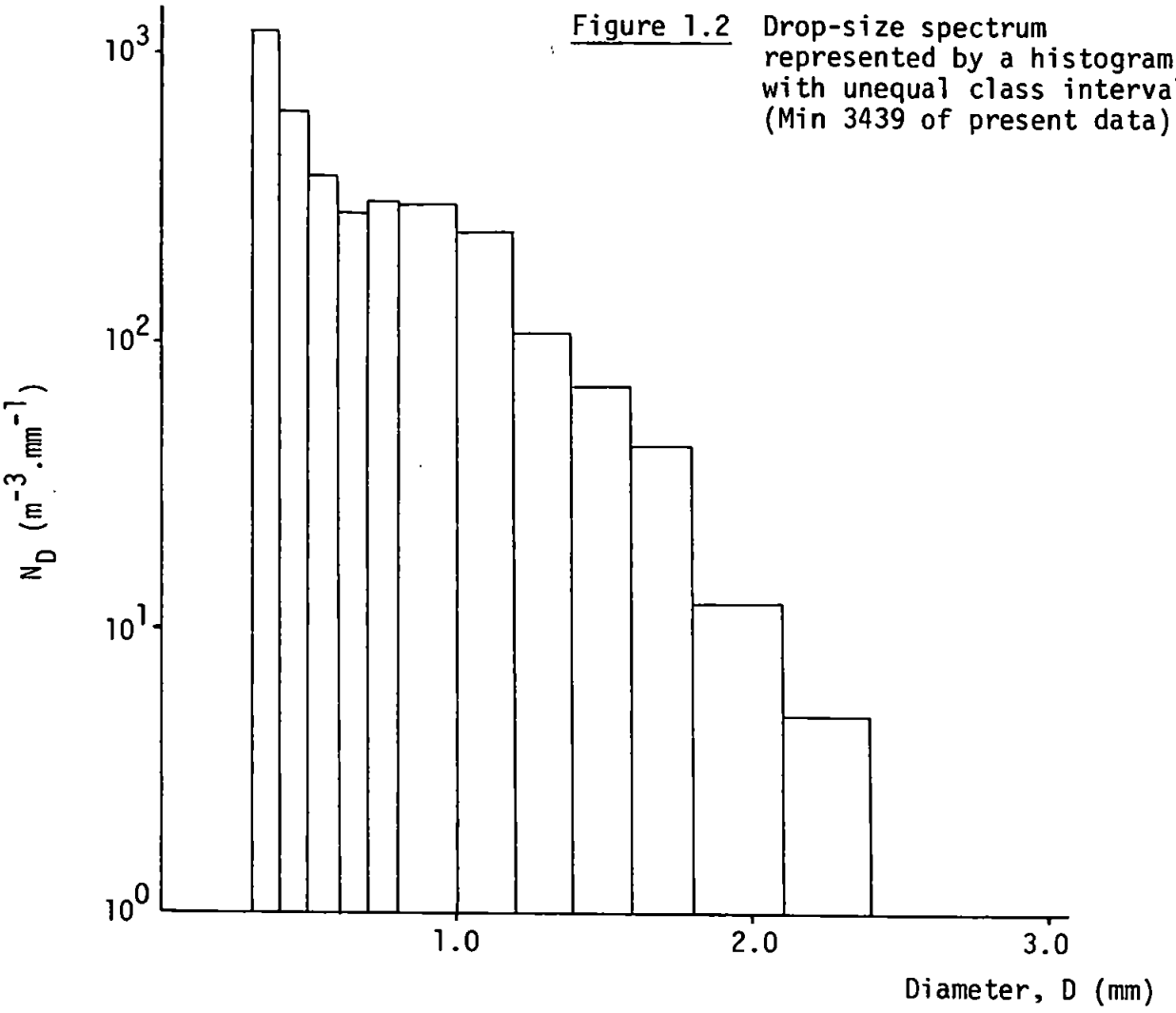

Figure 1.2 Drop-size spectrum represented by a histogram with unequal class intervals. (Min 3439 of present data)

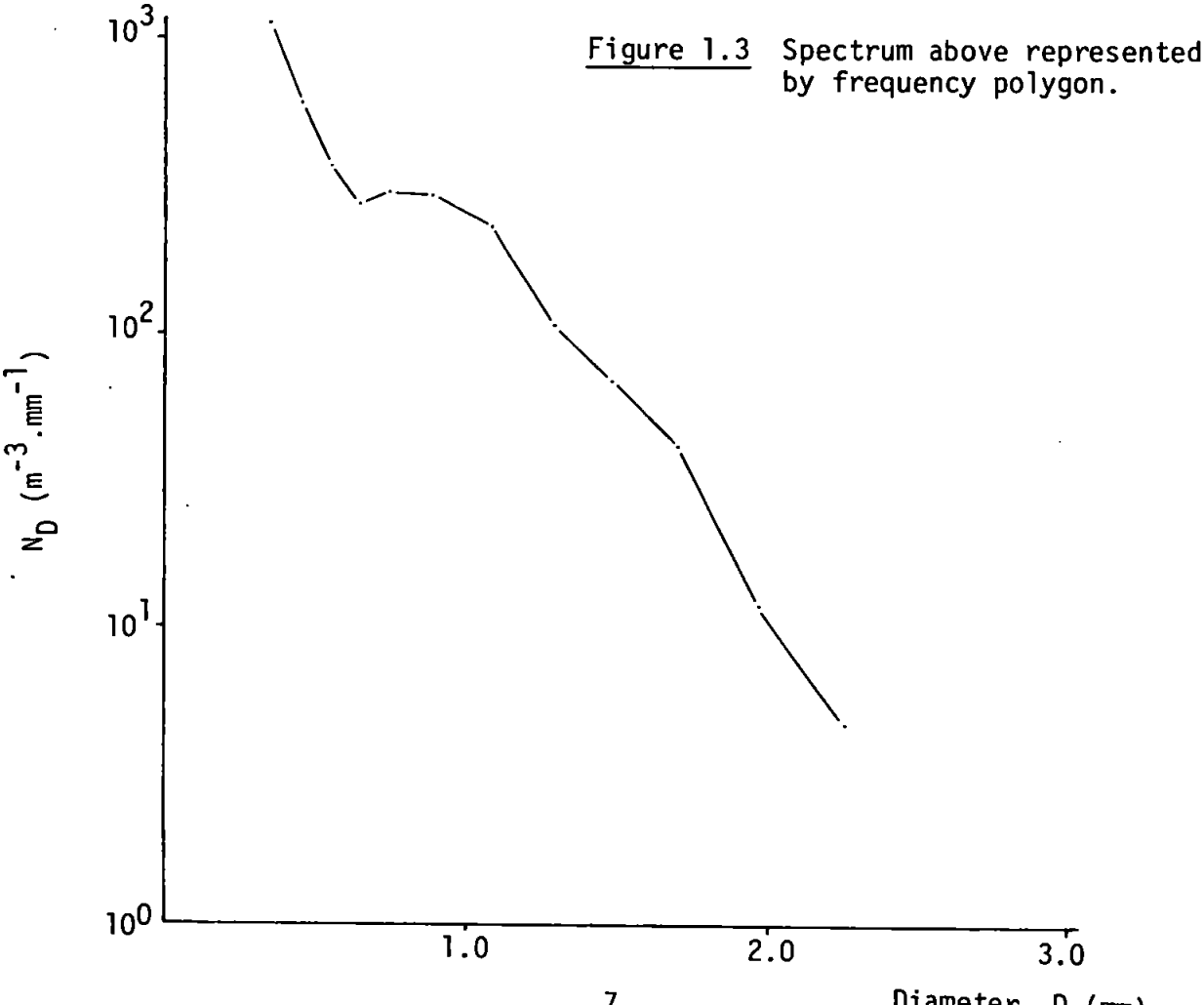

Figure 1.3 Spectrum above represented by frequency polygon.

1.1.2 The Marshall-Palmer distribution function

The previous two examples of actual raindrop-size distributions have a similar range in respect of each variable. Furthermore, the distributions have a markedly similar shape, there being many more small drops than large drops and evidence of a simple log-linear relationship. Many raindrop spectra produce this shape of distribution and an exponential distribution function was first proposed by MARSHALL and PALMER (hereafter abbreviated to M-P) in 1948. (*13*)

These authors used filter paper data and the results of LAWS and PARSONS (*14*) and found that, except at small diameters, both sets of observations could be fitted by a general relation:

$$N_D = N_o e^{-\lambda D} \qquad \ldots (i)$$

where D is the diameter, $N_D \delta D$ is the number of drops of diameter between D and D + δD in unit volume of space, and N_o is the value of N_D for D = 0.

It was found that:

$$N_o = 0.08 \text{ cm}^{-4} \quad (8 \times 10^3 \text{ m}^{-3} \text{ mm}^{-1})$$

for any intensity of rainfall, and that:

$$\lambda = 41 R^{-0.21} \text{cm}^{-1} \quad (4.1 R^{-0.21} \text{ mm}^{-1}) \qquad \ldots (ii)$$

where R is the rainfall rate in mm hr^{-1}. (See 1.2.2.)

These data are shown in Figure 1.4 and the trend towards a common value of N_o for all rates of rainfall is evident. This is perhaps a surprising result for such a complex and variable phenomenon as rainfall and it is only achieved consistently by measuring a number of

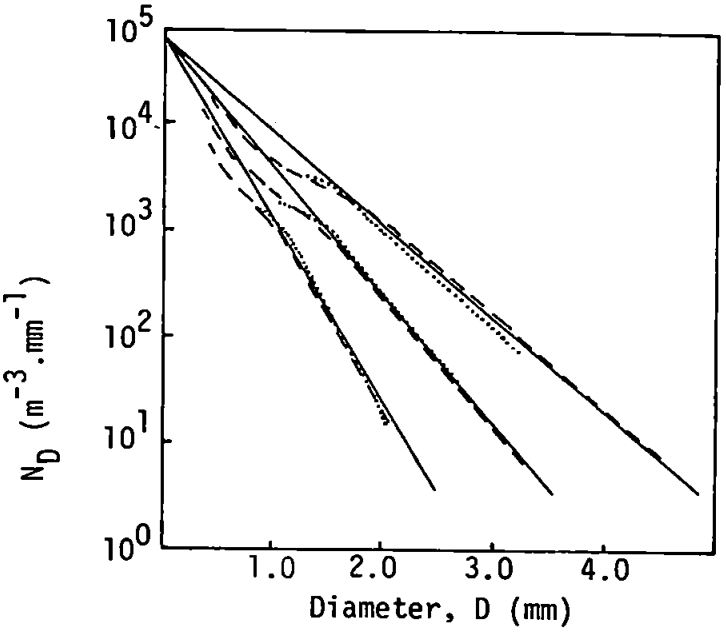

Figure 1.4 Distribution function (solid straight lines) compared with the results of LAWS and PARSONS (*14*) (broken lines) and Ottawa observations (*13*) (dotted lines).

spectra of similar rainfall rates, although individual spectra may occasionally produce the same numerical results.

It is now established that the value of N_0 for averaged spectra varies considerably (*15*) and indeed the change of N_0 over short intervals of time may be of some interest (*12*). However, the M-P distribution is a most useful "yardstick" in this work and has been used as such by many workers. (See for instance *7*, *12*, *16*.)

If the rainfall rate is known, the distribution is easily computed from (i) and (ii) and may be compared with an observed distribution having the same value for R. Figure 1.5 shows the spectrum of Figures 1.2 and 1.3 compared with the appropriate M-P distribution. The deficiency of small drops in the observed distribution is apparent and the fit is quite good for diameters above 1.0 mm.

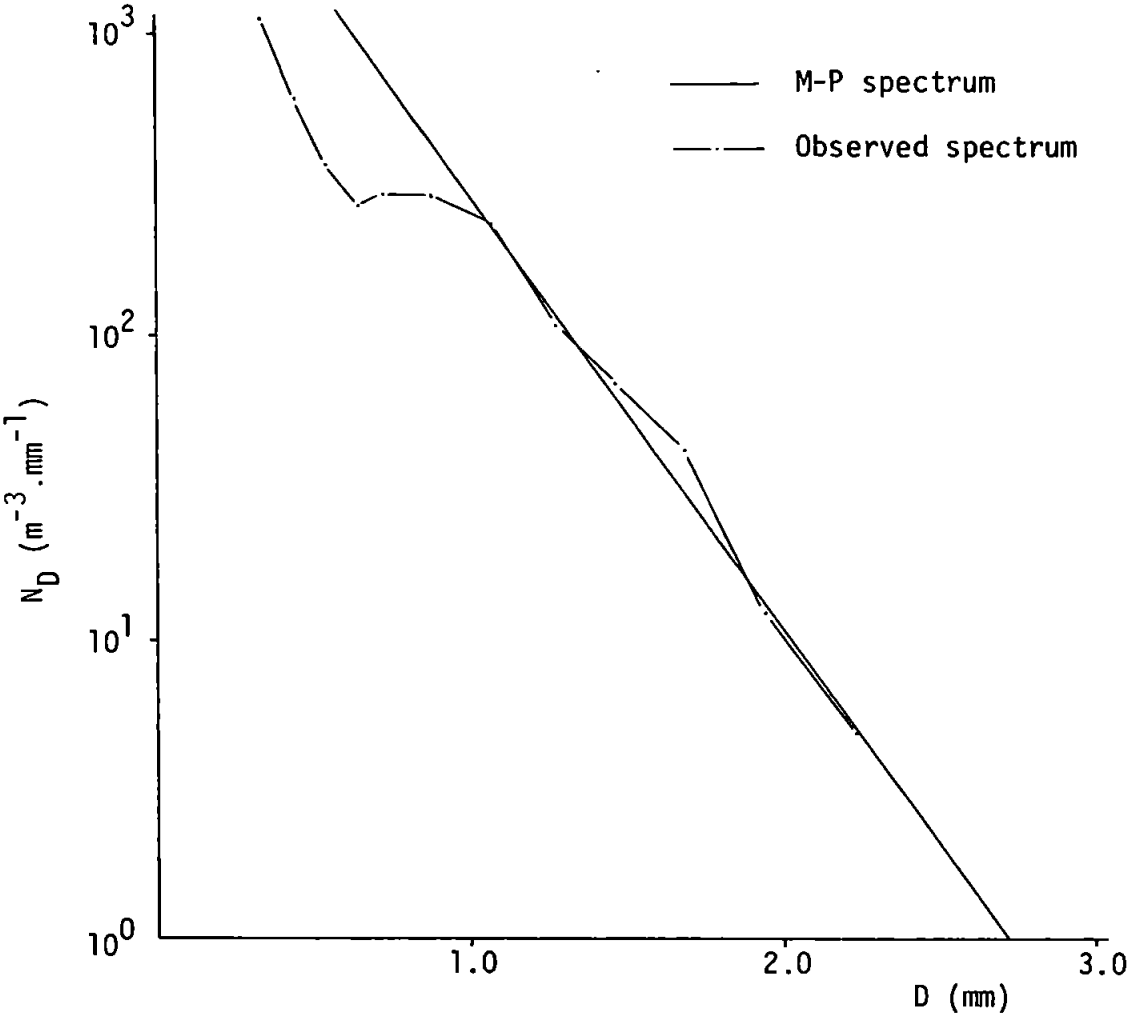

Figure 1.5 Spectrum 3439 compared to M-P distribution for same rainfall rate. R = 2.95 mm hr^{-1}.

1.2 PHYSICAL RELEVANCE

1.2.1 Integration of the spectrum

Raindrop spectra may be integrated in several ways to produce results of physical relevance. For instance the total volume of all the raindrops in a spectrum may be expressed as:

$$W = \frac{\pi}{6} \int_0^\infty N_D \, D^3 dD \ \text{mm}^3 \ \text{m}^{-3} \qquad \ldots \text{(iii)}$$

where W is the liquid water content. This result and the result of other integrations will be discussed in the following sections.

A general form of this expression may be written:

$$P(n) = C \cdot \int_0^\infty N_D \, D^n dD \qquad \ldots \text{(iv)}$$

where P(n) is the "integral parameter" (*17*) for a particular integer value of n ($0 < n \leq 6$) and C is a constant. It may be seen that (iii) is a particular case of (iv) with $C = \frac{\pi}{6}$ and $n = 3$.

In practice the spectrum is integrated between definite limits, corresponding to the upper and lower measuring limits of the instrument, and N_D is the number of drops in the range D to D + δD. Hence for each step of the integration $D^n \delta D$ must be computed from the finite-difference approximation:

$$D^n = \tfrac{1}{2} \left(D_i^{\,n} + D_{i+1}^{\,n}\right) \left(D_{i+1} - D_i\right) \qquad \ldots \text{(v)}$$

where D_i and D_{i+1} are the limits of a particular size interval and $D_{i+1} > D_i$. In the case of the Joss distrometer the interval $(D_{i+1} - D_i)$ varies for reasons explained in 2.2.2.

1.2.2 Rainfall rate

The rainfall rate, R, is the depth of water collected on a horizontal surface in unit time if R remains constant. The depth is conventionally measured in millimetres and the time unit is one hour.

It is well established (*16*, *18*, *19*, *20*) that rainfall rate is a very variable quantity over even very short time intervals. Hence R is never constant for one hour but a unit of mm hr^{-1} is satisfactory for manipulation and as a basis for crude comparison between spectra. It is also essential for constructing the M-P distribution.

Rainfall rate may be determined by several methods all of which involve an averaging process. The approach to an instantaneous value improves as the sampling interval is reduced. An average value of R over a period of some hours may be obtained from conventional rain gauge records or over shorter intervals by measuring the slope of the hyetogram from an autographic gauge. NORBURY and WHITE (*20*) developed a rapid response raingauge which could be interrogated at 10 sec. intervals and yield near instantaneous rates up to 200 mm hr^{-1} with an error of not more than 10%. SEMPLAK and TURRIN (*21*) reported a gauge with a collecting area of 730 cm^2 and a sampling time of 1 sec.

The Joss distrometer in the present work uses a collecting area of 50 cm^2 and a sampling time of 1 minute. Rainfall rates are calculated in mm hr^{-1} for each spectrum hence the total depth of precipitation represented by each spectrum is $R/60$ mm.

R may be derived from (iii) by including the velocity of the falling drops thus:

$$R = \frac{\pi}{6} \int_0^\infty N_D D^3 V_D \, dD \text{ mm}^3 \text{m}^{-3} . \text{ m sec}^{-1}$$

which reduces to:

$$R = \frac{3.6\pi}{6000} \int_0^\infty N_D D^3 V_D \, dD \text{ mm hr}^{-1} \qquad \ldots \text{(vi)}$$

where V_D is the terminal velocity of raindrops of diameter D mm.

1.2.3 Liquid water content

The liquid water content, W, was introduced in 1.2.1 and may be computed from (iii). It is related to the rainfall rate and has considerable significance in meteorology especially when determined within a cloud. In this case the magnitude and spatial distribution of W facilitates the study of cloud dynamics, particularly the growth mechanisms of precipitation elements. It is also of direct relevance in the study of ice accretion on aircraft (*22*). Measurement of W at the surface is perhaps of less direct value, but may be of use indirectly in describing spectra, as discussed in 1.3.

1.2.4 Radar reflectivity factor

Radar is now a highly-developed tool in the hands of the meteorologist and one of its most useful applications is in the detection and measurement of precipitation. Consideration of raindrop-size distributions is fundamental in this respect.

PROBERT-JONES (*23*) has shown that, provided the pulse volume is uniformly filled with rain, then:

$$\overline{P} = C_1 \, C_2 \, K \frac{Z}{r^2} \qquad \ldots \text{(vii)}$$

where $\overline{P}$ is the average power returned to the radar from the rain at range r, C_i is a constant known from the radar parameters (e.g. wavelength, aerial dimensions etc.), C_2 is approximately constant and related to the dielectric properties of raindrops, K is the coefficient of attenuation, mainly due to the rain in the path between the aerial and the pulse volume under consideration, and Z is the radar reflectivity factor defined as the sum of the sixth powers of the drop diameters per unit volume, i.e.:

$$Z = \int_0^\infty N_D \, D^6 \, dD \qquad \ldots \text{(viii)}$$

which is equation (iv) with C = 1 and n = 6.

This simple relationship arises from the Rayleigh scattering law which is applicable when the radar wavelength is long compared with the diameter of the scattering particles. It has been shown (*24*) that at wavelengths between 3 and 10 cm (which includes most meteorological radars) the Rayleigh approximation is valid for the observation of rain.

For a single spherical drop, the back scattering cross section is given by:

$$\sigma_i' = \frac{\pi^5}{\lambda^4} \, |K|^2 \, D_i^6 \qquad \ldots \text{(ix)}$$

where λ is the wavelength (*25*). This is known as the "Rayleigh approximation". Hence for a population of spherical drops $\Sigma n_i D_i^6$ is required and this is known as the "Radar reflectivity factor".

1.2.5 Other physical parameters

Several other parameters may be computed from the spectrum; for instance if $C = \pi/4$ and $n = 2$ in equation (iv) we produce the optical extinction cross section σ where

$$\sigma = \frac{\pi}{4} \int_0^\infty N_D \, D^2 \, dD \; mm^2 \; m^{-3} \qquad \ldots (x)$$

which is the total surface area of all the drops in one cubic metre. This parameter is also related to the washout in a cloud.

ATLAS (*26*) has defined the median volume drop diameter, D_o, as that diameter which divides the drop distribution in such a way that half of the liquid water content is contained in drops greater than D_o. This result is not directly useful but may be used as a descriptive parameter, especially if the same concept is used in a more developed form as described in 1.3.2.

1.2.6 Relationships between physical parameters

The relationships that exist between these physical parameters generated by the spectra may be examined empirically and this is a most fruitful area to explore. For instance, if a well-defined relationship exists between R and Z, then the radar equation (vii) may be used to enable radar to measure rainfall.

These relationships are most easily examined by plotting one parameter against the other on logarithmic axes. This almost inevitably leads to a straight line from which an empirical power relationship in the form:

$$X = A.Y^B$$

may be deduced, where X and Y are two physical parameters and A and B

are constants. The Z-R relationship is the most commonly used and will be described in the following discussion.

MARSHALL and PALMER (*13*) proposed a relationship $Z = 220\ R^{1.6}$ in 1948 and $Z = 200\ R^{1.6}$ has been commonly quoted (*27*) and used for reduction of radar data for some years. It is now accepted that there are no absolutely reliable values for the constants A and B and in a number of studies many relationships have been proposed (see *25* for a summary). This is due to the complex variability of rainfall leading to variations in the Z-R relationship between synoptic types, locations and small scale features of rainfall events. The relationship is also very sensitive to the existence of hail or snow in the population and an approximate relationship $Z = 2000\ R^{2.0}$ is appropriate for aggregate snowflakes (*28*).

The first 7253 minutes of the present data were examined and a linear regression of log R and log Z for all raindrop spectra representing rainfall rates of 0.1 mm hr^{-1} and above (4586 minutes) yielded the relationship $Z = 269\ R^{1.68}$ with a correlation coefficient of +0.94. This is well within the compass of the many published relationships and may be compared with $Z = 296\ R^{1.47}$ which is the result obtained by the direct integration of the M-P distribution assuming Rayleigh scattering. These relationships and some others appear in Figure 1.6.

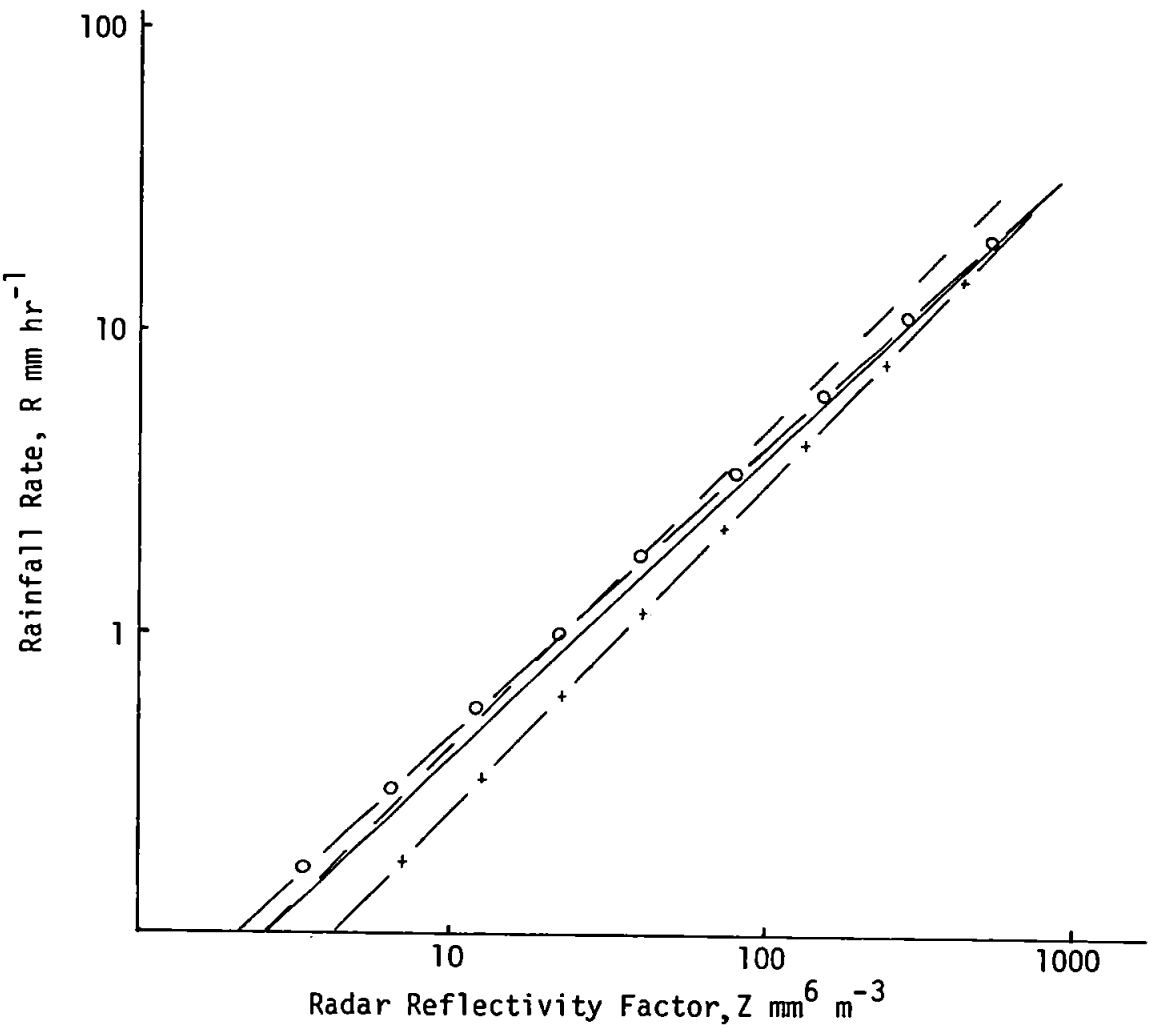

Figure 1.6 Various Z-R relationships

———	$Z = 269\ R^{1.68}$	Present data
— —	$Z = 220\ R^{1.6}$	M-P (*13*)
—o—	$Z = 250\ R^{1.8}$	NICHOLASS and LARKE (*16*)
—×—	$Z = 296\ R^{1.47}$	Direct integration of M-P distribution

1.3 DESCRIPTIVE PARAMETERS

1.3.1 Intercept and slope

It is useful to be able to describe a raindrop-size distribution with some characteristic parameters which would ideally define the spectrum completely. This facilitates the comparison of spectra without the need to resort to simply comparing the numbers of drops in each size interval which is inconvenient, especially when using data from different instruments, which may use different size intervals.

There are a variety of possibilities, and the use of intercept (N_0) and slope (λ) of the exponential distribution was first proposed by MARSHALL and PALMER (*13*). This method suffers from the main disadvantage that few spectra are perfect exponential distributions. These authors proposed that N_0 had a common value of 8×10^3 mm^{-1} m^{-3} for all rainfall rates. As noted earlier this result is only possible when many spectra are averaged and so such a parameterisation, using a fixed value for N_0, is useful for generalised relationships, such as the Z-R curve, but ignores small scale fluctuations in the raindrop spectra.

The variability of the N_0 value may be exploited to improve its use as a descriptive parameter as demonstrated by WALDVOGEL (*12*). This author used a simple transformation from equations (i), (iii) and (vii) to show that:

$$N_0 = 446 \left(\frac{W}{Z}\right)^{\frac{4}{3}}.W \qquad \ldots \text{(xi)}$$

$$\text{and} \quad \lambda = 6.12 \left(\frac{W}{Z}\right)^{\frac{1}{3}} \qquad \ldots \text{(xii)}$$

The results were interpreted as follows:

> "large values of N_0 ($N_0 > 2 \times 10^4$ m^{-3} mm^{-1}) mean spectra whose balance between small and large drops is shifted towards small drops (drizzle) whereas small values of N_0 ($N_0 < 2 \times 10^3$ m^{-3} mm^{-1}) mean spectra whose balance between small and large drops is shifted towards large drops (local thunderstorm) as compared to a distribution found in a steady-state widespread rain situation ($N_0 \sim 10^4$ m^{-3} mm^{-1})."

Figures 1.7 and 1.8 show examples of spectra with small and large values of N_0. These distributions from the present data set have almost identical rainfall rates but in the case of the large drop spectrum (2202) the value of Z is much larger than would be expected from the conventional Z-R relationship ($Z = 200\ R^{1.6}$) and more than double the value of the small drop spectrum (9656). The exponential distribution for the computed values of N_0 and λ is shown and provides a better fit to the data than an M-P distribution.

The variation of these shape parameters with time will be discussed later (4.1) and an interpretation of their significance given.

1.3.2 Joss-Gori parameterisation

The values N_0 and λ have no direct physical relevance, N_0 being the number of drops with zero diameter - clearly an abstract quantity. JOSS and GORI (*17*) have proposed a more sophisticated parameterisation based on the values of σ, W, R and Z. This technique is suited to the Joss distrometer and well defined up to rainfall rates of 100 mm hr^{-1}.

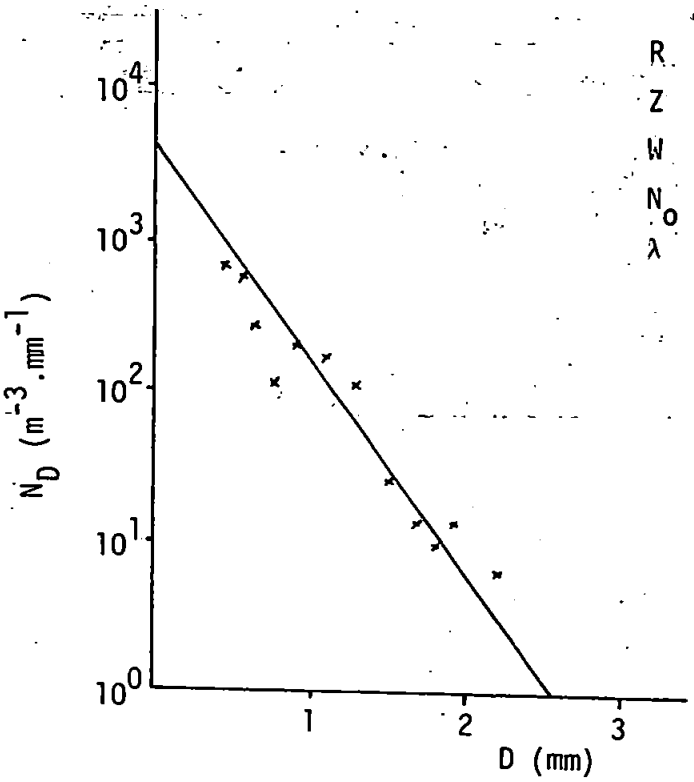

$R = 2.20$ mm hr^{-1}
$Z = 859.3$ $mm^6 m^{-3}$
$W = 129.5$ $mm^3 m^{-3}$
$N_o = 4630.6$ $m^{-3} mm^{-1}$
$\lambda = 3.26$ mm^{-1}

Figure 1.7 Spectrum for min. 2202 (Low N_o)

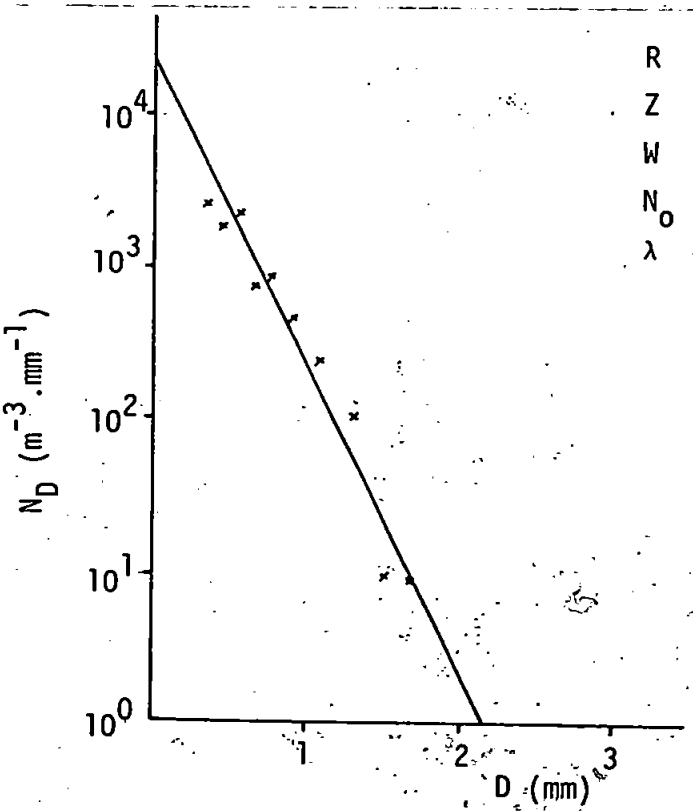

$R = 2.23$ mm hr^{-1}
$Z = 365.3$ $mm^6 m^{-3}$
$W = 173.5$ $mm^3 m^{-3}$
$N_o = 28689.3$ $m^{-3} mm^{-1}$
$\lambda = 4.78$ mm^{-1}

Figure 1.8 Spectrum for min. 9656 (High N_o)

These authors propose 12 parameters divided into 3 sets:

Integral parameters	σ, W, R, Z
Median parameters	DM(σ), DM(W), DM(R*), DM(Z)
Shape parameters	S(W, σ), S(R*, W), S(Z, R*), S(Z, σ)

The first set are the magnitudes of parameters of direct physical relevance, described in 1.2 and are used as the basis for the other two sets which describe the drop-size distribution in more detail.

The median parameters are a set of diameters which indicate the region of the distribution which contributes most to the associated integral parameter. The parameter DM(W) is synonymous with D_o described in 1.2.5 and the other median parameters are similarly defined. R* is given by equation (iv) with C = 1 and n = 4 and is used in preference to R to simplify comparison of the observed data with an exponential distribution.

The third set of parameters describes the deviation of the observed spectrum from the exponential over certain portions of interest. A concept analogous to a second differential or curvature is used to indicate the form of the distribution contributing to the specified pairs of integral parameters. For example, if S(W, σ) = 1, an exponential distribution is appropriate for the drops contributing to W and σ and as this shape parameter tends to zero the distribution tends to monodispersity.

Some of the present data were analysed using this relatively sophisticated parameterisation technique and the relationship to other published work was considered (*29*, *30*). In view of the line of research subsequently pursued, which would relate to an actual

operational problem, it appeared that the relative complexity of the JOSS-GORI parameterisation was not suited to this investigation and that only studies which would be concerned primarily with the micro-physical meteorological implications of precipitation would warrant such sophistication.

CHAPTER TWO

DATA COLLECTION AND PRIMARY ANALYSIS

2.1 THE SITE

2.1.1 St. Mawgan, Cornwall

St. Mawgan is a village in north west Cornwall some 25 km north of Truro and near to an RAF base. RAF St. Mawgan is an operational base which houses a Meteorological Forecasting Office in the control tower building. The airfield is an extensive flat area with runways extending up to the coast and some distance inland. The area is open to Watergate Bay and the Atlantic Ocean to the west; south westerly air arrives having travelled over approximately 160 km of land. The area is generally elevated, the Meteorological Office instrument compound being 103 m above mean sea level. The locations referred to in this work are shown in Figure 2.1.

2.1.2 Meteorological Office Instrument Compound, St. Mawgan

The relationship of the compound to the surrounding buildings and roads is shown in Figure 2.2. A general view appears in Plate 1. The distrometer was installed close to the 5 inch station gauge and approximately 3 m from the autographic gauge with which comparisons were made. Some shelter was to be expected from a support of the chain link fence, although the effect was not serious (3.1.2). As can be seen in the plan, the compound is not significantly affected by the nearby buildings.

2.1.3 Installation

The makers recommend that the transducer be mounted with the sensor level with the ground to reduce the turbulent effects of strong winds. Care must be taken to prevent the transducer from becoming flooded and

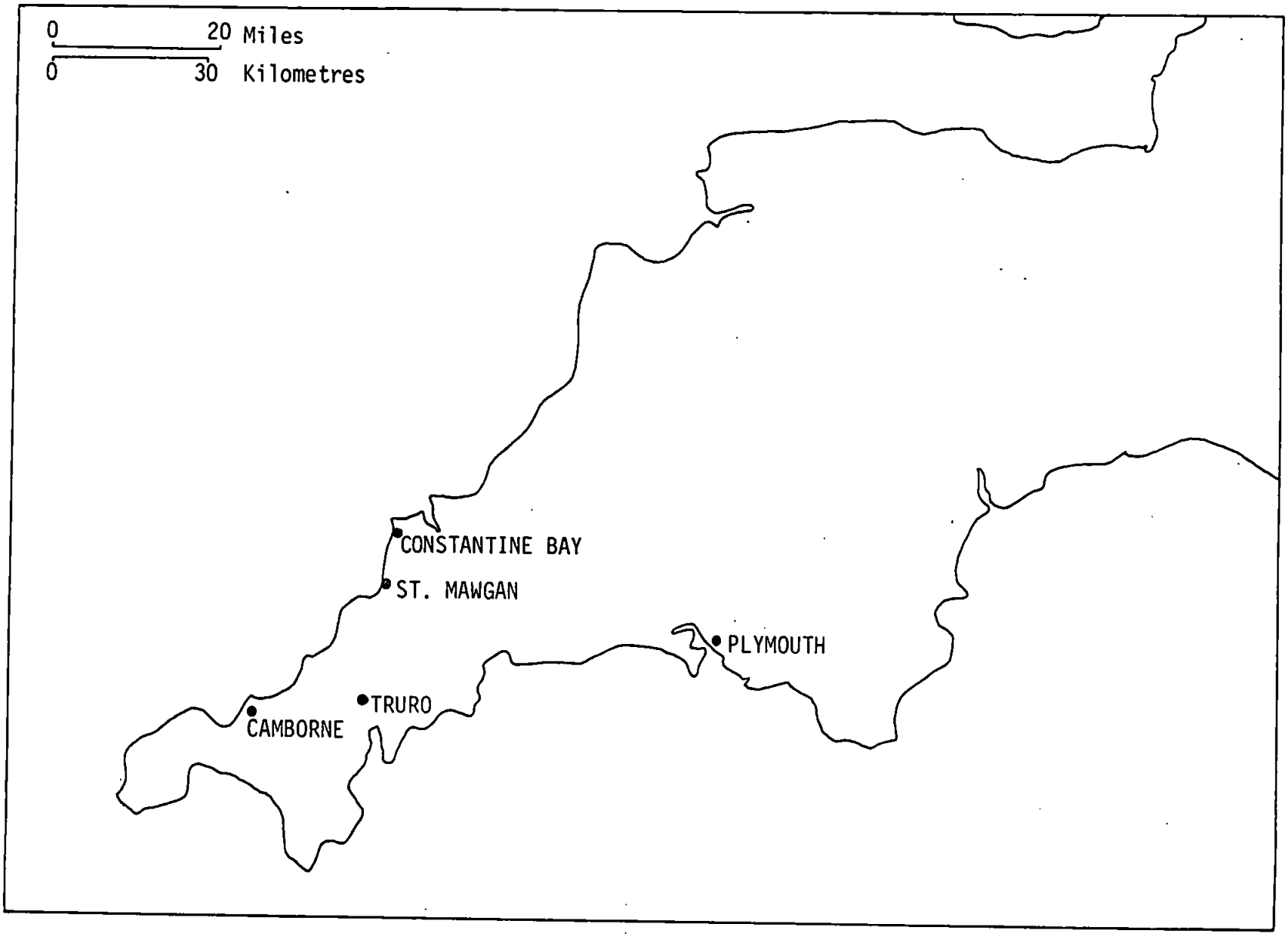

Figure 2.1 Map of Devon and Cornwall showing places referred to.

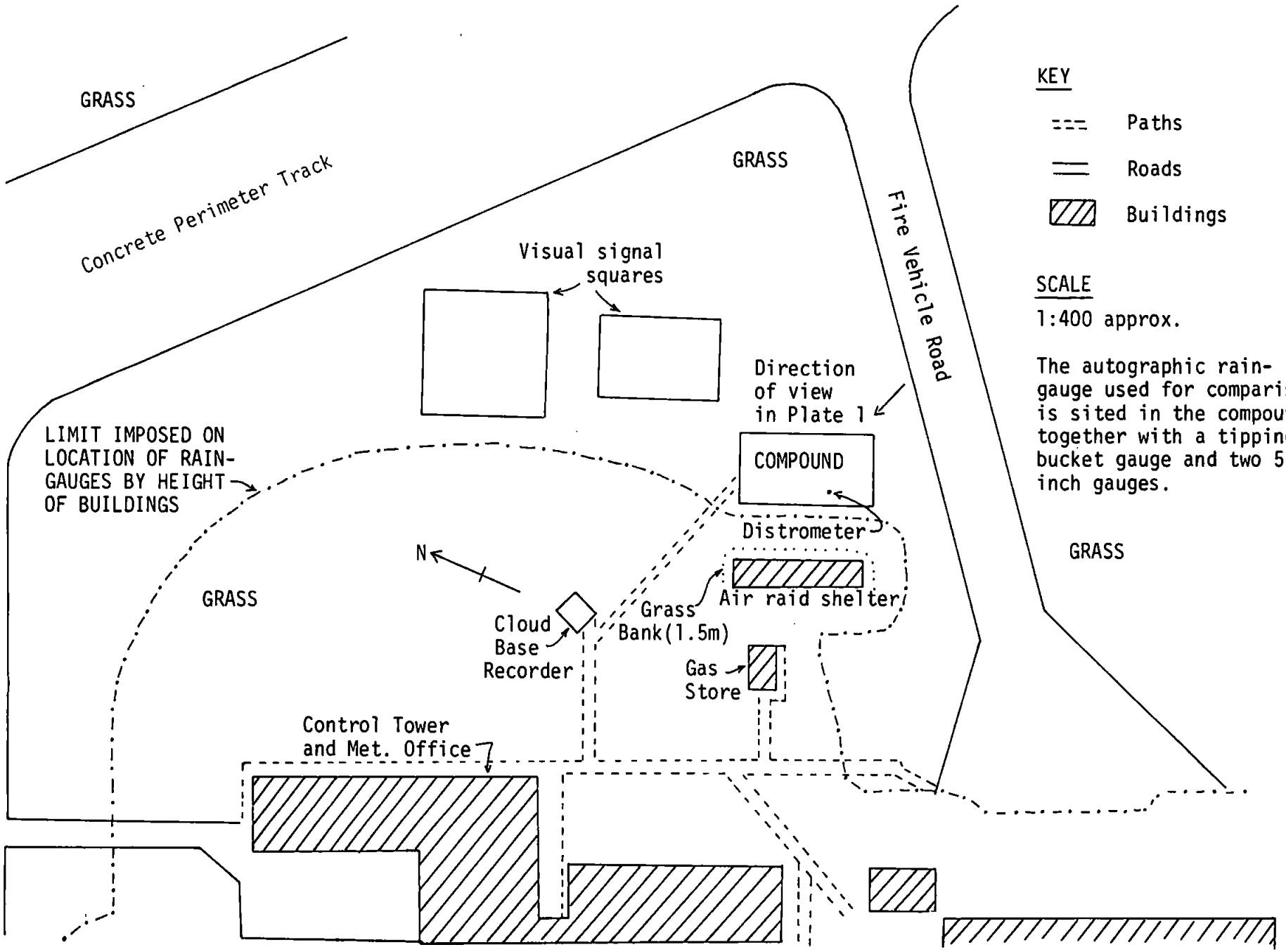

Figure 2.2 RAF St. Mawgan. Meteorological Office Instrument Compound and environs

it must be surrounded by a surface that will not cause raindrops landing nearby to splash onto the receiving body. A foam rubber surround is suggested (*31*) but in the present experiment the advice of Meteorological Office technical staff was sought and this resulted in the installation as described below. This is similar to that used in the Dee Weather Radar Project.

A varnished, open-ended plywood box 60 cm x 60 cm x 20 cm deep was sunk into the ground and the bottom of the pit so formed was filled with coarse gravel to a sufficient depth to bring the sensor level with the ground (Plate 2). An anti-splash surround was fixed to the corners of the box (Plate 3). This was constructed from a plastic light diffuser having a 1 cm x 1 cm mesh. A hole was left in the centre for the sensor and the surround was orientated approximately East-West. It was anticipated that much of the rain would be blown from a westerly quadrant and such orientation would provide the maximum benefit from the dimensions available. Exhaustive experiments (*32*) have shown that for absolute rainfall measurement, a gauge set with the rim at ground level, surrounded by an anti-splash surround, gives the best results.

The cable from the transducer (which can be seen in Plate 2) was buried in the grass and connected to a junction box on a pedestal near to the Stevenson screen (Plate 1). From there the cables pass underground to the Meteorological Office area in the Control Tower, 50 m distant. The installation proved satisfactory throughout the experiment; it was inspected regularly and the cover removed to keep the grass cut as necessary.

2.2 THE INSTRUMENT

2.2.1 Principle of operation

> "The Distrometer for raindrops is an instrument for measuring raindrop-size distributions continuously and automatically. It was developed because statistically meaningful samples of raindrops could not be measured previously without a prohibitive amount of work. The instrument transforms the vertical momentum of an impacting raindrop into an electric pulse, whose amplitude is a function of the drop diameter. A conventional pulse height analysis yields the size distribution of the raindrops" (*31*).

A Joss distrometer, together with its supporting hardware, was obtained on loan from the Meteorological Office Radar Research Laboratory. This instrument had previously been used in the Dee Weather Radar Project (DWRP) and some published results were available (*16*).

The distrometer consists of two units:

- the transducer which is exposed to rain (Plate 4)
- the processor (Plate 5)

The specification of the instrument is contained in Appendix I.

The distrometer transforms the mechanical momentum of an impacting raindrop into an electric pulse. This transformation is achieved by a feedback system consisting of two coils in magnetic fields and an amplifier (see Figure 2.3). The raindrops are intercepted by a rigid cone made of hard styrofoam which has a non-absorbent top surface. Two coils are firmly attached to this element and the whole is supported by two springs which constrain any movement to be axial. On the impact of a raindrop, the cone and coils are driven downwards inducing a voltage in the lower coil as it is moved through a magnetic

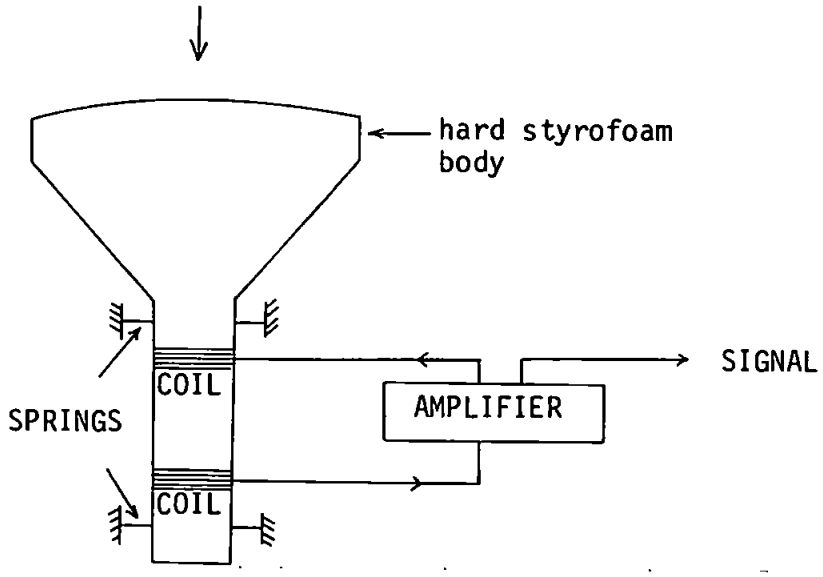

Figure 2.3 Schematic diagram of transducer

field. This voltage is then amplified and fed back to the upper coil which produces an axial force in a direction opposite to the original deflection. The system is thus electronically-damped and the amplitude of the current in the upper coil is a measure of the drop size.

The amplitude of the electric pulse is proportional to the mechanical momentum of the falling raindrop, given by the product of the mass and the terminal velocity. (It is assumed throughout that raindrops are at terminal velocity on impact.) Thus the amplitude is roughly proportional to the fourth power of the drop diameter:

$$U \sim D^4$$

The large ratio in the dynamic ranges of the measured signals (U) and the diameters (D) leads to a high order of accuracy even for small drops. (See Figure 2.4.) The makers claim that the standard deviation of the measured drop diameters is less than 5% (*33*).

As seen in Figure 2.4 the output pulses for drops from 0.3 mm to 5.0 mm range from 0.3mV to 10V corresponding to a dynamic range of 90 db. The processor compresses this to a range of 36 db to facilitate signal processing. The compressed signal output (U_c) varies from 0.16V to 10V for drops in this size range. A simple relationship is found between U_c and D and is illustrated in Figure 2.5. (An individual calibration is provided with the instrument - this is contained in Appendix I.)

The processor also contains circuits to eliminate unwanted signals, mainly due to acoustic noise. Hence when a high level of acoustic noise is encountered, the instrument will fail to record drops which produce a signal below the level of interfering noise. Although this results in drops being eliminated from the record on occasions, it is

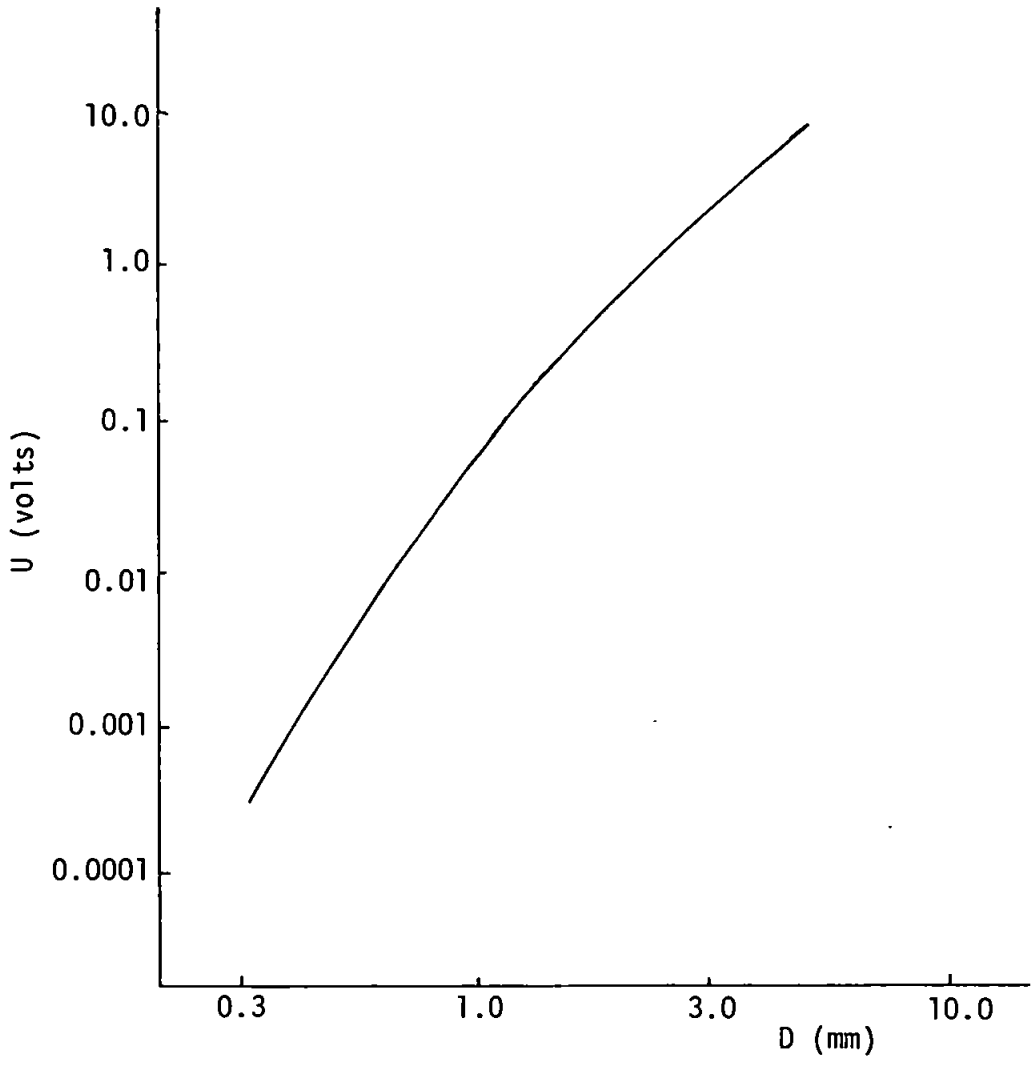

Figure 2.4 Relationship of output signal (U) to drop diameter (D) (33)

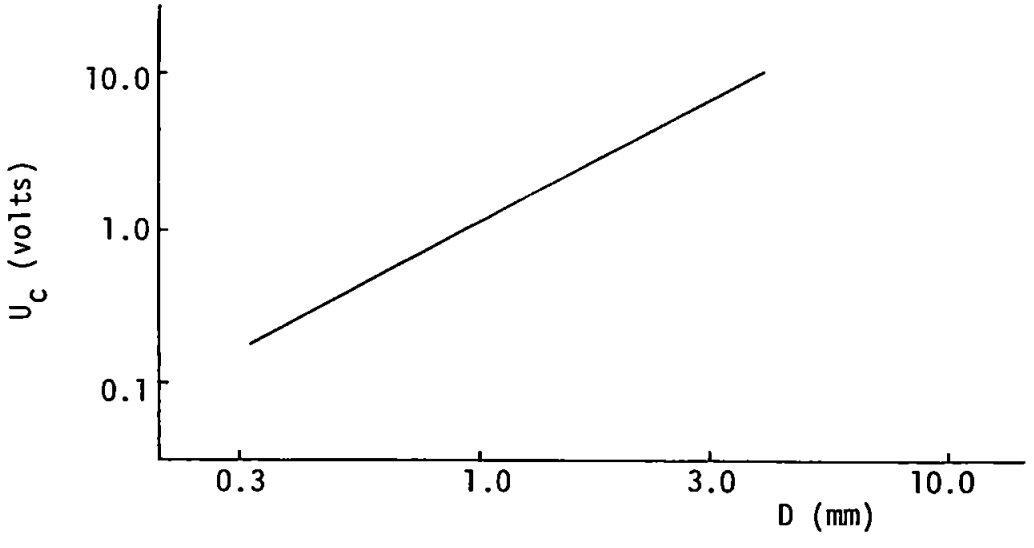

Figure 2.5 Relationship of compressed output signal (U_c) to drop diameter (D) (33)

preferable to the alternative of a burst of noise being recorded as a number of perhaps large and non-existent impacts.

2.2.2 Supporting Hardware

The signal from the processor must be fed to a pulse-height analyser in order that pulses may be converted to appropriate drop sizes. These data must then be recorded together with a timing reference.

The makers of the Distrometer also produce a pulse-height analyser which is designed to be compatible and render the data easily recordable on a variety of devices. The specifications of this device (Analyser AD 69) are given in Appendix I and it can be seen in Plate 5. A visual indication of raindrop impacts is given by a set of 20 red indicator lamps on the front panel, one for each channel, corresponding to 20 ranges of drop diameters. These are given in Table 2.1, together with input/output information. The class limits of the channels are arranged so that the ratio between the class intervals and the relevant drop diameters remains nearly constant. This ensures a proportionally wider sampling range for the relatively infrequent impacts of the larger drops.

These signals are fed to a FACIT 4070 paper tape punch as a permanent record. This device is specified in Appendix I and also receives signals from a crystal-controlled digital clock to provide a uniquely-coded frame on the paper tape at intervals of one minute.

The clock is a VENNER type TSA 6686 and is modified to produce the required pulses and fed to the processor via the "clock connection box" supplied by the Meteorological Office. The entire configuration is shown in Plate 5 and schematically in Figure 2.6.

CHANNEL No.	DROP DIAMETER (mm)	INPUT AMPL. circuit a (volts)	20 LINE OUTPUT pulse at pin No.	BINARY OUTPUT logic level at pin No. A	B	C	D	E
1	0.3 - 0.4	0.16 - 0.245	A	1	1	1	0	1
2	0.4 - 0.5	0.245- 0.34	B	1	1	1	0	0
3	0.5 - 0.6	0.34 - 0.44	C	1	1	0	1	1
4	0.6 - 0.7	0.44 - 0.56	D	1	1	0	1	0
5	0.7 - 0.8	0.56 - 0.68	E	1	1	0	0	1
6	0.8 - 1.0	0.68 - 0.94	F	1	1	0	0	0
7	1.0 - 1.2	0.94 - 1.22	H	1	0	1	1	1
8	1.2 - 1.4	1.22 - 1.55	J	1	0	1	1	0
9	1.4 - 1.6	1.55 - 1.90	K	1	0	1	0	1
10	1.6 - 1.8	1.90 - 2.25	L	1	0	1	0	0
11	1.8 - 2.1	2.25 - 2.80	M	1	0	0	1	1
12	2.1 - 2.4	2.80 - 3.40	N	1	0	0	1	0
13	2.4 - 2.7	3.40 - 4.05	P	1	0	0	0	1
14	2.7 - 3.0	4.05 - 4.75	R	1	0	0	0	0
15	3.0 - 3.3	4.75 - 5.45	S	0	1	1	1	1
16	3.3 - 3.7	5.45 - 6.40	T	0	1	1	1	0
17	3.7 - 4.1	6.40 - 7.50	U	0	1	1	0	1
18	4.1 - 4.5	7.50 - 8.60	V	0	1	1	0	0
19	4.5 - 5.0	8.60 -10.00	W	0	1	0	1	1
20	5.0 -	10.00 -	X	0	1	0	1	0
Auxiliary input 1 (pin F)			-	0	0	0	1	0
Auxiliary input 2 (pin H)			-	0	0	0	0	1
Auxiliary input 3 (pin J)			-	0	0	0	0	0

Table 2.1 Channel Calibration

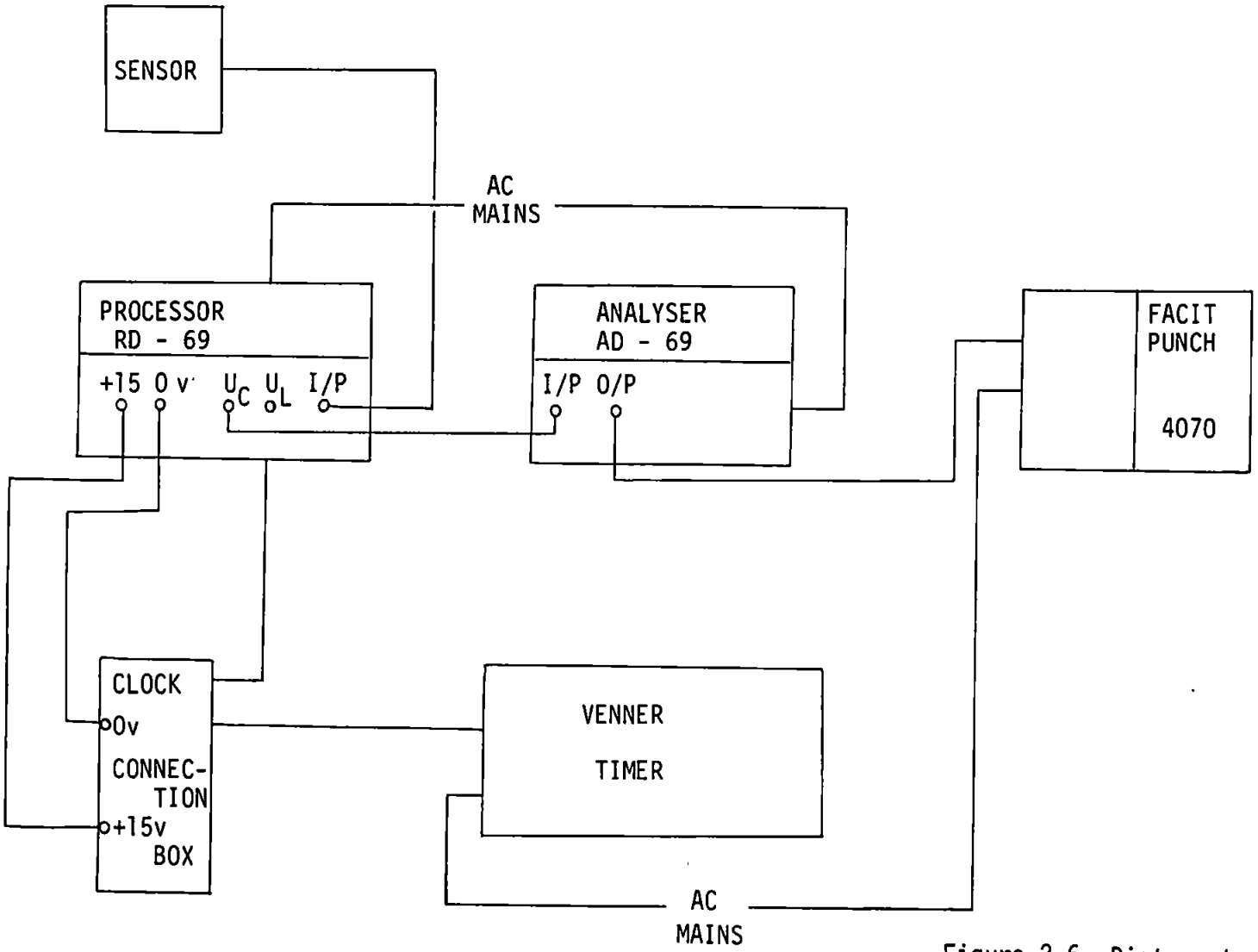

Figure 2.6 Distrometer System Wiring Diagram

2.2.3 Sources of error

The potential sources of error recognised in this experiment are:-

Acoustic noise at distrometer site
Incorrect calibration of distrometer
Variation in fallspeed of raindrops of same size
Variation in shape of raindrops
Inadequacy of sampling volume
Inadequate response time in high rainfall intensities
Insplash to sensor from surroundings
Splash products formed on sensor
Timing errors.

The first error is unique to a particular experimental site and will be discussed separately in the next section. The calibration is described in 2.2.5. The remaining potential sources of error are common to all distrometer experiments, and are discussed below:

Variation in fallspeed of raindrops of same size

As explained in 2.2.1, the instrument relies on the existence of a fixed relationship between the amplitude of the signals produced and the mechanical momentum of the raindrops striking the transducer. This assumes that raindrops of the same size are travelling at the same speed when arriving at the transducer. This velocity is assumed to be the terminal velocity of the drops in still air.

Furthermore when computing the raindrop-size distribution in the conventional form of number per unit volume per unit size interval, the terminal velocity is again introduced. Clearly any fluctuation

in the fallspeed of raindrops of the same size will lead to errors. The most likely mechanism to cause such fluctuation would be vertical air motion (VAM).

This matter has been widely discussed (see for instance *10*, *35*, *37*) and the conclusion is that errors due to this mechanism are unlikely to be serious. In fact the Joss distrometer has been used as an independent measure of the spectrum of raindrop sizes in an experiment to investigate VAM using Doppler radar (*34*). The authors (BROWNING et al) state "The influence of VAM on the accuracy of the distrometer has been shown to be negligible in most practical circumstances".

Variation in the shape of raindrops

It has been suggested by KINNELL (*35*) that if raindrops of a different shape to those used to calibrate the distrometer occur in natural rain, then the relationship between the signal pulse and the drop diameter (described in 2.2.1) will not hold. Such a situation may arise during high wind velocities.

Freely falling raindrops develop a concave depression in the base when the diameter exceeds 5 mm (*36*). Such raindrops are counted in the largest size category measured by the distrometer (Channel 20) and in the present data no drops were recorded in this category. From the results discussed in 3.1.2, comparing gauge and distrometer-derived rainfall with wind velocity, there does not seem to be any systematic variation which suggests that if errors due to drop shape changes are present, then they are small and do not systematically affect the observations.

The designers of the distrometer (JOSS & WALDVOGEL) reply to KINNELL's paper and largely discount the results since the latter specified extreme conditions which are unlikely to occur in natural rainfall (*37*). These authors also stress that the distrometer is necessarily a compromise to optimise the contradicting specifications for the instrument:-

- statistically significant raindrop samples (large receiving body)
- small ringing time constant: few drops lost (small receiving body of damping material, broad band width)
- no dependence on the impact location (small receiving body, low frequency response)
- no dependence on drop shape (low frequency response)
- no dependence on acoustic noise and wind (high frequency response, small receiving body)

The optimisation is achieved by the correct choice of two parts of the instrument, firstly the receiving body (geometry and material) and secondly the electronic processing circuitry (centre frequency and bandwidth).

Inadequacy of sampling volume

Raindrop-size distributions are quantified as a number of drops per cubic metre. In the present experiment the volume of atmosphere sampled in each channel is given by:

$$\text{VOLUME} = A \times V_{D_i} \times t \ m^3$$

where i = channel number ($1 \leq i \leq 20$)

A = collecting area (0.005 m^2)

V_{D_i} = terminal velocity of drops in channel i

t = sampling interval (60 secs.)

The volume sampled in each channel for this interval is given in Table 2.2. It is not until channel 6 that at least one cubic metre is sampled and this is not necessarily typical of the rainfall situation.

The effect of this error depends on the integral parameter under consideration. Clearly to measure Z accurately requires the sampling of a larger volume than that required to measure R with the same degree of accuracy, because the largest drops, which contribute very significantly to Z, are much scarcer than the smaller drops.

The sample size required to measure R with a probability of 95% which deviates less than 10% from the mean has been calculated theoretically (*38*). For a filter paper technique (which is identical in principle to the distrometer calculation) 1.5 m^2sec. is required and for a drop camera (where a volume is sampled directly) 11 m^3 is required. The sample provided by the distrometer is 0.3 m^2sec. which suggests that a longer interval, perhaps 5 minutes, should be used. However, such an approach would mask some of the interesting short-term fluctuations in rainfall and since a 60 second interval is most commonly used, it would render the results less easily comparable with other published work. The use of the results without a correction is therefore a compromise between a high order of accuracy (difficult to achieve with such a random and fluctuating phenomenon as rainfall) and the most complete qualitative description of the event.

It is likely that the wide range of Z-R relationships which have been deduced by various techniques is due in some part to the statistically-induced variability in observations arising from this sort of error, for which it would be difficult to compensate.

Channel number	Volume sampled (m^3)
1	0.42
2	0.55
3	0.68
4	0.80
5	0.92
6	1.10
7	1.30
8	1.47
9	1.62
10	1.76
11	1.92
12	2.09
13	2.24
14	2.36
15	2.46
16	2.55
17	2.63
18	2.69
19	2.72
20	2.74

Table 2.2 Sample volume of each distrometer channel for an interval of one minute

Inadequate response time in high rainfall intensities

Raindrops which are intercepted by the sensor whilst the system is recovering from a previous impact will not be counted. The recovery time of the transducer is only a few milliseconds (e.g. for 1 mm drops the recovery time is about 1 ms. (*29*)). The operational speed of the paper tape punch is 75-80 rows per second (see Appendix I). This determines the maximum rate at which the system can count raindrops and corresponds to a response time of 13 ms.

The manufacturers claim that significant errors due to coincidence counting are only likely at high rainfall intensities. Although there is much published work based on distrometer observations, there has apparently been no attempt to quantify this error. Hence an investigation was made into the likely effect of missing impacts whilst the system is recovering. These effects are normally considered in the case of other particle counters - in particular Geiger counters and Coulter counters. For a raindrop-size distribution the problem is complicated by the need to know the size distribution of the impacts missed if the error is to be quantified with any degree of certainty.

Two methods of calculating the error were devised and applied to the observed average drop-size distributions (discussed in 3.2). The first method is based on the distribution statistics and the second simply on average counting rates. Two different results are obtained and detailed in Table 2.3. The methods are outlined below.

METHOD 1

Theoretical and experimental investigations have shown (*39*) that the numbers of drops in each size interval in a given volume will be

distributed according to the Poisson distribution. Assuming that all drops are equally likely to be missed, then it is possible to estimate the effects of coincidence counting when 2 or more drops arrive at the sensor within the response time of the system.

If N drops arrive at the sensor in 1 minute the average number of drops arriving during the response interval (0.013 secs.) is:

$$\bar{N}_t = \frac{0.013 \times N}{60}$$

$$\bar{N}_t \doteq 2.2 \times 10^{-4}.N \text{ drops.}$$

The probability that at least two drops will arrive before the system has recovered is given by:

$$P(x \geq 2) = 1 - (P(o) + P(1))$$

where P(x) is the probability of x drops arriving.

Hence $P(x \geq 2) = 1 - (e^{-\bar{N}t} + \bar{N}_t e^{-\bar{N}t})$

If N = 1000 (a number which would be appropriate for a rainfall rate of about 9-10 mm hr^{-1} - see Table 2.3), then

$$P(x \geq 2) = 1 - (e^{-0.22} + 0.22\, e^{-0.22})$$

$$\doteq 0.02$$

Therefore in 2 out of every 100 periods of 0.013 secs. coincidence may occur and at least one drop could be lost.

There are $\frac{60}{0.013} \doteq 4615$ periods of 0.013 secs. in one minute.

Hence 4615 x 0.02 = 92.3 drops may be missed.

This calculation was repeated for each of the first 8 ranges of rainfall rates for which average raindrop-size distributions were deduced. The results appear in Table 2.3. As expected, at the lower rainfall rates (when N is small) the numbers of impacts missed are small. As R increases more drops are missed, rising from about 3% of the observed impacts at rainfall rates about 1 mm hr^{-1} to 10% in the highest category.

To quantify the effect of these losses in terms of the integral parameters R, Z and W, it was assumed that the drops missed would be distributed in the same proportions as the drops observed. Then by re-forming the spectrum using the calculation described in 2.4.2 it was possible to compute the contributions to R, Z and W by using equations (vi), (viii) and (iii). These results are given in Table 2.3; again the losses are small in both absolute and percentage terms at first but increasing as the precipitation becomes heavier.

METHOD 2

An alternative method was investigated by considering the average counting rate and deducing the amount of "dead time" during which it was assumed that drops would be arriving at the same rate and therefore being missed.

Average counting rate = $\frac{N}{60}$ impacts per second.

Dead time per second = $\frac{N}{60} \times 0.013$ sec.

Drops lost per minute = $\frac{N}{60} \times 0.013 \times \frac{N}{60} \times 60$

$$\doteq 2.2 \times 10^{-4} N^2.$$

If N = 1000, as in the example above, then 220 drops would be lost.

The results of this calculation for each rainfall rate are given in Table 2.3 and are seen to be approximately twice the size of the numbers for method 1. The contributions to R, Z and W are also larger.

The effect of these losses in relation to the rainfall total may be deduced by calculating the amount represented by all the observed average raindrop-size distributions (given by the product of the number of spectra in each category and the average rainfall rate divided by 60 - see 3.2.2). Thus the losses by methods 1 and 2 represent 4.5% and 9.5% of the rainfall total, respectively. This difference is partly due to method 1 only predicting co-incidence and the loss of at least one drop. Method 2 offers a more comprehensive solution, based on average counting rates, and should include all the drops missed. These results may be regarded as the upper and lower limits of the loss due to this factor.

When the distrometer data are compared with raingauge records (3.1.1) it is shown that the distrometer over-reads by a few percent overall (a result in agreement with other published results (*16*)). Therefore no correction procedure for coincident passages was devised. The application of such a correction would also render the present results less comparable with those published by other workers who have apparently without exception regarded this source of error as unimportant.

Insplash to sensor from surroundings

Raindrops which land in the vicinity and break up may cause impacts on the sensor leading to erroneous results due to the counting of splash

Rainfall rates about: ($mm\ hr^{-1}$)	Number of spectra	Number of spectra as a percentage of all spectra (17655)	Number of impacts	Impacts missed		Contribution to:						Mean rainfall rate of average distribution ($mm\ hr^{-1}$)	Rainfall total (mm)	Contribution of impacts missed to rainfall total (mm)	
						R $mm\ hr^{-1}$		Z $mm^6\ m^{-3}$		W $mm^3\ m^{-3}$					
				Method 1	Method 2	Method 1	Method 2	Method 1	Method 2	Method 1	Method 2			Method 1	Method 2
1.0	3968	22.5	275	8	16	0.030	0.060	11	23	2	4	0.90	59.52	1.98	3.97
2.0	1374	7.8	381	14	31	0.086	0.178	40	83	5	11	1.93	44.20	1.97	4.08
3.0	500	2.8	460	21	46	0.152	0.326	83	179	9	17	2.91	24.25	1.27	2.72
4.0	160	0.91	525	28	60	0.214	0.465	112	244	12	26	3.89	10.37	0.57	1.24
5.0	58	0.33	551	30	66	0.314	0.682	271	589	16	35	4.90	4.74	0.30	0.66
6.5	39	0.22	673	45	98	0.469	1.031	367	808	25	54	6.31	4.10	0.30	0.67
8.5	26	0.15	868	72	163	0.692	1.566	390	881	38	85	8.24	3.57	0.30	0.70
10.5	10	0.06	1153	122	288	1.101	2.640	742	1782	56	140	10.21	11.70	0.18	0.44
												TOTAL	152.45	6.87	14.48
														4.5%	9.5%

Table 2.3 The effects of coincidence counting

products as well as direct raindrop impacts. It has been shown (4) that large raindrops may produce a large number of splash drops which may rise to a height of some 65 cm. This effect varies with drop size and the surface onto which the drops fall. Drops smaller than 2.5 mm produce very few splashes.

To reduce the effects of insplash the transducer must be surrounded by a suitable absorbing surface. In the present experiment a plastic grid was used (see 2.1.3). Most of the raindrops landing in the vicinity of the sensor will fall through the grid into either the instrument pit or grass and those which strike the mesh will find a cutting edge which will severely disrupt them and reduce the chance of splash products reaching the sensor.

Splash products formed on sensor

Raindrops which land on the sensor may form splash products which will fall back onto the sensor and be counted again in a lower channel. MASON and ANDREWS (4) have shown that the number of splash drops and the height to which they rise decrease considerably as the drop size decreases and also many fewer splash drops are produced from a dry surface than from the same surface when it is wet.

This source of error may be minimised by ensuring that the sensor stays dry - hence a non-absorbent convex surface from which the water drains rapidly. Only splash drops with a near vertical trajectory are likely to fall back onto the sensor. In the present data, few very large drops were measured, reducing still further the chance of large errors due to this factor.

Timing errors

The chronology of the data relies on the accuracy and continuous operation of the crystal-controlled clock which produces a signal pulse every minute. The minute count from each paper tape was compared with the elapsed time between the start and finish times entered on the log sheets at the instrument site. In many cases an exact agreement was obtained although sometimes there was a discrepancy of a few minutes which was perhaps due to an observational error in the log.

More serious discrepancies occur on four paper tapes when the clock stopped (notably PT25, see Table 2.6) due to an instrument or power failure. By careful editing these discrepancies were removed although this was not possible in the case of PT25. Hence the times on PT's 25 and 26 are suspect.

Where these data are compared with autographic raingauge and anemograph records, there exists the further possibility of timing discrepancies due to errors in those instruments. These factors are discussed in 3.1.1. The accuracy of the clock was checked by comparison with an independent time reference and a wholly acceptable agreement was found.

2.2.4 Effects of noise

The signal produced by a raindrop striking the transducer is a distinct 0.5 ms pulse. The signal recognition circuit in the processor can distinguish between these signals and the more uniform oscillations caused by acoustic noise. For raindrops to be counted in a noisy situation it is necessary for the amplitudes of these pulses to exceed those of the oscillations caused by acoustic noise.

The distrometer site at RAF St. Mawgan is generally very quiet with infrequent bursts of noise at a high level when aircraft take off and land or taxi nearby. Observations have indicated that these high levels of noise occur for only a few seconds at a time and total only a few minutes per day. It was thought improper to request or compile a detailed log of aircraft movements at the Base.

The equipment was observed in operation during both dry conditions and when precipitation was being recorded to assess the effects of aircraft noise. It was noted that these high levels of noise did not produce any signals when it was not raining, showing that the noise limiter in the processor was working satisfactorily. During rainfall the smaller drops were not recorded when an aircraft used the runway and therefore some small drops were lost from the record. This interruption usually lasted for 10 seconds or less.

Since these interfering noises occupy only a very small proportion of the time and do not necessarily occur during rainfall, they are unlikely to cause the loss of such a large number of drops that the record of many thousands of minutes will be noticeably affected. However, any analysis that examines individual minutes must be scrutinized carefully to ensure that any unrepresentative distributions polluted by noise are eliminated. Under conditions of a high background sound level the recording of small drops will be eliminated. Such a situation occurred during the GATE experiment when a Joss distrometer was operated on the ship "RESEARCHER", as reported by CUNNING and SAX (*40*). In the presence of continuous generator and motor noise all drop sizes less than 1 mm were eliminated and the number of drops in the 1-2 mm range was greatly reduced. The authors devised a technique to overcome this problem by extrapolating a best-fit curve to the distribution of drop sizes, not affected by the noise problem, back to small drop diameters

in a consistent manner. This resulted in a better agreement between distrometer-derived rainfall and gauge catches as shown in Table 2.4. The results of this comparison for the present experiment are discussed in 3.1.1 and are appreciably better than even the corrected values in the GATE experiment; this suggests that a similar procedure for the present data would be unnecessary.

At the beginning of the experiment it was noted that occasional signals were generated by the equipment when no precipitation was evident. To ensure that these signals were not generated by foreign objects being blown onto the transducer or by wind turbulence deflecting the sensor, the distrometer and surround were covered with a metal lid. The occasional signals were still observed, but they were very infrequent and at a low level (i.e. mainly in Channels 1 & 2). They were attributed to local electrical interference from the large amount of electronic equipment and switchgear in the Control Tower building in which the distrometer hardware was situated.

Several hours of operation without precipitation on PT3 were examined to determine a level at which to reject minutes with few impacts as being due to these spurious interfering signals. Failure to do so would result in the records containing these signals alone being written to the main body of data and wasting storage space.

By far the worst case of interference in this period was when 6 frames occurred between timemarks as detailed in Table 2.5. Even this level of noise represents an insignificant contribution to rainfall rate, although the contribution to the N_D value is noticeable. It must be emphasised that the example under consideration is an extreme case - normally the interference consisted of a solitary signal in Channel 1

6 minute averages, July 8 1974 - Researcher			
Time	Siphon Gauge (mm)	Distrometer	
		Uncorrected	Corrected
1745-51	6.2	3.5	4.6
1751-57	10.9	6.7	12.0
1757-1803	9.3	5.1	7.8
1803-09	7.6	3.0	6.3
1809-15	6.7	1.7	2.4
1815-21	3.9	1.0	1.4
1821-27	7.3	2.6	4.5
1827-33	6.4	2.1	3.3
TOTAL	53.8	24.7	42.3

Table 2.4 Comparison of distrometer-derived rainfall with that from siphon gauge on board "Researcher" (*40*)

CHANNEL	No.	N_D	R mm hr^{-1}	% total R
1	1	24.0	0.0003	4
2	4	72.5	0.0024	32
6	1	4.6	0.0048	64
TOTAL	6	101.1	0.0075	100

Table 2.5 Example of signals recorded during a dry period on PT3.

or 2 (this was the only example of a signal in Channel 6). If this noise is also present during rainfall then it must be expected that the N_D values for Channels 1 or 2 may be incremented occasionally.

There was no convenient method of separating the electrical noise from the record and therefore it was decided to reject all minutes when 6 signals or less were recorded in one minute. This task was carried out by RAINSPECTRA (see 2.4.2). Despite this procedure a small number of records were still produced during dry periods but again the interference was at a very low level representing rainfall rates of a few thousandths of a millimetre per hour. These could be eliminated when analysing large portions of data (e.g. to calculate Z-R relationships) by using only minutes with rainfall rates > 0.1 mm hr^{-1}. (0.1 mm is the smallest quantifiable amount of precipitation measured on a conventional raingauge.)

2.2.5 Calibration

The distrometer was received directly from a manufacturer's overhaul when the calibration of the transducer against the processor had been carried out. It remained only to check the calibration of the pulse height analyser.

This calibration check was carried out in accordance with the directions given in the manufacturer's manual (*41*). It was found that the analyser was correctly calibrated and no adjustment was necessary. The opportunity was taken to connect the paper tape punch and verify the codes given in Table 2.7.

2.3 ORGANIZATION OF DATA

2.3.1 Paper tape retrieval

At the start of the experiment it was not known exactly how many data would be collected. Observation was expected to last for some months which would require the archiving of at least 10^5 minutes of records. Clearly in an exercise of this magnitude it is essential to organize the data properly.

When the instrument was previously operated by the Meteorological Office, the exercise was served by a small team of personnel, both on site and elsewhere, to collect, compute and archive the data. The author was faced with the task of developing software from first principles and installing and operating the equipment at a remote station. Thus the paper tape retrieval organization had to be both simple and flexible to make the experiment feasible. It had to be accepted that gaps might occur in the observations and that in any event, a considerable amount of travelling was inevitable.

Ideally the distrometer system should have a dedicated on-site operator to switch on the equipment at the onset of precipitation and log all the necessary details, switching off at the end of the rainfall event. This ensures that no precipitation is missed and the records consist almost entirely of the data of interest - raindrop-size distributions. RAF St. Mawgan has a very busy operational Meteorological Office and it was determined that the most suitable method of observation was to leave the instrument running continuously and to change the paper tape only when it ran out; if at all possible changing the tape during rainfall was to be avoided. The author would then travel to the station at approximately 3 week intervals to collect completed tapes, log sheet and station data and also to check the equipment.

Although previously mentioned in the Acknowledgements, the author records again, in this context, the excellent co-operation of the Meteorological Office staff at RAF St. Mawgan in playing their part in this programme. The instructions left on site are included in Appendix II. When the author visited the site the staff were informed of progress in the experiment, the station records were made available and much useful advice and discussion offered.

Having already developed the software in principle, using dummy data, it had been decided that ten blank frames would be necessary at the start and finish of the paper tape record. Hence the requirement to run out tape at the start and finish, and to avoid switching off in the middle. Also when the ancillary devices (processor, analyser and timer) were switched on, some spurious signals were always punched on the tape and these had to be eliminated from the record. This method of creating clean run-out was simpler and more flexible than punching and splicing special header sequences, and, in general, it worked well throughout the experiment.

Having collected the paper tapes from the instrument site it was necessary to check that the blank frames were present at the end of the record, rewind the tape and check the starting frames. The tape was then ready for reading and it was considered essential that the record should be duplicated for security reasons so that if any data became corrupted it would be possible to recreate the original record. Each minute of data required the storing of 25 integer variables (see 2.4.1) and this applied even during periods of no rain. Hence for 10^5 records, storage space for 2.5×10^6 values was required. The only practicable facilities for storing such a mass of data were magnetic tapes or discs. The flexibility and simplicity of magnetic tape data files was chosen and this is described in the next section.

It was desirable that there should be a facility for examining the paper tape record for errors at an early stage in processing and the minutes suspected of containing errors to be printed out on reading the tape, together with a summary of the data. This led to the development of a three-level data-processing system as depicted in Figure 2.7.

Table 2.6 contains a summary of the 32 paper tapes used in this analysis. Only 17655 distributions are used due to discrepancies in tapes 25 and 26 as explained in the table. It can be seen that in the 131127 minutes (~91 days) of the experiment, 116615 minutes were recorded (89%) and 17821 were during rainfall (15%).

2.3.2 Magnetic tape archives

The paper tapes were read by the package RAINDROPS (described in some detail in 2.4.1) and the data written to a generation of magnetic tapes called ECCRAIN. On reading each new paper tape, the previous magnetic tape record was re-written to a scratch tape and the new data added. This ensured further duplication in the event of data becoming corrupted during processing. The data were split into three portions to economise on computer time in this copying process. All data then appeared on three tapes:

ECCRAIN	11*	PT 1 - 12
ECCRAIN	25	PT 13 - 25
ECCRAIN	37	PT 26 - 32

* file generation number

On reading each paper tape a summary and error profile was output to the line printer and a sample of this is included in Appendix III.

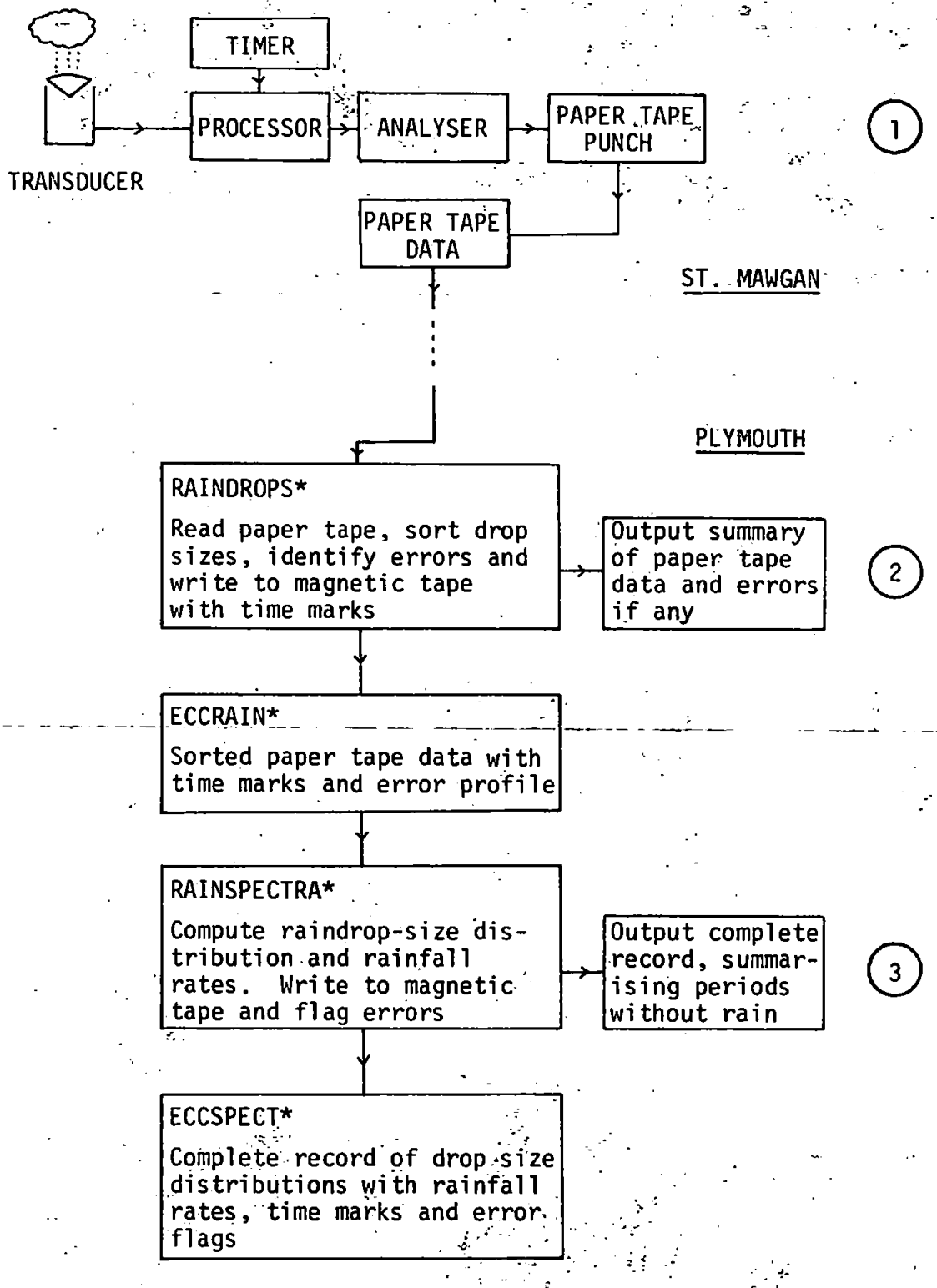

Figure 2.7 Three-level data-processing system for distrometer experiment

* RAINDROPS and RAINSPECTRA are the identifications of computer jobs. ECCRAIN and ECCSPECT are magnetic tape files.

PT No.	MINUTES START	MINUTES FINISH	MINUTES TOTAL	MINUTES RAINFALL	MINUTES ERRORS
1	1	2870	2870	894	3
2	2884	(3653)	769	694	0
3	3845	5603	1758	251	0
4	5608	6524	916	459	1
5	6560	7859	1299	545	0
6	7876	10907	3031	367	1
7	11596	13783	2187	768	0
8	13982	16169	2187	597	0
9	16180	22319	6139	577	0
10	22448	29363	6915	595	0
11	29418	(31004)	1586	814	0
12	31410	(34834)	3424	693	0
13	37936	38880	944	415	0
14	38944	39951	1007	502	2
15	39960	(42456)	2496	387	1
16	42546	(46346)	3890	623	0
17	46504	49134	2630	506	1
18	49143	49953	810	598	0
19	51040	(51590)	550	549	1
20	52115	(55502)	3387	442	0
21	55623	55883	260	90	0
22	55902	57105	1203	571	0
23	57643	69341	11698	475	0
24	69342	71625	2383	503	6
25	*76290	82060	5770	413	0
26	*82061	(83872)	1811	627	0
27	85217	91078	5861	414	0
28	91155	98349	7194	1323	0
29	98528	101903	3375	287	0
30	101930	105308	3378	604	0
31	105541	115013	9472	727	1
32	115712	131127	15415	511	1
TOTALS	--	--	116615	17821	18

Table 2.6 Summary of paper tape records

Times are given in minutes from 1600 GMT 20 FEB 1978.

Times in brackets were recreated from paper tape record when tape ran out unnoticed and no accurate finish time was logged.

* Approximately 166 minutes more data appeared on PT25 than was expected. This has been eliminated from the magnetic tape file. Hence the times for tapes 25 and 26 are suspect.

This generation of tapes was read at intervals to compute raindrop-size distributions and carry out preliminary analysis. In view of the small number of errors encountered in the data, editing was carried out at a later stage. These tapes were read, using the same duplicating procedure described above and under control of RAINSPECTRA (described in detail in 2.4.2) and a generation of tapes ECCSPECT resulted:

ECCSPECT	3	MINS 1 - 34834
ECCSPECT	6	MINS 37936 - 81818
ECCSPECT	8	MINS 81819 - 130870

RAINSPECTRA also output a line printer record of distributions and rainfall rates with minutes containing errors flagged. A sample of this output is included in Appendix III.

These three tapes were read onto a single tape:

ECCSPECT	12	MINS 1 - 130870

and at this stage minutes with a serious error profile (3 in all) were eliminated. The errors shown on PT14 in Appendix III were not considered serious enough to warrant exclusion.

2.4 ANALYSIS OF DATA

2.4.1 Reading the paper tapes

As described earlier, the paper tape record contained a series of coded frames giving information on raindrop impacts with a time mark each minute. The paper tape code was supplied with the equipment (table 2.7) and this was used as the basis to develop RAINDROPS, a package to read the paper tapes.

As seen in the table there are 23 codes in the set but in fact 25 possible frames had to be allowed for. In addition to the 20 channels, time marks and reference marks it was possible that a blank frame might occur (other than at the start and finish of the record) or a spurious code might be punched which was not in the character set.

A further complication was that the code is a non-standard, 6-track code and therefore a binary-imaging technique had to be employed to read it. To decode a frame the holes must be converted to their binary image and then fed to a program to sort them as required. This technique requires a level of computer peripheral control not available in a FORTRAN program. Hence a PLAN program (TPRD) which had been developed elsewhere in Plymouth Polytechnic, to read tapes from a remote weather station, was obtained and adapted by compiling it as a segment of RAINDROPS.

This program segment was called as a subroutine from the FORTRAN master segment (SORT) to supply the binary images of the coded frames in groups of ten. It was required that the FORTRAN segments should:-

1 Copy previous data from input magnetic tape to a scratch tape

2 Call TPRD to supply binary images

3 Recognise time marks and increment time reference

Channel No.	Tracks						Binary Eq.	Remarks
	1	2	3	4	5	6		
1		O				O	34	0.3 - 0.4 mm
2	O	O					3	0.4 - 0.5 mm
3			O			O	36	0.5 - 0.6 mm
4	O		O				5	0.6 - 0.7 mm
5		O	O				6	0.7 - 0.8 mm
6	O	O	O			O	39	0.8 - 1.0 mm
7				O		O	40	1.0 - 1.2 mm
8	O			O			9	1.2 - 1.4 mm
9		O		O			10	1.4 - 1.6 mm
10	O	O		O		O	43	1.6 - 1.8 mm
11			O	O			12	1.8 - 2.1 mm
12	O		O	O		O	45	2.1 - 2.4 mm
13		O	O	O		O	46	2.4 - 2.7 mm
14		O	O	O	O		30	2.7 - 3.0 mm
15					O	O	48	3.0 - 3.3 mm
16	O				O		17	3.3 - 3.7 mm
17		O			O		18	3.7 - 4.1 mm
18	O	O			O	O	51	4.1 - 4.5 mm
19			O		O		20	4.5 - 5.0 mm
20	O		O		O	O	53	5.0 -(5.4)mm*
Aux 1	O	O	O		O		23	Above Reference **
Aux 2	O					O	33	Below Reference **
Aux 3	O	O	O	O	O	O	63	Time mark

Table 2.7 Distrometer paper tape code

O = Hole

* Channel 20 counts all drops over 5.0 mm diameter, however for calculation purposes it is necessary to set an upper limit to the class. This was chosen arbitrarily to be 5.4 mm.

** These codes are generated when the voltage comparators in the hardware determine that the equipment is not operating within its designed tolerances. Only 4 such occurrences were found in the present data.

4 Sort the frames between time marks into drop sizes or errors and increment a counter for each channel

5 Write new data to scratch tape

6 Write end-of-file mark on scratch tape

7 Output to line printer a summary of data and minutes containing errors.

The program listing is included in Appendix III. The input to each run consisted of the previous ECCRAIN tapes and the paper tape to be read. 4 cards were changed, namely the INPUT and CREATE statements in the Program Description and the tape number and starting time in the master segment. The paper tape was read on line with the binary image board in place on the paper tape reader. The program was run without using the TRACE mode, thus reducing the mill time on these jobs which was usually several thousand seconds.

Early tests on the data using unformatted magnetic tape records proved to be impractical due to the large amount of tape written. Hence a formatted data file was developed to make best use of storage space. All 25 values in each record are integers which occupy one word under 'A' format; thus records were written in blocks of 2502 words which gave 100 records per block with two words for control.

2.4.2 Computing the raindrop-size distribution

The ECCRAIN tapes contain the numbers of impacts at the distrometer; this is not a convenient form to describe the drop-size distribution, especially if comparison with the results of other workers is required. These data are for a particular sampling area and sampling interval. It is desirable to standardize the results to numbers of drops per unit volume per unit size interval (as described in 1.1.1).

To obtain N_D (the number of drops per cubic metre per millimetre), the equation:

$$N_{D_i} = n_{D_i}/(A.V_{D_i}.t.(D_{i+1} - D_i))m^{-3}.mm^{-1}$$

was used where:

i = distrometer channel no. ($1 \leq i \leq 20$)

N_{D_i} = number of drops in channel i

n_{D_i} = number of impacts observed in channel i in t secs. (t = 60)

A = area of transducer head (0.005 m^2)

V_{D_i} = terminal velocity of drops in channel i

D_{i+1}, D_i = upper and lower limits of measuring interval.

This equation takes account of the varying class intervals for each channel ($D_{i+1} - D_i$). The values for the terminal velocities of the drops are those used widely by other authors (e.g. *12*, *13*) and are given in Table 2.8.

To obtain rainfall rate (R) the following equation was used:

$$R = \frac{\text{Period}}{\text{Area}} \sum_{i=1}^{20} n_{D_i} \frac{4}{3}\pi\frac{1}{2}\left(\frac{D_i^3}{2} + \frac{D_{i+1}^3}{2}\right) \text{mm hr}^{-1}$$

which reduces to:

$$R = \frac{\pi}{10^3} \sum_{i=1}^{20} n_{D_i} (D_i^3 + D_{i+1}^3) \text{ mm hr}^{-1}$$

where: Period = 60 mins

Area = 5000 mm^2

The distrometer observations were converted to raindrop-size distributions in the desired form under control of RAINSPECTRA. The requirements of this package were:

Channel No.	Mean diameter	Velocity $m.sec^{-1}$
1	0.35	1.40
2	0.45	1.84
3	0.55	2.26
4	0.65	2.67
5	0.75	3.07
6	0.90	3.65
7	1.10	4.33
8	1.30	4.90
9	1.50	5.41
10	1.70	5.87
11	1.95	6.40
12	2.25	6.98
13	2.55	7.48
14	2.85	7.88
15	3.15	8.21
16	3.50	8.50
17	3.90	8.77
18	4.30	8.95
19	4.75	9.05
20	5.20	9.12

Table 2.8 Terminal velocity of raindrops (*42*)

1 Copy previous data from input magnetic tape to a scratch tape, if required.

2 Eliminate observations with less than seven impacts (see 2.2.4).

3 Summarize all other periods without precipitation and output on line printer record.

4 Compute raindrop-size distribution and rainfall rate for minutes when precipitation was observed and output on line printer record, with minutes containing errors flagged (1 = error, 0 = no errors).

5 Write new data to scratch tape in compact form.

6 Write end-of-file mark on scratch tape.

The program listing is given in Appendix III. The input to each run consisted of an ECCRAIN tape and, if required, the previous ECCSPECT tape. The INPUT and CREATE statements were altered to the appropriate tape generation numbers. The input data is first scrutinized by the master segment (DROP) and then, if required, control is transferred to a subroutine (SPECR) to compute the raindrop-size distribution and rainfall rate and write to magnetic tape data file.

In view of the large amount of data to be written, careful consideration was given to the format of the ECCSPECT tapes to economise on space. Each observation consisted of 23 values, 2 integers and 23 real numbers. The 20 real numbers comprising the N_D values were written as integers by converting them to $10^3 \times \log_{10} N_D$, preserving the desired accuracy and using only half the space that would be required for real numbers. These data were written to the line printer as logarithms to 2 decimal places, a form that was convenient for any further off-line processing.

The rainfall rates were first multiplied by 10^3 before writing to the magnetic tape as integers but are printed as real numbers on the line printer. As with the ECCRAIN tapes the blocks contained 100 records, giving a block length of 2302 words.

2.4.3 Computing the integral parameters

In 1.2 the integration of the spectrum of raindrop sizes was discussed. Three integral parameters are identified as being of particular interest and the equations used to compute them in the various programs are given below:

$$\text{Rainfall Rate } (R) = \frac{3.6\pi}{6000} \sum_{i=1}^{20} N_{D_i} . V_{D_i} . \tfrac{1}{2} (D_i^3 + D_{i+1}^3).(D_{i+1} - D_i) \text{ mm hr}^{-1}$$

(Except in RAINSPECTRA, see 2.4.2).

$$\text{Liquid water content } (W) = \frac{\pi}{6} \sum_{i=1}^{20} N_{D_i} . \tfrac{1}{2} (D_i^3 + D_{i+1}^3).(D_{i+1} - D_i) \text{ mm}^3$$

$$\text{Radar reflectivity factor } (Z) = \sum_{i=1}^{20} N_{D_i} . \tfrac{1}{2} (D_i^6 + D_{i+1}^6).(D_{i+1} - D_i) \text{ mm}^6 \text{ m}^{-3}$$

The programs used data sets for V_{D_i} (given in Table 2.6), D_i (the class limits for the diameters, 21 values 0.3 - 5.4 mm) and N_{D_i} read from the magnetic tapes.

CHAPTER THREE

EXPERIMENTAL RESULTS

3.1 CHECKING THE ACCURACY OF THE DISTROMETER

3.1.1 Comparison with syphon gauge readings

It is desirable to have an independent check of the distrometer observations and this may be achieved to a first approximation by comparing the distributions integrated for rainfall amount with raingauge readings.

Autographic syphon raingauge totals for all the whole hours of precipitation within the distrometer record were abstracted from the appropriate copies of Metform 3440, tabulated at the Meteorological Office, RAF St. Mawgan. This form records, for each hour of the day, the number of tenths of that hour when the rainfall rate exceeded 0.1 mm hr^{-1}. To ensure a reliable comparison only whole hours of continuous precipitation were used. Thus the data are for non-showery type rainfall, although there is no reason to suppose that the distrometer should perform any less accurately than a gauge during showers. This allowed 79 hours of data for comparison, comprising 4740 distributions or about 27% of all the data.

The distrometer hourly rainfall totals were computed by adding all the rainfall rate values for the appropriate minutes of the distrometer magtape record (ECCSPECT 12) and dividing by 60. These data, together with the relevant gauge totals, are detailed in Table 3.1.

Figure 3.1 compares the results and indicates the area between which the gauge records 80% of the distrometer total and 120%. Figure 3.2 shows the cumulative totals for gauge and distrometer over the 79 hours. The gauge total was 81.3 mm and the distrometer total was 83.86 mm. The results for Figure 3.2 are not sequential; three periods are identified in Figure 3.3, for a number of sequential hourly totals given in Table 3.2.

FROM (mins)	TO (mins)	GAUGE (mm)	DISTR. (mm)
121	180	0.1	0.10
181	240	0.1	0.01
2161	2220	1.2	1.49
2221	2280	1.7	1.91
2281	2340	2.3	2.07
2341	2400	0.7	0.72
3061	3120	1.5	1.40
3121	3180	0.2	0.42
3241	3300	0.7	0.88
3301	3360	0.6	0.77
3361	3420	0.4	0.50
3421	3480	1.6	1.36
3481	3540	1.0	1.18
3541	3600	0.8	1.08
6601	6660	3.0	2.72
6661	6720	1.1	1.15
7741	7800	0.7	0.72
14041	14100	0.7	0.74
14101	14160	0.5	0.60
14161	14220	0.5	0.67
14221	14280	0.5	0.54
15961	16020	0.9	1.18
16021	16079	1.6	1.76
16081	16140	2.6	2.94
39661	39720	1.2	0.80
39721	39780	0.8	0.52
39841	39900	0.6	1.45
39961	40020	2.2	1.93
40021	40080	2.6	2.54
48961	49020	0.9	1.12
49021	49080	2.2	1.98
49261	49320	0.6	0.34
49321	49380	0.5	0.51
49741	49800	1.4	0.73
51061	51120	1.0	1.22
51121	51180	1.7	1.58
51181	51240	2.0	2.17
51242	51300	0.9	1.07
51301	51360	0.2	0.39
51361	51420	0.6	1.06
51421	51480	1.5	0.80
51481	51540	0.2	0.47

FROM (mins)	TO (mins)	GAUGE (mm)	DISTR. (mm)
55321	55380	1.4	1.40
55381	55440	1.8	1.17
55441	55500	0.8	1.10
71161	71220	1.0	0.91
71221	71280	0.2	0.32
73981	74040	0.7	0.75
74041	74100	1.5	1.32
74101	74160	0.2	0.24
74161	74220	1.3	1.21
80941	81000	2.7	2.83
81001	81060	0.3	0.43
81541	81600	0.7	0.54
81601	81660	0.8	0.87
83461	83520	1.8	1.72
83521	83580	1.0	1.04
83581	83640	1.1	1.00
83641	83700	0.2	0.32
90781	90840	1.4	1.76
90941	90900	3.0	2.73
90901	90960	1.2	1.10
91861	91920	0.5	0.76
91021	91080	2.9	2.93
91081	91140	1.8	1.87
91141	91200	0.6	0.82
92641	92700	0.1	0.23
92701	92760	0.1	0.16
98461	98520	1.0	1.28
98521	98580	0.2	0.31
98581	98640	0.1	0.12
103081	103140	0.4	0.57
103141	103200	0.4	0.49
103201	103260	0.2	0.31
105301	105360	1.0	1.28
110581	110640	1.3	1.20
110641	110700	0.4	0.17
110761	110820	0.5	0.51
110821	110880	0.6	0.50
TOTAL	79 hours	81.3	83.86

Table 3.1 Gauge and distrometer hourly totals

The 1st data set comprises 17655 spectra representing a total rainfall of 186.8 mm.

The data above represent 27% of all records and 45% of the measured rainfall.

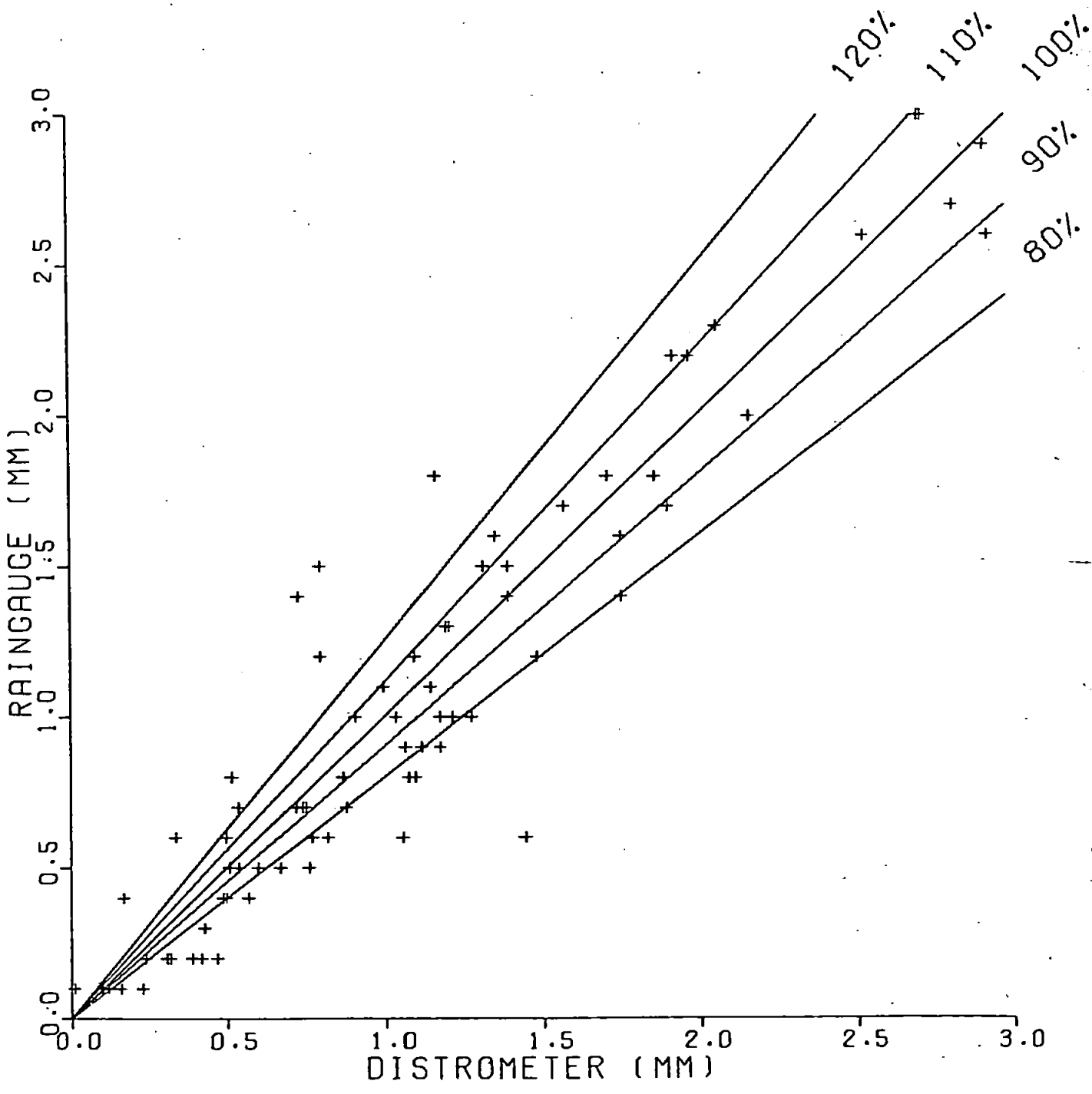

Figure 3.1 Comparison of gauge and distrometer hourly catches

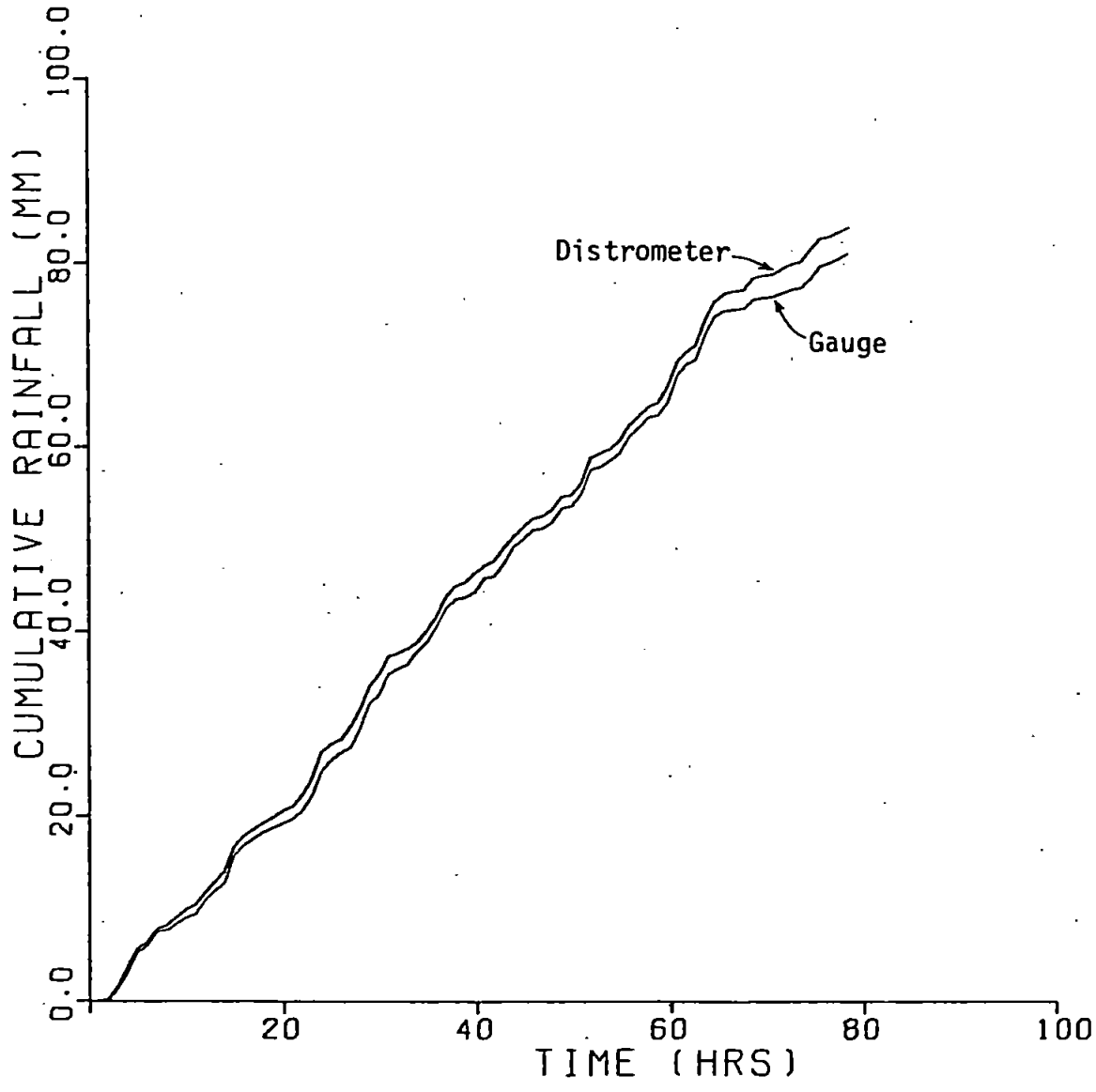

Figure 3.2 Comparison of gauge and distrometer cumulative totals

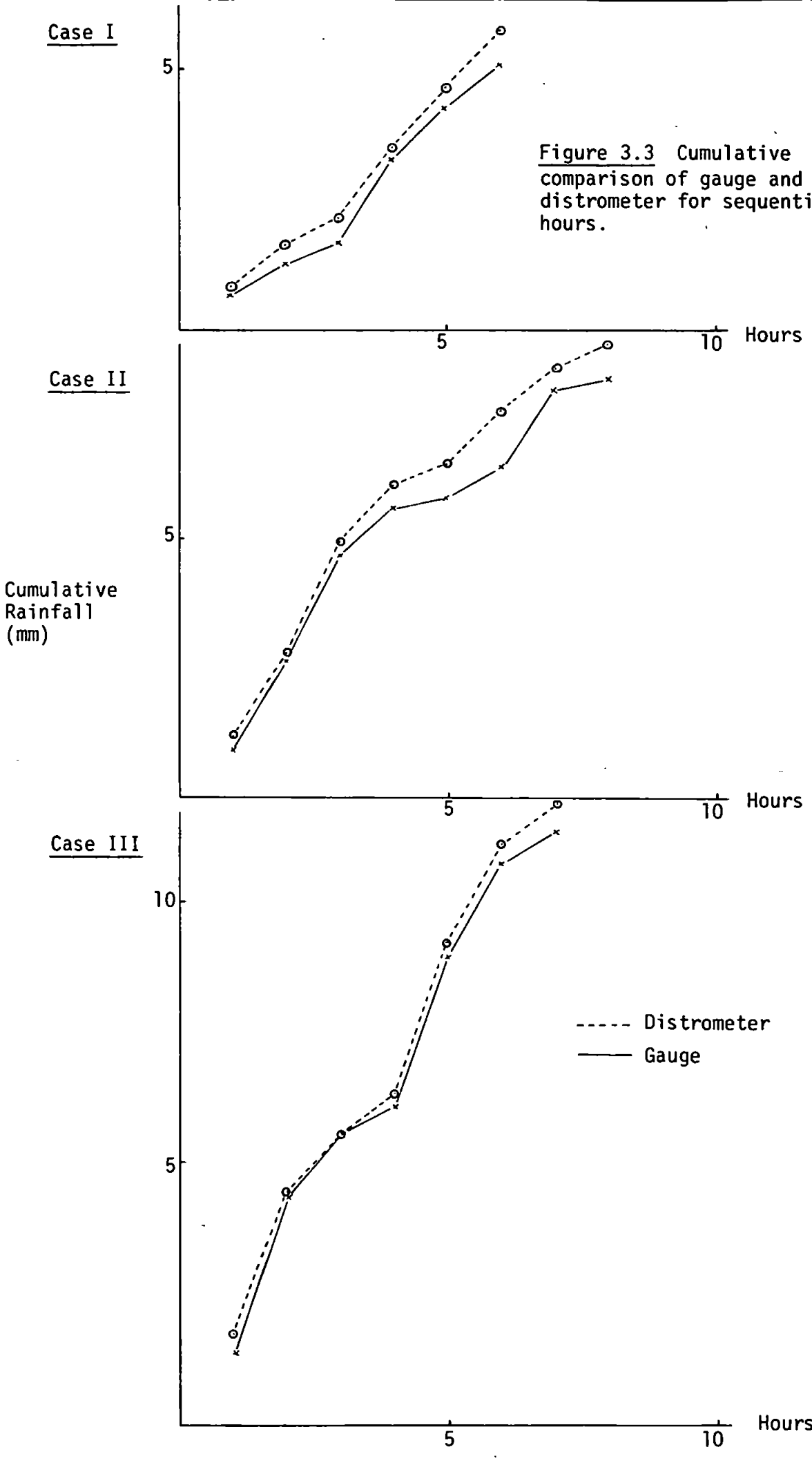

Figure 3.3 Cumulative comparison of gauge and distrometer for sequential hours.

		Cumulative Totals (mm)	
		Gauge	Distrometer
Case I	22/23 FEB 2300-0400 Mins. 3301 - 3600	5.1	5.77
Case II	28 MAR 0400-1100 Mins. 51061 - 51540	8.1	8.76
Case III	24 APR 1800-2400 Mins. 92641 - 91200	11.4	11.97

Table 3.2 Details of sequential hourly totals shown in Figure 3.3.

Year	Gauge	Distrometer	Hours of data	$\frac{\text{Gauge}}{\text{Distr.}} \times 100$
1972	104.0	119.1	1580	87.3%
1973	145.6	154.6	2256	94.2%
1974	93.6	82.2	1275	113.9%
TOTAL	343.2	355.9	5111	96.4%

Table 3.3 Rainfall measured by gauge and distrometer
After NICHOLASS and LARKE (*16*).

All these results demonstrate that the distrometer records more rainfall than the autographic gauge. The gauge total is 96.9% of the distrometer total. This result has been reported before; for example NICHOLASS and LARKE (*16*) gave results for the comparison between a Plessey MM 37 tipping-bucket gauge and distrometer derived rainfall (Table 3.3). These data were obtained during summer rainfall in Wales and, taking the three years together, it is found that the gauge total is 96.4% of the distrometer total -- a result comparable to the present data. These authors conclude that although errors are likely with both the gauge and the distrometer, the measurements are sufficiently alike to assume that the distrometer correctly measures raindrop-size distributions.

There are several reasons for the differences; indeed the precipitation intercepted by the two devices should differ because they are both effectively point-measuring instruments and since they are at different locations, experiencing different exposures, they could only agree exactly when the rainfield was perfectly homogenous for a whole hour.

The syphon gauge operates on a completely different principle from the distrometer and the latter will continue recording whilst the gauge is syphoning. The distrometer will not suffer loss due to evaporation, although this loss is very small for a gauge. Other reasons for the distrometer recording too many drops have been discussed in 2.2.3. It is also well known that a gauge mounted with its rim at ground level will catch more than one mounted some distance above it. Figure 3.4 shows the variation in catch ratio for unshielded gauges compared with the sophisticated 9-hole gauge used as a standard by GREEN (*32*). At a height of 30 cm (the height of the syphon gauge at St. Mawgan) the catch ratio is about 0.96.

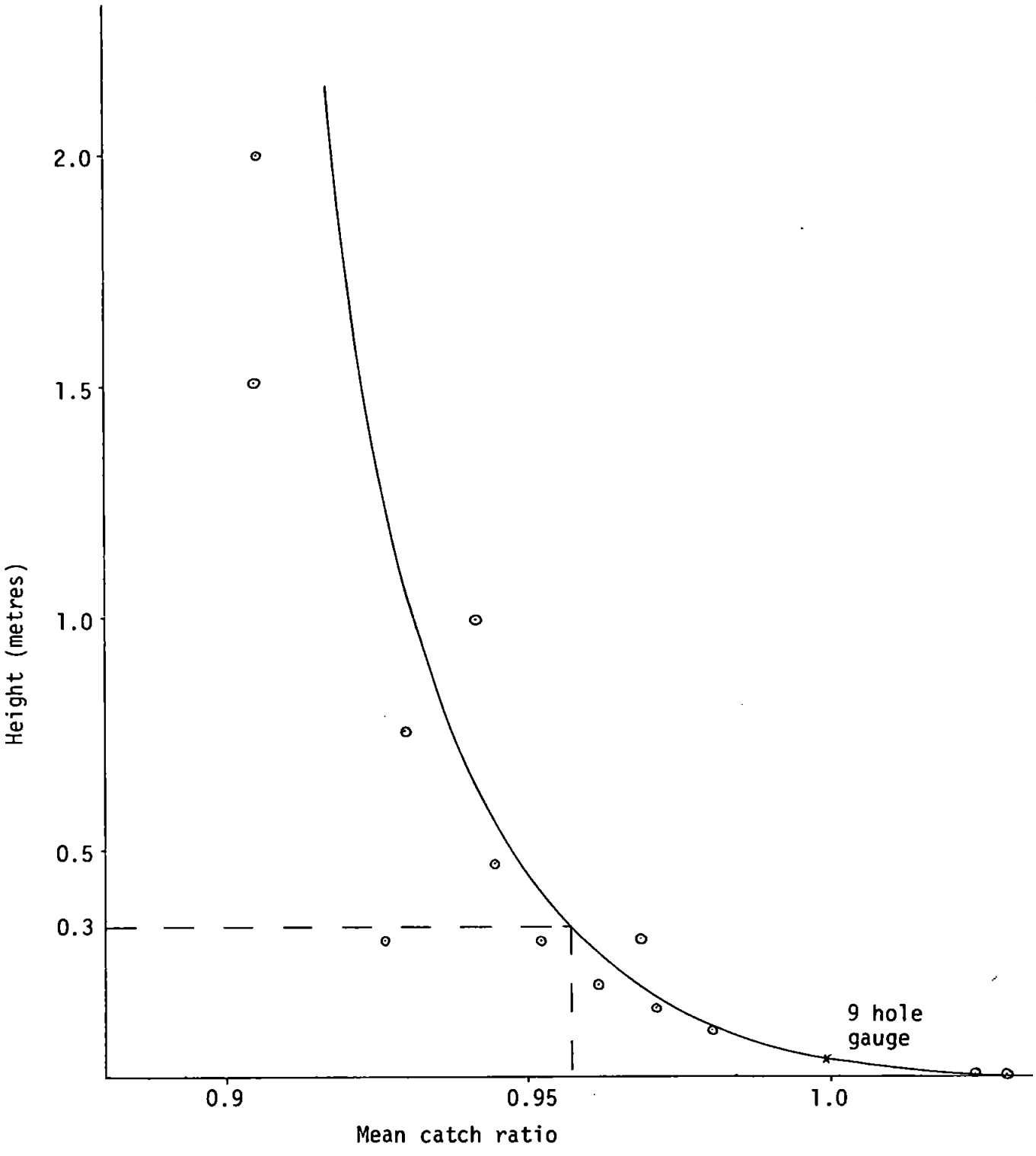

Figure 3.4 Comparison of catch ratios for 9 hole gauge and other unshielded gauges at various heights. After GREEN (*32*).

This is in fair agreement with the present data and suggests that most, if not all, of the difference is due to the variation in exposure as a function of vertical separation.

Autographic gauge readings are "adjusted" so that the 12-hourly totals agree with the station gauge measurements and this introduces the possibility of gross errors. Typically any difference between station gauge and syphon gauge totals is distributed as an addition to, or subtraction from, the largest hourly totals.

Gross errors due to timing are possible since different clocks are used as a timing standard and a discrepancy of even a few minutes, particularly in heavy rain, can lead to a significant discrepancy in hourly totals. Other inaccuracies may occur in the calibration of the distrometer and the interpolation of the hyetograms from the syphon gauge.

Thus the comparison between the gauge and distrometer is favourable; many of the data are within the tabulated accuracy of the autographic gauge (±0.1 mm) and the occasions when larger differences occur may be due to gross errors in timing or interpolation. Such errors do not affect the accuracy of the distrometer as a drop-size measuring device and it is reasonable to assume that the raindrop-size distributions produced are representative.

3.1.2 The effects of wind on the distrometer catch

As noted earlier, the performance of the distrometer in high wind velocities has been criticised (*35*). In order to investigate the effect of both wind direction and speed on distrometer catches, the

anemograph records at RAF St. Mawgan were abstracted for the same times as the gauge records discussed in the previous section. Hourly mean wind directions and speeds were compared with the distrometer-gauge differences for each of the 79 hours. The results of this comparison appear in Figures 3.5 and 3.6.

Maximum shelter is on a south-westerly bearing, notably from a post supporting the chain link fence, clearly visible in Plate 1. The data in Figure 3.5 show that this effect is not serious and the only systematic trend (apart from the general trend for the distrometer to over-read, as discussed in 3.1.1) is for a positive distrometer-gauge difference for winds in a northerly quadrant. However, these differences are very small, half of them being 0.1 mm or less.

The catch differences in relation to wind speed (Figure 3.6) also show little or no systematic variation, both positive and negative differences occurring throughout the range of wind velocities.

To investigate in more detail the effect of high wind velocities on results, some data collected during a three hour period when winds were relatively strong were compared to the data set as a whole. The period considered was from 0501 - 0800 on 22 FEB 1978 (mins. 2221 - 2400). The relevant catches and anemograph data are given in Table 3.4.

Figure 3.7 shows the meaned distribution for the whole data set for rainfall rates about 2 mm hr^{-1} (discussed in more detail in 3.2) and the distribution for the same range of rainfall rates from this subset of data. The former (Distribution A, solid line) is derived from 1374 distributions and the latter (Distribution B, broken line) from 77 distributions.

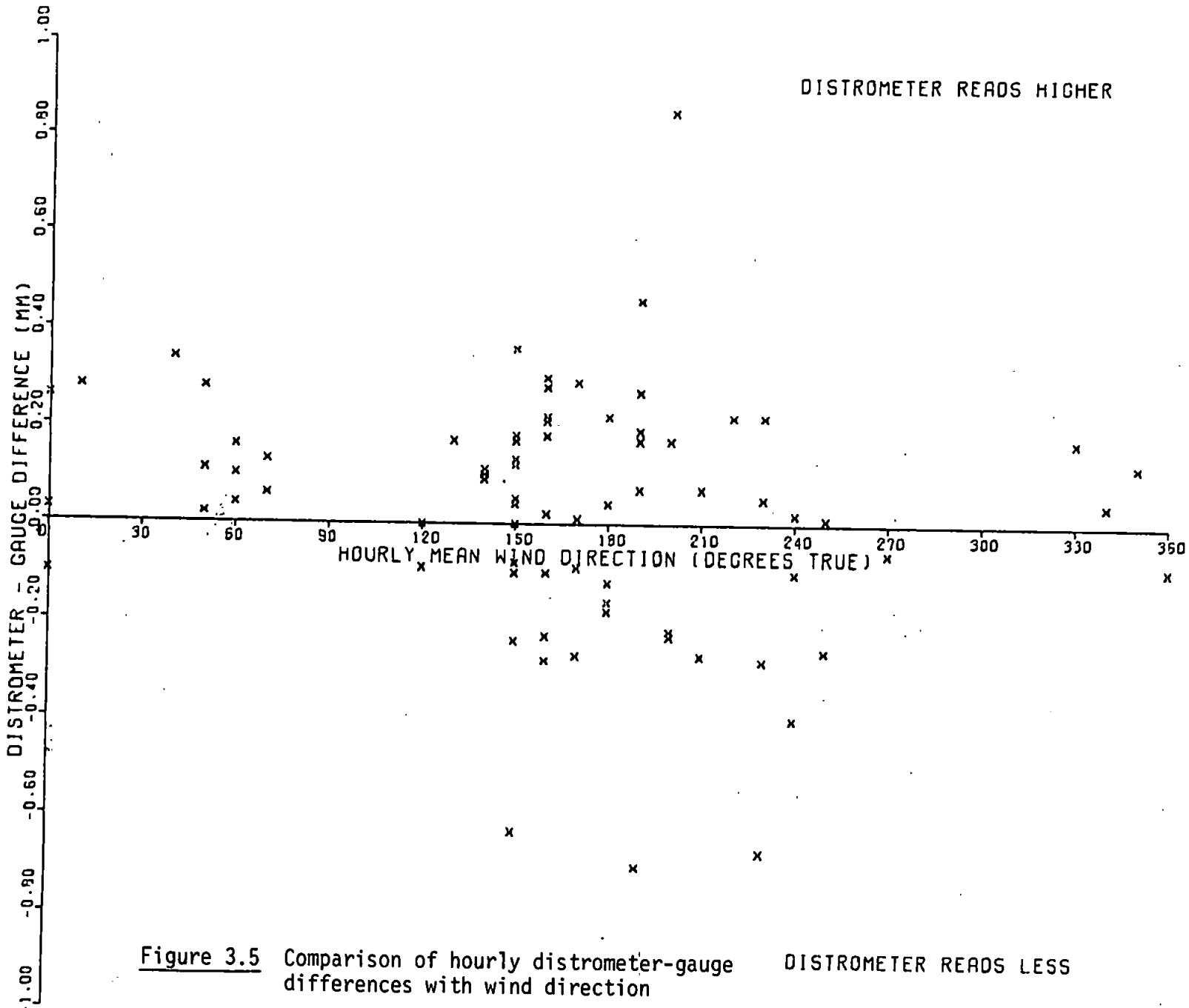

Figure 3.5 Comparison of hourly distrometer-gauge differences with wind direction

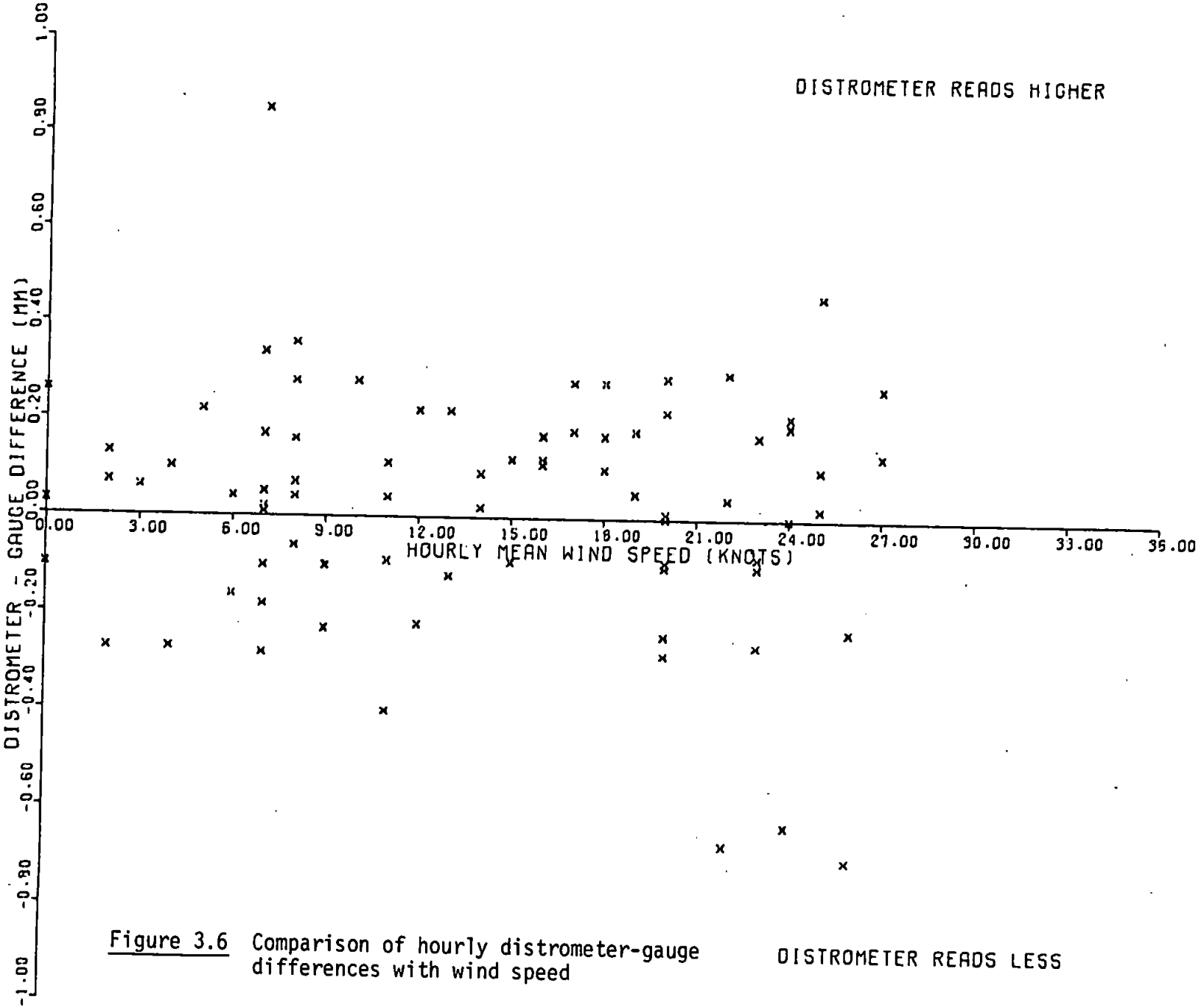

Figure 3.6 Comparison of hourly distrometer-gauge differences with wind speed

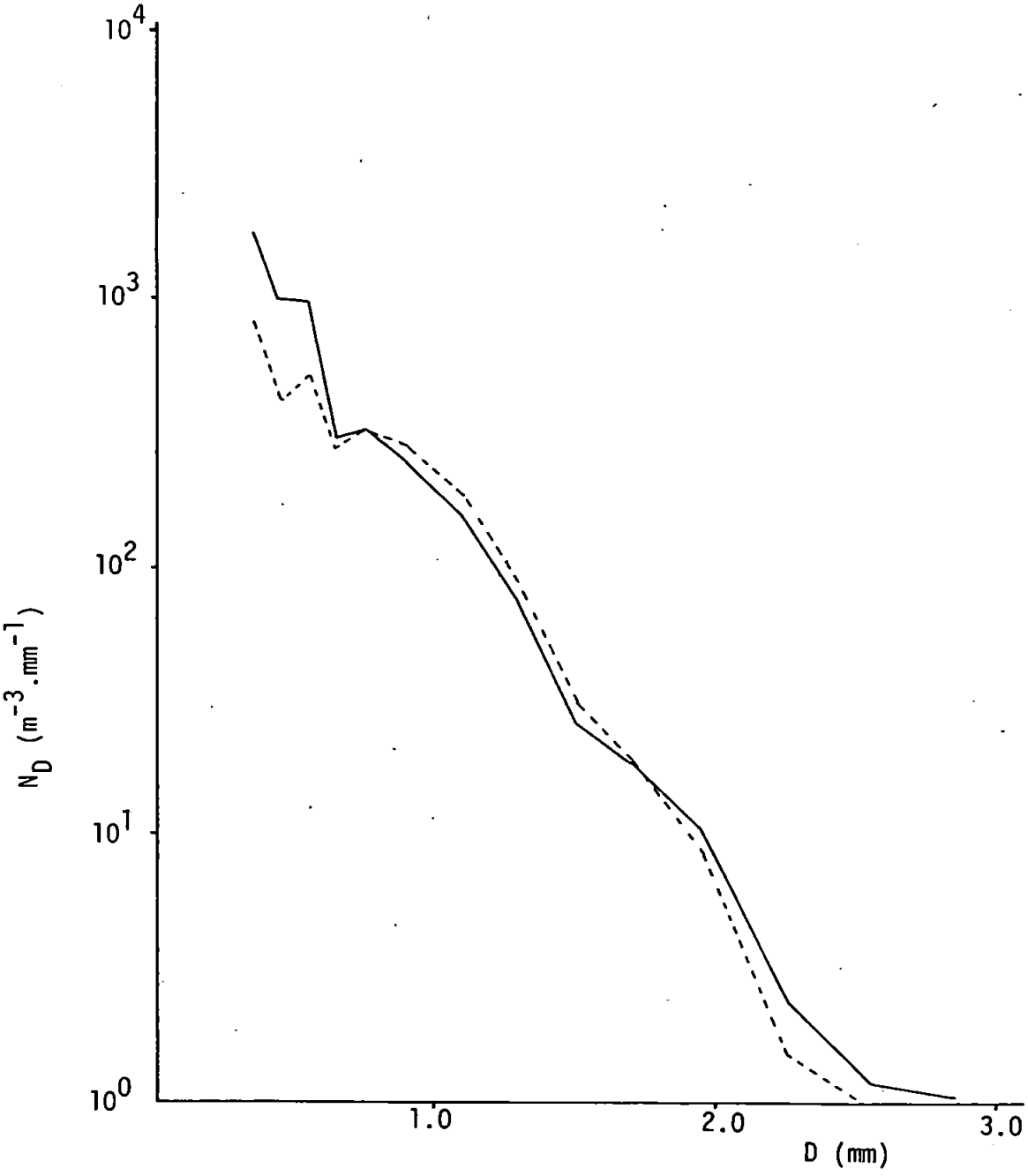

Figure 3.7 Average raindrop-size distributions for rainfall rates about 2 mm hr^{-1}.

——— All data (1374 distributions)

- - - - - Mins 2221-2400 during winds ~ 25 knots (77 distributions)

FROM (mins)	TO (mins)	Gauge (mm)	Distr. (mm)	Wind	
				Direction (°T)	Speed (kts)
2221	2280	1.7	1.91	160	24
2281	2340	2.3	2.07	160	26
2341	2400	0.7	0.72	160	25
TOTALS		4.7	4.70	160	25

Table 3.4 Gauge, distrometer and anemograph data relevant to Figure 3.7.

	Channel No.							
	1	2	3	-----	11	12	13	14
Distribution A	1737	977	933		10.2	2.5	1.2	1.0
Distribution B	794	417	501		8.3	1.5	1.0	0
B as a percentage of A	46	43	54		81	60	83	0

Table 3.5 Numbers of drops in Distributions A and B

Distribution A - all data, rainfall rates about 2 mm hr^{-1} (1374 spectra)

Distribution B - 2221-2400, rainfall rates about 2 mm hr^{-1} during winds ~ 25 kts (77 spectra)

The spectra are broadly similar although the data for high wind velocity show a substantial reduction in the number of small drops intercepted and a smaller reduction in the largest drops. The numbers of drops in the three smallest intervals and the four largest intervals which appear in these data are detailed in Table 3.5. The effect of losing drops in the smallest intervals is very slight compared to the loss of the larger drops; these effects are examined in Table 3.6 in terms of the values of the integral parameters R, Z and W and shape parameters N_0 and λ.

It is readily apparent that many small drops may be lost without seriously affecting the integral parameters, although the shape parameters are somewhat altered. However, when larger drops are lost the effects are more pronounced, particularly for the Radar Reflectivity factor, Z (which depends on the sixth power of the drop diameter). The differences in the shape parameters are of a similar magnitude to those which occur during rainfall as a consequency of real variations of a meterological nature (see for example *12* and *43*). Thus this difference may be due to a real change in the shape of the distribution rather than an experimental error resulting from the high wind velocity.

The subset of data considered here was obtained in conditions which would represent the extreme effects of wind velocity for this experiment. Although some differences in integral and shape parameters may occur in such a situation they are not serious enough to warrant the evolution of a wind velocity-dependent correction scheme.

	1	2	3	4	5	6	7	8
R	1.93	1.93	1.90	1.87	1.80	1.87	1.64	1.58
Z	681.4	902.0	901.6	900.7	897.8	900.0	548.8	546.8
W	123.6	128.8	124.6	119.8	111.5	120.3	117.8	109.3
N_o	5658.9	4283.0	3971.2	3626.4	3078.7	3667.8	6747.0	5701.4
λ	3.46	3.2	3.16	3.12	3.05	3.13	3.66	3.58

Table 3.6 The effect on integral and shape parameters when drops of various sizes are lost

1 Distribution B
2 Distribution A
3 Reducing channel 1 in A to a single drop
4 Reducing channels 1 and 2 in A to a single drop
5 Reducing channels 1, 2 and 3 in A to a single drop
6 Reducing channels 1, 2 and 3 in A by 50%
7 Reducing channels 11, 12, 13 in A by percentages in Table 3.5
8 Combination of 6 and 7. (cf. 1)

3.2 AVERAGE DROP-SIZE DISTRIBUTIONS

3.2.1 The significance of average drop-size distributions

As noted earlier (1.1.2) the M-P exponential distribution is only consistently obtained by meaning a number of spectra of similar rainfall rates. Such a procedure seems obligatory in studies of raindrop-size distributions although the variations in individual spectra may be more interesting than similarities in smoothed or averaged data. (4).

However, the grouping of data in this way provides a useful check of their validity, particularly when compared with the results of other workers. If the results from the present data showed any large deviation from the M-P distribution or differences when compared with raindrop-size distributions from other sources (different measuring techniques, different locations etc.), then there would be reason to suspect either experimental error or a real difference due to other factors, such as location (e.g. Maritime Locale).

3.2.2 Results from the present data

Figures 3.8 to 3.17 show average raindrop-size distributions from the present data for the following ranges of rainfall rates:

$0.5 \leq R \leq 1.5$ mm hr^{-1}
$1.5 < R \leq 2.5$ mm hr^{-1}
$2.5 < R \leq 3.5$ mm hr^{-1}
$3.5 < R \leq 4.5$ mm hr^{-1}
$4.5 < R \leq 5.5$ mm hr^{-1}
$5.5 < R \leq 7.5$ mm hr^{-1}
$7.5 < R \leq 9.5$ mm hr^{-1}
$9.5 < R \leq 11.5$ mm hr^{-1}
$11.5 < R \leq 15.5$ mm hr^{-1}
$15.5 < R$

The R value given in each figure is the average for the distributions in each range and the straight line is the appropriate M-P distribution.

The data are a good fit to the M-P yardstick, particularly at the lower rainfall rates for which more data are available. The deviation from an exponential is well known and has been observed by other workers using different techniques (see for example *9* (Doppler radar) and *44* (Photoelectric spectrometer)). The results of MARSHALL and PALMER (*13*) also show the same trend.

In Figures 3.16 and 3.17 (for 10.2 and 39.2 mm hr^{-1} respectively) some points appear above the M-P line at the smallest diameters, which are contrary to this trend. It should be noted that these distributions are based on a small and perhaps unrepresentative number of spectra and that in Figure 3.17 the result is based on a very wide range of rainfall rates ($R > 15.5$ mm hr^{-1}).

When all the meaned distributions are plotted on the same axes (Figure 3.18), two kinks are accentuated; one at the smallest diameters (Channels 1-5) and another at about 1.5 mm (Channel 9). A similar result was obtained when the same distrometer was used in DWRP, as reported by NICHOLASS and LARKE (*16*).

In that work, the first kink was attributed to a slight inaccuracy in calibration and was overcome by pairing size intervals, reducing the first 8 intervals to 4. However the effect of allocating some drops to the wrong channel at small diameters is very slight when the integral and shape parameters are considered (see Table 3.6). In addition there is evidence to show that some alteration in slope

generally occurs at this end of the spectrum (*5*, *9*, *45*) and such a procedure would tend to mask this effect.

The kink in the middle of the spectrum was in evidence in the DWRP work although it passed without written comment. The fact that this feature appears in results which are independently derived in all respects, except that the same instrumentation was used, strongly suggests that it is attributable to the hardware and not to any real meteorological factor or fault in interpretation of data. Although a noticeable feature of the distribution when represented diagrammatically, it is not significant in numerical terms when the integral and shape parameters are considered. The drops involved are of moderate size but it appears that only a small percentage of all the drops in channels 8-10 are involved.

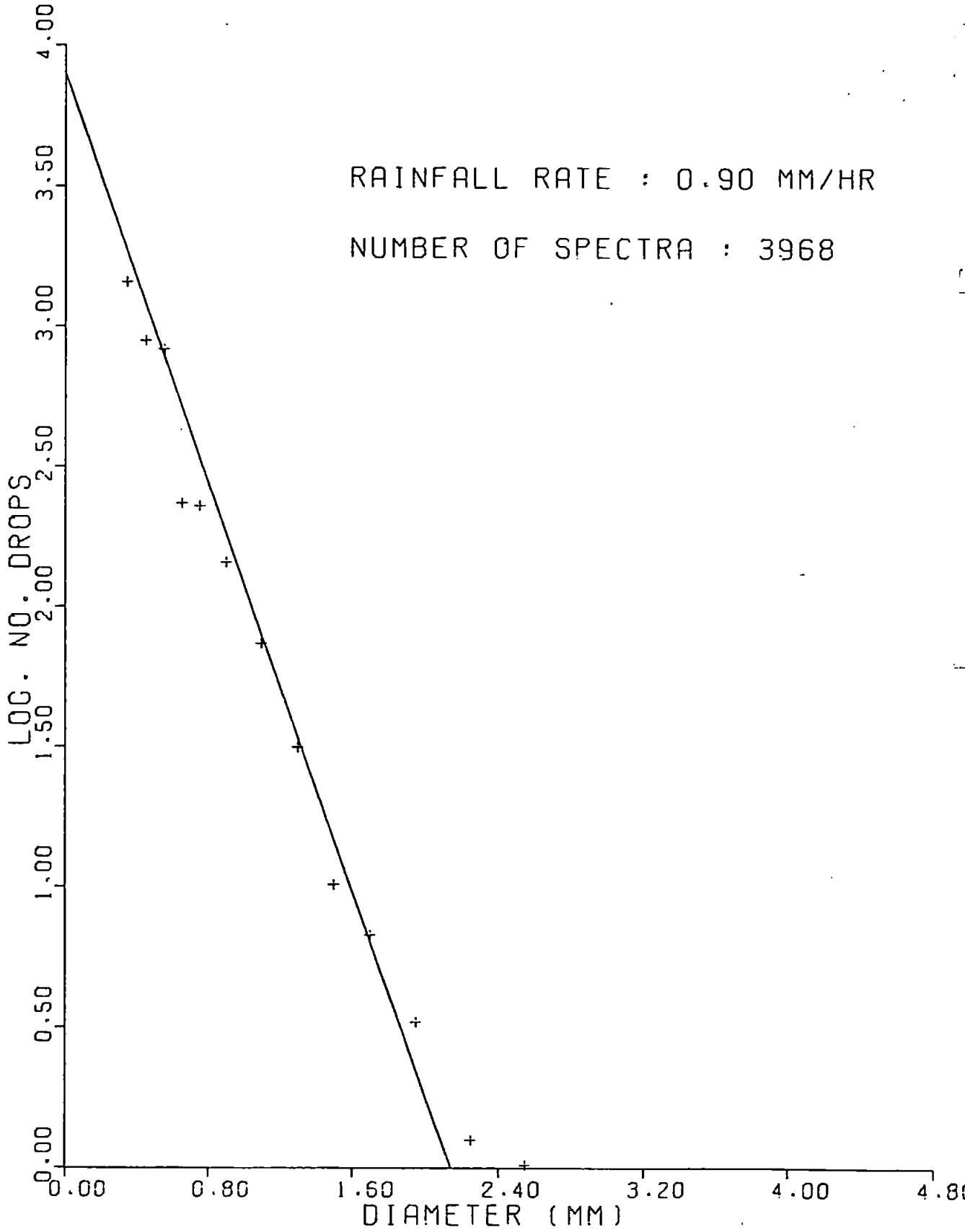

Figure 3.8 Average raindrop-size distribution (1ST DATA SET) Rainfall rates about 1.0 mm hr^{-1}.

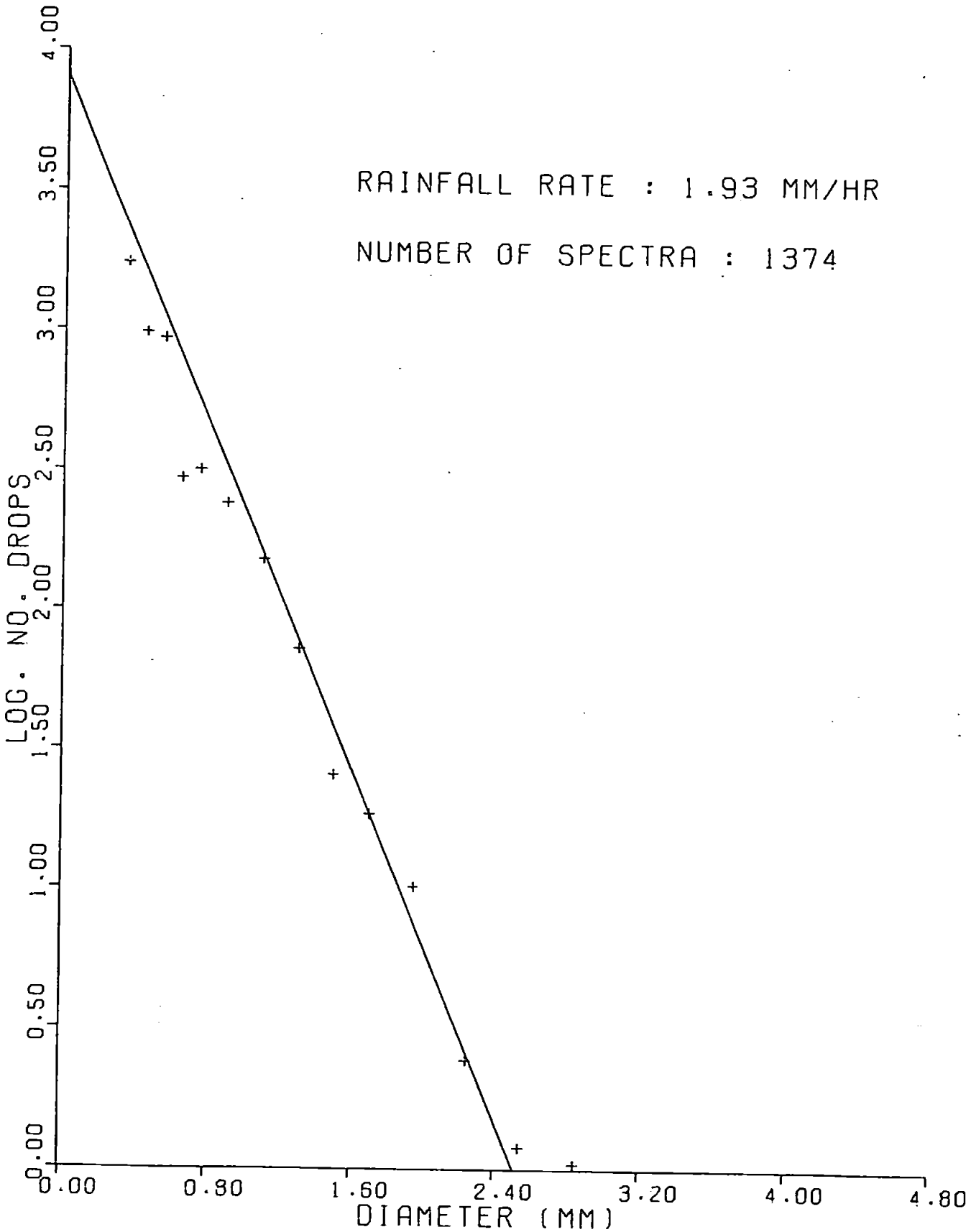

Figure 3.9 Average raindrop-size distribution (1ST DATA SET) Rainfall rates about 2.0 mm hr^{-1}.

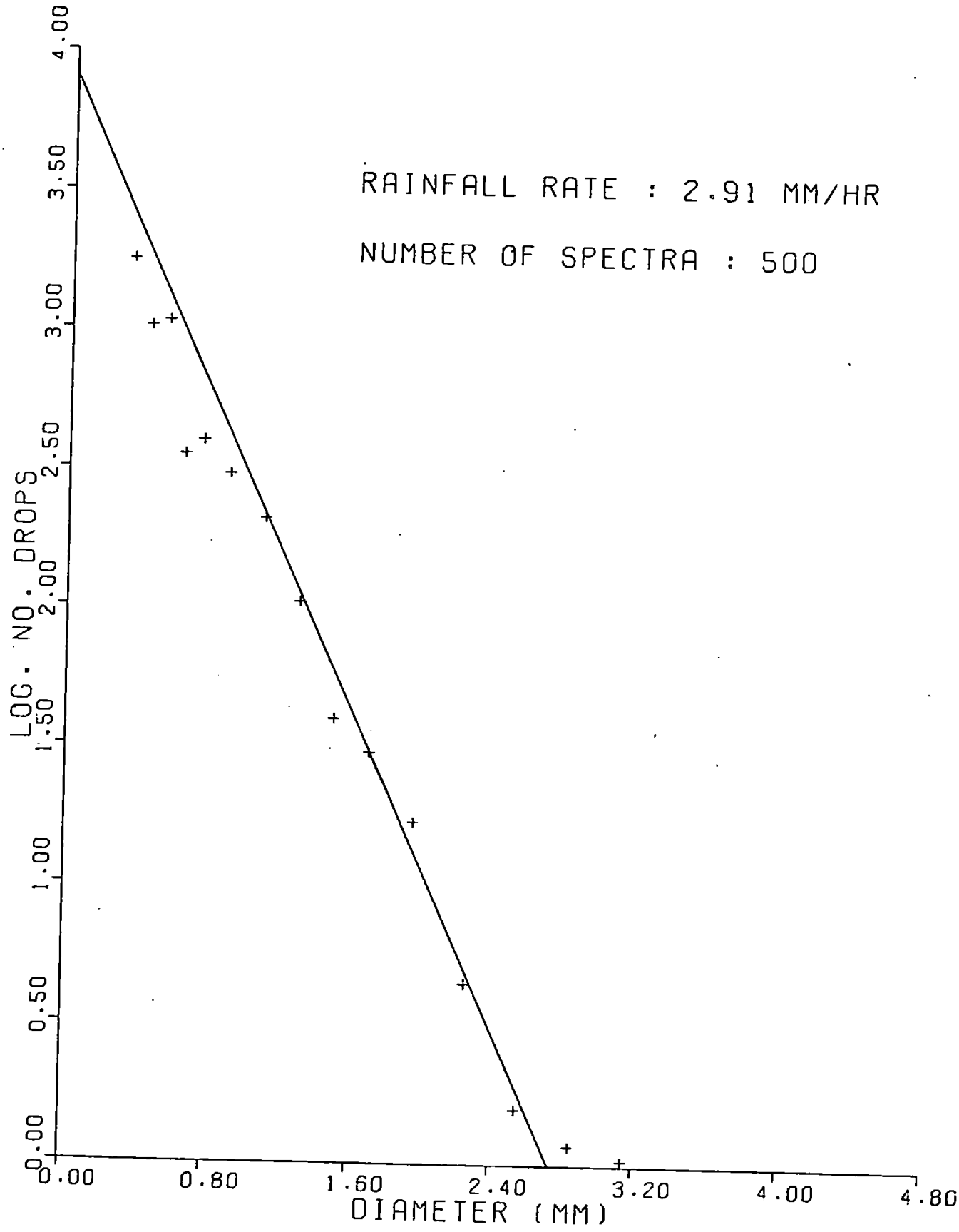

Figure 3.10 Average raindrop-size distribution (1ST DATA SET) Rainfall rates about 3.0 mm hr^{-1}.

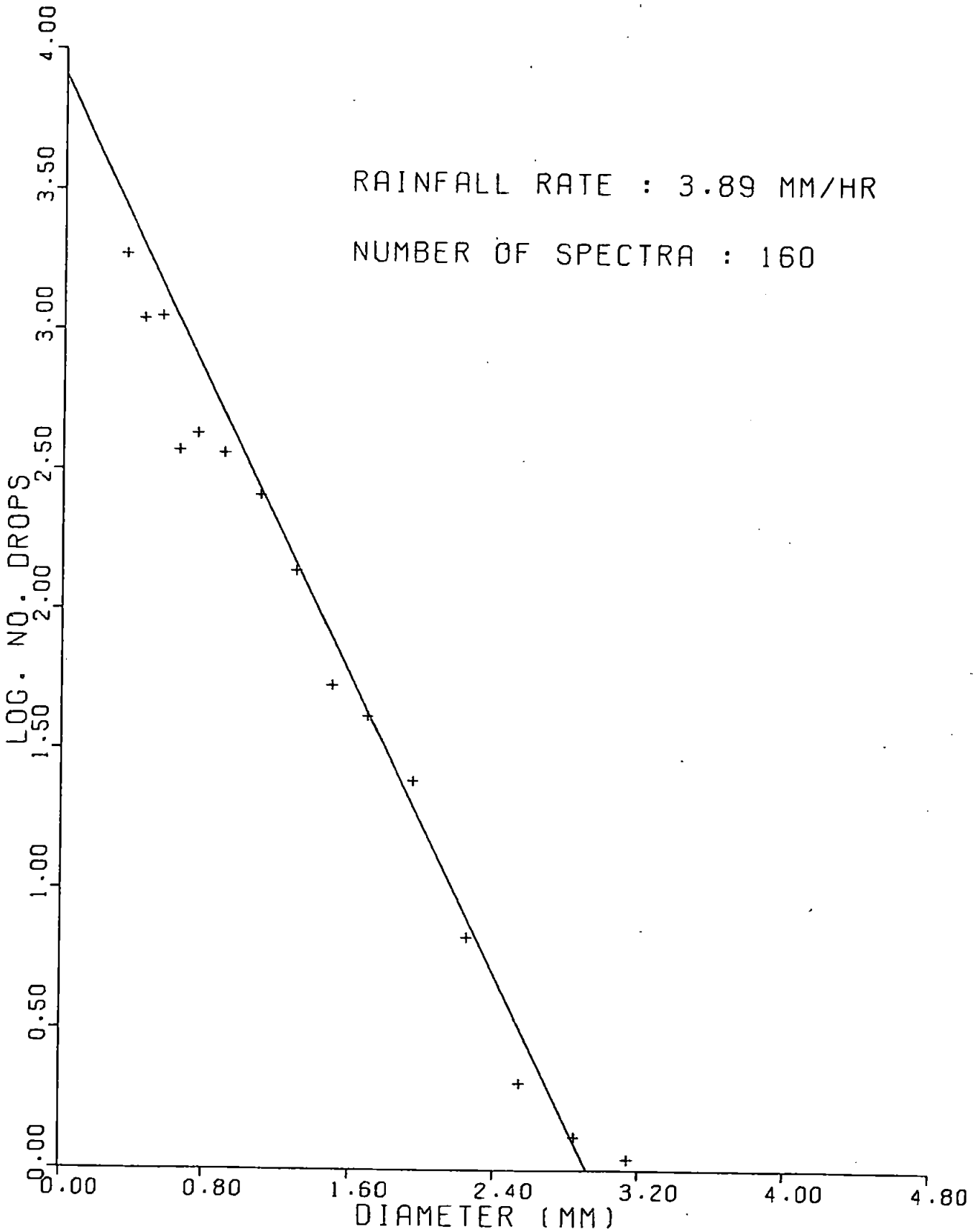

Figure 3.11 Average raindrop-size distribution (1ST DATA SET) Rainfall rates about 4.0 mm hr^{-1}.

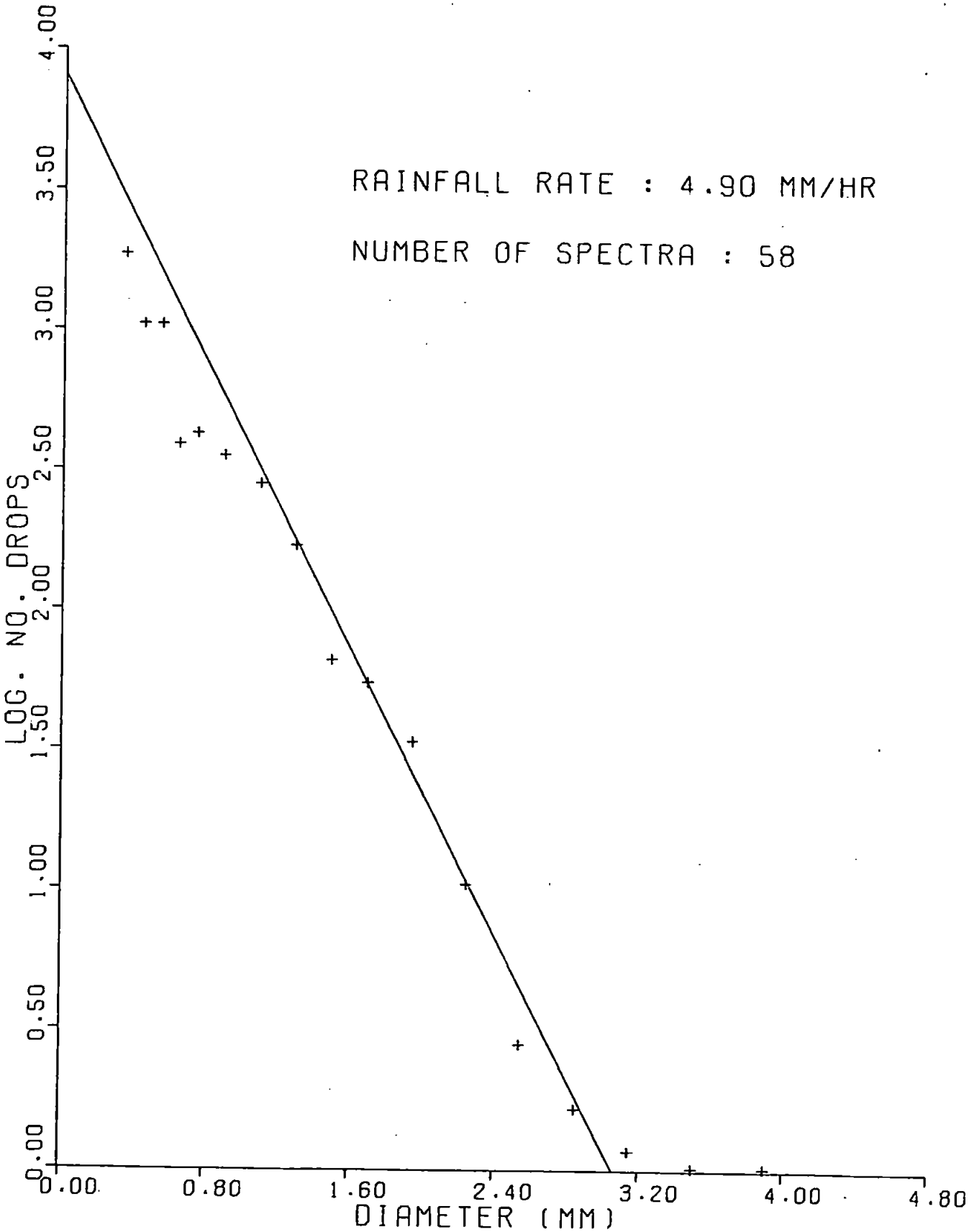

Figure 3.12 Average raindrop-size distribution (1ST DATA SET) Rainfall rates about 5.0 mm hr^{-1}.

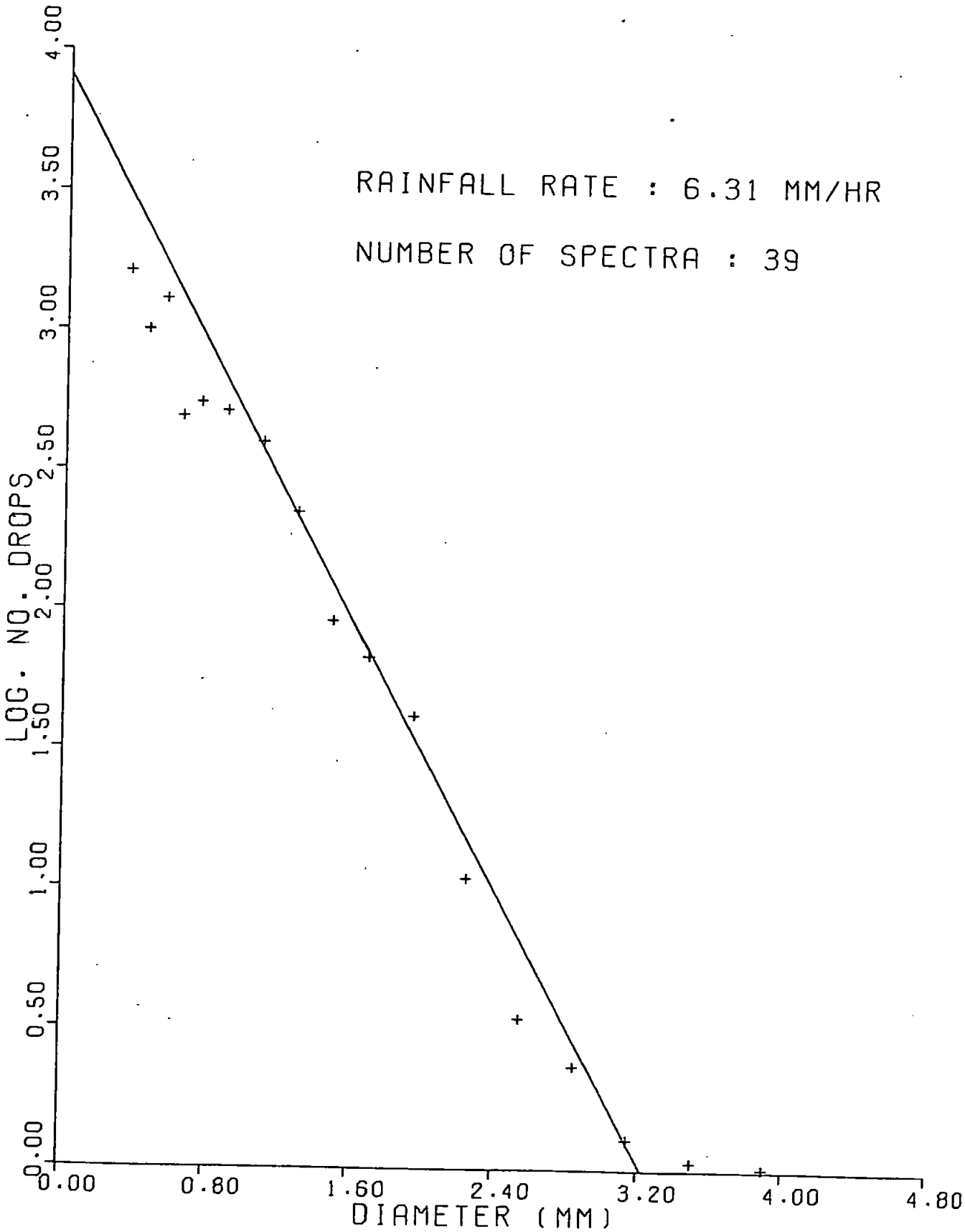

Figure 3.13 Average raindrop-size distribution (1ST DATA SET) Rainfall rates about 6.5 mm hr^{-1}.

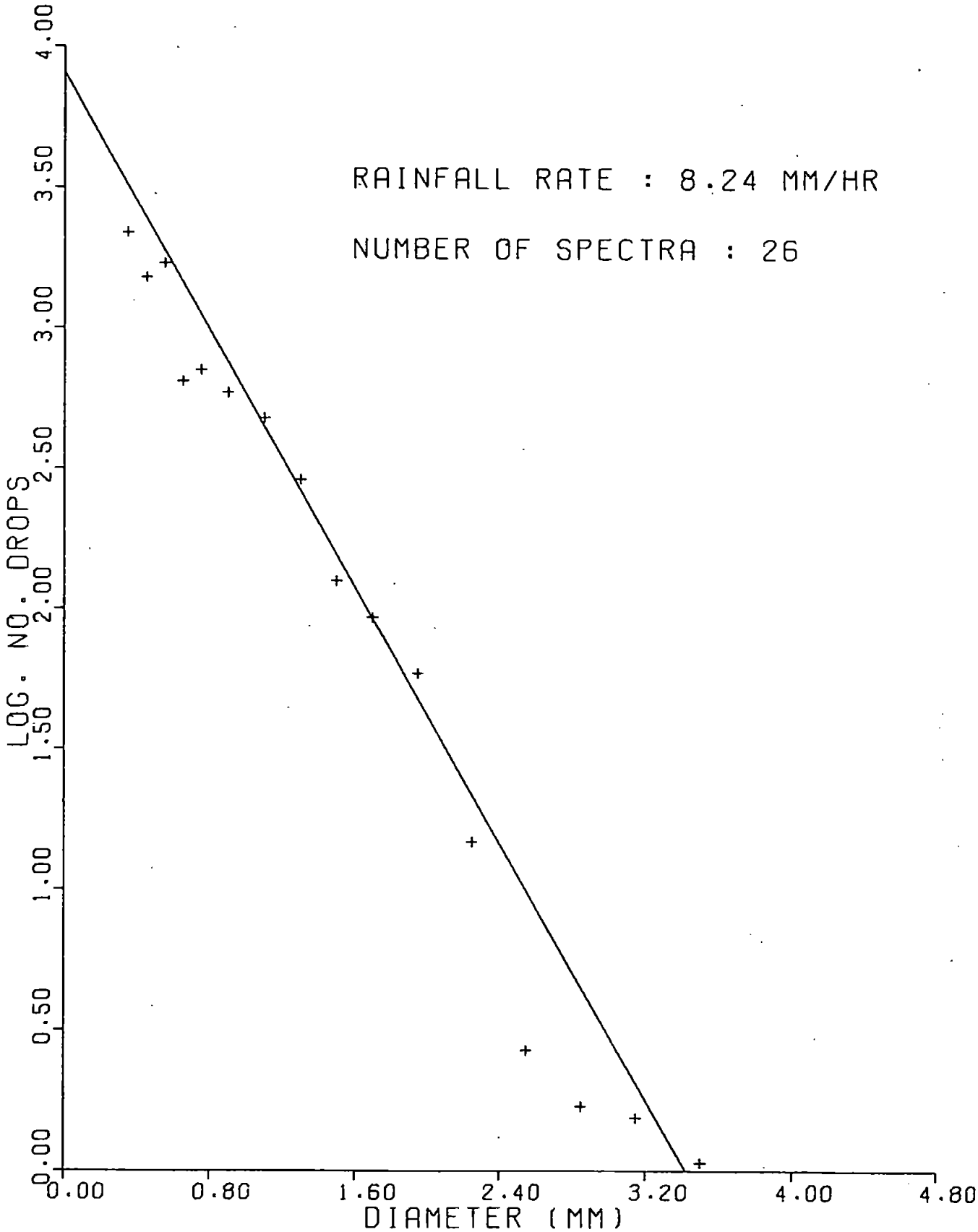

Figure 3.14 Average raindrop-size distribution (1ST DATA SET) Rainfall rates about 8.5 mm hr^{-1}.

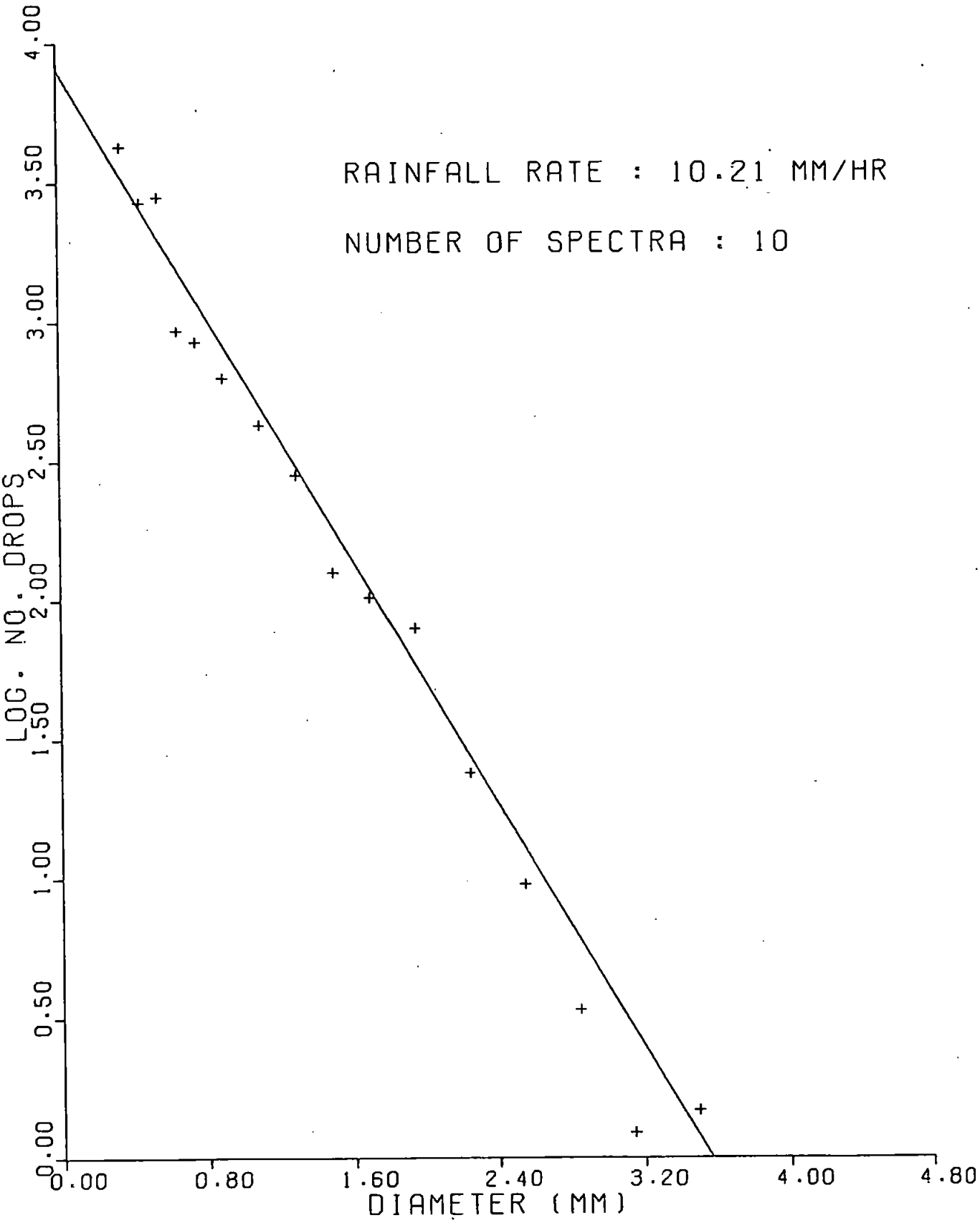

Figure 3.15 Average raindrop-size distribution (1ST DATA SET) Rainfall rates about 10.5 mm hr^{-1}.

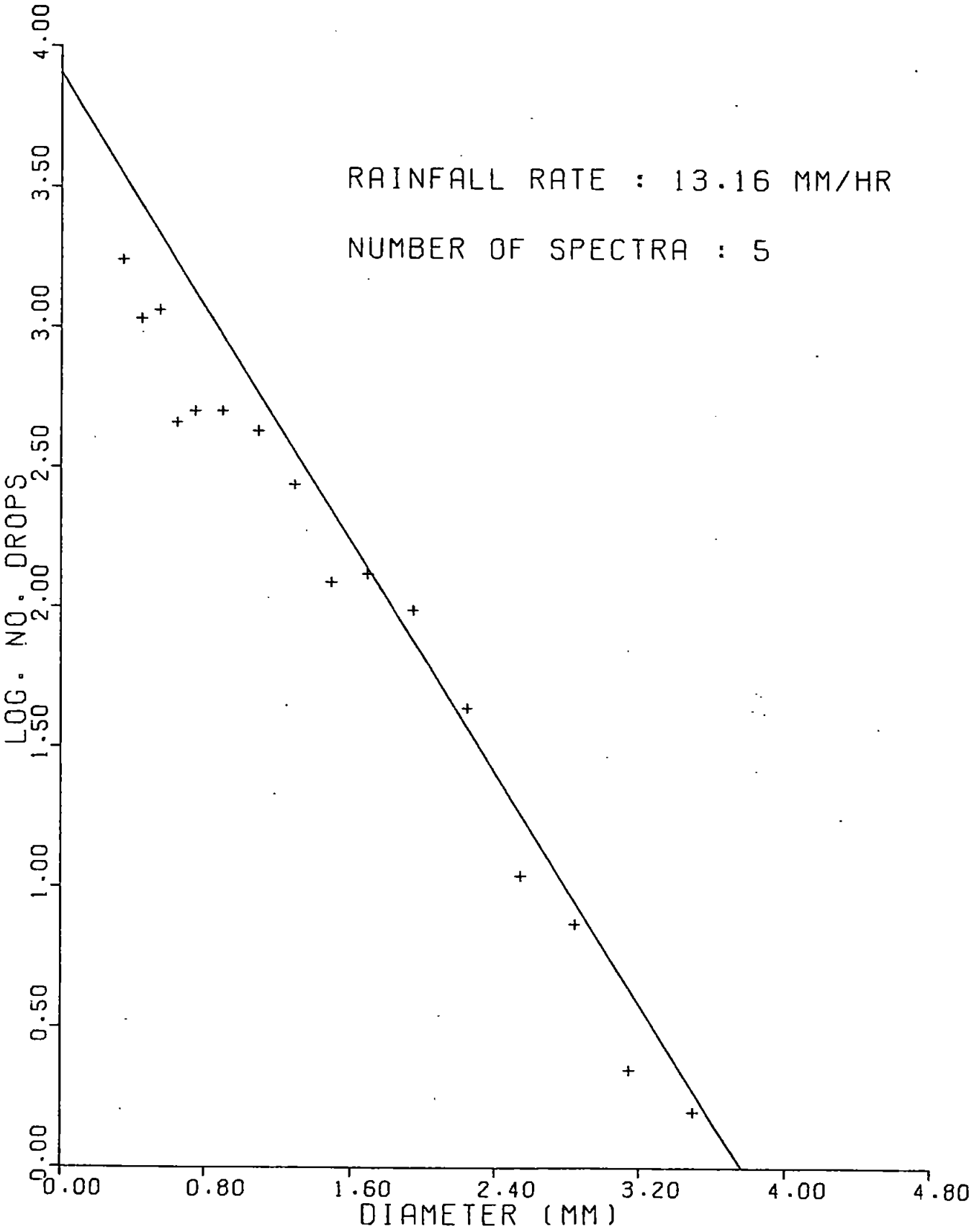

Figure 3.16 Average raindrop-size distribution (1ST DATA SET) Rainfall rates about 13.5 mm hr^{-1}.

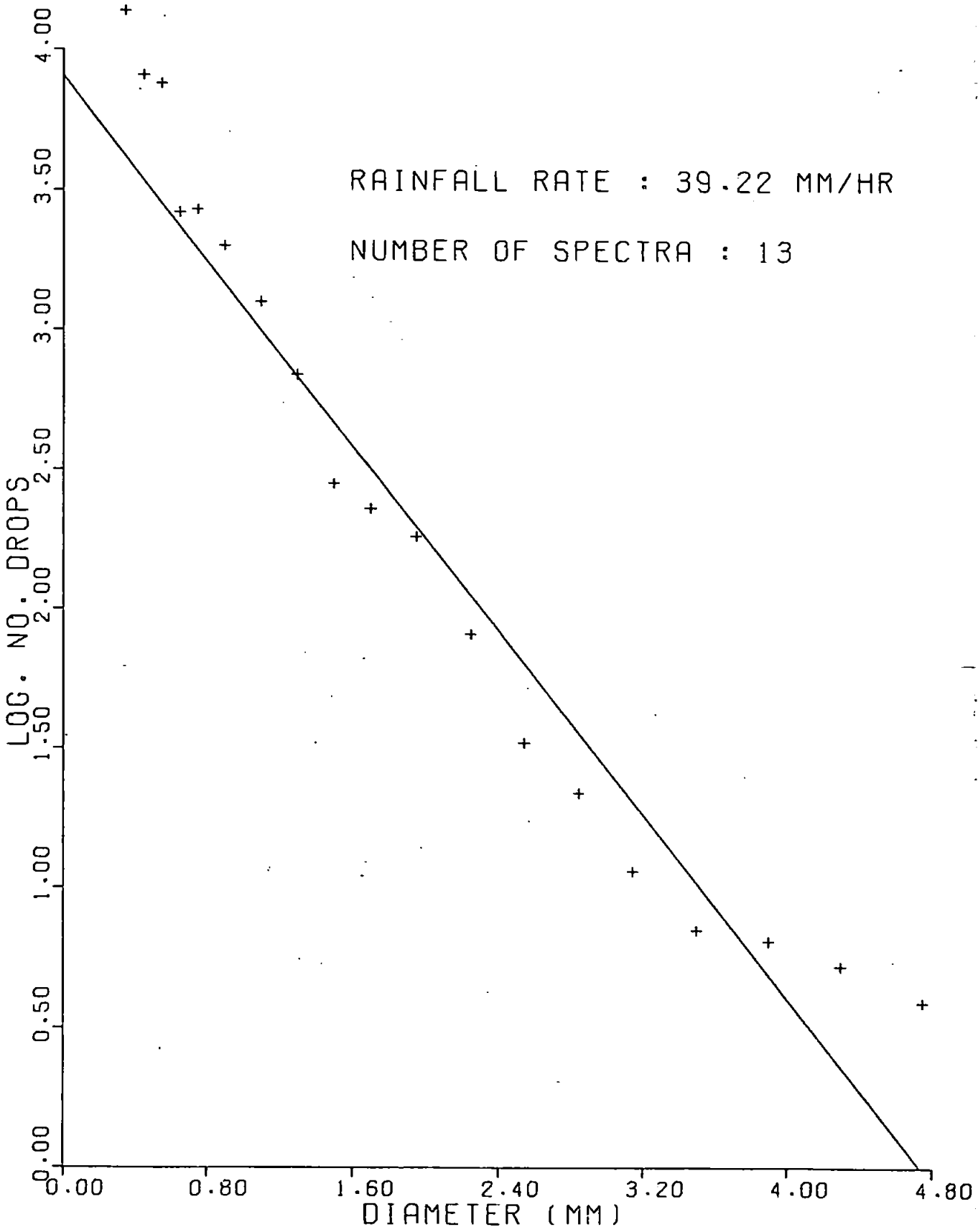

Figure 3.17 Average raindrop-size distribution (1ST DATA SET) Rainfall rates above 15.5 mm hr^{-1}.

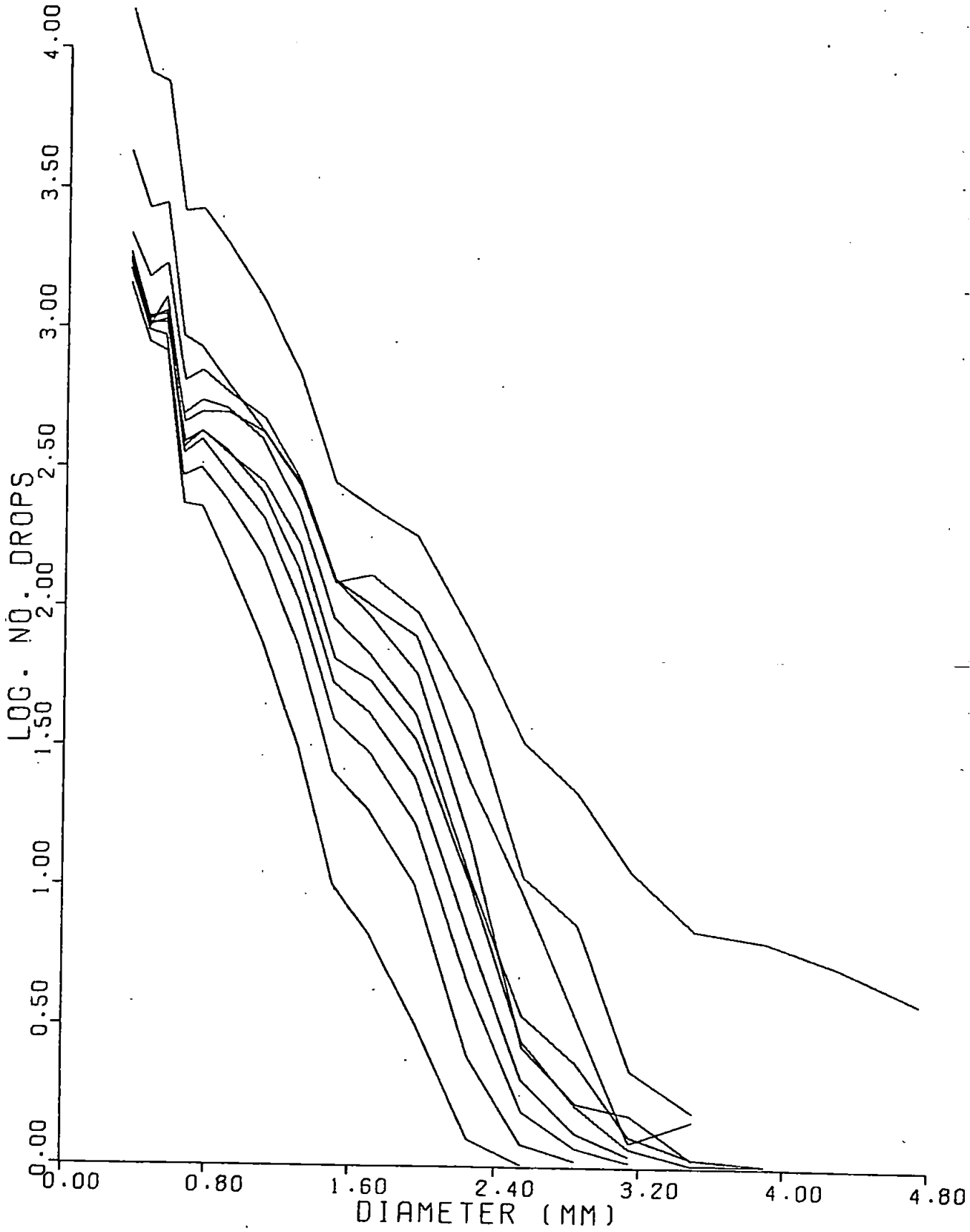

Figure 3.18 All average raindrop-size distributions (1ST DATA SET)

3.3 Z-R RELATIONSHIPS

3.3.1 Conventional Z-R relationships

As noted earlier (1.2.4 and 1.2.6) an empirical relationship between Radar Reflectivity factor and Rainfall Rate may be used to derive meteorological and hydrological information from radar data. Much of the research concerning raindrop-size distributions is directed towards obtaining these relationships and there are almost as many Z-R relationships as there are studies (*46*). A summary of results from many different locations and covering a period of 32 years has been published by BATTAN (*25*).

Such relationships are generally produced by obtaining raindrop-size distribution data and then performing a least squares linear regression on the logs of the derived Z and R values. In the context of radar meteorology, it is logical to treat Z as the independent variable and hence perform the regression of log R on log Z. It is sometimes not clear whether published relationships have been deduced in this way or by regressing log Z on log R; the effect of so doing is to reduce the values of A and B in the relationship $Z = AR^B$ for a particular set of data.

The present data were analysed by performing a linear regression of log R on log Z for all minutes with rainfall rates above 0.1 mm hr^{-1}; this gave the relationship $Z = 264\ R^{1.68}$ for 11087 data pairs with a correlation coefficient of +0.93. (When all data are used the result $Z = 251\ R^{1.45}$ is obtained for 17654 data pairs with a correlation coefficient of +0.98.)

3.3.2 Comparison with other published relationships

The result obtained from the present data is well within the compass of other published results and is typical for widespread rain. Some studies have taken account of the effects of synoptic, seasonal and geographical variations and published a range of Z-R relationships (see for example *6*, *16*, *47*). Results often show that in thunderstorms A has a large value and for drizzle a smaller value is found for the same value of the exponent B. The range of values for A is typically 100 - 500 and B lies between 1 and 2. Therefore the values obtained in the present data are those expected in an exercise that did not involve any consideration of synoptic type or seasonal differences and may be compared with the value suggested by JOSS (*47*) for 'widespread' rain.

3.3.3 Variable Z-R relationships

Because Z depends on the sixth power of the drop diameter, then the Z-R relationship depends critically on the raindrop-size distribution, which is known to have a wide temporal and spatial variability (*48*, *49*). Most authors note that a single Z-R relationship is not an ideal solution to the radar problem. Many studies have shown that the appropriate relationship varies both in time and space (see for instance *50*, *51*).

JOSS (*47*) suggested various values for A with B fixed at 1.5 and typical N_o values as follows:

	Z-R relationship	N_o
Drizzle	$Z = 140\ R^{1.5}$	30000
Widespread rain	$Z = 250\ R^{1.5}$	8000
Thunderstorm	$Z = 500\ R^{1.5}$	1400

The author derives a relationship between N_o and A thus:

$$A = 230\sqrt{\frac{8000}{N_o}} \quad \text{for } 0.5 < R < 100 \text{ mm hr}^{-1}$$

and suggests the possibility of using radar data alone to identify different precipitation patterns, with typically different values for N_o and hence continuously adjust the parameters A and B to improve the radar estimation of precipitation.

The possibility of deploying distrometers in the radar field and telemetering observations in real time to the radar to adjust continuously and automatically the Z-R relationship, is generally discounted because of the complexity and cost of the instrumentation required to monitor adequately the temporal and spatial variations in the Z-R relationship.

To examine the possibility of combining these concepts the present data were analysed to investigate the relationship of the shape parameter N_o and the 'constant' A and to test this relationship on simulated and real radar data. The observations of N_o were related to the radar echo structure to investigate the viability of the suggestion made by JOSS (*47*). These investigations required the archiving of more distrometer observations, co-ordinated with actual radar data and the results are presented in the remainder of this work.

CHAPTER FOUR

MEASUREMENT OF PRECIPITATION BY RADAR

4.1 VARIABLE Z-R RELATIONSHIP FROM DISTROMETER OBSERVATIONS

4.1.1 Variation of rainfall parameters with time

The interpretations of the present data discussed thus far have been concerned with the grouping of numbers of spectra to produce hourly totals, averaged distributions and Z-R relationships. This type of procedure reduces some of the errors present in individual spectra, discussed previously in 2.2.3. However, some of the features of rainfall may be usefully investigated by examining the variation of spectra, or integral and shape parameters derived therefrom, with respect to time.

Such investigations have been carried out by a variety of methods and in numerous locations, notably HARDY and DINGLE (*44*), DU TOIT (*9*), SIVARAMAKRISHNAN (*6*), JOSS and GORI (*21*), WALDVOGEL (*12*), NORBURY and WHITE (*20*), PASQUALUCCI (*52*), BROWNING et al (*34*). All those investigations point to the variability of rainfall and this was investigated in the present data by producing time-series of rainfall rate together with computed N_0 and A values.

Figure 4.1 shows one hour of data (mins. 40021 - 40080) during which gauge and distrometer catches were almost the same (2.6 and 2.54 mm respectively; see Table 3.1). During this period the value of R_D (distrometer-derived rainfall rate) varied between 5.9 and a few tenths of a millimetre per hour. The shape parameter - the intercept, N_0 - was at a high value at the beginning of the hour (almost $2 \times 10^4 \, m^{-3} mm^{-1}$) and progressively decreased to a value much lower than the value which MARSHALL and PALMER (*13*) postulated as an appropriate value. The other shape parameter - the slope λ - also showed a similar downward trend.

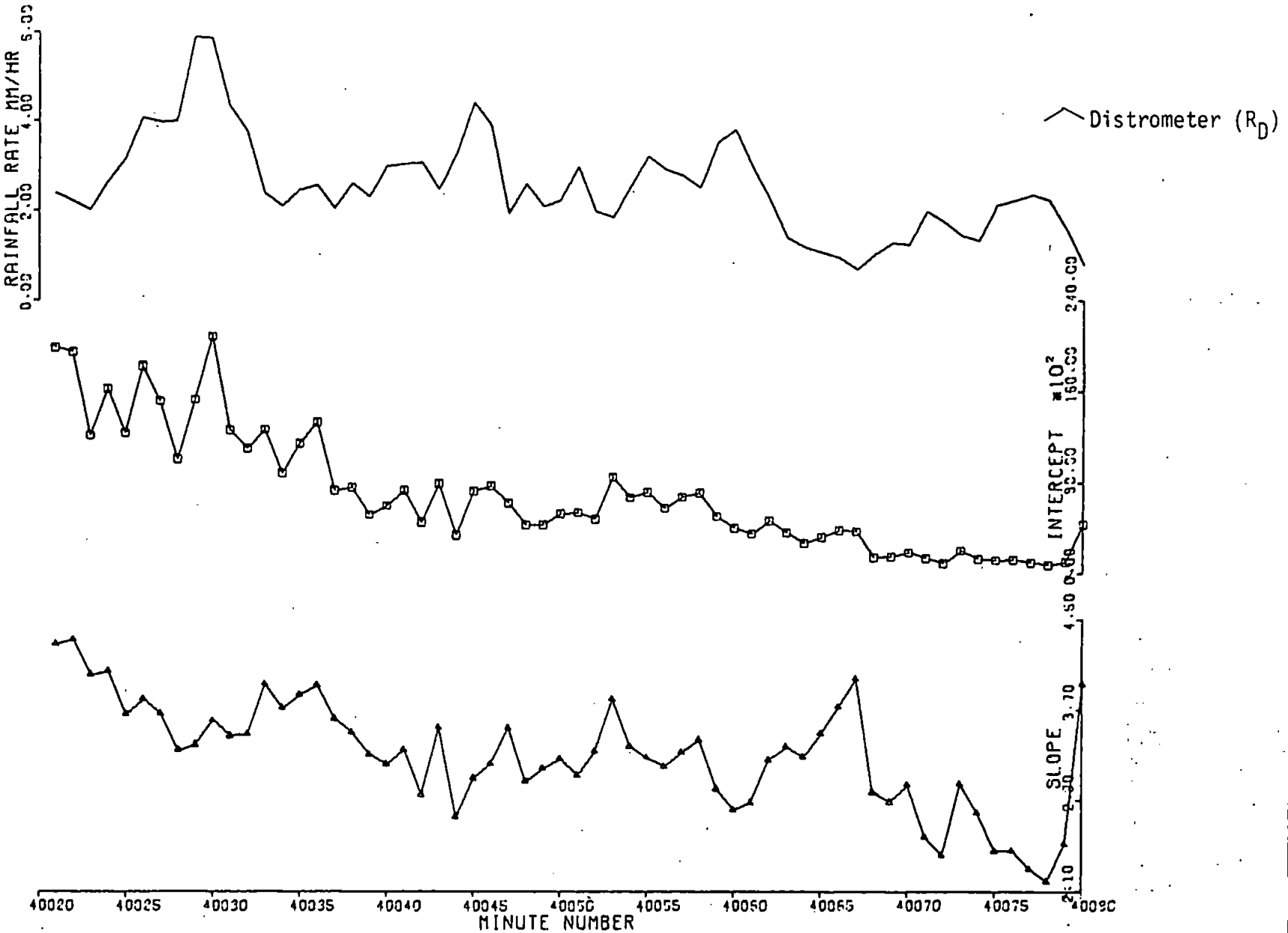

Figure 4.1

Totals

R_G : 2.6 mm

R_D : 2.54 mm

These data were recorded during a prolonged warm sector rainfall on 20.3.78 when the wind was westerly with a mean speed of 8 knots. Under these conditions of continuous moderate rainfall there is a marked variability in all the parameters. When it is required to measure the variations of the integral parameter R by radar, the variation in the drop-size distribution, indicated by the fluctuation in the shape parameters, is of great significance.

There are instances in these data where spectra with similar rainfall rates have markedly different shapes, representing a shift to larger or smaller drops. As discussed earlier (3.3.3) this has a significant effect on another integral parameter - the radar reflectivity factor, Z.

4.1.2 Simulated radar rainfall rate

To investigate the effect of the changing shape of the drop-size distribution on what a radar might measure if observing the same situation, a simulated radar rainfall rate is introduced.

The simulated radar rainfall rate, R_Z, is computed by integrating the spectrum to produce Z and then converting this to rainfall rate by using a selected Z-R relationship. This approach will not give perfect results, since there are great differences between the way a distrometer measures rainfall rate and the operation of radar to perform the same task. These differences are due to both the physical differences in the hardware (electromechanical v. radio) and the statistical differences arising from the sampling technique (the distrometer measures for a fixed interval and then a spatial distribution is deduced; the radar may be made to measure the spatial distribution directly). However, this approach is at least as acceptable as using

a distrometer to produce empirical Z-R relationships for use on operational radars, a method which is bound by the same constraints, but widely reported. (*16*, *40*, *47*)

Figure 4.2 shows the same hour of data with R_Z plotted for each minute using the widely accepted Z-R relationship, $Z = 200\ R^{1.6}$ (*27*). This shows that R_Z agrees quite well, the minute-by-minute differences being generally less than 1 mm. The total for the hour also compares favourably with both the gauge and the catch derived directly from the distrometer. The agreement is best during the middle of the period when the intercept is closer to the M-P value. The most striking feature of the comparison between R_D and R_Z is that when N_o is high, R_D consistently exceeds R_Z and when N_o is low, R_Z consistently exceeds R_D.

Figure 4.3 shows the same data using $Z = 264\ R^{1.68}$, the best-fit Z-R relationship deduced from the present data. A similar result is obtained, the hourly total in this case not agreeing as well as before, but the portions in which over-estimation and under-estimation take place are the same. It is noticeable that the relationship with the higher value for the constant A performs better at the end of the hour when N_o is low and that the conventional relationship with A = 200 is better at the beginning when N_o has a relatively high value.

The behaviour described above may result in the calculated hourly total being in fair agreement with the measured total (in this case the difference is 0.32 mm). However, the minute-to-minute differences may be significant, and particularly undesirable in a system which is intended to produce data in real-time. In order to quantify this effect the rms error for each hour was derived by computing the

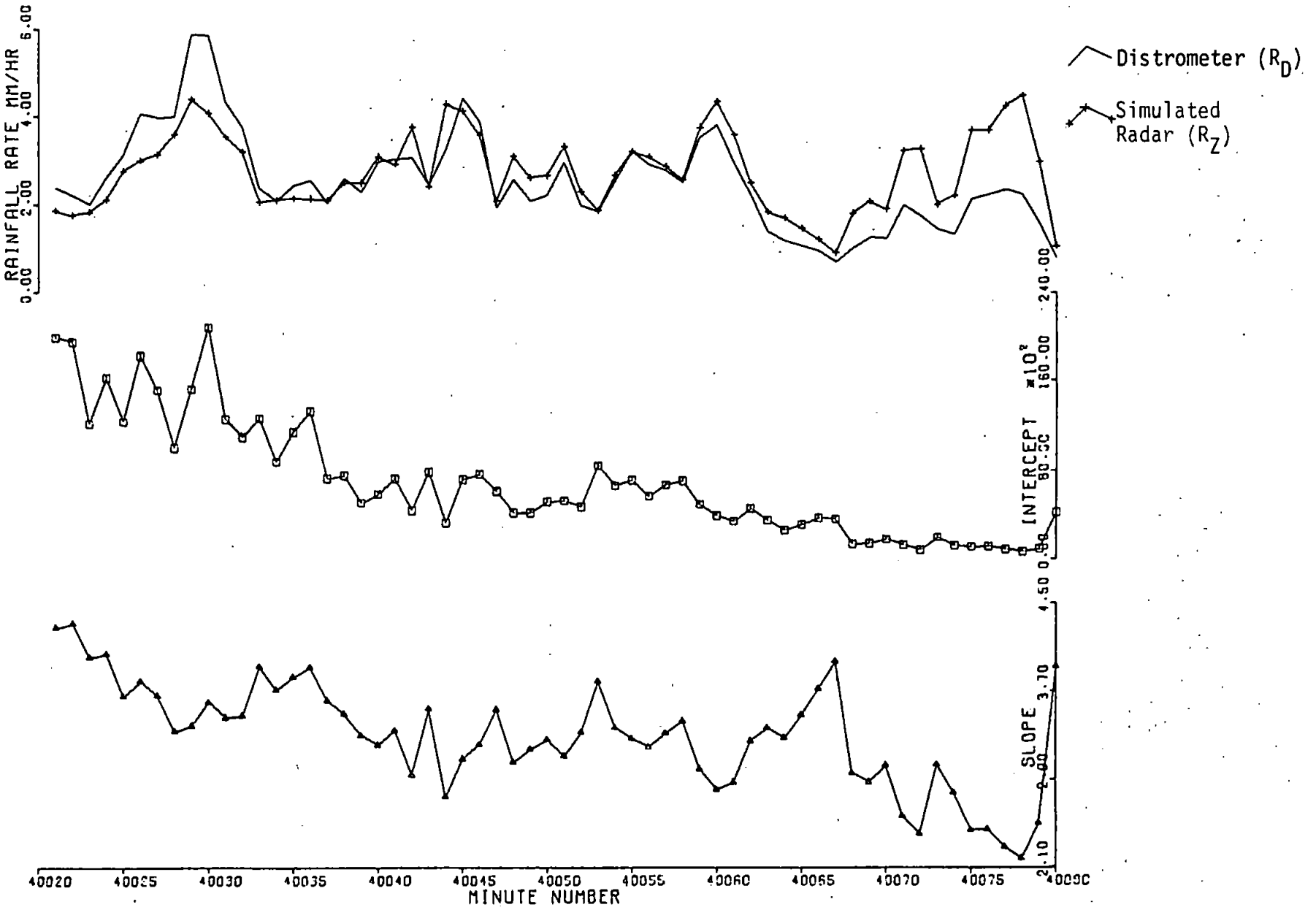

Figure 4.2

Totals

R_G : 2.6 mm

R_D : 2.54 mm

R_Z : 2.75 mm

(rms error: 0.399)

$Z = 200\ R^{1.6}$

Figure 4.3

Totals

R_G : 2.6 mm

R_D : 2.54 mm

R_Z : 2.22 mm

(rms error: 0.683)

$Z = 264\ R^{1.68}$

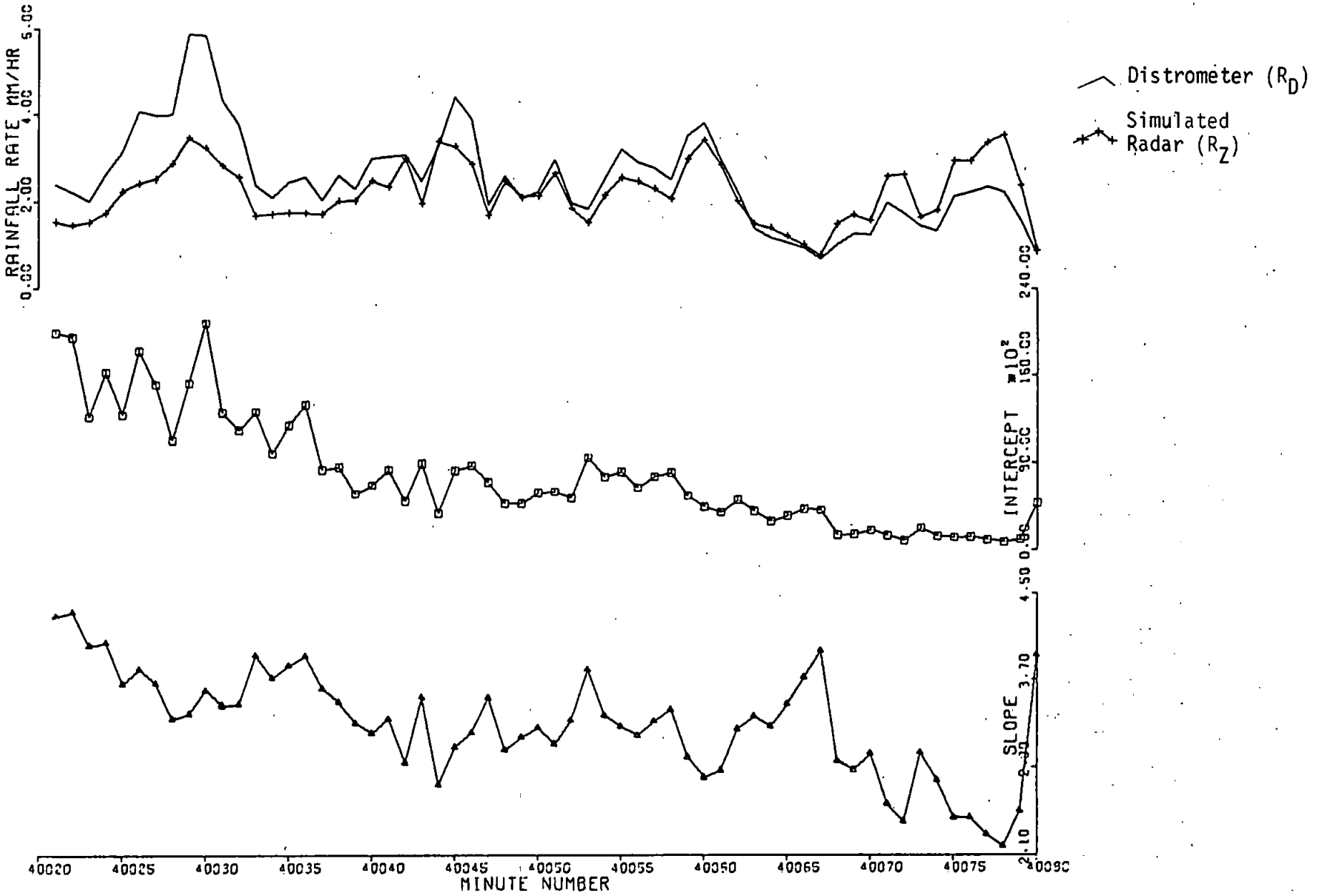

linear differences between the simulated radar rainfall rate and the distrometer values for each minute. As already noted, each method (gauge, distrometer and radar) can be expected to produce different results; in this analysis the distrometer rainfall rate values were used as the base measurement and the deviation from them as an "error".

Any method adopted to improve the radar estimate should ideally both improve the hourly total and reduce the rms error.

4.1.3 The effect of spectrum shape on radar rainfall rate

Although only one hour of data was presented in the previous section, many hours were examined in this way and similar results obtained. It appears, therefore, that when the balance in the drop-size distribution is shifted towards the smaller drops (high N_0), the radar will under-estimate because the value of Z is less than expected and A is too high; when the balance is shifted towards the larger drops (low N_0), the radar will over-estimate because the value of Z is more than expected and A is too low.

This effect may be shown quantitatively by considering two spectra with similar rainfall rates but different shapes - and hence different N_0 values. Minutes 40053 and 40072 of the data shown in Figure 4.3 are detailed in Table 4.1, which shows the R_Z values when the relationship $Z = 264\ R^{1.68}$ is used; the final column indicates the magnitude of the discrepancy which may arise through the use of inappropriate values for A and B.

Minute Number	R_D mm hr^{-1}	Z mm^6 m^{-3}	N_o m^{-3} mm^{-1}	λ mm^{-1}	R_Z mm hr^{-1}	$R_Z - R_D$ mm hr^{-1}
40053	1.84	540	8511	3.80	1.53	-0.31
40072	1.73	1331	863	2.41	2.62	+0.89

Table 4.1 Spectra 40053 and 40072 - simulated radar rainfall rates

Thus an inverse relationship between N_0 and A emerges - as predicted theoretically (*47, 53*). If a stable relationship between the observed value of N_0 and the appropriate value for A can be found, more reliable estimates of R from Z may be obtained by reference to N_0 at the time in question - a variable Z-R relationship.

4.1.4 Applicability of shape parameters

The shape parameters N_0 and λ have been used by many workers as discussed in 1.3.1. The work of WALDVOGEL (*12*) and PASQUALUCCI (*52*) in particular has indicated the possibilities offered by a detailed consideration of the intercept parameter. Thus the present investigation was directed towards this end, ignoring to some extent the possibilities that may be offered by a further consideration of the slope of the spectrum. This should not be interpreted as a statement that, in the author's opinion, λ may not be as useful in this respect as N_0.

From a purely statistical viewpoint N_0 may be criticised as an estimator of spectrum shape because it depends so strongly on the existence of a relatively small number of large drops in the spectrum. This may lead to a variability which is statistically rather than meteorologically induced. In Figure 4.3, particularly during the first 20 minutes, there is a considerable variation in the value of N_0 from one minute to the next and doubtless some of this variation is statistically induced, i.e. the sampling interval is too small in these circumstances. However, the trend is very clear and there are many examples in the present data where even shorter term trends are obvious, where the N_0 value shows a steady rise or fall over several individual spectra and then continues at a new mean value. Indeed

N_0 may sometimes 'jump' from one level to another, indicating a mesoscale change in the atmosphere, as discussed by WALDVOGEL (*12*).

An example of an hour's data when short term but sequentially consistent trends in N_0 occurred is displayed in Figure 4.7*(drawn from the 2nd data set, discussed in 4.2). In this case the intercept value peaks at minute 520109, preceded by three ascending values and followed by four descending values. A secondary peak is seen at minute 520136, possibly caused by another mesoscale change in the atmosphere, taking place over a period of a few minutes.

These data also show an example of what was probably a statistically induced peak, at minute 520155, when the intercept value rises suddenly from a relatively steady value (although the rainfall rate was varying considerably) and then drops again to the previous level. This occurred at a very low rainfall rate and therefore a relatively small number of drops was sampled.

4.1.5 Frequencies of N_0 values

The M-P results (*13*) suggest that a value of 8000 for N_0 might be typical. 17505 spectra from the present data were analysed to reveal the relative frequency with which particular N_0 values occur. The results appear in Figure 4.4.

The most frequent value of N_0 is in the range 2000-3000 with the percentages dropping away quite rapidly after N_0 = 10000. (Over 70% of the spectra have N_0 values < 10000.) The large percentage which occurs for $N_0 >$ 50000 is mainly attributable to spectra with very low

* p. 116

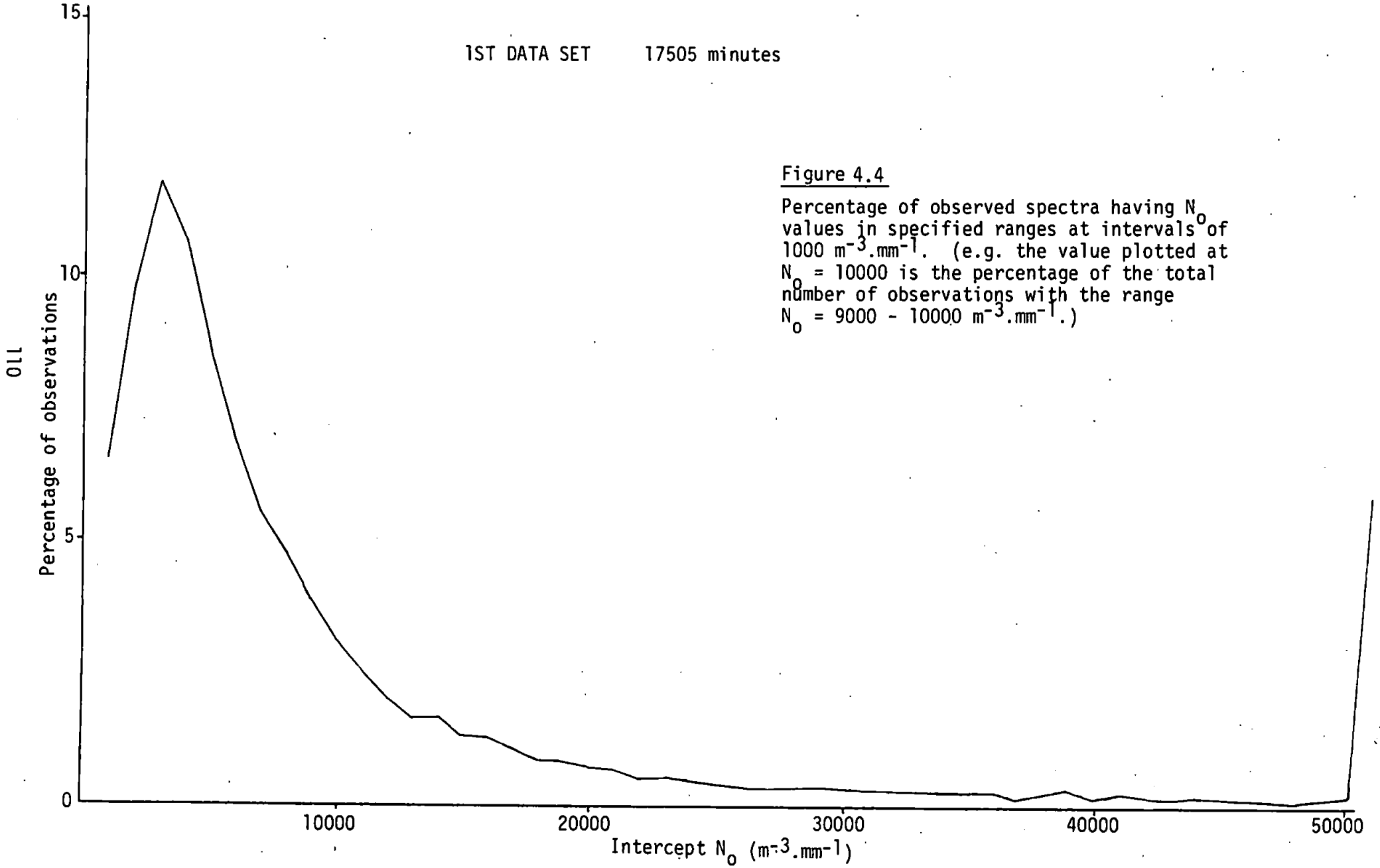

Figure 4.4

Percentage of observed spectra having N_o values in specified ranges at intervals of 1000 $m^{-3}.mm^{-1}$. (e.g. the value plotted at N_o = 10000 is the percentage of the total number of observations with the range N_o = 9000 - 10000 $m^{-3}.mm^{-1}$.)

rainfall rates and which are not included in the analyses which involve rainfall rates > 0.1 mm hr^{-1}.

Hence the most frequent values of N_0 observed by distrometer at St. Mawgan were of the same order as the value suggested by MARSHALL and PALMER. The fact that a difference exists is almost certainly due to the quite different methods of computing N_0. As already noted the present data, when considered in the form of average raindrop-size distributions (3.2.2), compare favourably with the M-P result when N_0 = 8000 m^{-3} mm^{-1}.

4.1.6 The relationship between spectrum shape and the constant A

As noted in 4.1.3 a qualitative investigation of the relationship between spectrum shape and rainfall rate suggests an inverse relationship between N_0 and A. To test this hypothesis quantitatively, values of N_0 and A were calculated for the same 11087 data points as for the derivation of the static Z-R relationship (3.3.1). A was determined directly from the standard power law form ($Z = A.R^B$) with B fixed at 1.6 and Z and R obtained from the integrated spectrum. Thus each computed A value is that which would give the correct value of R from Z because the shift in drop-sizes has been taken into account.

These computed N_0 and A values were used in a least squares regression for a power curve fit with A as the dependent variable. The regression was carried out by a linear fit to the logarithms of the variables. The curve of best fit was found to be

$$N_0 = 1.54 \times 10^9 A^{-2.24}$$

with a correlation coefficient of -0.95. Thus a relationship between N_0 and A is found; the precise values for the "constants" are likely to vary from one instrument/atmosphere system to another.

This technique was tested on a large portion of the distrometer record. Improvements in rainfall totals were often found and the rms error was consistently reduced. Although the best fit relationship above was derived from the whole data set, it was found that for many of the hours considered in this part of the analysis, a curve slightly lower than the best fit gave the best results and this was used in subsequent investigations. This relationship, $N_0 = 3.1 \times 10^8 A^{-2}$, is shown in Figure 4.5 with some representative points chosen to cover a suitable range of N_0 and A values. This experimentally determined relationship agrees very well with WALDVOGEL's findings on a theoretical base (*53*, *54*).

The spectra detailed in Table 4.1 have different N_0 values and, as already shown, produce different values of R_Z. When the relationship above is used to adjust the value of A and produce an enhanced radar rainfall rate - R_{ZN} - it is seen that the result obtained is much closer to the distrometer-derived value (Table 4.2).

Applying this technique to the example under consideration (minutes 40021 - 40080) yields the result in Figure 4.6. The total for the hour agrees more closely with both the gauge and the distrometer and the rms error is reduced considerably.

Figure 4.7 shows the results for another set of data collected on 7.12.78 during the passage of an occlusion and analysed in the same way. These data are distinct from those used to derive the N_0-A

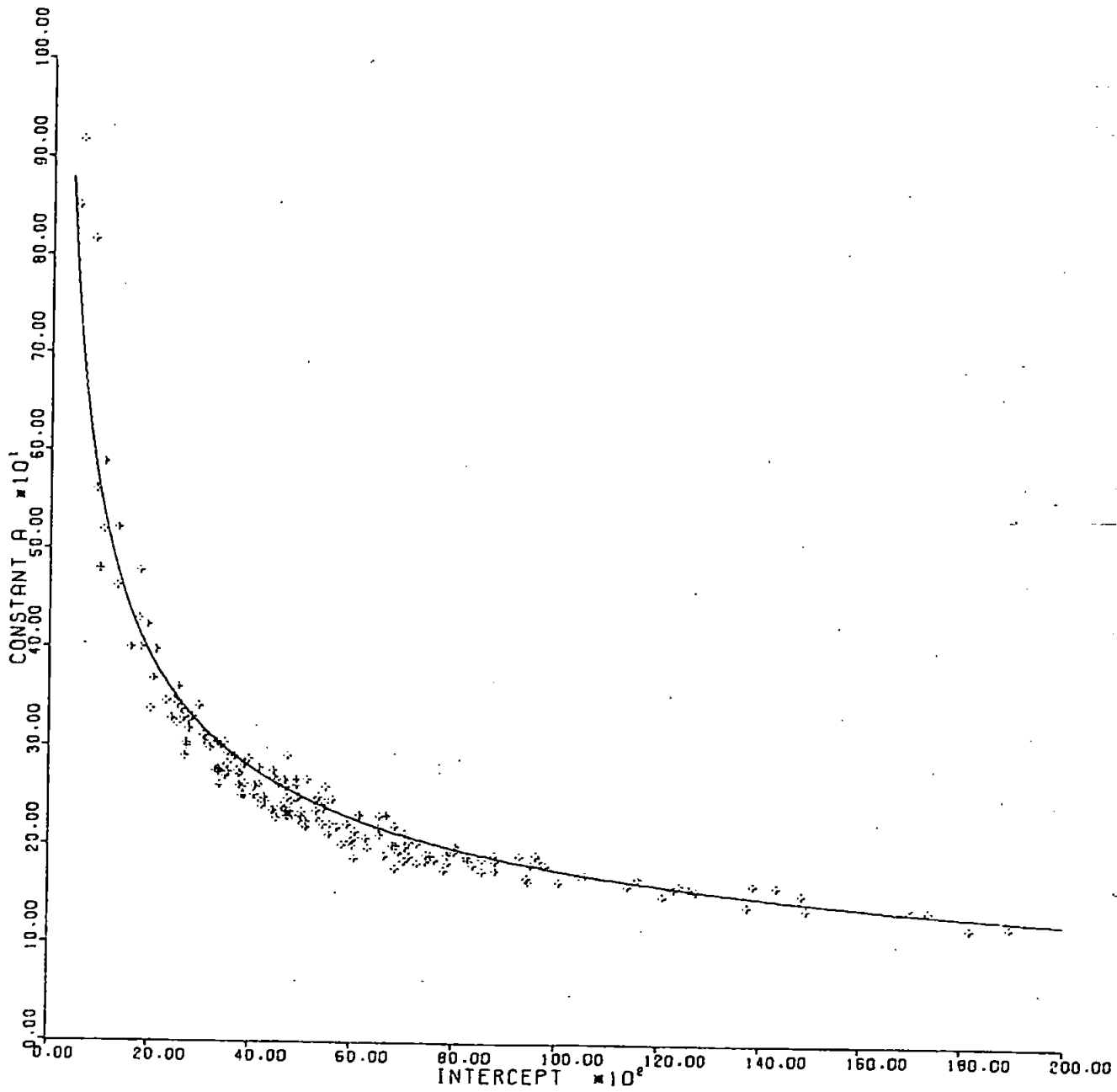

Figure 4.5 Relationship between N_o and A.
The data plotted are for mins. 15990-16185.
The curve $N_o = 3.1 \times 10^8 A^{-2}$ is shown.

Minute Number	R_D mm hr^{-1}	Adjusted A	B	R_{ZN} mm hr^{-1}	$R_{ZN} - R_D$ mm hr^{-1}
40053	1.84	191	1.6	1.91	+0.07
40072	1.73	599	1.6	1.64	-0.09

Table 4.2 Spectra 40053 and 40072 - enhanced radar rainfall rates

Figure 4.6

Totals

R_G : 2.6 mm

R_D : 2.54 mm

R_{ZN}: 2.48 mm

(rms error: 0.092)

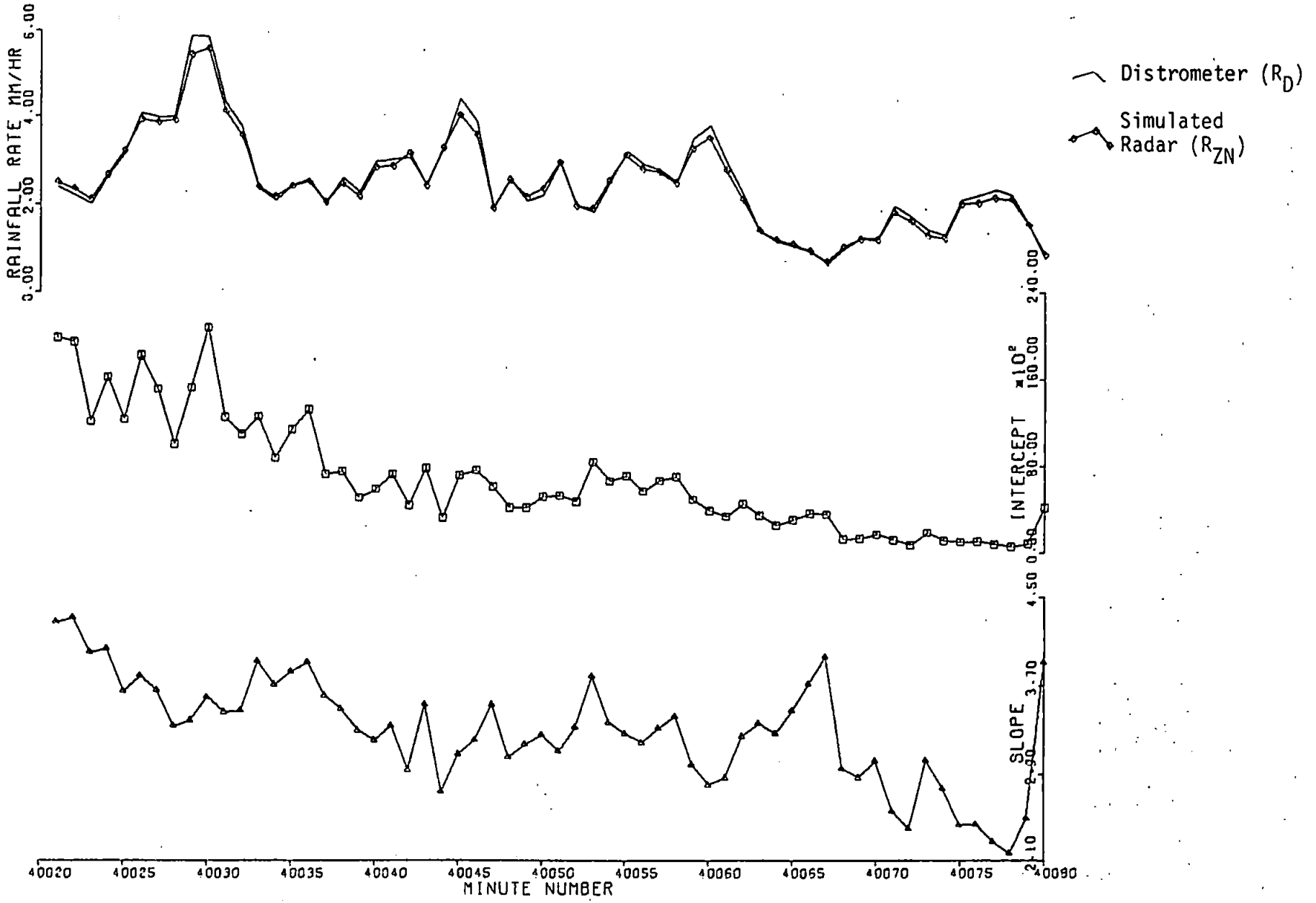

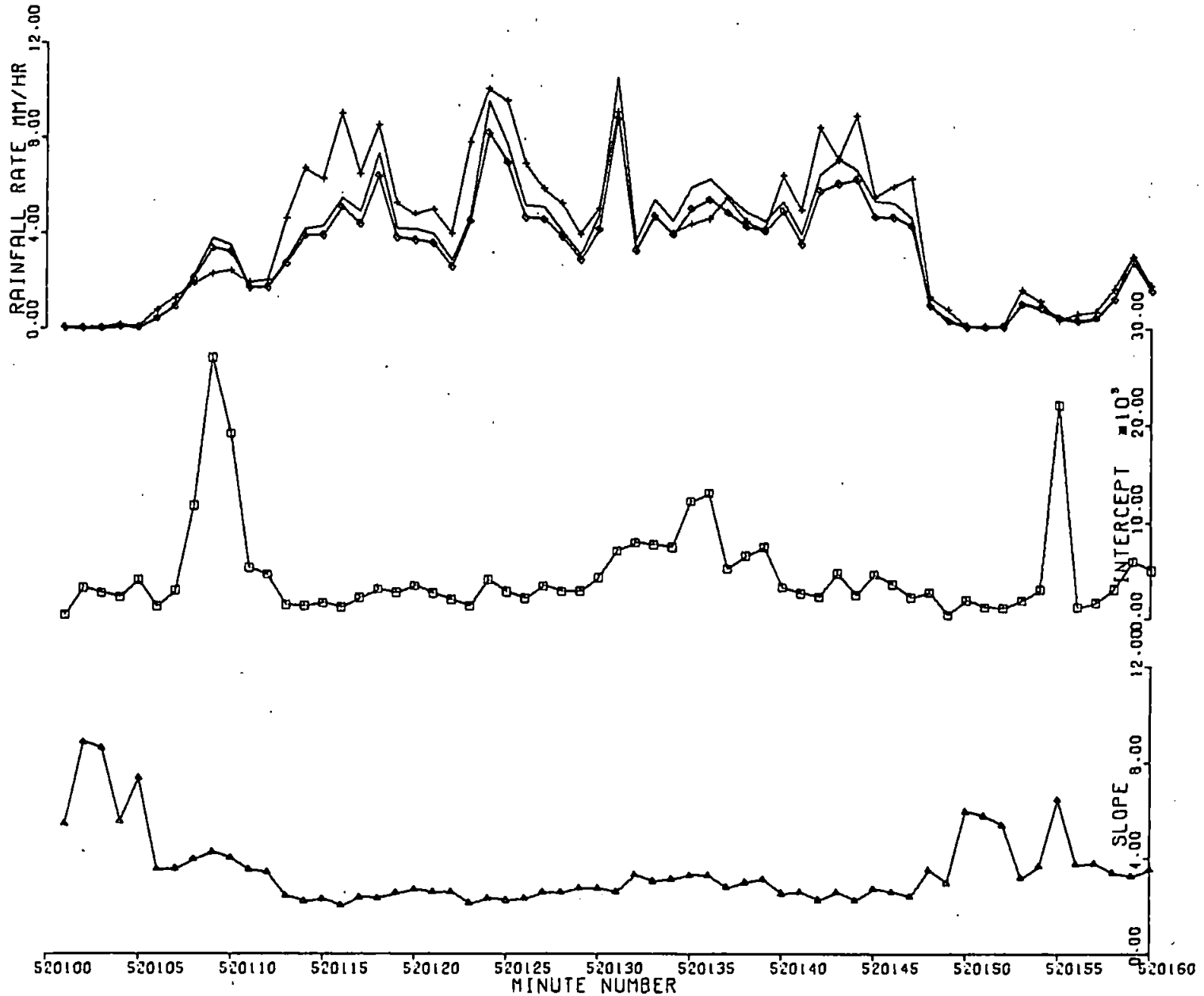

Figure 4.7

Totals

R_D : 3.49 mm

R_Z : 4.00 mm
(rms error: 0.769)

R_{ZN}: 3.16 mm
(rms error: 0.186)

$Z = 200\ R^{1.6}$

relationship presented here and the results show a slight improvement in the hourly total, reducing the rms error by more than half.

It is interesting to note that substituting the original M-P Z-R relationship ($Z = 220\ R^{1.6}$) into the curve of best fit yields $N_o = 8.7 \times 10^3\ m^{-3}\ mm^{-1}$, which is in fair agreement with their observed value ($8 \times 10^3\ m^{-3}\ mm^{-1}$).

4.1.7 Application of N_o-A relationship

It is a relatively simple matter to compute N_o from distrometer observations, but to apply a similar variable Z-R relationship to an operational radar would require a quite different technique to estimate N_o.

Implicit in the description of these distributions as 'large' or 'small' drop spectra is a consideration of the growth processes in the vertical. WALDVOGEL (*12*) made such observations in conjunction with a vertically-pointing radar and showed that these distribution shapes may be characterised by differing reflectivity profiles. A bright-band type echo (when the radar beam intercepts snow or ice just below the 0°C isotherm) corresponded to a large drop spectrum whilst a high altitude and no bright-band echo was observed above a small drop spectrum. In the first case the growth of large snowflakes would be possible, causing a large drop spectrum at the ground and in the latter, the melting of small graupel may lead to a predominance of small drops.

When a meteorological radar is operated to produce data at a series of elevations, it may be possible to estimate N_o at the ground by

considering the changing vertical Z profile. To investigate the applicability of this approach to the real-time calibration of an operational radar, a second data collection exercise was initiated.

4.2 THE SECOND DATA SET

4.2.1 Philosophy

The first data set collected from FEB 1978 to MAY 1978 consisted of distrometer and St. Mawgan gauge observations. To investigate the possibility of applying a variable Z-R relationship to actual radar data, a second data set was collected to which were added radar observations made from Camborne and gauge records at Constantine Bay.

The aim was to co-ordinate radar and distrometer observations, deducing variable Z-R relationships for the radar by computing N_0, and comparing the results with the "ground truth" calibration technique (*55*, *56*). If this approach proved acceptable the observed N_0 values would be examined with reference to the growth processes aloft, as revealed by the radar data in the vertical. To carry out this work, information on the operational procedure of the radar was obtained and an original interpretation technique developed.

4.2.2 Distrometer record

The first distrometer data set was obtained from the continuous operation of the instrument over a period of several months. The second distrometer data set was obtained from selected observations between DEC 1978 and MAY 1979. These observations were continuously monitored to eliminate any uncertainty about equipment malfunction and to note any high acoustic noise levels which might affect the results.

The paper tapes were again analysed using RAINDROPS and a modified version of RAINSPECTRA, producing a continuous record even when no rain was falling.

Data were obtained on 5 occasions identified by the numbers 51, 52, 53, 54 and 55 as detailed in Table 4.3. These data were all written to one magtape - ECCSPECT 44. The data on PT51 and PT52 were not subsequently examined for reasons discussed in 4.3.2.

To ensure that the distrometer was performing satisfactorily, and that the second data set would be consistent with the first, several checks were carried out. As before, the distrometer hourly catches were compared with the St. Mawgan gauge (detailed in Table 5.2) and average raindrop-size distributions computed (see Appendix IV). The relative percentages of N_0 values falling into specified intervals was computed as before (Figure 4.8) and compared to the first data set (Figure 4.4). All these comparisons show that the distrometer performance was satisfactory. The slight displacement of the peak in Figure 4.8 to smaller N_0 values in the case of the second data set is due to the fact that only occasions when some moderately heavy rain was expected were chosen whereas in the first data set all data collected over a longer period were considered. Thus in the latter case the proportion of low rainfall rates will be greater and such spectra typically produce high N_0 values - hence an apparent shift to lower N_0 values in the second set.

4.2.3 Radar record

The meteorological radar located at Camborne in Cornwall (see Figure 2.1) forms part of a mini-network of radars covering part of the UK (*57*) which in turn is part of the FRONTIERS plan (*58*). This 10 cm radar has an on-site minicomputer dedicated to detecting and measuring rainfall over the south west of Britain. During 1978 the onsite hardware was being commissioned using software developed by the Meteorological Office Radar Research Laboratory, Malvern (MORRL).

PT No.	Date	Commenced	Mins		Mins	Total Rainfall (mm)
			From	To		
51	3 DEC 78	1606	510000	510033	33	0.71
52	7 DEC 78	1133	520000	520212	212	4.10
53	27 MAR 79	1132	530000	530431	431	2.64
54	9 APR 79	1300	540000	540480	480	3.78
55	22 MAY 79	1600	550000	550272	272	5.73
				TOTAL	1328	16.96

Table 4.3 Second data set - Distrometer record

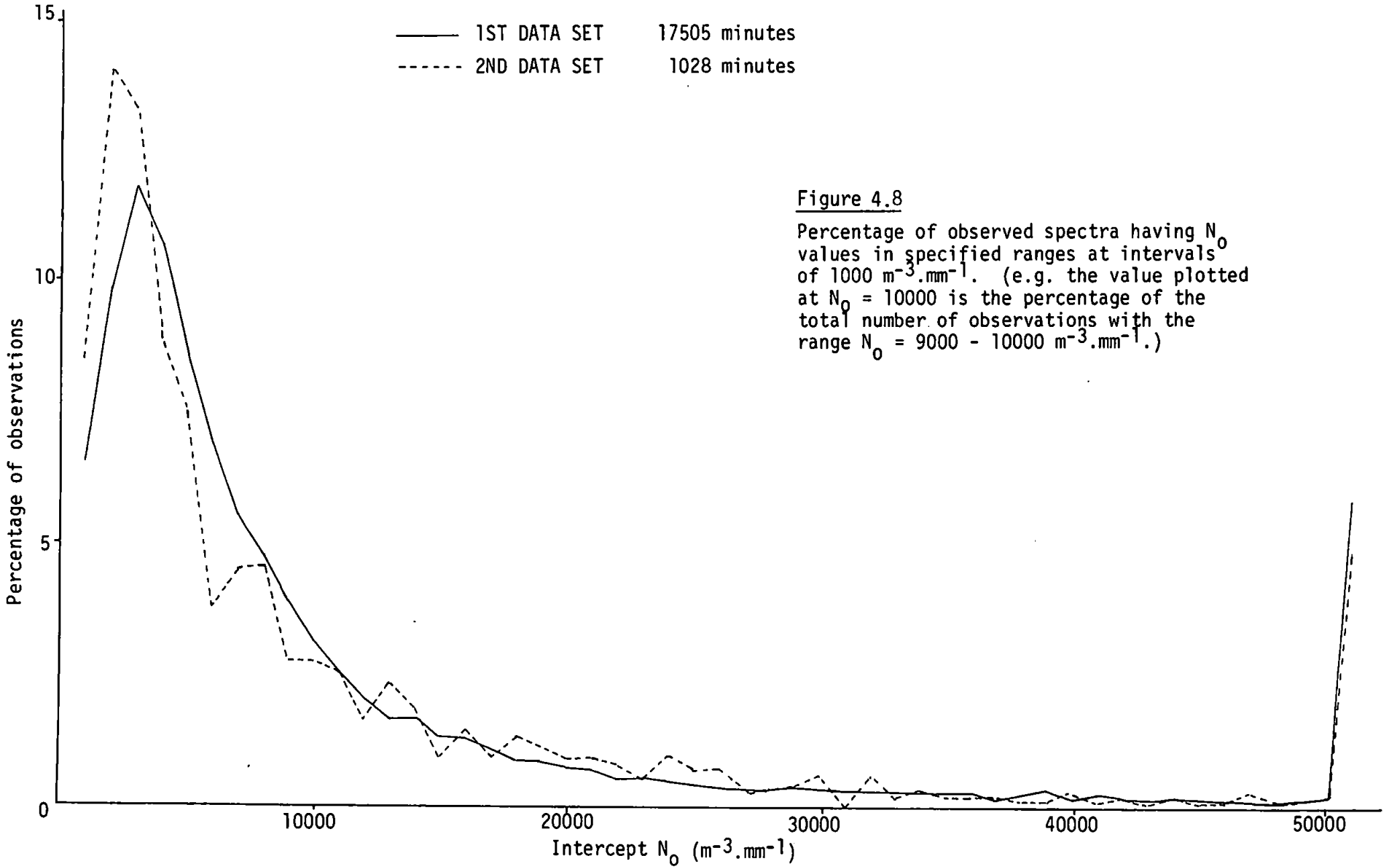

Figure 4.8

Percentage of observed spectra having N_o values in specified ranges at intervals of 1000 $m^{-3}.mm^{-1}$. (e.g. the value plotted at N_o = 10000 is the percentage of the total number of observations with the range N_o = 9000 - 10000 $m^{-3}.mm^{-1}$.)

The radar aerial revolves once every minute and makes observations at four elevations. The time taken to elevate is approximately 15 secs. or a quarter of a revolution. Thus a set of elevations is completed every 5 minutes and a "12 beam task" performed 4 times in an hour. Some modifications are made to the scans to allow for nearby trees and other topography, but these do not affect observations in the sector which includes Constantine Bay and St. Mawgan. Only the operational features of the radar which relate directly to the surface rainfall measurement were considered. The method of converting the azimuthal data to a Cartesian format and the statistical considerations involved in integrating many signal pulses were not investigated in any detail since there was no easy way to affect these features of the operation and the output data had to be accepted as transmitted. However, particular attention was paid to the method of producing rainfall rate data from the radar reflectivity observations and to the proposed method of calibration.

The overall philosophy of the operation of this radar is to measure areal rainfall. It has been shown (*58*, *59*) that this is cost effective in relation to a network of telemetering gauges over areas larger than 3000 km^2. Data are available in real time in the form of colour video displays of the lowest elevation every 15 minutes. Such a display is in use at Camborne Met. Office and the Regional Forecasting Office at RAF Mountbatten, Plymouth, transmitted by GPO line.

Alternatively the data are available in hard-copy form approximately three weeks in arrears. This format includes the data at four elevations for every scan and was thus more comprehensive and most suitable for the present purpose. The Meteorological Office Radar

Research Laboratory very kindly made these data available to the author, free of charge.

An example of one page of hard copy data is given in Figure 4.9, comprising the results of a single scan. The key to the rainfall rate symbols appears in Table 4.5.* The grid squares in this case are 5 km x 5 km; a representation of the lowest elevation data on a 2 km x 2 km grid was also available, but not used in the present investigation.

Radar data were requested to correspond with the distrometer records and the required St. Mawgan and Constantine Bay observations abstracted by hand using a transparent overlay. The results were transferred to cards and subsequently written to a magtape archive. The reduction of these data to a convenient form for calculating hourly totals and producing vertical profiles is discussed in 4.3.

The points at which observations were made (St. Mawgan and Constantine Bay) were not at the centre of the grid squares containing them. This is shown in Figure 4.10 and illustrates one of the many problems which are encountered in the comparison of point and areal measurements.

The advantages of radar over a raingauge network are best exploited by measuring the precipitation areally. Because of the spatial variations in Z-R relationships already discussed, the evaluation of R and Z at a point to produce such relationships is not an ideal solution, although widely reported. However, any other method which employs such direct measurements is likely to be very complex and probably uneconomic. A method which uses the areal radar data themselves to regulate the calibration is more likely to overcome this problem. Therefore in

* p. 134

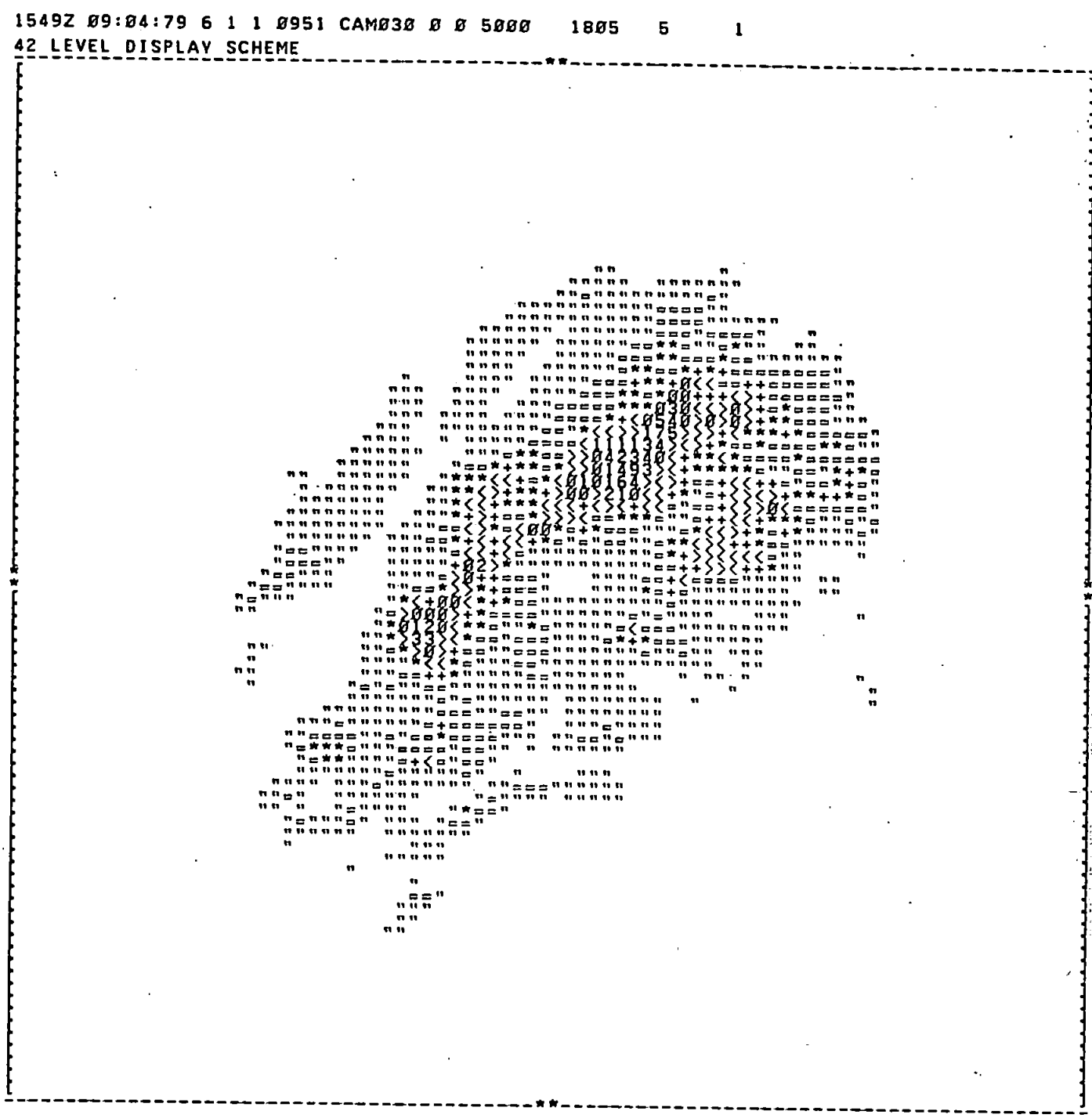

Figure 4.9 Example of radar hard copy data at 1549 on 9 APR 1979 (PT 54) showing 5 km grid data at lowest elevation ($0^{o}.5$).

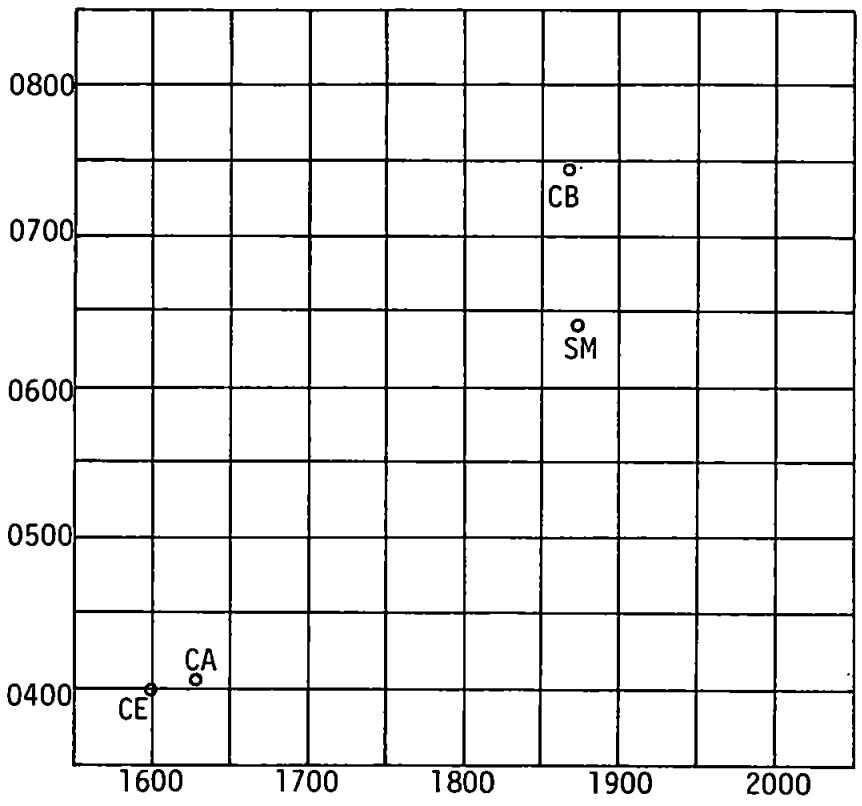

Figure 4.10 5 km grid over part of Cornwall showing National Grid and relative positions of the locations referred to. Scale; 1 : 500000.

		National Grid Reference		
CE	Centre of radar display	1600	0400	(see Fig. 4.9)
SM	St. Mawgan distrometer	1871	0642	
CB	Constantine Bay autographic gauge	1867	0745	
CA	Camborne radar	1627	0406	

analysing the Camborne data an approach which allowed for a good spatial and temporal representation was adopted.

4.2.4 Constantine Bay record

The integration of radar and raingauge data to improve surface rainfall measurements was demonstrated by the National Severe Storms Laboratory, Oklahoma (*55*) and the technique has been tested and developed further in the UK, notably during DWRP (*59*). The principle of this "ground truth" technique is that one or more calibration sites are chosen within the radar field and telemetering gauges are installed. The amount measured by the gauge is compared in real time with the rainfall measured overhead by the radar. A calibration factor, given by the ratio of these values, is determined and applied to the remainder of the radar field, sometimes with a weighting factor based on the geography of the area.

In DWRP the radar estimates of areal rainfall were greatly improved by using this technique and three rules were adopted:

(i) No gauge cluster shall be used for calibration unless the rainfall rate is greater than 1 mm hr^{-1}.

(ii) No gauge cluster shall be used if the ratio between the gauge value and the radar measured value is greater than 5 or less than 0.2. Further experience may modify this rule.

(iii) Inverse distance weighting factors shall be applied.

The basis for comparison was by one-hourly totals which to some extent smoothes out the short-term fluctuations in the point measurements

which would not be observed by the areal measurements. Subsequent work on the calibration factors for the Camborne radar (*60*) has used a lower limit of 0.4 mm hr^{-1} for hourly comparisons.

This operational report assesses the performance of Camborne radar against 13 autographic gauge archives. It was found that the ratio between the radar and gauge hourly totals was reduced from 1.5 in November 1978 to about 0.4 in May 1979. The mean values for March, April and May were 0.36, 0.42 and 0.43 respectively, indicating that the radar performance had become more stable. This improvement was attributed to more effective removal of clutter - unwanted return signals which are produced by targets other than precipitation elements, discussed in 4.3.2.

The possibility of improving the radar-derived measurement of areal rainfall by the application of these calibration factors alone is not seriously contemplated. Such an approach would ignore the short term meteorological fluctuations which have been discussed earlier but any seasonal variations might be compensated for. However, the analysis of the second data set includes the results of applying these factors on a monthly basis.

The rainfall, measured at a site other than Camborne (radar) or St. Mawgan (distrometer), was required to enable a "ground-truth" calibration of the radar to be carried out. Operational considerations required that the author should make these measurements personally, which precluded the use of other rainfall archives. The Meteorological Office intended to use the Constantine Bay site for real-time calibration at some later date and therefore permission was sought to site recording equipment at the same location. Two advantages accrued from this decision - gauges could conveniently be placed at the site en

route for RAF St. Mawgan and subsequently recovered on the return journey to Plymouth, and any unexpected anomalies that might arise by calibration from a site, other than the site intended for when the radar was fully commissioned, would be removed.

A "Casella" tilting syphon autographic gauge was sited at the Constantine Bay Golf and Country Club, a few metres from the site to be used subsequently by the Meteorological Office. A 5 inch check gauge was also placed a short distance away. These gauges were operated during the collection of the data on the last 3 tapes in Table 4.3. A hyetogram from the gauge is shown in Figure 4.11 and the catch totals appear in Table 4.4.

The hyetograms were measured in half hour periods to facilitate subsequent analysis and radar calibration. These results together with the relevant radar totals are shown in Table 5.2*

* p. 154

PT No.	Autographic gauge total (mm)	5 inch check gauge total (mm)
53	2.4	2.4
54	8.1	7.9
55	5.3	5.2

Table 4.4 Comparison of Constantine Bay gauges

PT 54

Gauge No..... Year 1979 Month APRIL Time on 9 d.....hrs. Time off .....d.....hrs. Duration of Rainfall.....h.....m.

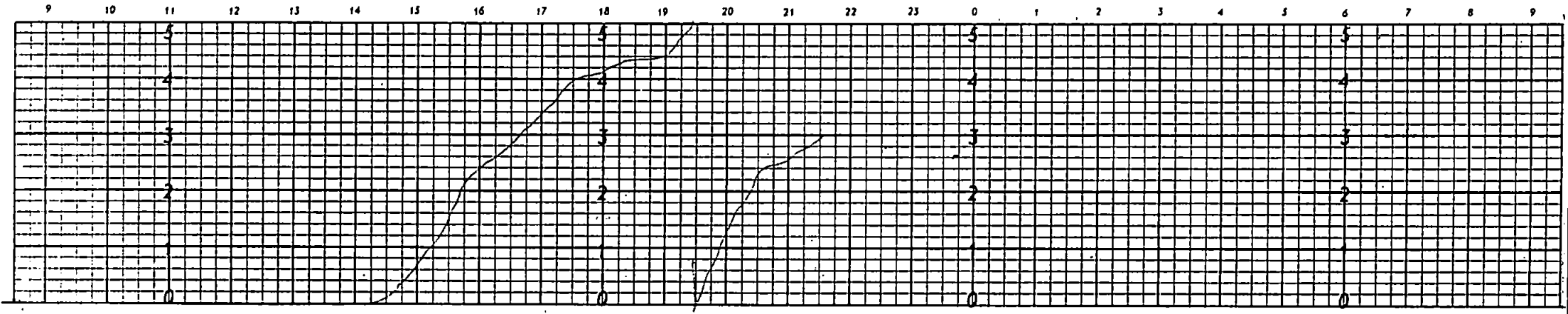

Scale, 1 mm = 10 mm on chart Station..... CASELLA LONDON ~~Total 9h to 9h~~ Recorder 8·1 mm Check gauge 7·85 mm PRINTED IN ENGLAND No. 345

Figure 4.11 Hyetogram from Constantine Bay gauge. (PT 54)

4.3 ANALYSIS OF RADAR DATA

4.3.1 Conversion to Z values

The radar data were received in hard copy form (Figure 4.9) which shows R values at each scan. Table 4.5 shows the meaning of the symbols displayed together with an integer code which was used by the author to facilitate off-line processing. The data presented here are therefore rainfall rates allocated to 43 specified ranges and not exact values. More precise data are available only in a magnetic tape format which was not compatible with the available computer facilities.

The nature of the investigation required an analysis of the Radar Reflectivity factor values. The onsite computer employs a fixed Z-R relationship - $Z = 200\ R^{1.6}$ - and therefore these R values could be easily converted to the appropriate Z values. This was achieved by converting the upper and lower class limits for each interval to their Z values and then converting the mean back to R. For example the rainfall rate denoted by the symbol '+' (integer code 39) represents $0.75 \leqslant R < 1.0$ mm hr^{-1} which is equivalent to $126 \leqslant Z < 200$ mm^6m^{-3}. The mean is 163 mm^6m^{-3} ($\overline{Z}$) which by $Z = 200\ R^{1.6}$ gives $\overline{R} = 0.88$ mm hr^{-1}.

The full set of $\overline{R}$ values is given in Table 4.5 together with the decibel equivalent of Z (dBZ : given by $10 \log_{10} Z$) which is used later (4.3.5). An arbitrary upper limit of 500 000 $mm^6\ m^{-3}$ was set for the largest category although no rainfall rates this high were observed. Errors which could arise through this interpretation of the data are discussed in 4.3.6.

SYMBOL	INTEGER CODE	R mm hr^{-1}	$\overline{Z}$ mm^6 m^{-3}	$\overline{R}$ mm hr^{-1}	dBZ
"	36	< 0.25	11	0.16	10
=	37	< 0.5	44	0.39	16
*	38	< 0.75	96	0.63	20
+	39	< 1.0	163	0.88	22
<	40	< 1.375	267	1.20	24
>	41	< 1.875	440	1.64	26
Ø	42	< 2.5	707	2.20	28
1	1	< 3.0	1013	2.76	30
2	2	< 3.5	1322	3.26	31
3	3	< 4.0	1661	3.75	32
4	4	< 4.5	2029	4.26	33
5	5	< 5.0	2423	4.75	34
6	6	< 5.5	2843	5.25	35
7	7	< 6.0	3288	5.75	35
8	8	< 6.5	3757	6.25	36
9	9	< 7.0	4248	6.75	36
A	10	< 7.5	4762	7.25	37
B	11	< 8.0	5299	7.75	37
C	12	< 10	6767	9.03	38
D	13	< 12	9311	11.03	40
E	14	< 14	12150	13.02	41
F	15	< 16	15266	15.02	42
G	16	< 18	18641	17.02	43
H	17	< 20	22265	19.02	43
I	18	< 22	26125	21.02	44
J	19	< 24	30213	23.01	45
K	20	< 26	34520	25.01	45
L	21	< 28	38809	27.01	46
M	22	< 30	43764	29.01	46
N	23	< 32	48689	31.01	47
O	24	< 40	62185	36.13	48
P	25	< 48	85561	44.11	49
Q	26	< 56	111652	52.09	50
R	27	< 64	140281	60.08	51
S	28	< 72	171303	68.07	52
T	29	< 80	204602	76.06	53
U	30	< 88	240076	84.06	54
V	31	< 96	277642	92.05	54
W	32	< 104	317222	100.05	55
X	33	< 112	358752	108.04	56
Y	34	< 120	402171	116.04	56
Z	35	> 120	462173	126.58	57
	43	0	0	0	0

Table 4.5 Radar data - 43 level display symbols

4.3.2 Occultation and clutter

Occultation and clutter are factors which affect the operation of all types of radar. Occultation of the radar beam is caused by the screening effect of the land and therefore affects the lowest elevation only. This attenuation can be allowed for by using an azimuth-dependent correction factor. The values for St. Mawgan and Constantine Bay (1.33 and 1.16 respectively) were obtained from MORRL. The onsite computer was not programmed for this correction until 2.7.79 and therefore all subsequent processing of the radar data presented here involved applying the correction manually to the lowest elevation.

The rainfall rate values produced by this procedure are shown in Table 4.6. All the data analysed are encompassed by the first 17 intervals and therefore only those rainfall rates are tabulated.

Other sources of attenuation, for example the range-dependent effect, are dealt with automatically by the radar computer.

The term "clutter" describes strong return signals which are not desirable; the interpretation of what is desirable depends on the requirements of the user. In the case of a marine radar the operator is interested in permanent echoes caused by land or ships and attempts to remove the transitory clutter which may be due to waves or rain. For the radar meteorologist it is this transitory clutter which is of interest and if an attempt is to be made to quantify the level of signals returned from rain, then the existence of strong and permanent clutter can lead to serious errors.

The Camborne radar is corrected for this effect by making "clutter maps" in dry spells and then applying them in a negative sense to the

Symbol	Integer Code	St. Mawgan		Constantine Bay	
		$\overline{Z}$ $mm^6\ m^{-3}$	$\overline{R}$ $mm\ hr^{-1}$	$\overline{Z}$ $mm^6\ m^{-3}$	$\overline{R}$ $mm\ hr^{-1}$
"	36	15	0.20	13	0.19
=	37	59	0.47	51	0.43
*	38	128	0.76	111	0.70
+	39	217	1.06	189	0.97
<	40	355	1.44	310	1.32
>	41	585	1.96	510	1.80
Ø	42	940	2.64	820	2.42
1	1	1347	3.30	1175	3.03
2	2	1758	3.90	1533	3.58
3	3	2209	4.49	1927	4.13
4	4	2699	5.09	2354	4.67
5	5	3223	5.69	2811	5.22
6	6	3781	6.28	3298	5.77
7	7	4373	6.88	3814	6.32
8	8	4997	7.48	4358	6.87
9	9	5650	8.08	4928	7.41
A	10	6333	8.67	5524	7.96

Table 4.6 Radar data - St. Mawgan and Constantine Bay values with occultation correction applied

data, thus removing the areas of strong permanent echo caused by the local topography. To minimise this problem at close range the data from scans at the lowest 2 elevations are combined automatically on site up to a range of 30 km. (The St. Mawgan and Constantine Bay sites are both more than 30 km from Camborne.) This technique became effective in March 1979 (*60*) and therefore data collected before this date were not fully analysed because of the possibility of significant errors arising.

4.3.3 Interpolation of Z values

As noted in 4.2.3, the radar produces 48 sets of data per hour but at any particular elevation values are produced at approximately 5 minute intervals. The distrometer data are available at one minute intervals and therefore to provide the most detailed comparison some interpolation of the radar data was required.

The Z values under consideration are representative of relatively large volumes of atmosphere and therefore a reasonably smooth transition from one observation to the next would be expected. Interpolation was performed by taking four adjacent observations and fitting a cubic to the logs of the Z values; the interpolated values were then obtained from the curve between the 2nd and 3rd observations. This approach preserves the trend of the values in the five minute intervals before and after the period under consideration.

This technique is more fully described in Appendix V and illustrated graphically in Figures 4.12, 4.13 and 4.14 with some data from PTs 53, 54 and 55. These interpolated data were written to a magnetic tape file - ECCRADAR 3, together with the one minute time-marks to coincide with the distrometer record.

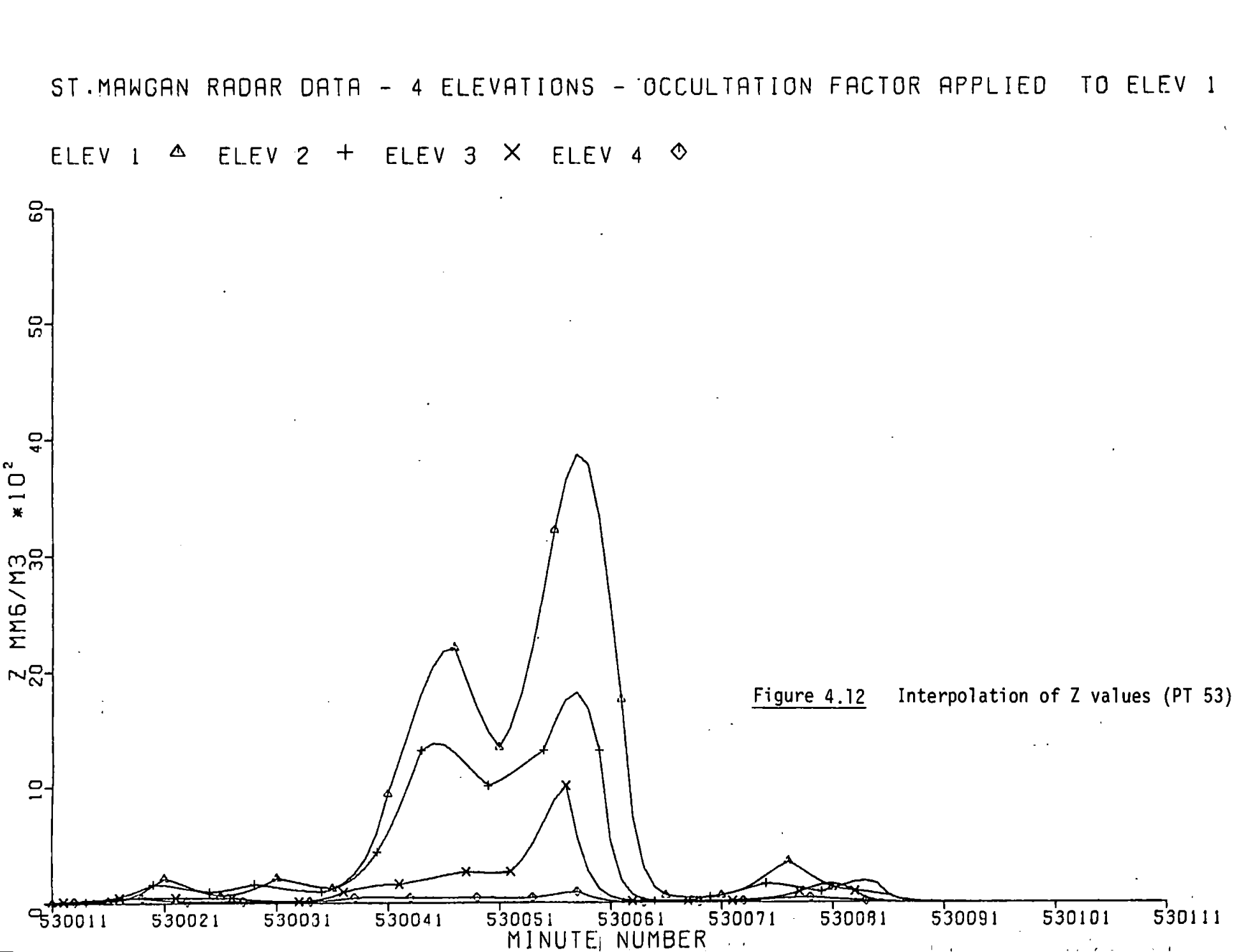

Figure 4.12 Interpolation of Z values (PT 53)

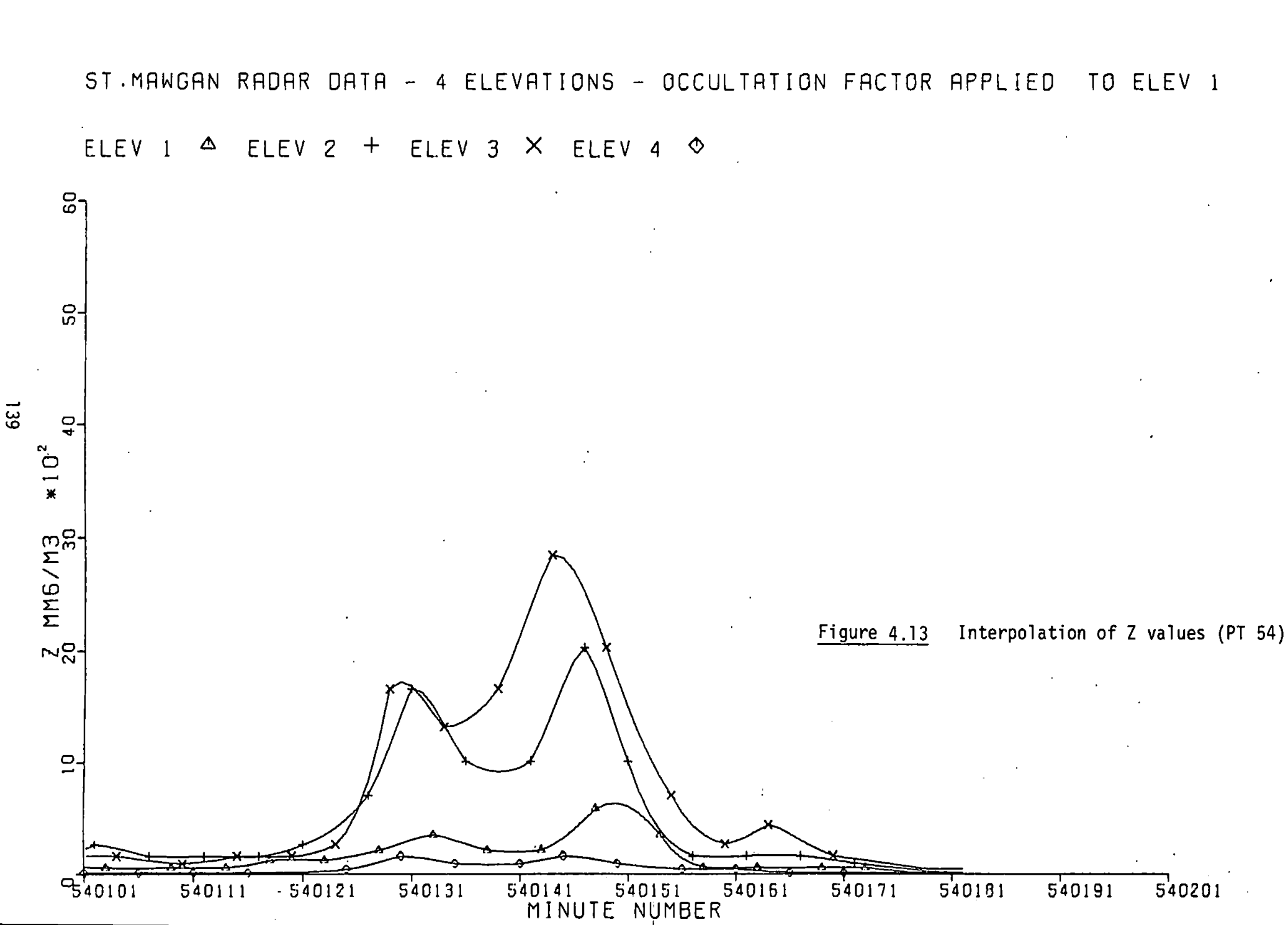

Figure 4.13 Interpolation of Z values (PT 54)

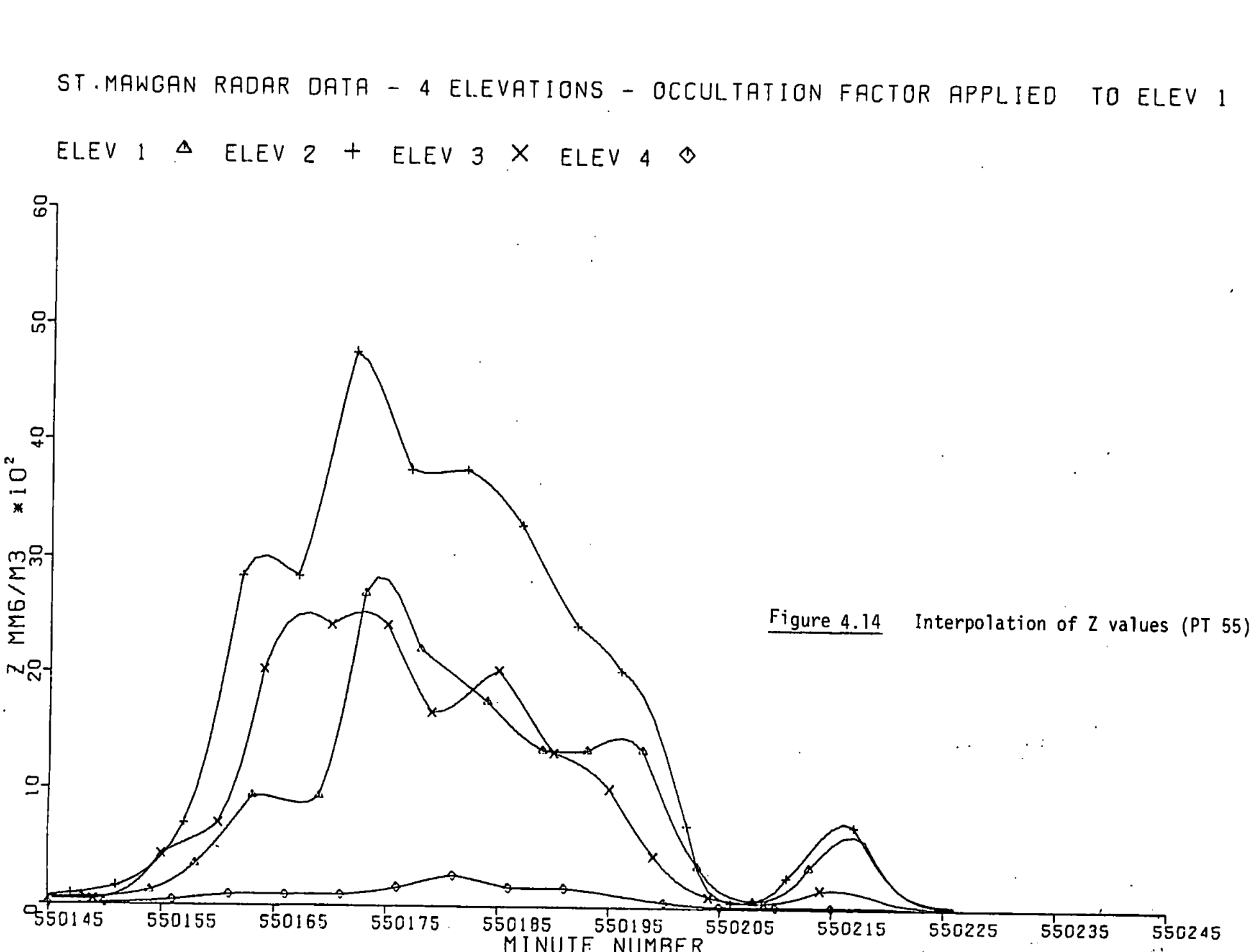

Figure 4.14 Interpolation of Z values (PT 55)

4.3.4 Half-hourly totals

The basic interval for comparison of gauge, distrometer and radar data was chosen to be 30 minutes. This would allow a more detailed study than if hourly totals were used (as in the "ground-truth" calibration technique described in 4.2.4).

The radar rainfall total for the 30 minute interval is given by the sum of the 6 R values for that period divided by 12. The total derived from the interpolated radar values was also calculated for comparison.

4.3.5 Time-height profiles

The representation of radar data as a time-height display has been reported (*61*, *62*, *63*) and is a useful technique since it allows a comprehensive appreciation of the observations. Such profiles are normally produced by Doppler or vertically-looking radar but a similar representation was obtained from the present data by plotting contours through the interpolated Z values described earlier (4.3.3).

The height of each elevated beam over St. Mawgan was calculated and the values of Z (in dBZ) for alternate minutes at these heights were used as the input data for a computer program which produced time-height plots such as the example in Figure 4.15. The contouring package available (CONB) required data at all grid points which meant that the 64 values (16 time ordinates x 4 elevations) had to be expanded to 96 values (16 time ordinates x 6 elevations) covering 0-2.5 km above St. Mawgan. This was achieved by further interpolation, performed objectively and by a linear process.

The example in Figure 4.15 shows how the original data (underlined) relate to the time-height contours. The representation satisfies all the values except for 2 which are slightly in error. This arises because they occur on the odd minutes which were not used as input data. This somewhat coarse interpretation was inevitable due to the relative inflexibility of the contouring package. Hence this diagram must be considered as a qualitative representation, indicating the general structure of the atmosphere above St. Mawgan. The patterns revealed in the time-height profiles generated from the second data set are discussed in the next chapter.

4.3.6 Errors

There are several possible sources of error in this analysis; some of these errors are already in the data when received and others arise through the analytical techniques employed. One of the major errors in the former category is due to the "bright-band" effect.

This effect is observed when the radar beam intersects the 0°C isotherm where melting snow or ice particles may be present. It is revealed as an increase in echo intensity in a narrow altitude range and is mainly due to changes in the dielectric properties of the reflectors causing an increase in reflectivity of typically 6dB (*64*). This causes the radar to over-estimate the amount of precipitation. A radar scanning in azimuth at a low elevation will show a roughly annular band of enhanced echo at ranges where the radar beam intersects the sleet (*65*). The Camborne radar will eventually apply a correction for this effect based on work carried out by the Meteorological Office (*65* and *66*).

530058 - 087
1230-59
27.3.79

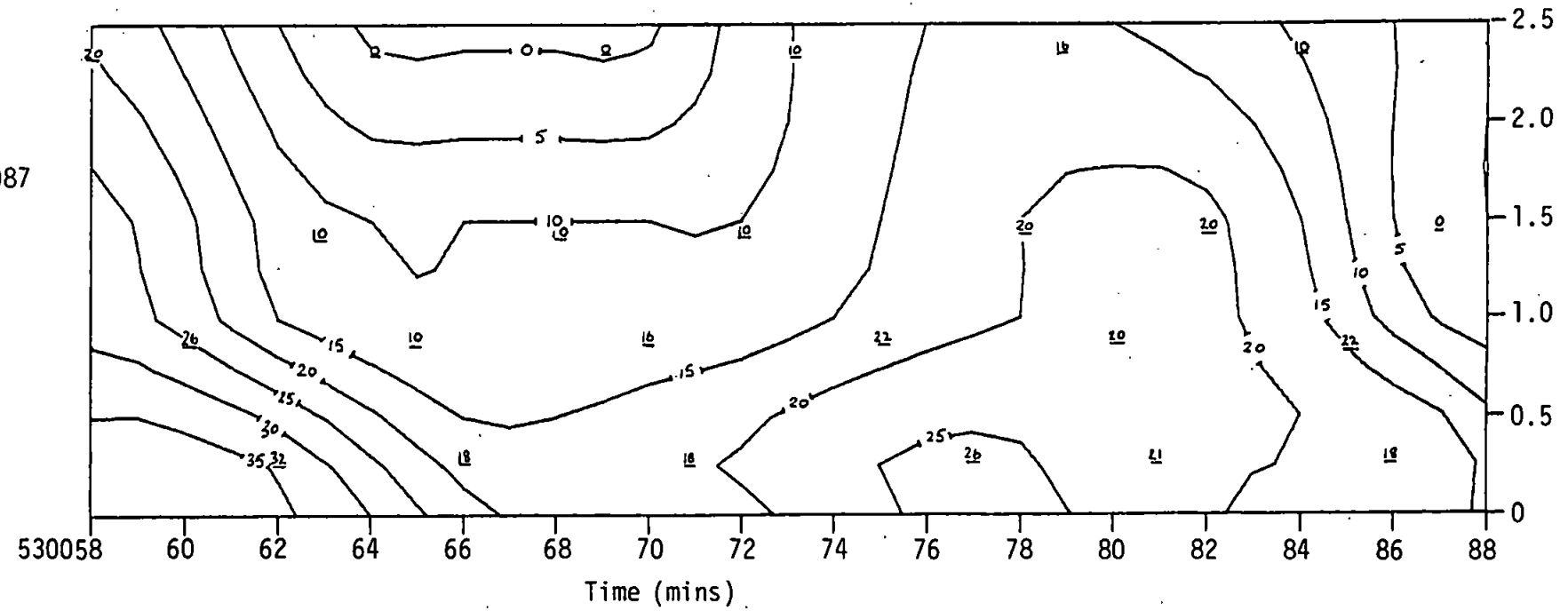

Figure 4.15 Time-height radar profile showing radar reflectivity contours at 5 dBZ intervals. The original radar data are shown underlined.

The average height of the melting layer in England during the winter is about 1 km (*67*). Ascent data from Camborne (Appendix VI) reveal that for the times under consideration the 0°C isotherm was at about this level and therefore would not affect the data in the lowest elevation. Hence the "bright-band" effect should not lead to errors in the surface rainfall totals but may affect the time-height profiles above 1 km.

The time shown on each page of the radar hard copy data is the time at which the data were written to the magnetic tape file on site and could be up to 2 minutes after the actual time at which they apply. This introduces a possible timing error which was alleviated to some extent by using a five-minute moving average of distrometer data as described in 5.1.1.

Some difference is likely to exist between the precipitation measured in the lowest elevation (which is approximately 300 m above the ground over St. Mawgan), and the surface rainfall. This may be due to the drift of precipitation in the wind and growth or evaporation of the raindrops below the cloud base. Such an error is difficult to accommodate and is further complicated by the fact that the measuring points are not central in the grid squares (Figure 4.10). Allowance for wind drift has been made in previous work (*56*) and some reduction in error achieved; however in this investigation no attempt was made to effect such corrections. The aim ultimately is to simplify the variety of input data to the radar measurement of precipitation (e.g. by removing the need for calibrating gauges) and a further input of anemograph and possibly other observational data introduces more complexity.

The method of conversion of R values to Z values, described in 4.3.1, introduces an error because a rainfall rate at approximately the mid-point of a range is used rather than an exact value. The magnitude of this error depends on the amount of rainfall recorded. At low rainfall rates the intervals span only a few tenths of a millimetre per hour whereas at higher rates the interval may be 2.0 mm or more. The extreme errors which could occur in the half hour total would be when all 6 values were either at the lowest end of the range or at the highest.

For the first half hour period analysed (see Table 5.2), the total obtained by using the values in Table 4.6 was 1.50 mm. If all the values had actually been the lowest possible, then a total of 1.36 mm is obtained and if the highest values are selected then a larger total of 1.62 mm results. This represents an error of approximately ±8%. Such extreme cases are unlikely to arise and, since the example chosen was for the highest rainfall amount, even if they did the error would be smaller than this.

CHAPTER FIVE

COMBINING DISTROMETER AND RADAR DATA

5.1 METHOD

5.1.1 Averaging of data

The second data set forms the basis of a quantitative exercise to test the efficacy of using distrometer observations to improve the accuracy of radar rainfall measurement. This approach is limited by the ability of a point measurement to represent an area. To improve the representation of a gauge for areal calibration it has been recommended (*68*) that mean calibrations over a period of time should be used.

A period of 30 minutes was used as the basic time unit to compare rainfall measurements. Thus each time unit includes 30 raindrop-size distributions, 24 radar observations and two autographic gauge totals.

The radar completes a set of elevations every 5 minutes and thus offers a near real-time display with a relatively fast update. To relate the distrometer record, five minute moving averages were computed for each minute by meaning the four previous and the current values of R and N_o. This has the effect of making the raindrop-size distribution more representative because it is applied over a longer period of time. The computed value also appears about 2 minutes "late" which improves temporal correlation with the radar because of the delay in writing the data on site. (See 4.3.6.)

5.1.2 Selection of data

Three portions of data were selected from the second data set for detailed analysis. It was desirable to combine variety with continuity and to this end 16½ hours was selected in three continuous sets which included the heaviest rain observed on PTs 53, 54 and 55 and for which a full set of gauge and radar data was archived. Some of the half hour

periods included have no rainfall recorded by one or more of the devices. These were included to preserve continuity and also to see the effect on the results. It is obviously as important that the radar should not record rain when it is not raining as that it should record accurately when it is raining.

The selected data are detailed in Table 5.1 in 33 numbered half hour periods. These numbers will be referred to hereafter to identify each period.

5.1.3 Processing of data

Radar and distrometer data from the magtape archives described earlier were read simultaneously by a computer program called PANORAMA. This program calculated N_0 values and performed the averaging process described above, in addition to computing the radar-derived rainfall totals for each half hour period at all four elevations. The data for the lowest elevation were enhanced by applying the variable Z-R relationship technique using the curve described in 4.1.6. In simulation of real time, each interpolated Z value was converted to its equivalent R value using a relationship determined by reference to the 5 minute moving average of N_0. When an average N_0 value was not available (when there were not 4 consecutive values preceding the minute under consideration) the spot value was used. Where neither the averaged nor the spot value was available, the Z-R relationship reverted to the conventional form ($Z = 200\ R^{1.6}$).

The program also contained options for using a different Z-R relationship, such as the one reported in 3.3.1 and the possibility of altering the raw Z value. A further option allowed the application

Half hour period no.	PT No.	Date	Time (GMT)	Time (mins)
1	53	27.3.79	1200 - 29	530028 - 057
2			1230 - 59	530058 - 087
3			1300 - 29	530088 - 117
4			1330 - 59	530118 - 147
5			1400 - 29	530148 - 177
6			1430 - 59	530178 - 207
7			1500 - 29	530208 - 237
8			1530 - 59	530238 - 267
9			1600 - 29	530268 - 297
10			1630 - 59	530298 - 327
11			1700 - 29	530328 - 357
12			1730 - 59	530358 - 387
13			1800 - 29	530388 - 417
14	54	9.4.79	1330 - 59	540030 - 059
15			1400 - 29	540060 - 089
16			1430 - 59	540090 - 119
17			1500 - 29	540120 - 149
18			1530 - 59	540150 - 179
19			1600 - 29	540180 - 209
20			1630 - 59	540210 - 239
21			1700 - 29	540240 - 269
22			1730 - 59	540270 - 299
23			1800 - 29	540300 - 329
24			1830 - 59	540330 - 359
25			1900 - 29	540360 - 389
26			1930 - 59	540390 - 419
27			2000 - 29	540420 - 449
28	55	22.5.79	1730 - 59	550090 - 119
29			1800 - 29	550120 - 149
30			1830 - 59	550150 - 179
31			1900 - 29	550180 - 209
32			1930 - 59	550210 - 239
33			2000 - 29	550240 - 269

Table 5.1 Selected data

of the mean monthly calibration factors described in 4.2.4. The three relevant records, R_Z, R_D and N_o were then plotted to facilitate comparison with the time-height radar profiles.

The results presented here, which use the fixed Z-R relationship, are confined to the widely accepted version with A = 200. The use of the relationship derived from the first data set ($Z = 264\ R^{1.68}$) makes a small difference to the rainfall totals. The intention here is to compare the new technique with an established method rather than yet another slight variation on the conventional approach.

5.1.4 Representation of data

The processed data described above have a considerable range of values and many discontinuities. To facilitate the comparison with the time-height profiles a representation was devised which used the largest scale possible whilst allowing all the data to be plotted on the same axes. This was achieved by using a truncated logarithmic scale for the meteorological variables and the same linear scale on the horizontal time axis. Values of R_Z and R_D below 0.1 mm hr^{-1} are therefore omitted and N_o values appear only when the corresponding R_D value is to be plotted. These plots together with the relevant time-height profiles appear in Appendix VII.

5.1.5 Comparison of results

The minute-to-minute correlation of the distrometer and radar derived rainfall rates may be judged by eye from the Figures in Appendix VII. To compare the half-hourly totals, a numerical approach was adopted.

Comparison of radar and gauge data has previously been made by comparing mean percentage differences, regardless of sign (e.g. *59*). This method suffers from three main disadvantages. Firstly, when rainfall rates are very low, small absolute differences result in large percentage differences and may distort any conclusions. Secondly, it is impossible to compare results in this way when one of the totals under consideration is zero, and finally, when a result is obtained it does not directly indicate the magnitude of the difference.

Despite these disadvantages, this method was used to analyse the results to facilitate comparison with previous work and, in addition, two other methods were considered. The work already referred to at the National Severe Storms Laboratory, Oklahoma (*55*), used a root mean square (rms) error as a comparative measure. Reductions of over 20% in the rms error were achieved when the radar was calibrated with one gauge. This method also has disadvantages - particularly if most of the linear differences are of the same sign. A small rms error may be obtained from a succession of small differences, but if they are all deficits, the net effect may be quite serious. Hence a rms cumulative error was also computed. This is obtained by calculating the rms value of the cumulative differences. The methods used to calculate these comparative measures are explained in Appendix V.

A further problem encountered in making these comparisons is the choice of the base measurement. Rms errors have been cited previously in this work (4.1.2) where the distrometer was used as the base measurement, deviations from this being described as "errors". For the comparison of the half hour totals from the second data set the choice is not so obvious - either the gauge or the distrometer could be used to assess the radar performance. In the DWRP work an "optimum field" (*56*) was

used for comparison. In this case, data from 62 gauges were interpolated by reference to the radar-derived intensity pattern. A rainfall field is computed which, based on the assumption that each gauge reads correctly, was denoted the "optimum rainfall field". This method approaches the ideal solution more closely, but was beyond the scope of the present work.

Other comparisons are also of interest - for example the difference between the half hour totals derived from 6 actual radar observations and the 30 interpolated values would show the validity of the latter as a reasonable representation of the original data. Therefore the comparisons presented here provide a comprehensive analysis showing the relationship between all the methods used to calculate the half hour totals. The effect of removing the periods when the smallest totals were measured (determined by the St. Mawgan gauge reading less than 0.1 mm) was also examined.

5.2 RESULTS

5.2.1 Distrometer, Gauge and Radar totals

Table 5.2 shows the distrometer, gauge and radar totals at St. Mawgan and Constantine Bay for each of the 33 half hour periods. The various methods produce different totals for the whole 16½ hours although the distrometer and calibrated radar results at St. Mawgan agree well. The ratios between the uncalibrated radar and gauge totals at both St. Mawgan and Constantine Bay also agree very well (0.66 and 0.67 respectively). This indicates that the radar performance is consistent for different grid squares. These ratios are higher than the factors noted in 4.2.4 but the latter did not take account of the occultation correction (*60*). This results in a lower radar-derived total and hence a lower ratio.

5.2.2 Further modification of radar data

The uncalibrated radar totals for both locations are considerably less than the gauge totals which would suggest that the radar is recording a consistently low result. This may be due to a variety of factors, some of which are meteorological, and others associated with hardware considerations. When the radar beam diverges and intercepts precipitation at a greater height, an underestimate may occur through low-level growth remaining undetected. It has been noted previously (4.2.4) that this underestimate may be due to the clutter removal process and the correction factors derived indicated that the radar measured less than half the actual rainfall (*60*). This has been affirmed in a later operational report (*69*) which recommends a range-dependent correction factor to be applied to the radar data to make them more representative. For St. Mawgan this factor is 2.39, applied to the rainfall rate values.

Half hour period no.	St. Mawgan				Constantine Bay		
	Distrometer	Gauge	Radar		Gauge	Radar	
	(mm)	(mm)	Uncal. (mm)	Cal. (mm)	(mm)	Uncal. (mm)	Cal. (mm)
1	1.00	1.6	1.50	1.29	0.5	0.58	0.62
2	0.77	0.8	0.63	(0.63)	0.0	0.29	0.37
3	0.35	0.5	0.40	0.57	0.5	0.35	0.44
4	0.01	0.0	0.02	0.02	0.0	0.00	(0.00)
5	0.10	0.0	0.14	0.09	0.1	0.16	(0.16)
6	0.00	0.0	0.05	(0.05)	0.0	0.02	(0.02)
7	0.00	0.0	0.04	(0.04)	0.0	0.00	(0.00)
8	0.00	0.0	0.02	(0.02)	0.0	0.00	(0.00)
9	0.07	0.1	0.03	(0.03)	0.0	0.03	0.10
10	0.00	0.0	0.03	(0.03)	0.0	0.00	(0.00)
11	0.00	0.0	0.00	0.00	0.0	0.11	(0.11)
12	0.11	0.1	0.11	0.20	1.0	0.54	0.54
13	0.03	0.1	0.03	(0.03)	0.0	0.00	0.00
14	0.00	0.0	0.02	(0.02)	0.0	0.08	(0.08)
15	0.03	0.0	0.07	0.04	0.1	0.18	(0.18)
16	0.29	0.3	0.24	0.21	0.6	0.68	0.85
17	0.71	0.7	0.61	0.69	0.9	0.80	0.92
18	0.52	0.6	0.29	0.26	0.8	0.88	1.82
19	0.22	0.2	0.10	0.18	0.4	0.22	0.44
20	0.27	0.3	0.12	0.36	0.6	0.20	0.50
21	0.35	0.4	0.10	0.33	0.6	0.18	0.72
22	0.07	0.1	0.10	0.10	0.1	0.10	0.10
23	0.01	0.0	0.00	0.00	0.2	0.06	(0.06)
24	0.10	0.2	0.10	0.13	0.1	0.08	0.16
25	0.33	0.5	0.17	0.85	0.8	0.16	0.47
26	0.41	0.8	0.26	1.41	1.3	0.24	0.74
27	0.36	0.4	0.08	0.36	1.0	0.22	1.10
28	0.19	0.2	0.12	0.60	0.1	0.02	0.03
29	0.22	0.3	0.15	(0.15)	0.0	0.06	0.12
30	1.62	1.1	1.42	0.56	0.2	0.51	0.40
31	2.59	3.2	1.31	1.46	2.7	2.43	5.94
32	0.42	0.6	0.36	0.90	2.0	0.80	1.33
33	0.01	0.0	0.00	0.00	0.3	0.06	(0.06)
Total	11.16	13.1	8.62	11.61	14.9	10.04	18.38

Table 5.2 Half-hourly totals

When no rainfall was recorded at the calibration site the uncalibrated radar total is carried forward and contained in brackets.

An underestimate by the radar may also be attributed to the use of a fixed Z-R relationship (*69*, *56*). The latter reference notes that the existence of a systematic error is not in itself of major importance in this application of radar since once known it could be allowed for. Such an error is not serious in a gauge calibration exercise (as evidenced by these results and discussed in 5.3.1) but will significantly affect the variable Z-R relationship approach which is under consideration here.

Therefore to alleviate some of this systematic error a correction was applied to the data by doubling all the interpolated Z values and calculating new totals. This correction procedure was preferred to modification of the R values, as described above, since the radar reflectivity factor is the parameter measured directly. The application of a linear correction factor to rainfall rate, which is related in a non-linear fashion to reflectivity, may introduce a further undesirable variation in the results.

The variable Z-R relationship technique was applied to these modified data and to the original data. The results for these and other methods are tabulated in Table 5.4 which summarises nine different ways of estimating rainfall at St. Mawgan for the times under consideration. These nine methods are explained in Table 5.3.

5.2.3 Comparison of half-hourly totals

The totals in Table 5.4 were compared using the techniques described in 5.1.5. Table 5.5 shows the mean percentage differences, regardless of sign. These comparisons omit the periods when very small or zero rainfall amounts were measured, leaving 22 periods when the St. Mawgan

1	Autographic gauge (G)	
2	Distrometer (D)	
3	Radar - 6 values	$Z = 200\ R^{1.6}$ (R6F)
4	Radar - 30 values	$Z = 200\ R^{1.6}$ (R30F)
5	Radar - 30 values	Variable Z-R relationship (R30V)
6	Radar - 6 values	Gauge calibrated (R6GC)
7	Radar - 6 values	Average monthly correction factors (R6MF)
8	Radar - 30 values (x 2)	$Z = 200\ R^{1.6}$ (R30x2F)
9	Radar - 30 values (x 2)	Variable Z-R relationship (R30x2V)

Table 5.3 Explanation of methods 1-9

The much-abbreviated form in brackets is used to facilitate the identification of methods 1-9 in the tables that follow.

Half hour period no.	Method								
	1 G	2 D	3 R6F	4 R30F	5 R30V	6 R6GC	7 R6MF	8 R30x2F	9 R30x2V
1	1.6	1.00	1.50	1.39	1.29	1.29	3.85	2.14	1.71
2	0.8	0.77	0.63	0.79	0.63	0.63	2.19	1.22	0.97
3	0.5	0.35	0.40	0.36	0.57	0.57	0.99	0.55	0.46
4	0.0	0.01	0.02	0.01	0.02	0.02	0.04	0.02	0.02
5	0.0	0.10	0.14	0.13	0.09	0.09	0.36	0.20	0.18
6	0.0	0.00	0.05	0.04	0.05	0.05	0.12	0.06	0.06
7	0.0	0.00	0.04	0.03	0.04	0.04	0.09	0.05	0.05
8	0.0	0.00	0.02	0.02	0.02	0.02	0.04	0.02	0.02
9	0.1	0.07	0.03	0.03	0.03	0.03	0.08	0.04	0.04
10	0.0	0.00	0.03	0.03	0.03	0.03	0.09	0.05	0.05
11	0.0	0.00	0.00	0.00	0.00	0.00	0.00	0.00	0.00
12	0.1	0.11	0.11	0.09	0.11	0.20	0.25	0.14	0.16
13	0.1	0.03	0.03	0.05	0.03	0.03	0.13	0.07	0.06
14	0.0	0.00	0.02	0.01	0.02	0.02	0.03	0.02	0.02
15	0.0	0.03	0.07	0.06	0.07	0.04	0.15	0.10	0.08
16	0.3	0.29	0.24	0.22	0.24	0.21	0.52	0.34	0.23
17	0.7	0.71	0.61	0.58	0.61	0.69	1.39	0.90	0.63
18	0.6	0.52	0.29	0.34	0.29	0.26	0.81	0.52	0.31
19	0.2	0.22	0.10	0.10	0.10	0.18	0.23	0.15	0.16
20	0.3	0.27	0.12	0.12	0.12	0.36	0.28	0.18	0.20
21	0.4	0.35	0.10	0.10	0.10	0.33	0.23	0.15	0.17
22	0.1	0.07	0.10	0.10	0.10	0.10	0.23	0.15	0.16
23	0.0	0.01	0.00	0.00	0.00	0.00	0.01	0.00	0.00
24	0.2	0.10	0.10	0.09	0.10	0.13	0.23	0.15	0.27
25	0.5	0.33	0.17	0.16	0.17	0.85	0.38	0.24	0.33
26	0.8	0.41	0.26	0.25	0.26	1.41	0.58	0.38	0.41
27	0.4	0.36	0.08	0.09	0.08	0.36	0.22	0.14	0.18
28	0.2	0.19	0.12	0.12	0.12	0.60	0.28	0.18	0.25
29	0.3	0.22	0.15	0.14	0.15	0.15	0.32	0.21	0.22
30	1.1	1.62	1.42	1.32	1.42	0.56	3.07	2.04	1.34
31	3.2	2.59	1.31	1.38	1.31	1.46	3.21	2.13	1.69
32	0.6	0.42	0.36	0.35	0.36	0.90	0.81	0.54	0.44
33	0.0	0.01	0.00	0.00	0.00	0.00	0.00	0.00	0.00
Totals (mm)	13.1	11.16	8.62	8.50	7.06	11.61	21.21	13.08	10.87

Table 5.4 Rainfall estimates at St. Mawgan

Method	Totals (mm)	COMPARED TO								
		1 G	2 D	3 R6F	4 R30F	5 R30V	6 R6GC	7 R6MF	8 R30x2F	9 R30x2V
1	13.1	-	40	115	108	111	62	38	56	53
2	11.00	24	-	72	72	77	49	43	41	39
3	8.23	43	34	-	8	23	40	59	34	30
4	8.17	42	37	10	-	24	45	59	34	30
5	6.75	45	41	22	23	-	41	59	36	34
6	11.30	47	61	115	121	106	-	62	79	61
7	20.28	63	98	151	145	166	122	-	62	76
8	12.56	37	43	54	52	66	64	38	-	24
9	10.39	35	42	54	33	53	48	39	23	-

Table 5.5 Mean percentage differences (St. Mawgan gauge ≥ 0.1 mm)

The magnitude of the mean percentage difference depends on which total is being compared. The larger difference for any given pair occurs when the larger is compared to the smaller.

gauge measured at least 0.1 mm. The mean percentage difference for any method in relation to any other may be examined and this comprehensive treatment includes some comparisons which are of little interest. However, the comparisons between either of the direct surface measurements (gauge and distrometer) with any of the radar-based methods are important. The comparison between methods 3 and 4 (6 and 30 Z values) is of interest because it shows whether or not the interpolation is reasonable and the comparison between the radar-derived totals from fixed and variable Z-R relationships shows the extent to which the former are modified.

Table 5.6 shows the same data interpreted as average and cumulative rms errors whilst Table 5.7 includes all 33 half hour periods. There are some differences between these tables, but they do not affect the results in a qualitative sense. Although not presented here, the mean percentage errors for the whole data set were computed, but only show similar, relatively small differences. Table 5.7 slightly favours the results from applying the variable Z-R relationship technique (because at very low rainfall rates the absolute differences, and hence the rms differences, are very low) and therefore discussion will be confined mainly to Tables 5.5 and 5.6.

The smallest difference which occurs in these tables is between methods 3 and 4. This demonstrates that the interpolation, which was used to expand the radar data to suit the format of the distrometer record, results in only a small deviation from the original data. The difference between the overall totals is also very small, reflected in the cumulative rms error.

Method	TOTAL (mm)									
1	13.1	1 G								
2	11.00	0.24 1.09	2 D							
3	8.23	0.46 1.29	0.32 0.70	3 R6F						
4	8.17	0.44 1.30	0.30 0.71	0.05 0.12	4 R30F					
5	6.75	0.51 1.56	0.38 1.12	0.16 0.87	0.14 0.86	5 R30V				
6	11.30	0.45 0.79	0.44 0.75	0.39 1.03	0.38 1.04	0.36 1.34	6 R6GC			
7	20.28	0.74 2.25	0.80 2.49	0.86 2.59	0.86 2.60	0.99 2.73	0.97 2.38	7 R6MF		
8	12.56	0.37 0.74	0.31 1.31	0.31 1.49	0.31 1.50	0.45 1.72	0.51 1.08	0.56 2.12	8 R30x2F	
9	10.39	0.36 0.76	0.27 0.77	0.14 1.05	0.13 1.05	0.24 1.36	0.35 0.19	0.76 2.37	0.22 1.06	9 R30x2V

COMPARED TO

Table 5.6 Average and cumulative rms differences (St. Mawgan gauge ≥ 0.1 mm)

The upper numbers in each box are the average rms differences; the lower are the cumulative rms differences.

Method	Total (mm)				COMPARED TO				
1	13.1	1 G							
2	11.16	0.20 0.99	2 D						
3	8.62	0.37 1.06	0.26 0.37	3 R6F					
4	8.50	0.36 1.08	0.25 0.43	0.04 0.24	4 R30F				
5	7.06	0.42 1.37	0.31 0.95	0.13 0.88	0.06 0.35	5 R30V			
6	11.61	0.36 0.61	0.36 0.78	0.32 0.87	0.31 0.90	0.29 1.23	6 R6GC		
7	21.21	0.61 2.37	0.65 2.57	0.70 2.59	0.71 2.60	0.81 2.74	0.79 2.45	7 R6MF	
8	13.08	0.30 1.02	0.25 1.43	0.25 1.47	0.25 1.49	0.36 1.71	0.42 1.19	0.46 2.14	8 R30x2F
9	10.87	0.29 0.22	0.22 0.97	0.12 1.03	0.11 1.06	0.19 1.36	0.29 0.57	0.62 2.38	0.18 1.05

9
R30x2V

Table 5.7 Average and cumulative rms differences (all data)

The upper numbers in each box are the average rms differences; the lower are the cumulative rms differences.

The results discussed in 3.1.1 suggest that the gauge and distrometer measurements should agree very well. However in this instance, although the average rms error is low, the cumulative error is relatively high and the overall totals differ by almost 2 mm. In the previous discussion, relating the distrometer catches to syphon gauge readings, hourly differences of this magnitude were observed but over the somewhat longer period under consideration (79 hours), they tended to compensate for each other. In the present data, periods 30 and 31 have large differences, one positive and one negative, and these contribute significantly to the rms errors. These particular differences may be due to the difficulty in accurately interpreting the hyetogram when the rainfall rate is high. This is supported by the fact that the totals for 30 and 31 taken together agree very well.

The hyetogram may only be realistically interpolated to the nearest 0.1 mm and when compared to the distrometer totals (given to 2 decimal places) this adds to the errors. It should also be noted that the distrometer total agrees well with the gauge-calibrated radar total. This illustrates the problem of arriving at an objective analysis - discussed in 5.3.2.

The mean percentage difference of the basic radar data (method 3) compared to the distrometer result is 34% which agrees well with 35% obtained in DWRP (*59*). The comparison with the gauge is not as good (43%). The overall total when the radar is calibrated by reference to the Constantine Bay gauge is much closer to both the St. Mawgan gauge and distrometer totals but the mean percentage and rms differences both suggest that this calibration has actually been detrimental to the results. Compared to the gauge, the mean percentage rises from 43% to 47%, the average rms differences are similar

but the cumulative difference reduces from 1.29 to 0.79. As discussed in 5.1.5 the latter is a more effective comparison of the results since it combines both the individual differences with the overall effect reflected in the final total.

The use of mean monthly calibration factors is not, on this evidence, very successful. The errors associated with method 7 in these tables are much larger than any of the others and the overall total represents a considerable over-estimate, reflected in the high cumulative rms error. The reason for this may be that the rainfall events under consideration here are not representative of the mean monthly weather and this long time base method of calibration cannot react to variations on a smaller scale. Also this type of correction may be more appropriate when applied to the raw radar data, as discussed in the previous section.

The main object of this exercise was to compare the effect of applying a variable Z-R relationship with the result obtained by existing methods of measurement. The relevant results are drawn from the larger tables and reproduced in Table 5.8. These cumulative rms differences show that the difference between the gauge and distrometer (methods 1 and 2), both of which should represent a good estimate of the surface rainfall, is larger than some of the differences in relation to the less direct methods (5, 6 and 9). The variable Z-R relationship technique, when applied to the unmodified radar data (5) produces a relatively poor result. However, when applied to the modified data (9) the rms cumulative difference compared to either the gauge or the distrometer is almost identical to the difference in relation to the proposed "ground truth" calibration (6). When all the data are considered (Table 5.7) method 9 clearly produces the best result.

Method	Total (mm)	COMPARED TO 1 G	2 D	5 R30V	6 R6GC	9 R30x2V
1	13.10					
2	11.00	1.09				
5	6.75	1.56	1.12			
6	11.30	0.79	0.75	1.34		
9	10.39	0.76	0.77	1.36	0.19	

Table 5.8 Cumulative rms differences - Methods 1, 2, 5, 6, 9 only

5.2.4 Comparison of radar profiles

The final stage of this investigation is to examined the possibility of deducing a value for N_0 from the vertical radar profile. These data, in the form of the time-height profiles described in 4.3.5, appear in Appendix VII. Some examples chosen to illustrate particular features are included in Figures 5.1 to 5.8.* The surface data are also shown in the form described in 5.1.4. There are no plots for periods 11 and 33 because no rain was detected by the radar. Period 23 is plotted because, although no rain was detected at the lowest elevation, there were returns from aloft and some distrometer data at the surface.

The profiles reveal a variety of patterns which may be examined in terms of the atmospheric processes which they represent. There are examples of continuous and relatively homogenous patterns, as well as discontinuous and more varied types. The most frequently observed feature is that the reflectivity increases towards the ground. Horizontal reflectivity gradients are also observed and they may be positive to left or right. The relative dominance of these gradients determines the overall structure of each profile. Smaller scale features exist in the form of closed contours, usually embedded in the structure between 1 and 2 km.

When the vertical reflectivity gradient dominates, the structure may be described as "laminar". This represents the growth of raindrops by accretion and coalescence under the influence of a gravitational field. The raindrop-size distribution aloft will comprise mainly small cloud droplets and this results in a low reflectivity. The growth of the drops by accretion and coalescence during their descent increases the concentration of large drops and produces the

* p. 172-180

higher Z values found near the surface. These processes are important in stratiform clouds although when occurring in isolation they may only produce light rain. Profiles 16-19 (Figures 5.4 - 5.7) show this laminar structure with continuous light rain at the surface and during this period stratus cloud types predominated. (See Appendix VI.)

These four profiles, although dominated by the vertical reflectivity gradient, also have areas with a horizontal gradient. These gradients are generally weaker and associated with changes in the rainfall rate at the surface. The horizontal gradient is positive to the right when the rainfall rate is increasing and to the left when it is decreasing.

When horizontal reflectivity gradients are more developed, such as in profiles 1, 2 and 3 (Figures 5.1 - 5.3) a "cellular" structure emerges. These patterns have been observed by ROGERS (*63*) using Doppler radar. This technique allows vertical velocities to be measured and in observations over Hawaii these cellular patterns were associated with strong updrafts and convective cloud types. The rainfall during profiles 2 and 3 was showery and associated with cumuliform cloud. A well-formed cell with strong gradients both vertically and horizontally is seen in profile 3 and this isolated cumulonimbus shower produced a short period of moderate rain at the surface.

During this shower the rainfall rates observed by the radar and distrometer show a broad agreement, the peak rates are comparable and over the half hour period the totals are similar. However, the fact that the shower lasts 9 minutes at the distrometer and 17 minutes over the whole grid square underlines the fundamental difference between the measurements. There are very few occasions when rainfall is observed

by the distrometer and not by the radar, but many minutes of radar rainfall occur when nothing was recorded at RAF St. Mawgan. This is a logical result of the comparison of areal and point measurements.

In view of this and the uncertainty over systematic errors in the radar measurements, discussed in 5.2.2, it is not possible to examine the minute-by-minute variations in R_D, R_Z and N_o. This unfortunately precludes the extraction of a semi-empirical relationship, such as that discussed in 4.1.6, which might improve on the results presented in 5.2.3. However, it is possible to note some broad correlations between the behaviour of N_o and the atmospheric processes revealed in the vertical profiles.

In the case of a laminar structure there is evidence to show an inverse relationship between N_o and the vertical reflectivity gradient. When the vertical gradient is strong, N_o tends to a lower value, reflecting the more effective growth processes aloft producing a higher concentration of large drops at the surface. This is seen in profiles 16-18 where continuous light rain was falling. At the beginning of the next half hour period the vertical gradient becomes less marked and N_o shifts to a higher value for the next 2 hours. The highest values of N_o occur in profile 24 when there is virtually no vertical gradient but a small horizontal gradient.

In the cellular structures N_o is generally more variable and when a horizontal gradient exists, where a cell is growing or decaying, the level changes to a lower value in the case of a positive gradient to the right (growth, e.g. profile 17). When the gradient is positive to the left (decay, e.g. profile 31) N_o shifts to a higher value.

WALDVOGEL (*12*) suggested that a large drop spectrum (low N_0) might be associated with a bright-band type echo. The observations in Appendix VI show that the 0°C isotherm could have been intercepted in any of these profiles, generally at about 1 km. In profile 17 there is evidence of a band of increased reflectivity at this height and the N_0 values at the surface are low, particularly at the end of the period when a strong echo exists between 1.0 and 1.5 km.

Thus there is evidence to show that trends in the value of N_0 could be deduced from the vertical radar profile. Any such deductions are likely to produce broad estimates and not the detailed record produced by the distrometer. In view of the discussion above it is possible that this approach would yield better results if N_0 were estimated on an areal basis and a similar deductive process to that followed in 4.1 were used to produce an N_0-A relationship based on a coarser time-scale.

5.2.5 Variation of rainfall rate with height

Table 5.9 shows the rainfall totals at each elevation for the data in the vertical radar profiles, calculated using the fixed Z-R relationship. These results are included because they give an indication of the strength of the vertical reflectivity gradient in each half hour period.

The fact that different rainfall rates occur at each elevation does not necessarily indicate that there is any variation in liquid water content through the profile. These rainfall rates are theoretical equivalents of the observed reflectivity and the magnitude of the rates depends on the relationship employed. As discussed above these measurements of reflectivity gradient may be related to the growth of raindrops during their descent. This results in a shift towards higher diameters and

Half hour period no.	Distrometer	Elevation 1	Elevation 2	Elevation 3	Elevation 4
1	1.00	1.39	1.06	0.48	0.17
2	0.77	0.79	0.47	0.21	0.09
3	0.35	0.36	0.26	0.08	0.00
4	0.01	0.01	0.03	0.04	0.05
5	0.10	0.13	0.06	0.02	0.00
6	0.00	0.04	0.01	0.02	0.00
7	0.00	0.03	0.00	0.00	0.01
8	0.00	0.02	0.04	0.00	0.01
9	0.07	0.03	0.03	0.01	0.01
10	0.00	0.03	0.01	0.00	0.00
11	0.00	0.00	0.00	0.00	0.00
12	0.11	0.09	0.04	0.02	0.00
13	0.03	0.05	0.02	0.01	0.00
14	0.00	0.01	0.00	0.00	0.02
15	0.03	0.06	0.12	0.12	0.08
16	0.29	0.22	0.42	0.37	0.10
17	0.71	0.58	1.40	1.68	0.31
18	0.52	0.34	0.50	0.73	0.14
19	0.22	0.10	0.10	0.16	0.08
20	0.27	0.12	0.18	0.26	0.08
21	0.35	0.10	0.10	0.19	0.06
22	0.07	0.10	0.08	0.08	0.05
23	0.01	0.00	0.01	0.01	0.01
24	0.10	0.09	0.08	0.05	0.04
25	0.33	0.16	0.15	0.13	0.06
26	0.41	0.25	0.19	0.23	0.10
27	0.36	0.09	0.07	0.07	0.05
28	0.19	0.12	0.08	0.04	0.00
29	0.22	0.14	0.14	0.11	0.02
30	1.62	1.32	2.26	1.64	0.30
31	2.59	1.38	1.95	1.21	0.32
32	0.42	0.35	0.38	0.18	0.05
33	0.01	0.00	0.00	0.00	0.00
Totals (mm)	11.16	8.50	10.24	8.15	2.21

Table 5.9 Rainfall totals at each elevation

larger Z values, rather than any increased accumulation of liquid water. Redistribution of the liquid water will take place due to the increased fallspeed of the larger drops and this will also affect the observed reflectivity profile.

The ratio between surface rainfall and rainfall aloft has been used previously as an indication of the existence of a bright-band aloft (*47*). A discontinuity in the ratio was often observed near the bright-band. In relation to the work referred to, the present data are not so detailed in the vertical (JOSS et al used 7 levels up to 3.5 km). However this behaviour is seen to some degree in the profiles presented here. Profile 17 (Figure 5.5) was previously used to illustrate evidence of a bright-band and in this case the ratios between the radar-derived rainfall at each elevation and the surface rainfall measured by the distrometer were as follows:

Elevation 1	(288 m)	0.82 mm
Elevation 2	(881 m)	1.97 mm
Elevation 3	(1474 m)	2.37 mm
Elevation 4	(2366 m)	0.44 mm

The discontinuity between elevation 1 and the next two elevations suggests the existence of a bright-band between 288 m and 1474 m. The 0°C isotherm was observed at 700 m by the ascent from Camborne three hours earlier. (Appendix VI.)

5.2.6 Modified data results

The best results from combining the distrometer and radar data were obtained when the variable Z-R relationship was applied to the modified radar data (method 9). As discussed above, this doubling of the raw

radar reflectivity values is quite arbitrary, but bears some relation to the real-time correction procedure implemented at the radar on an operational basis (*69*). The effect of making this modification may be seen in detail in Appendix VII. This shows that a doubling of the Z value results in a smaller proportional increase in the corresponding R value. The total for the whole period is increased by 75% to a value very close to the gauge total (Table 5.4).

The results obtained from these modified data generally support the theoretical behaviour deduced earlier (4.1) in a more convincing manner than the unmodified data. In some cases the improvement is quite noticeable in terms of both the half hour total and the minute-by-minute comparison (e.g. No. 30, Figure 5.9)*. There are occasions when although the agreement between half hour totals is improved, the detailed plot shows the effect to have been detrimental (e.g. No. 25, Figure 5.10)**. This supports the requirement to measure N_o on a coarser scale to relate more closely to the areal data.

The occasions when it is necessary either to increment or decrement the radar total in relation to the distrometer catch to improve the correlation may be deduced from Table 5.4. It is found that the application of the variable Z-R relationship predicts the correct sign of the increment on more occasions for the modified data than for the unmodified data. It is likely that the results could be much improved if the exact value of the correction factor to apply to the Z values were known and the most suitable values for the "constants" in the N_o-A relationship discovered. Some slightly different relationships were tried and it was found that the correlation between half hour totals could be improved. However, there was no direct observational evidence for these relationships and hence the results presented here are derived using the "constants" given in 4.1.

* p. 181 ** p. 182

Key to Figures 5.1 to 5.10

R_D - Distrometer surface rainfall rate (five-minute moving average)

R_Z - Radar rainfall rate at lowest elevation (interpolated values - method 4, Table 5.3)

N_o - Distrometer surface measurement (five-minute moving average)

In Figures 5.9 and 5.10* R_D and N_o are plotted as above but in the upper plot R_Z is derived from the modified radar data (method 8, Table 5.3) and in the lower plot R_Z is derived from these data after applying a variable Z-R relationship and the total is denoted R_{ZN} (method 9, Table 5.3).

* p. 181-182

Radar Reflectivity

Contours (dBz)

Figure 5.1

(1) 530028 - 057

1200-29 : 27.3.79

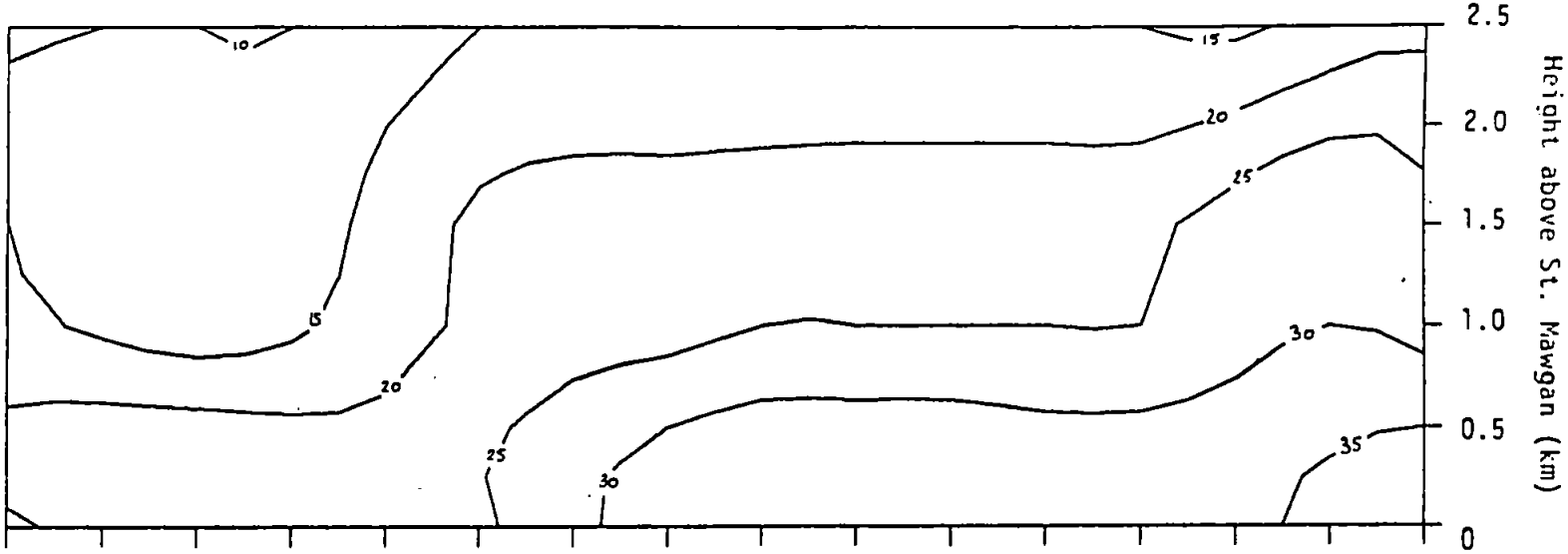

Totàls:

R_G : 1.6 mm

R_D : 1.00 mm

R_Z : 1.50 mm

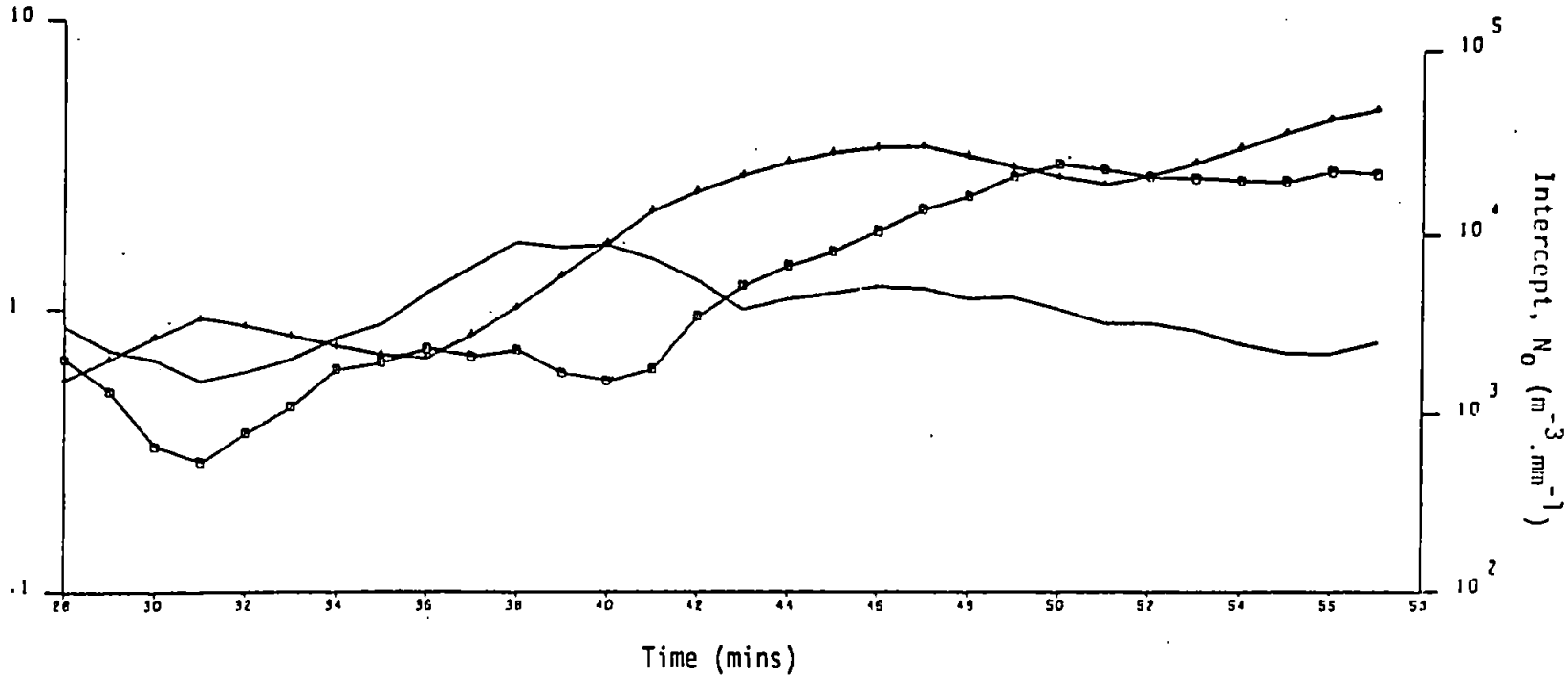

Radar Reflectivity

Contours (dBz)

Figure 5.2

(2) 530058 - 087

1230-59 : 27.3.79

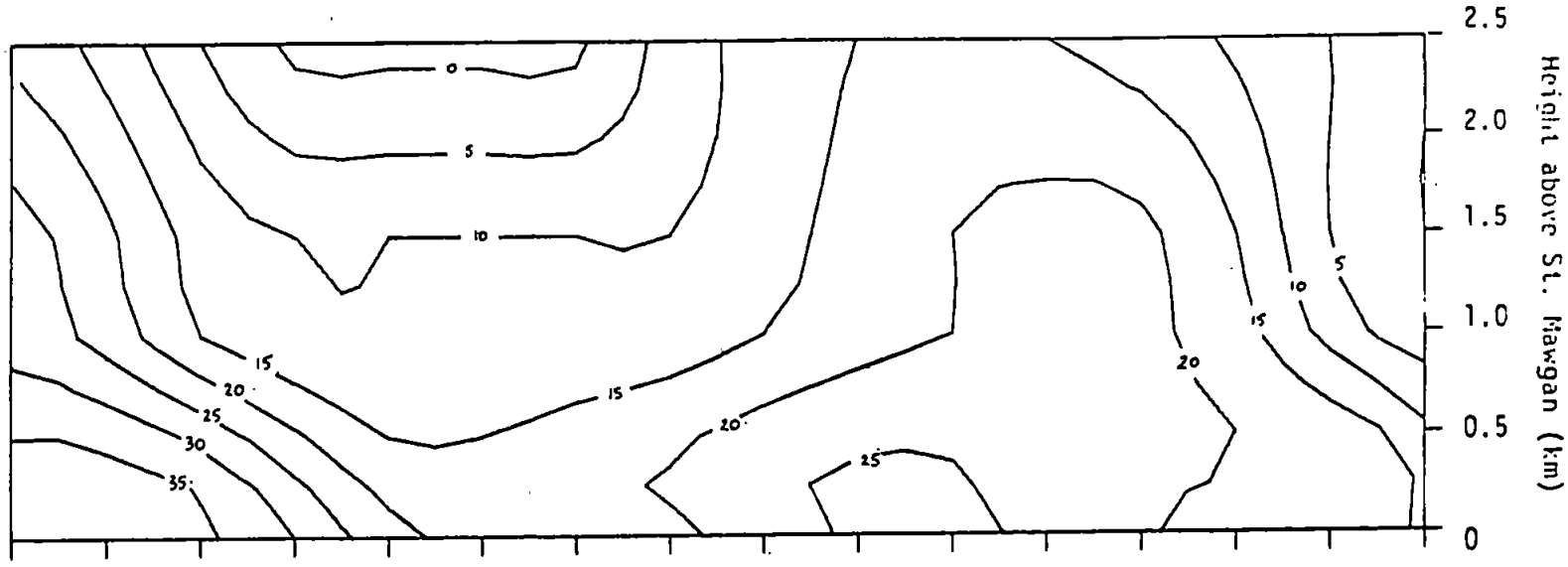

Totals:

R_G : 0.8 mm

R_D : 0.77 mm

R_Z : 0.63 mm

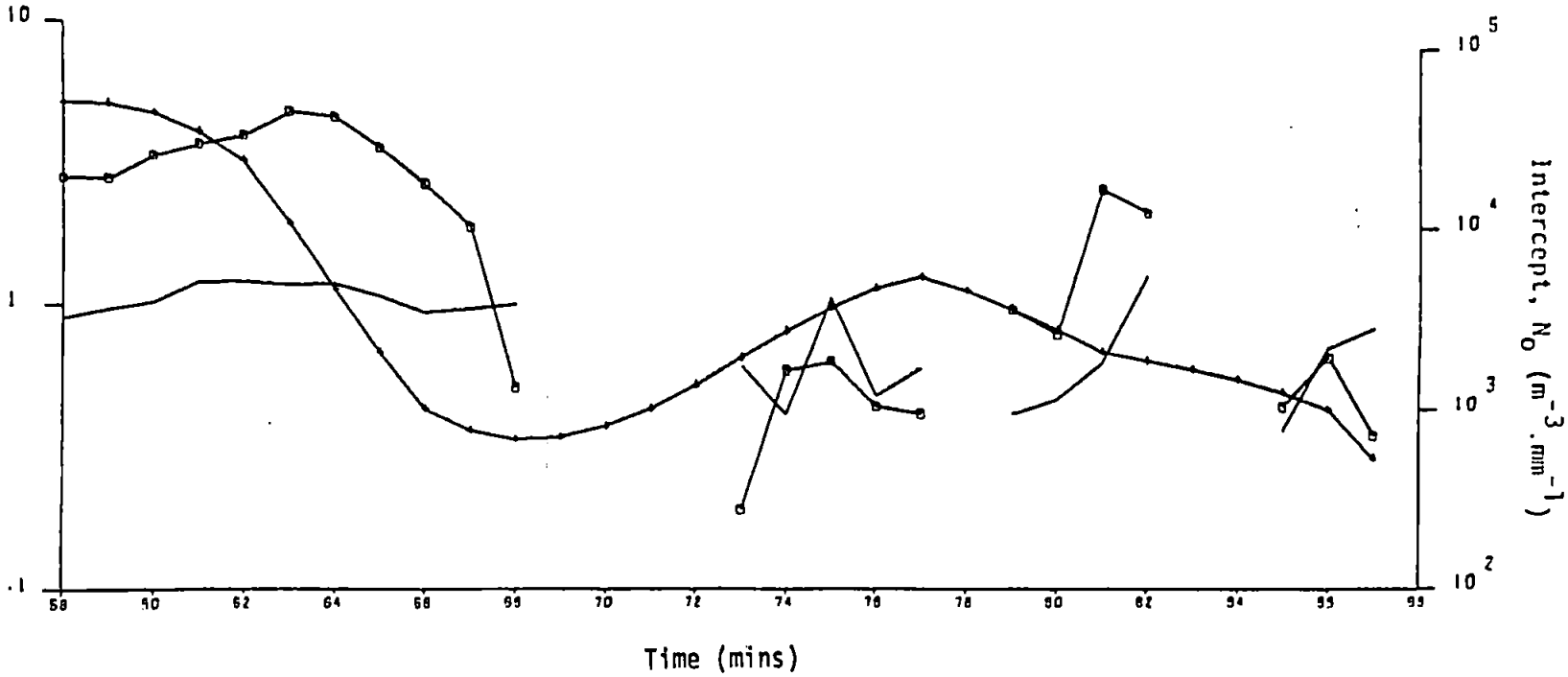

Radar Reflectivity

Contours (dBz)

Figure 5.3

(3) 530088 - 117

1300-29 : 27.3.79

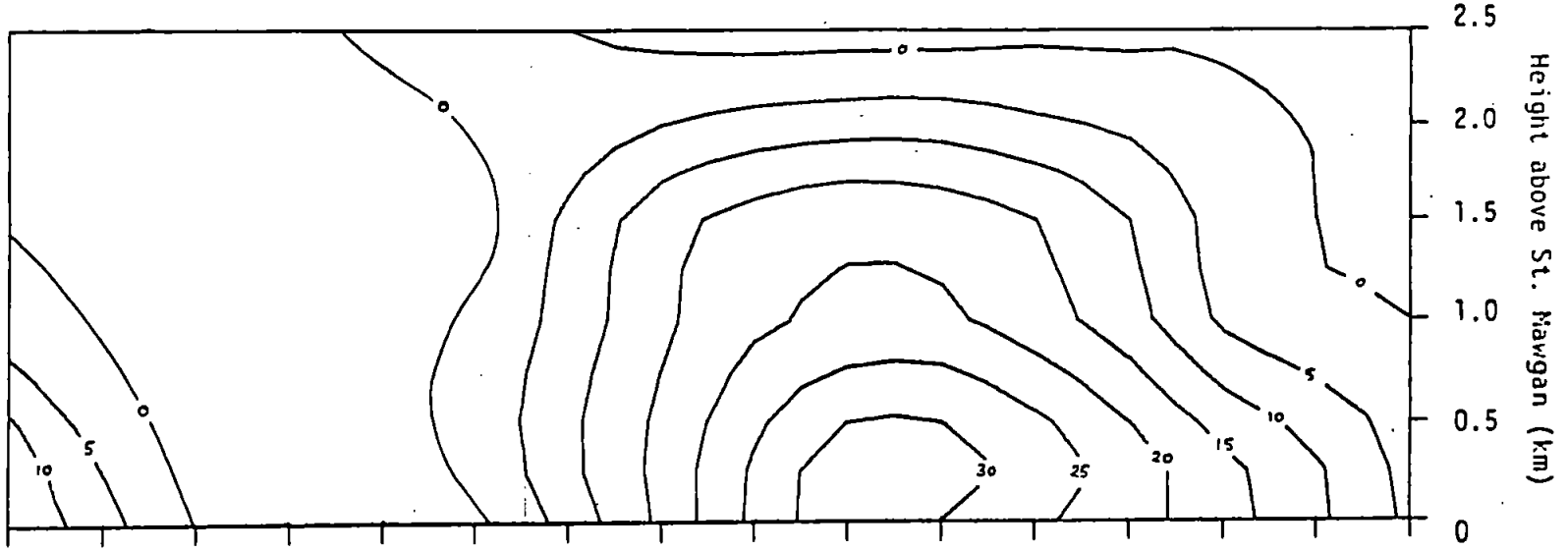

Totals:

R_G : 0.5 mm

R_D : 0.35 mm

R_Z : 0.40 mm

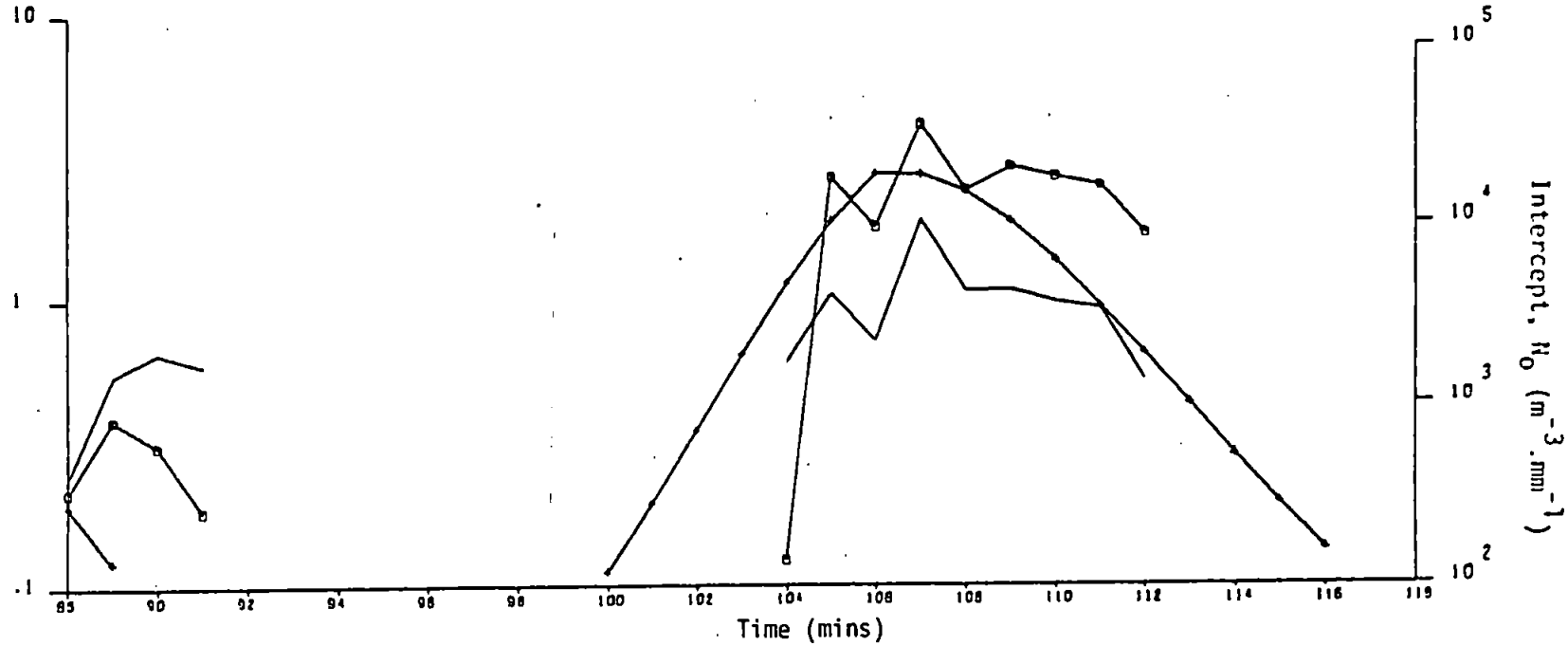

Radar Reflectivity

Contours (dBz)

Figure 5.4

(16) 540090 - 119

1430-59 : 9.4.79

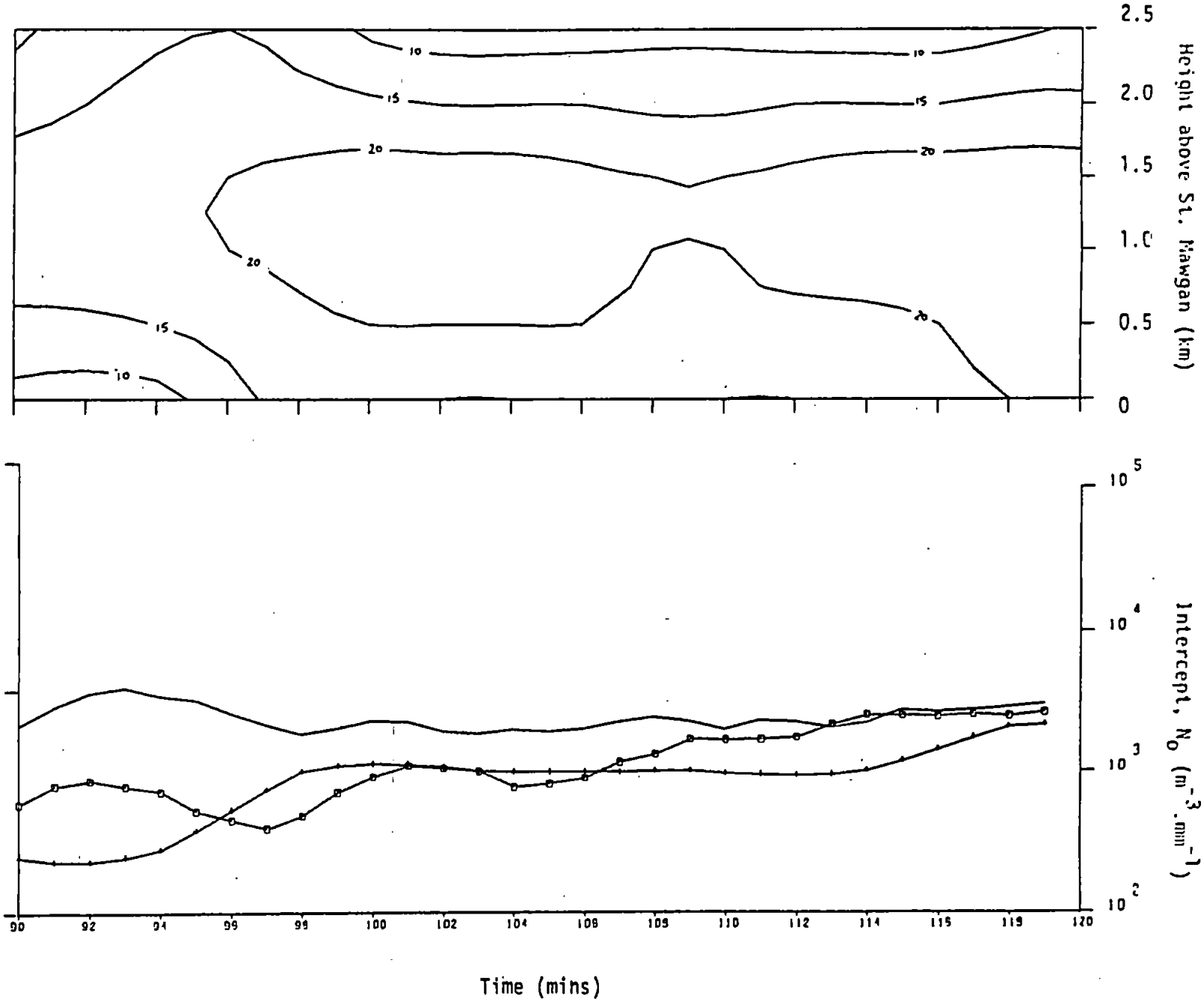

Totals:

R_G : 0.3 mm

R_D : 0.29 mm

R_Z : 0.24 mm

Radar Reflectivity

Contours (dBz)

Figure 5.5

(17) 540120 - 149

1500-29 : 9.4.79

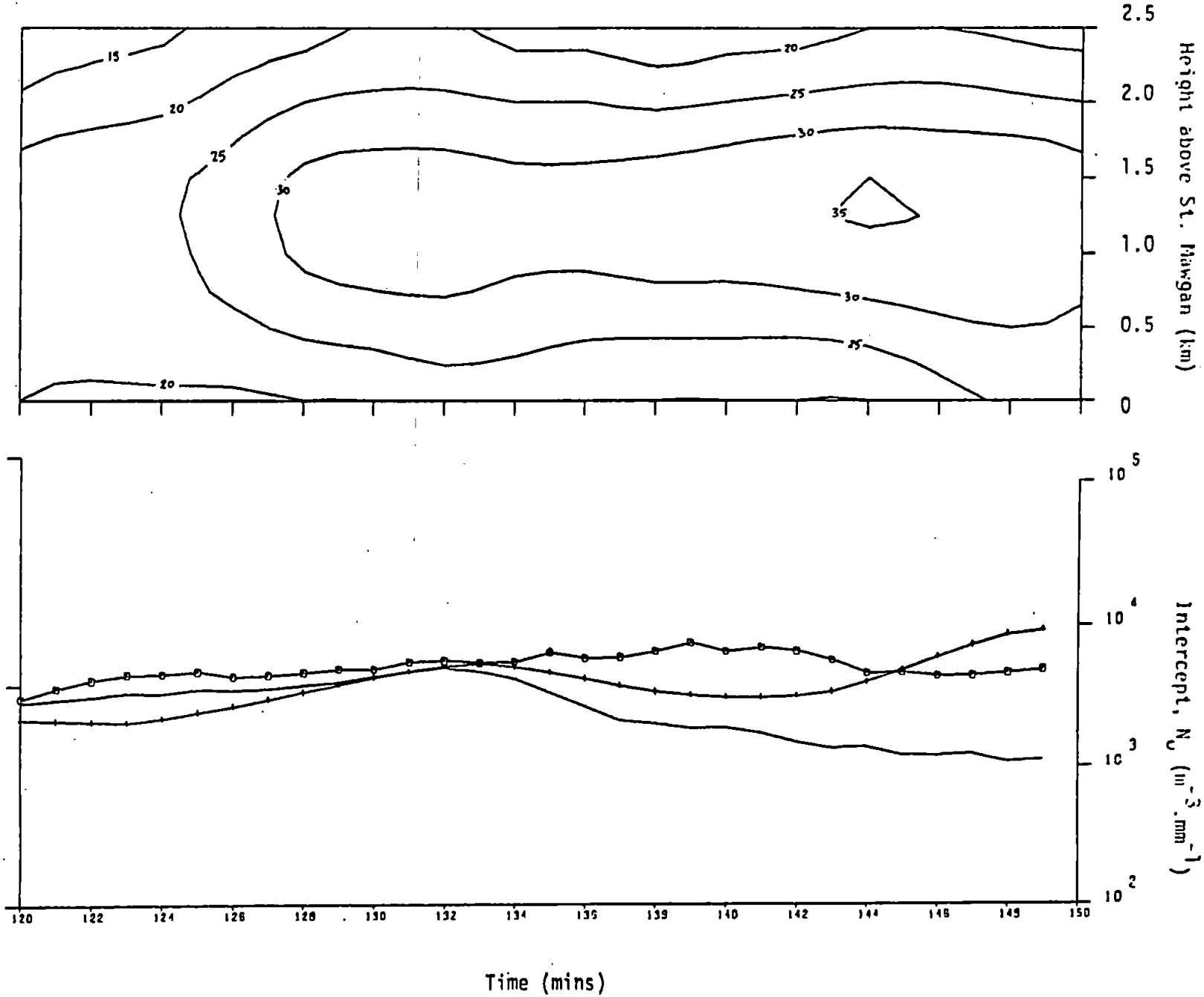

Totals:

R_G : 0.7 mm

R_D : 0.71 mm

R_Z : 0.61 mm

Radar Reflectivity

Contours (dBz)

Figure 5.6

(18) 540150 - 179

1530-59 : 9.4.79

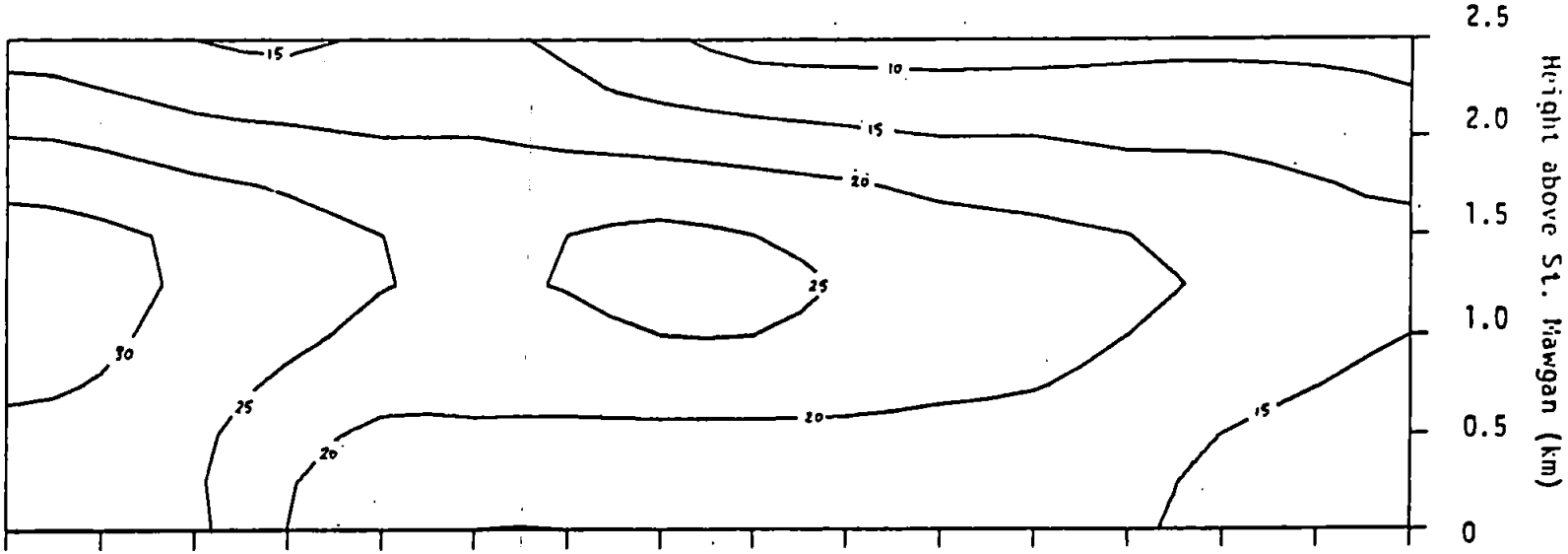

Totals:

R_G : 0.6 mm

R_D : 0.52 mm

R_Z : 0.29 mm

178

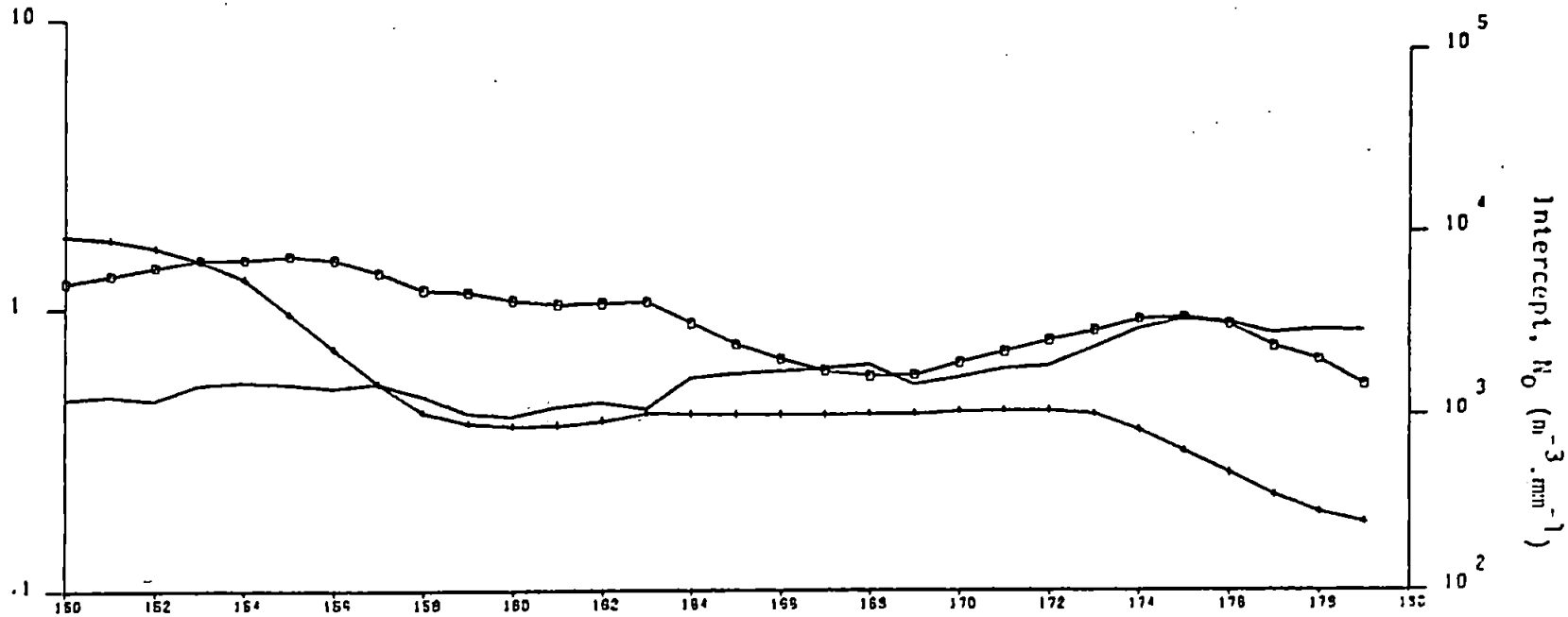

Radar Reflectivity

Contours (dBz)

Figure 5.7

(19) 540180 - 209

1600-29 : 9.4.79

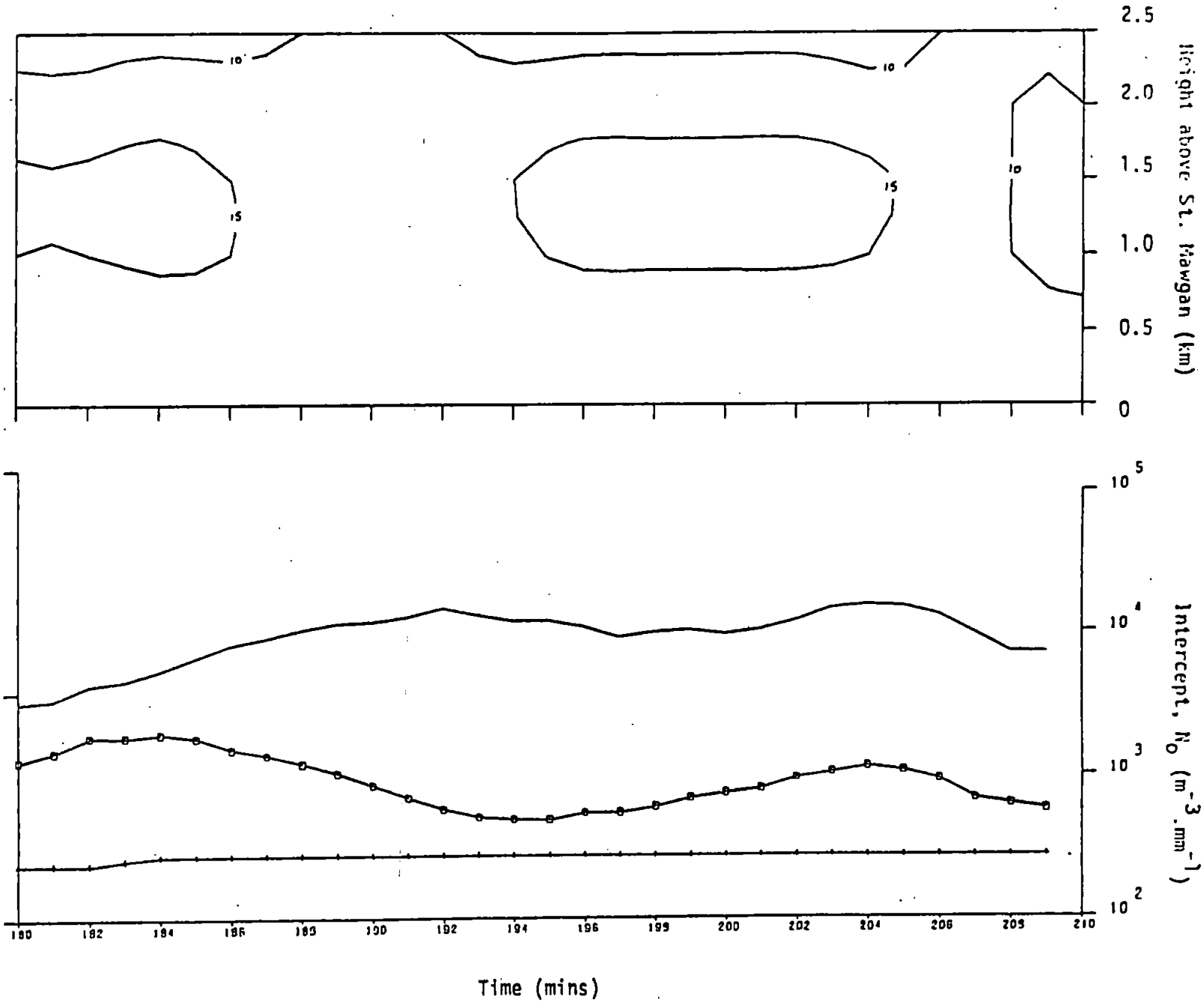

Totals:

R_G : 0.2 mm

R_D : 0.22 mm

R_Z : 0.10 mm

Radar Reflectivity

Contours (dBz)

Figure 5.8

(31) 550180 - 209

1900-29 : 22.5.79

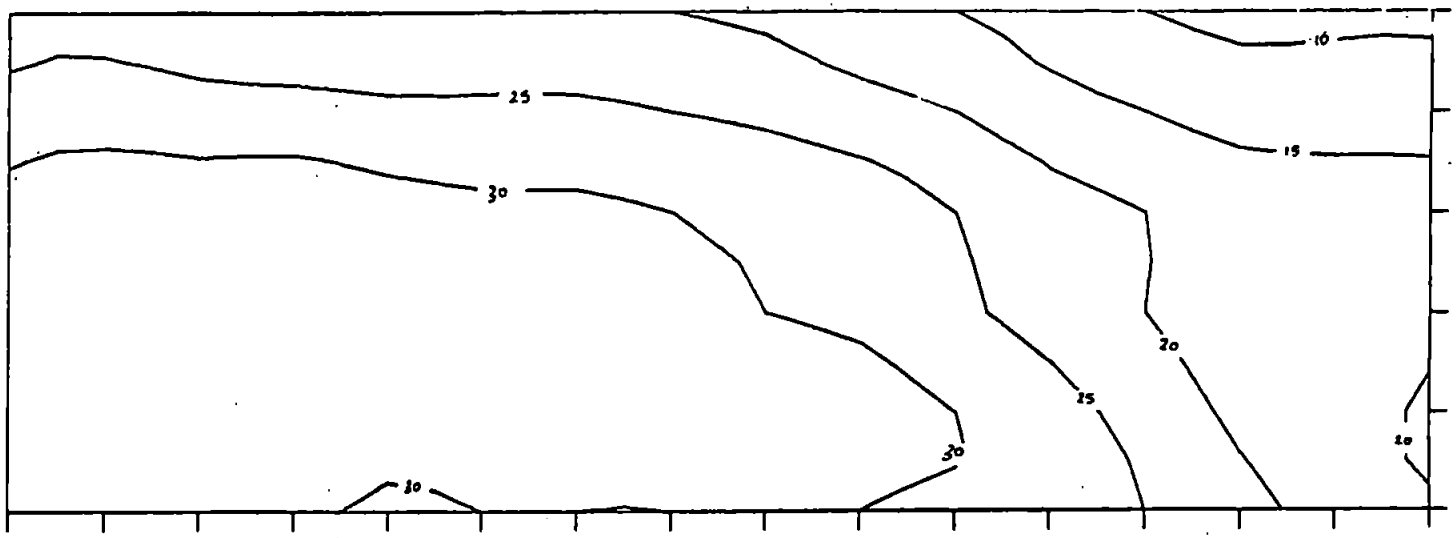

Totals:

R_G : 3.2 mm

R_D : 2.59 mm

R_Z : 1.31 mm

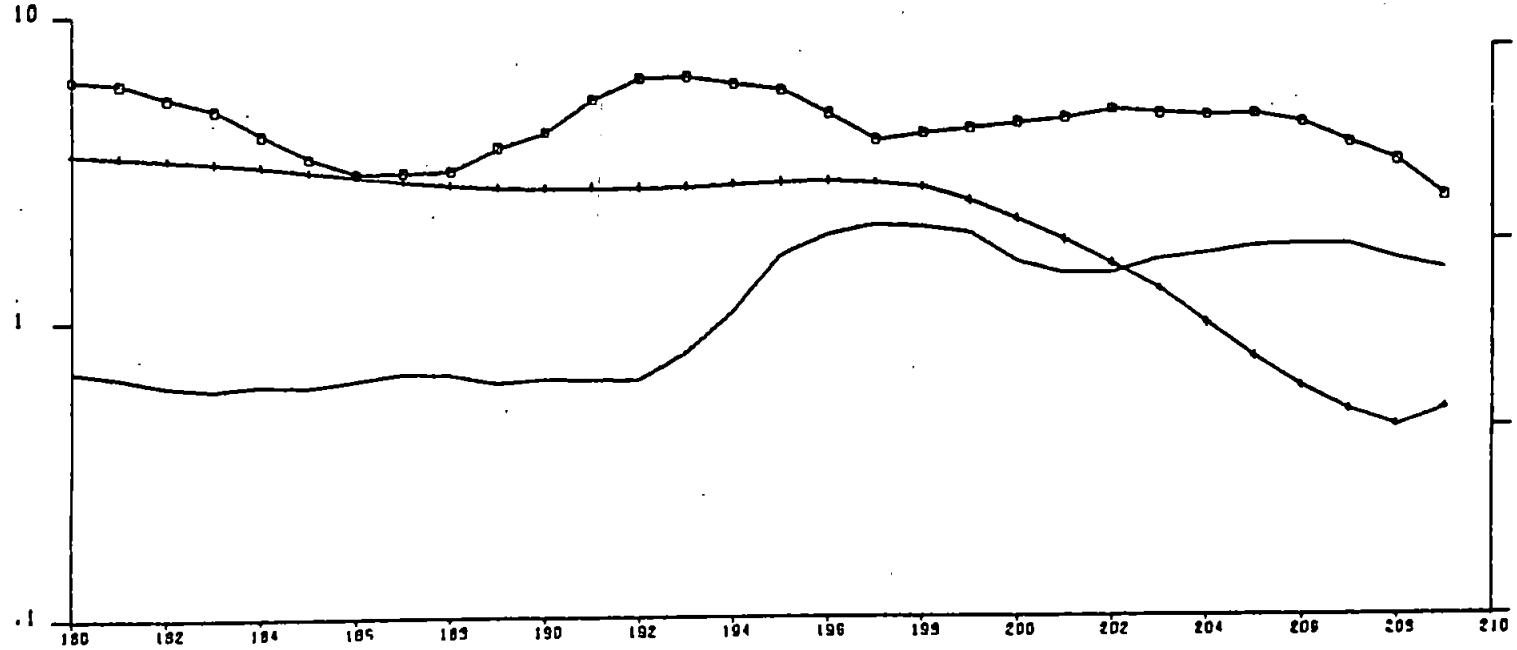

081

Figure 5.9

(30)

1830-59

22.5.79

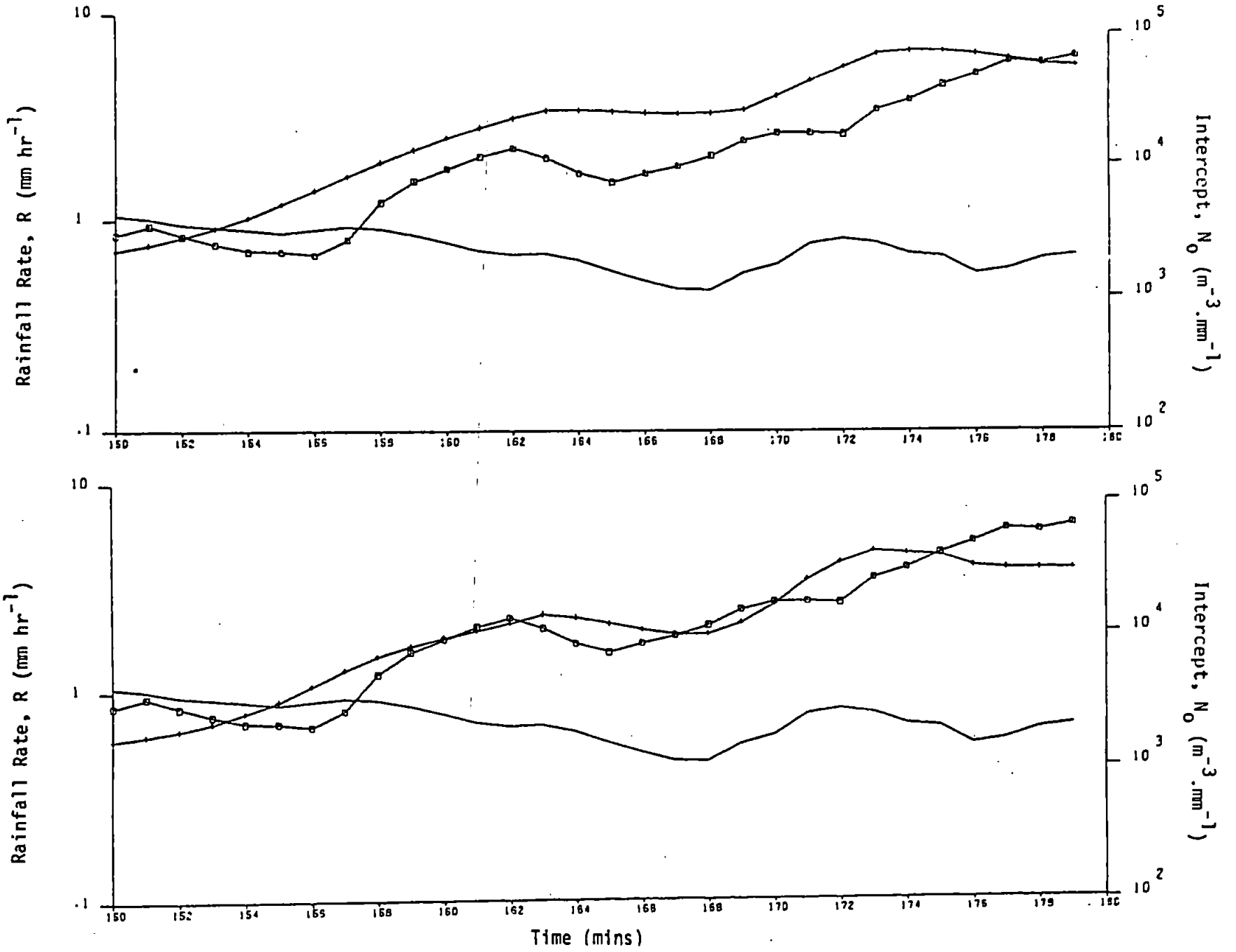

Totals:

R_G : 1.1 mm

R_D : 1.62 mm

R_Z : 2.04 mm

R_{ZN}: 1.34 mm

Figure 5.10

(25)

1900-29

9.4.79

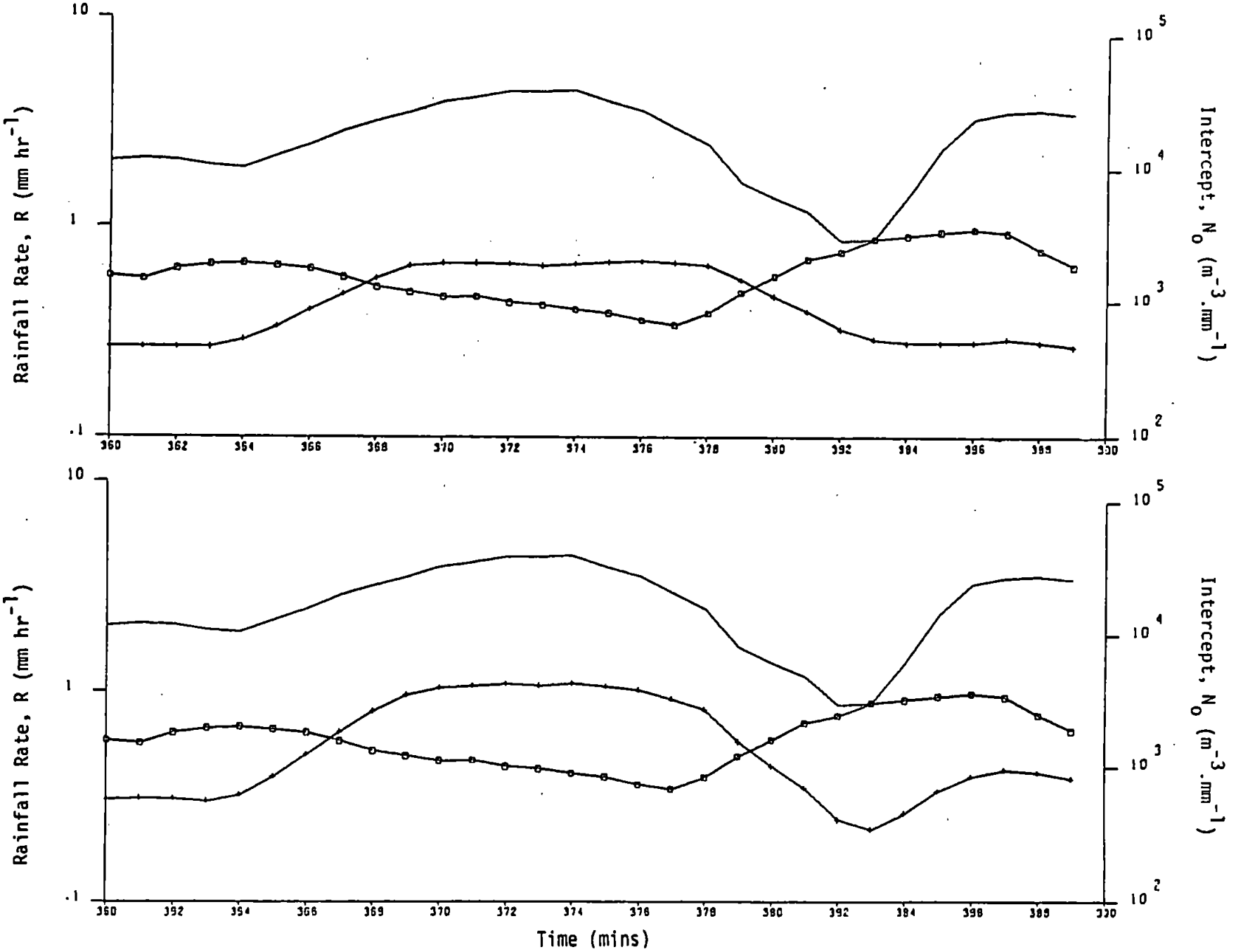

Totals:

R_G : 0.5 mm

R_D : 0.33 mm

R_Z : 0.24 mm

R_{ZN}: 0.33 mm

5.3 DISCUSSION

5.3.1 Distrometer versus gauge calibration

The results to be expected from this exercise depend to a significant extent on the performance of the radar. The gauge calibration method is relatively independent of this consideration. Providing the performance of the radar is consistent over the radar field for the relatively short periods of integration under consideration, any day-to-day variations, from whatever source, will be allowed for automatically. This is the major advantage of the "ground-truth" gauge calibration technique.

However, such a coarse method of characterising rainfall does not provide a suitable basis for the detailed interpretation of radar data which is necessary to understand the meteorological variations which lead to errors when the raindrop-size distribution is anything other than "average". These variations, which are revealed as fluctuations in the most appropriate values for the constants in the conventional Z-R relationship, can only be measured directly by a device which measures raindrop-size distributions. The use of a distrometer, or array of distrometers, to measure raindrop-size distributions and compute optimum Z-R relationships in real-time to improve radar measurements is often discounted on grounds of technical complexity and expense. The work presented here suggests that even if unlimited funds were available, there are scientific problems which remain to be solved before this approach is entirely successful.

5.3.2 Problems of objective analysis

A major problem in this analysis has been the difficulty in determining the true value of the measurements which are being compared. It is well known that differences may occur over relatively short intervals in the catches of raingauges which are quite close to each other. These differences arise through the innate variability of rainfall and the efficiency of the gauge itself. The efficiency may be affected by external conditions, but the situation is further complicated when the measuring devices are very different. The operational principles of the gauge and distrometer are very different and this doubtless contributes to their differing performance. The differences between them in the second data set were of the same order as the differences associated with the radar-based techniques under evaluation. This makes objective analysis very difficult. The use of an optimum rainfall field, described earlier, is likely to be a more satisfactory base for comparison, particularly for areal measurements.

In the present analysis this problem is recognised in the comprehensive treatment of the differences between the various methods, allowing as broad a base for comparison as possible. In all other respects the analysis has been thoroughly objective, with the intention of allowing any results to be readily translated to the radar operation which is largely automatic.

5.3.3 Generality of the data

The extent to which the data represent a general survey of the behaviour of the atmosphere affects the validity of this work. As noted earlier (4.2.2) the periods of observation were selected to include reasonable

amounts of precipitation to make the considerable amount of travelling and organisation worthwhile. This means that a higher percentage of the data represents continuous and moderately heavy rain than might occur over a longer period. During the collection of the first data set 79 hours were recorded when the autographic gauge recorded rain falling continuously for an hour. This represented 27% of the archive and 45% of the rainfall (3.1.1). In the second data set the gauge recorded a higher proportion of this type of rain. However, the feature which is under the closest scrutiny - namely the behaviour of the shape parameter N_0 - has a broadly similar distribution in relation to the first data set (see Figure 4.16), which covered 3 months of continuous observation.

This similarity is achieved partly by including a wide range of rainfall rates in the record. This requires the inclusion of some periods of little or no rain. Removal of these data would reduce the archive considerably in terms of the number of hours of observation, although not the total rainfall measured. The major criticism of this archive of data is that it should have been larger and therefore more representative.

The scope of this work was considerably limited by the remote experimental site and a forecast of suitable weather to determine if the journey to set up the equipment was worthwhile. It was also necessary that every hardware element should be working simultaneously. On one occasion, over 10 mm of rainfall passed unrecorded due to a minor fault in the digital clock. The radar data were not always available and the distrometer operation was ultimately terminated when the transducer was severely damaged by a third party.

CHAPTER SIX

CONCLUSIONS AND RECOMMENDATIONS

6.1 CONCLUSIONS

The work presented here emcompasses two main areas:

- the measurement of raindrop-size distributions in a maritime locale using a Joss distrometer;
- the combination of distrometer and radar data to enhance the measurement of precipitation.

Some previous results have been confirmed and an original contribution has been made to the understanding of the complex relationship between natural rainfall and the operation of a meteorological radar. The interpretation of distrometer data to calibrate a radar in this way is entirely new.

The operation of the Joss distrometer has been described in some detail and the inclusion of computer program listings which derive raindrop spectra from raw data should assist any researcher who might wish to operate this instrument in the future. The most important sources of error in the experiment, due to both instrumental and environmental factors, have been investigated and discussed. No corrections have been proposed; this would contradict previous practice and is vindicated by the good agreement of distrometer and raingauge catches.

The distrometer archive forms a useful data base for any investigation into raindrop-size distributions and is unique since previously published work has been concerned with continental data. This investigation has not been aimed towards examining any differences between maritime and continental archives. Although differences between the atmospheric physics in these locales undoubtedly exist, both in the sizes of condensation nuclei available and types of synoptic develop-

ment which dominate, no large differences between the distributions at St. Mawgan and other published data were observed.

The analysis of the distrometer data in the conventional manner, producing average drop-size distributions and a Z-R relationship, confirms the results of other workers and demonstrates the consistency of this method of measurement with other techniques. The data were also interpreted in a non-conventional manner to produce a variable Z-R relationship which has often been suggested as an improvement to the measurement of precipitation by radar. This variable relationship depends on describing the variation in the shape of the raindrop-size distribution by a parameter which may be deduced from the distrometer observations and is influenced by the growth processes in the atmosphere. The derivation of the relationship between this shape parameter (N_o) and one of the constants in the conventional Z-R relationship (A) from actual observations supports a result derived previously from theoretical considerations. This empirical relationship was predicted by a qualitative argument and its performance was tested on simulated radar data. Using this technique for the first time, a significant improvement resulted when compared with the conventional, static Z-R relationship.

The use of actual radar data to test the performance of the variable Z-R relationship required a further experiment including observations which allowed calibration of the radar using a ground-truth method. This method is well-tried and will be used in the operation of a network of radars to measure areal precipitation over the United Kingdom. The work here shows that this method is likely to perform well although difficulty was experienced in relating point and areal measurements and the data set was somewhat limited. Nine different estimates of rainfall over St. Mawgan were compared and it was found

that the proposed variable relationship approach only performed well when the radar data were modified. This modification is in line with that carried out by the operators of the radar and affects the distrometer based calibration much more than the ground-truth method.

The benefit of this approach to radar calibration is only fully realised if the shape parameter can be deduced from the radar data alone. In order to initiate an investigation into this possibility the radar data were displayed in the form of time-height profiles which were compatible with the distrometer archive. Some trends were observed in the surface data which could be related to the broad features of the atmospheric structure. It seems likely that further work might reveal a consistent and useful relationship between the shape parameter at the surface and the radar data aloft. Such a relationship would reveal relatively large scale behaviour and this is likely to be more representative of the areal nature of the data than the present point measurements are.

The measurement of areal rainfall by radar is now passing from the experimental stages to an operational status. It is known that good results can be obtained when the rainfall field is calibrated in real time by reference to telemetering raingauges. However, this will always be regarded as a slightly inelegant solution and a more satisfying result is obtained if the radar data alone can be used to produce the optimum result. There is evidence in the work presented here to show that, if the radar data set can be interpreted comprehensively, variations in the raindrop-size distribution can be detected. These variations are fundamental to the accuracy of the radar technique. If they can be compensated

for by the application of a variable relationship between the rainfall rate and reflectivity factor, a result is obtained which compares favourably with the ground-truth technique.

6.2 RECOMMENDATIONS FOR FUTURE WORK

This work has shown that the use of a variable Z-R relationship, based on direct observations of raindrop-size distributions, may lead to improvements in the measurement of areal precipitation by radar. It was necessary to use a simple measure of the shape of the spectrum and the parameter chosen was based on the intercept of the exponential which was used to approximate the distribution. This approach was adopted because the work of previous authors had indicated that its behaviour could be related to the growth processes observed in the atmosphere. These give rise to the variation in raindrop sizes which so profoundly affects the use of radar to measure rainfall. This ignores the possibility that the other shape parameter, described earlier and based on the slope of the exponential distribution, might be used in the same way. It would therefore be worthwhile to pursue a similar exercise to investigate this possibility, using the same data set.

Further work is required to relate the behaviour of the shape parameter near the surface to the radar reflectivity profiles. The difficulty of relating point and areal measurements limited this part of the exercise in the present work. This problem does not arise with vertically-looking radars which have been reported previously. Since these instruments are not suitable for measuring areal rainfall, it is necessary to make the point measurements more representative and this was achieved to some extent by using five-minute moving averages. Further lengthening of the timebase for comparison, to say thirty minutes, may improve this. The behaviour of the shape parameter over half-hour periods might be characterised by a simple parameter (perhaps the average value) which would set the Z-R relationship for that period. The St. Mawgan data set could be used for this, although

it might be better to devise a new experiment when the radar is fully operational with the calibrating gauges installed. A more sophisticated technique for estimating the true rainfall - for example, an optimum rainfield based on data from several gauges - would improve the objectiveness of the experiment, but would require more resources than were available to the present author.

The time-height profiles required a certain amount of interpolation to make them representative of one grid square. A similar approach might be adopted by using a line of twenty grid squares, perhaps arranged at right-angles to the line of an advancing front, to reveal atmospheric development over an area of interest. These cross-sections could be displayed to forecasters in a similar manner to the areal data which are presented as a digitised colour picture on a visual display unit. This would enhance the capability of the radar as a means of improving short period weather forecasting in addition to its use in measuring areal rainfall - thus increasing the benefits gained by society from the study of meteorology.

REFERENCES

1. WIESNER, J. 1895 Beiträge zur Kenntnis des tropischen Regens. Sber.Akad.Wiss.Wien 104, 1397.

2. MARSHALL, J.S., LANGUILLE, R.C., and PALMER, W.McK. 1947 Measurement of rainfall by Radar. J.Met. 4, 186-192.

3. ANDERSON, I.J. 1948 Drop-size distribution measurements in orographic rains. Bull.Am.Met.Soc. 29, 362.

4. MASON, B.J. and ANDREWS, J.B. 1960 Drop-size distributions from various types of rain. Q.J.R.Met.Soc. 86, 346-353.

5. ECCLESTON, A.J. 1976 Raindrop-size distributions in a maritime locale. B.Sc. (Hons.) Dissertation, School of Maritime Studies, Plymouth Polytechnic.

6. SIVARAMAKRISHNAN, M.V. 1959 Studies of raindrop size characteristics in different types of tropical rain using a simple raindrop recorder. Indian J.Met.Geophys. 12, 189-217.

7. MASON, B.J. and RAMANADHAM, R. 1953 A photoelectric raindrop spectrometer. Q.J.R.Met.Soc. 79, 490-495.

8. DINGLE, A.N. and SCHULTE, H. 1962 A research instrument for the study of raindrop-size spectra. J.Appl.Met. 1, 48.

9. DU TOIT, P.S. 1967 Doppler radar observation of drop sizes in continuous rain. J.Appl.Met. 6, 1082-1087.

10. ROWLAND, J.R. 1976 Comparison of two different raindrop distrometers. Proc.17th Weather Radar Conf., Amer.Met.Soc., 398-404.

11. JOSS, J. and WALDVOGEL, A. 1967 Ein Spectrograph für Niederschlagstropfen mit automatischer Auswertung. Pure & Appl.Geophys. 68, 240-246.

12. WALDVOGEL, A. 1974 The N_0 jump of raindrop spectra. J.Atmos.Sci. 31, 1067-1078.

13. MARSHALL, J.S. and PALMER, W.McK. 1948 The distribution of raindrops with size. J.Met. 5, 165-166.

14. LAWS, J.O. and PARSONS, D.A. 1943 The relation of raindrop size to intensity. Trans.Amer.Geophys.Union 24, 452-460.

15. JOSS, J., THAMS, J.C. and WALDVOGEL, A. 1968 The variation of raindrop distributions at Locarno. Proc.Int.Conf. on Cloud Physics, Toronto, Canada, 369-373.

16. NICHOLASS, C.A. and LARKE, P.R. 1976 Raindrop-size distributions in a hilly region. Met.Mag. 105, 361-381.

17. JOSS, J. and GORI, E.G. 1976 The parameterisation of raindrop-size distributions. Riv.It. di Geofis. 3, 275-283.

18 GERTZMAN, H.S. and ATLAS, D. 1977 Sampling errors in the measurement of rain and hail parameters. J.Geophys. Res. 82, 4955-4966.

19. DINGLE, A.N. 1960 The Microstructure of rain in a summer shower. Proc.8th Weather Radar Conf., Amer.Met.Soc., 99-106.

20. NORBURY, J.R. and WHITE, W.J. 1971 A rapid response raingauge. J.Phys. Part E 4, 601-602.

21. SEMPLAK, R.A. and TURRIN, R.H. 1969 Some measurements of attenuation by rainfall at 18.5 GHz. Bell Syst. Tech.J. 48(6), 1767-1787.

22. MASON, B.J. 1972 The Physics of Clouds. Clarendon Press, Oxford. 659 pp.

23. PROBERT-JONES, J.R. 1962 The radar equation in meteorology. Q.J.R.Met.Soc. 88, 485-495.

24. HERMAN, B.M., BROWNING, S.R. and BATTAN, L.J. 1961 Tables of the radar cross sections of water spheres. Tech. Report No. 9, Tucson Inst.Atmos.Phys.Univ. Arizona.

25. BATTAN, L.J. 1973 Radar Observation of the Atmosphere The University of Chicago Press. 274 pp.

26. ATLAS, D. 1953 Optical extinction by rainfall. J.Met. 10, 486-488.

27. WORLD METEOROLOGICAL ORGANISATION 1959 WMO Technical Note No. 78 Use of ground-based radar in meteorology.

28. GUNN, K.L.S. and MARSHALL, J.S. 1958 The distribution with size of aggregate snow flakes. J.Met. 15, 452-466.

29. JOSS, J. and GORI, E.G. 1978 Shapes of raindrop size distributions. J.Appl.Met. 17, 1054-1061.

30. SRIVASTAVA, R.C. 1978 Parameterization of raindrop size distributions. J.Atmos.Sci. 35, 108-117.

31. JOSS, J. and WALDVOGEL, A. 1970 Distrometer RD-69 Instruction Manual.

32. GREEN, M.J. 1969 Effects of exposure on the catch of raingauges. Water Res.Ass. Technical Paper No. 67.

33. JOSS, J. and WALDVOGEL, A. 1969 A distrometer for raindrops.

34. WILEY, R.L., BROWNING, K.A., JOSS, J. and WALDVOGEL, A. 1970 Measurement of drop size distribution and vertical air motion in widespread rain using pulsed doppler radar and distrometer. Proc.14th Weather Radar Conf., Amer.Met.Soc., 167-170.

35. KINNELL, P.I.A. 1976 Some observations on the Joss-Waldvogel Rainfall disdrometer. J.Appl.Met. 15, 499-502.

36. MASON, B.J. 1978 Physics of a raindrop. Phys.Bull. 29, 364-369.

37. JOSS, J. 1977 Comments on "Some observations on the Joss-Waldvogel Rainfall Disdrometer". J.Appl.Met. 16, 112-113.

38. JOSS, J. and WALDVOGEL, A. 1969 Raindrop size distribution and sampling size errors. J.Atmos.Sci. 26, 566-569.

39. SASYO, Y. 1965 On the probabilistic analysis of precipitation particles. Proc.Int.Conf. on Cloud Physics, Tokyo, 254-259.

40. CUNNING, J.B. and SAX, R.I. 1977 Raindrop size distributions and Z-R relationships measured in the NOAA DC-6 and the ship Researcher within the GATE β scale array. U.S. Dept. of Commerce Nat.Tech.Info.Service PB 269 659. (NOAA Boulder, Colorado).

41. JOSS, J. and WALDVOGEL, A. 1969 Analyser AD-69 Instruction Manual.

42. GUNN, R. and KINZER, G.D. 1949 The terminal velocity of fall for droplets in stagnant air. J.Met. 6, 243-248.

43. CARBONE, R.E. and NELSON, L.D. 1978 The evolution of raindrop spectra in warm-based convective storms as observed and numerically modeled. J.Atmos.Sci. 35, 2302-2314.

44. HARDY, K.R. and DINGLE, A.N. 1960 Raindrop-size distributions in a cold frontal shower. Proc.8th Weather Radar Conf., Amer.Met.Soc., 179-186.

45. KREUELS, R.W. 1976 Statistische Interpretation von 131750 Spektren aus 13 millionen an der Messstation Meckenheim-Merl bei Bonn elektrodynamisch erfassten Tropfen. Kleinheubacher Berichte Band - Nr. 19, 221-233 FT2 Darmstadt. (Unedited translation available at the National Meteorological Library, Bracknell.)

46. METEOROLOGICAL OFFICE RADAR RESEARCH LABORATORY 1977 Meteorological Applications of Radar. Research Report No. 4. (Copy available at Meteorological Office Radar Research Laboratory, Royal Signals and Radar Establishment, Malvern, England.)

47. JOSS, J., SCHRAM, K., THAMS, J.C., and WALDVOGEL, A. 1970 On the quantitative determination of precipitation by radar. Forschungsstelle der "Eidgenössischen Kommission zum Studium der Hagelbilding und der Hagelabwehr" amd Osservatorio Ticinese della Centrale Meteorologica Svizzera, Locarno-Monti.

48. BREWER, L.J. 1976 Anmerkungen zur Erforschung von Niederschlagstrukturen mit elektronischen Pulsmessgeraten. Kleinheubacher Berichte Band - Nr. 19, 235-250 FT2 Darmstadt. (Unedited translation available at the National Meteorological Library, Bracknell.)

49. CANTANEO, R. 1971-1972 Surface measurements of condensation nuclei and raindrop distributions. Summary of Metromex Studies.

50. ICHIRO IMAI 1960 Raindrop size distributions and Z-R relationships. Proc.8th Weather Radar Conf., Amer.Met.Soc., 211-218.

51. SIMS, A.L. 1964 Case studies in areal variation in raindrop size distributions. Proc. 11th Weather Radar Conf., Amer.Met.Soc., 162-165.

52. PASQUALUCCI, F. 1978 Radar observations of drop-size distributions and vertical air velocity in a squall line storm. Proc.18th Weather Radar Conf., Amer.Met.Soc., 121-128.

53. WALDVOGEL, A. 1975 Reply to "A comment on the N_o jump of raindrop spectra". J.Atmos. Sci. 32, 653-654.

54. JOSS, J. 1979 Personal communication, 25.5.79.

55. WILSON, J.W. 1970 Integration of radar and raingauge data for improved rainfall measurements. J.App.Met. 9, 489-497.

56. HARROLD, T.W., ENGLISH, E.J. and NICHOLASS, C.A. 1974 The accuracy of radar-derived rainfall measurements in hilly terrains. Q.J.R.Met.Soc. 100, 331-350.

57. METEOROLOGICAL OFFICE RADAR RESEARCH LABORATORY 1977 The short period weather forecasting pilot project. Research Report No. 1. (Copy available at Meteorological Office Radar Research Laboratory, Royal Signals and Radar Establishment, Malvern, England.)

58. BROWNING, K.A. 1979 The FRONTIERS plan: a strategy for using radar and satellite imagery for very short-range precipitation forecasting. Met.Mag. 108, 161-184.

59.	CENTRAL WATER PLANNING UNIT, METEOROLOGICAL OFFICE, PLESSEY RADAR LTD., WATER DATA UNIT, WATER RESEARCH CENTRE.	1977	Dee weather radar and real time hydrological forecasting project. Report by the steering committee. Central Water Planning Unit, Reading, U.K.
60.	METEOROLOGICAL OFFICE RADAR RESEARCH LABORATORY	1979	Assessment of performance of Camborne Radar from November 1978 to May 1979. OAG Report No. 34. (Copy available at Meteorological Office Radar Research Laboratory, Royal Signals and Radar Establishment, Malvern, England.)
61.	BATTAN, L.J. and THEISS, J.B.	1970	Measurement of vertical velocities in convective clouds by means of pulsed-doppler radar. J.Atmos.Sci. 27, 293-298.
62.	BATTAN, L.J. and THEISS, J.B.	1970	Depolarization of microwaves by hydrometeors in a thunderstorm. J.Atmos. Sci. 27, 974-977.
63.	ROGERS, R.R.	1967	Doppler radar investigation of Hawaiian rain. Tellus 19, 432-454.
64.	WEXLER, R.	1955	An evaluation of the physical effects of the melting layer. Proc.5th Weather Radar Conf., Eng.Lab., Signal Corps, USA., 329-334.
65.	METEOROLOGICAL OFFICE RADAR RESEARCH LABORATORY	1977	Assessment of a real-time method for reducing the errors in radar rainfall measurements due to the bright-band. Research Report No. 3. (Copy available at Meteorological Office Radar Research Laboratory, Royal Signals and Radar Establishment, Malvern, England.)
66.	HARROLD, R.W. and KITCHINGMAN, P.G.	1975	Measurement of surface rainfall using radar when the beam intersects the melting layer. Preprint Vol. 16th Weather Radar Conf., Amer.Met.Soc., 473-478.

67. COLLIER, C.G. 1976 The height of the freezing level during rainfall over the British Isles. Met.Mag. 105, 381-392.

68. CENTRAL WATER PLANNING UNIT, METEOROLOGICAL OFFICE, PLESSEY RADAR LTD., WATER DATA UNIT, WATER RESEARCH CENTRE. 1977 Dee weather radar and real time hydrological forecasting project. Report by operations systems group. Water Research Board, Reading, U.K.

69. METEOROLOGICAL OFFICE RADAR RESEARCH LABORATORY 1979 Assessment of radar performance to August 1979 and derivation of correction factors. OAG Report No. 40. (Copy available at Meteorological Office Radar Research Laboratory, Royal Signals and Radar Establishment, Malvern, England.)

PLATES

1. General view of St. Mawgan Meteorological Office compound and control tower.

2. Distrometer transducer in pit.

3. Distrometer transducer with anti-splash surround and 5 inch station gauge.

4. Distrometer transducer.

5. Processor, analyser, clock and paper tape punch.

Plate 1

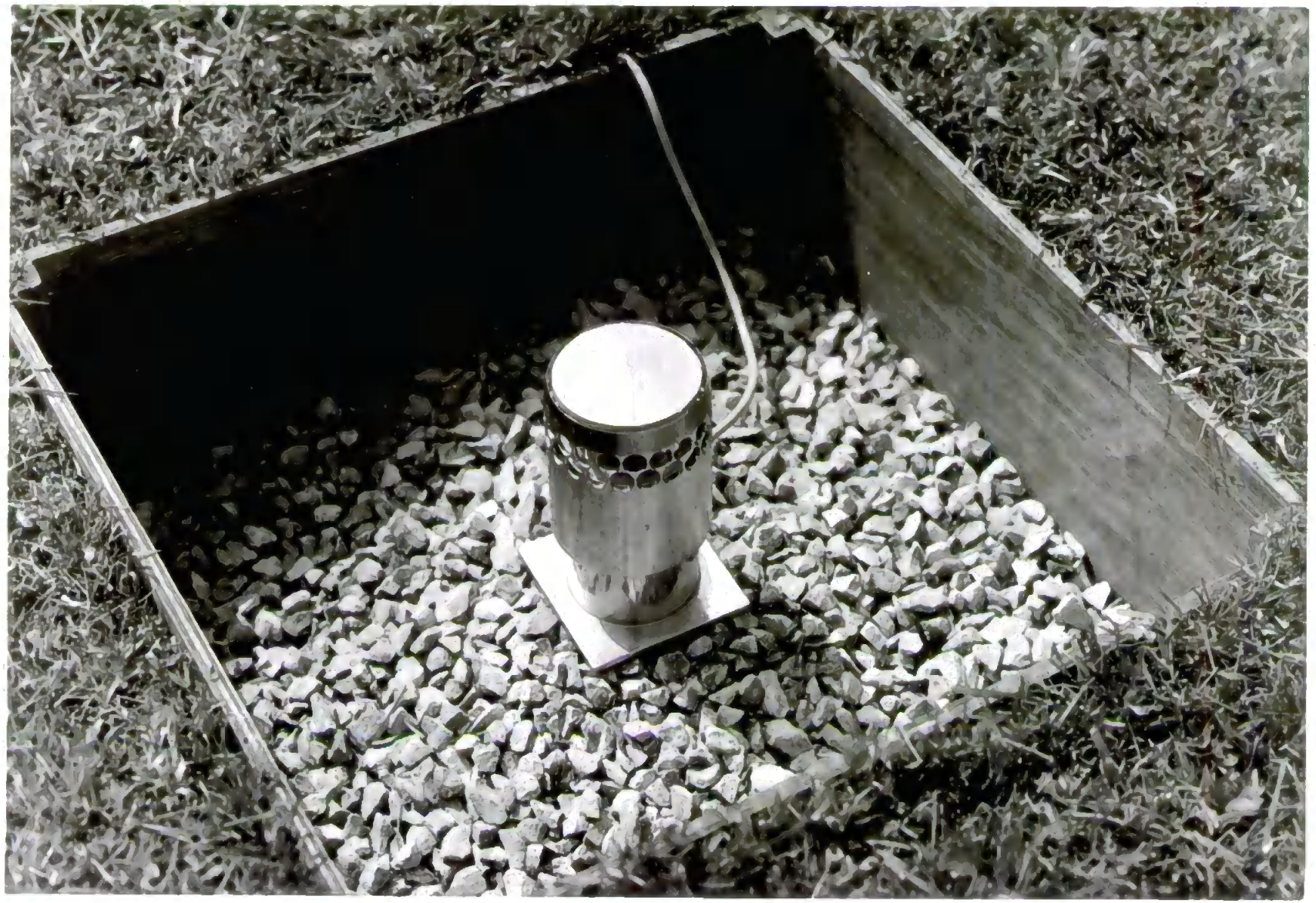

Plate 2

Plate 3

Plate 4

Plate 5

Appendix I

DISTROMETER HARDWARE SPECIFICATION

Specification of distrometer (RD 69)

Calibration curve for distrometer

Specification of analyser (AD 69)

Specification of paper tape punch (FACIT 4070)

Specification of crystal-controlled clock (Venner TSA 6686)

SPECIFICATION OF DISTROMETER (RD 69)

Range of drop diameter: 0.3 mm - 5 mm

Sampling area: 50 cm^2

Relation between drop diameter D and amplitude of output pulse U_c:

$$U_c = 0.94\ D^{1.52}$$

(U_c is measured in volts, D is measured in millimetres)

Accuracy: ± 5% of measured drop diameter

Power requirements: 115 volts AC ± 10% or 230 volts AC ± 10%
50 - 400 Hz, 5 watts
or ± 15 volts DC, 50 m A

Operating temperature range: 0° to 40°C

Size: transducer: 10 cm . 10 cm . 17 cm
processor: 10 cm . 23 cm . 27 cm

Weight: transducer: 2.4 kg
processor: 1.8 kg

Length of cable provided with the instrument: 10 metres

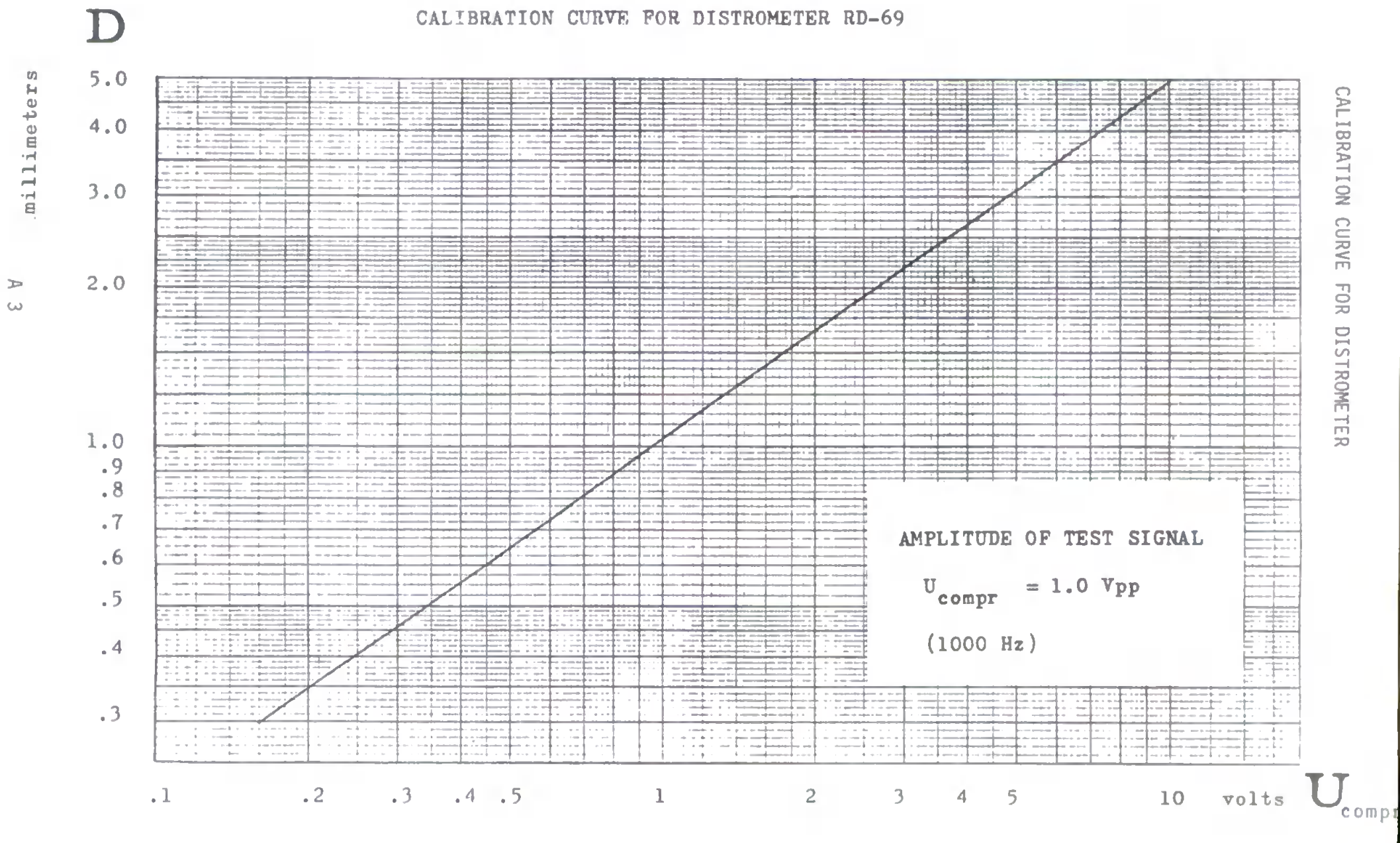
D
CALIBRATION CURVE FOR DISTROMETER RD-69
millimeters
5.0
4.0
3.0
2.0
1.0
.9
.8
.7
.6
.5
.4
.3
AMPLITUDE OF TEST SIGNAL
U_{compr} = 1.0 Vpp
(1000 Hz)
.1
.2
.3
.4
.5
1
2
3
4
5
10
volts
U_{compr}
A 3
CALIBRATION CURVE FOR DISTROMETER

SPECIFICATION OF ANALYSER (AD 69)

Number of channels:	20
Channel spacing:	individually adjustable, distributed over the range of input amplitudes to yield convenient drop size classes if operated in connection with the Distrometer Rd-69.
Input amplitude range:	for Processor Rd-69 signals: 160 mV - 10 V for tape recorder signals: 10 mV - 0.6 V
Pulse length:	0.1 msec - 1 msec
Accuracy:	± 2% of set value
Outputs:	a) twenty line output (one line per channel) suitable for driving electromechanical counters. b) parallel five bit binary output.
Power requirements:	220 V AC ± 10% or 110 V AC ± 10% 50 - 400 Hz, 10 watts
Operating ambient temperature range:	0° - 40°C
Size:	15 cm . 23 cm . 27 cm
Weight:	3.8 kg

SPECIFICATIONS PAPER TAPE PUNCH (FACIT 4070)

GENERAL DATA

Operation speed:	Up to 75 rows per second.
Tape feed:	Asynchronous, externally controlled.
Feed Accuracy:	Complies with or exceeds ISO standard. Adjacent rows, 3% 10 rows, 1% 50 rows, 0.5%
Backspacing:	Up to 10 steps.
Punch hole configuration:	5–8 track ISO standard, 6 track type-setting or 6 track Japanese telex.
Tape Widths:	5 track tape, 11/16 inch (17.5 mm ± 0.1 mm) and 8 track tape, 1 inch (25.4 mm ± 0.1 mm). Alternatively 6 and 7 track, 7/8 inch (22.2 mm ± 0.1 mm).
Thickness of tape:	0.08–0.11 mm. Optional control logic accomodates thicker tape.
Type of tape:	ISO-standardized paper tape.
Hub:	51 – 52 mm cores (2") as standard. Other types optional.
Outer diameter of tape reel:	Max. 200 mm (8").
Reel Capacity:	Approx. 300 m which corresponds to about 120,000 rows.
Store:	Built in, stores one row (max. nine bits).
Mark Character:	Customer-selected. Usually an all-hole delete character.
Noise level with cover on (distance of 1 metre):	Idling nil 5 ch/s punching one track 59 dB (B) 5 ch/s punching in all tracks 61 dB (B) 75 ch/s punching one track 75 dB (B) 75 ch/s punching in all tracks 77 dB (B)
Dimensions:	Length 432 mm (17"), width 220 mm (8 5/8") and height 198 mm (7 3/4").
Weight:	AC version: 13.5 kg (30 lb). DC version: 9.5 kg (21 lb).

INPUT SIGNALS

	Signals shorter than 10 μs at 6 V signal level are rejected as noise.
Punch Instruction signal (PI):	Min. pulse duration 0.1 ms. Input imp. min 2.2 kohms. Logical 1: +3.5 V to +12 V. Rise time: Max. 10 μs. Logical 0: −12 V to +1.5 V.
Data signals (Ch1 – Ch9):	Min. pulse duration 200 μs. Ch1 to Ch 8 – for tracks 1 to 8 – input imp. min 22 kohms. Ch9 – for feed hole track – input imp. min 22 kohms. Logical 1: +3.5 V to +12 V. Rise time: Max. 10 μs. Logical 0: −12 V to +1.5 V.
Stepping Direction signal (SD):	Input imp. min 2.2 kohms. Forward direction: −12 V to +1.5 V. Backward direction: +3.5 V to +12 V.
Remote Control:	−12 V signal voltage recommended to avoid interference.

OUTPUT SIGNALS

Punch Ready signal (PR):	From logical 1 to logical 0 when information is stored in register. From logical 0 to logical 1 when punching is completed. Logical 1: +6 V. Output imp. 1 kohm. Logical 0: Max. +0.4 V. Max. 10 mA.
Tape Low signal (TL):	From logical 0 to logical 1 when TL is generated. Logical 1: +6 V via reed relay. Max. 10 mA. Logical 0: 0 V via 470 ohms.
Error signal (Err):	From logical 0 to logical 1 when Err is generated. Logical 1: +5 V at 3 mA. Output imp. 100 ohms. Logical 0: Max. +0.6 V at 1 mA.
External signal (Ext):	0 V when EXT-key is depressed. (Floating when not depressed).

SUPPLY VOLTAGE

AC version:	115/127/220/240 V $^{+15\%}_{-10\%}$ 50 to 100 Hz. Optional 400 Hz. Max. power consumption 200 W. Min. power consumption 50 W.
DC version:	24 V $^{+25\%}_{-15\%}$ Max. power consumption 180 W. Min. power consumption 2–5 W.
	Both the AC and DC versions are dimensioned to provide extra DC outputs for additional electronics of 1 A at +6 V and +24 V.

VARIANTS

Four variants of both the AC and DC versions are available.

Facit 4070 for:	5 and 8-track standard tape 6 and 7-track standard tape 6 track typesetting tape 6 track Japanese telex tape

SPECIFICATION OF CRYSTAL-CONTROLLED CLOCK (VENNER TSA 6686)

Supply:

100 - 125V, 50 Hz
or 200 - 250V, 50 Hz
(N.B. Voltage adjustment at internal transformers)
Consumption: approx. 24W.

Timing Signal Source:

Oven-controlled crystal oscillator
Crystal frequency: 1MHz ± 2 parts in 10^6
Warm-up or stabilization period approx. 10 minutes

Display:

'Tens' and 'units' of Hours, Minutes & Seconds
(In 1-second increments to 23 hrs. 59 mins. 59 secs.)
Display presented by six in-line side-view neon indicator tubes.

Start & Stop Inputs:

(i) Signal:-

Signal : Negative pulse
Amplitude: min. 4V peak
max. 50V "
Rise time: 0.2μS max.

Input Impedance : 100kΩ shunted by 130pF for pulses up to 6V; shunted by 5000pF for pulses above 6V.

Accuracy of start : ± 1μS

(ii) Contact:-

Operation (start or stop) can be initiated by contact closure between centre-pin and shell of appropriate input socket.

Temperature Range:

-10° to +60° Centigrade

Dimensions & Weight:

Panel Width	Panel Height	Unit Depth (front to rear)	Weight
48.5 cm	14 cm	24 cm	6.4 Kg

Appendix II

DISTROMETER OPERATING INSTRUCTIONS

These are the instructions which were left at the Meteorological Office at RAF St. Mawgan for the guidance of the staff who changed the paper tapes as required.

OPERATION OF DISTROMETER EQUIPMENT

General

The equipment should run without any attention other than changing the paper tape when necessary and noting any unusual occurrences, e.g. power failure.

The instructions for changing the paper tape are given below in some detail, and it is important that they are carried out in the stated sequence to avoid any spurious signals being punched on the tape.

The time displayed on the clock unit is immaterial, since it is only required for punching a time mark every minute.

The experiment is designed to run continuously, even during lengthy periods without rain. It is important that none of the equipment is turned off and that the controls of the tape punch are left untouched except when replacing a paper tape.

Thank you very much for helping with this experiment. Should you have any queries, my name is

Andrew Eccleston

address School of Maritime Studies
Plymouth Polytechnic
Drake Circus
Plymouth PL4 8AA
Devon.

Telephone: (0752) 23483 or pass a message via Mrs. Eccleston
(0752) 21312 Ext. 223.

CHANGING PAPER TAPE

When the tape is nearly finished, the 'TAPE LOW' lamp lights.
Please avoid changing tape during a period of rain.

Removing used tape

Run out tape on 'FEED HOLES' for approx. 10 seconds.
Remove perspex cover and break tape at Ⓧ. (See diagram)
Remove take up spool by pulling up on perimeter and remove used tape from spool by pushing in sector on centre bobbin until a click is heard and plastic centre is released. Secure end of tape with small piece of sellotape.
Write finish time on log and write number on side of reel.
Switch off Processor, analyser and clock unit.
Break tape at Ⓨ and run out on 'TAPE FEED', removing remainder of unused tape off feed spool. Remove the plastic centre and discard remainder of tape.

Loading new tape

Place new tape on feed spool and push down until a click is heard and plastic centre is gripped.
Place take up spool on top of feed spool having moved drive-pedestal Ⓩ clear.
Remove garbage bin, open front lid and loop tape round rollers as shown to leave end of tape lying against roller Ⓐ.
Run tape through on 'FEED HOLES' for about 18".
Pass tape under roller Ⓑ which may be swung out clear of machine.
Pass tape round pedestal Ⓒ to raise to height of take up spool.
Replace plastic centre on take up spool and press down to secure, attach end of new tape with sellotape.
Replace perspex cover and switch on equipment (i.e. processor, analyser and clock unit, ensuring that the latter is set to "OPERATE" and that the "START" button is depressed and seconds digits are counting).
Run out on 'FEED HOLES' for approx. 10 seconds and log start time.

SCHEMATIC PLAN AND ELEVATION OF PAPER TAPE PUNCH.

Not to scale.

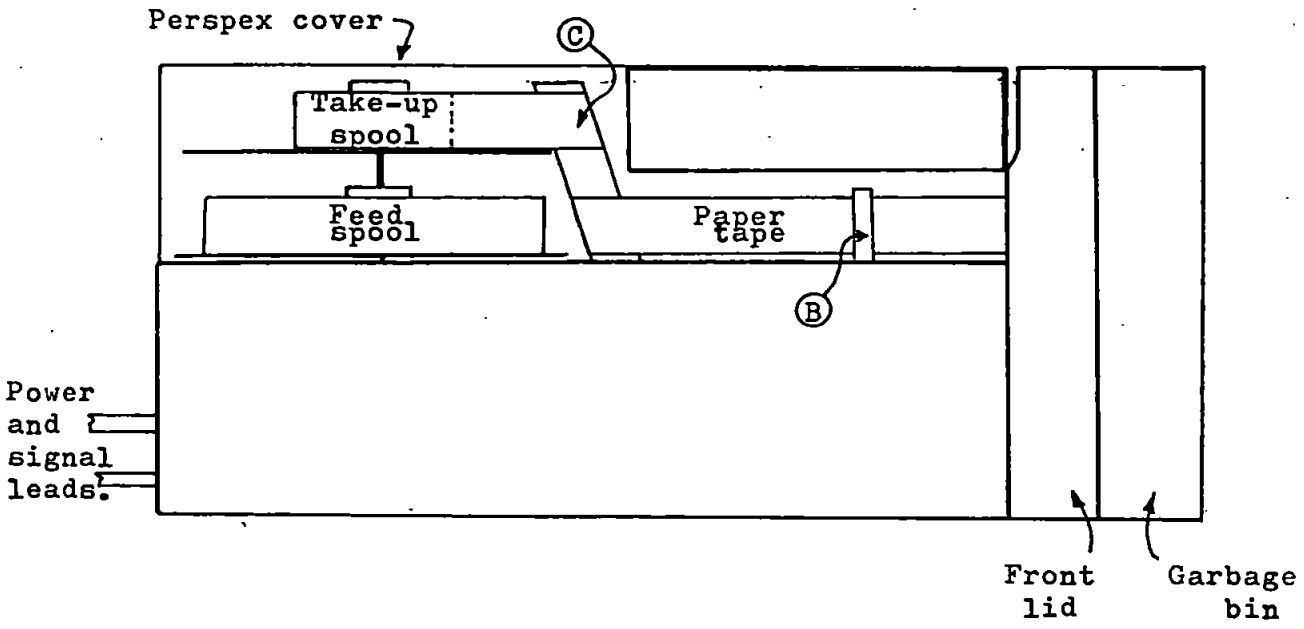

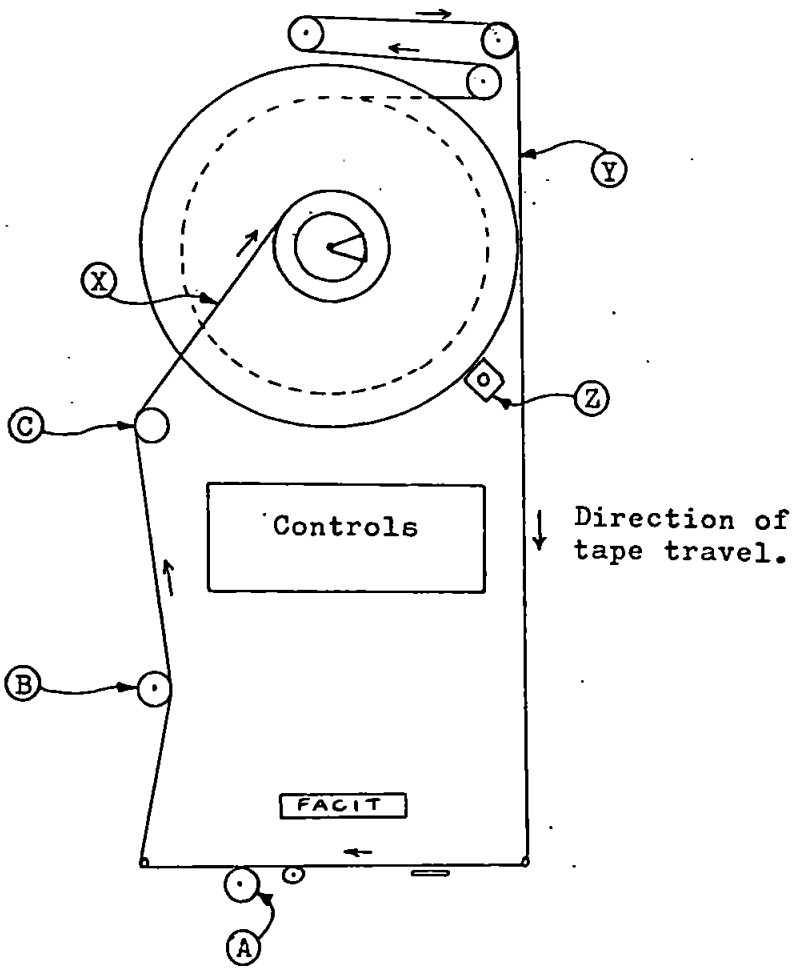

Appendix III

COMPUTER HARDWARE AND SOFTWARE

The data base for the distrometer experiment was created on magtape, as described in Chapter 2, using an ICL 1903 mainframe computer. Most of the processing of the distrometer and radar records was performed on this computer, making use of the CALCOMP plotter where appropriate. Some investigations and calculations which did not require access to the whole data base were performed interactively using either an ICL 2903, Commodore PET 2032 or TI57 programmable calculator.

The ICL 1903 was used interactively under the MAXIMOP system to create subfiles to be read as input for CONB to produce the time-height profiles as described in 4.3.5. CONB was the only "package" used in this work, the remainder of the software being developed to meet the particular requirements of the experiment. A brief summary of the FORTRAN programs (identified by job name) written for the ICL 1903 is included below. Listings of RAINDROPS and RAINSPECTRA (described in some detail in 2.4) are given together with some examples of output.

BLUEPETER	power curve fit to N_o and A values
CROSSROADS	interpolates radar data and creates MAXIMOP file
DISTAVER	computes average raindrop-size distributions
GRANDSTAND	computes 5 minute moving averages
JACKANORY	computes N_o and A from distrometer data
MTEDIT	utility program to edit magtapes

NATIONWIDE	computes and plots distrometer gauge differences in relation to anemograph data
PANORAMA	combines distrometer and radar data and plots results in half hour blocks
RADAR DATA	writes raw radar data from cards to magtape
RAINDROPS	reads distrometer paper tape data and creates ECCRAIN magtape
RAINCHECK	computes distrometer hourly totals
RAINMESS	utility program to edit magtapes
RAINPLOTS	plots average raindrop-size distributions
RAINSPECTRA	computes raindrop spectra and creates ECCSPECT magtape
RAINTIME	computes and plots time series of R, N_0 and λ
RGAGCHECK	computes distrometer hourly totals and plots comparison with raingauge
ZPROFILE	interpolates Z values from raw radar data and creates RADARDATA magtape
ZREL	computes Z-R relationships from distrometer data

Program Listing - RAINDROPS

```
JOB RAINDROPS,074006CF,ECCLESTON
PPLAN TPRD,,,X
PFORTPLUS SORT,1
PRUN SORT,,,,5000
****
```

→The statements marked by an arrow are altered on each run.

```
#STEER          LIST,OBJECT,MONITOR
#PROGRAM        /TPRD
#
#               SUBROUTINE TO READ DISTROMETER DATA FROM PAPER TAPE
#               IN IMAGE MODE AND UNPACK EACH FRAME INTO AN INTEGER
#               WORD
#
#               CALLED FROM FORTRAN WITH 3 ARGUMENTS
#               1   SWITCH PRESET -VE FOR FIRST CALL, ZERO OTHERWISE
#                   GETS SET TO 999 IF PAPER TAPE INPUT ERROR
#               2   ADDRESS FOR UNPACKED INTEGER DATA
#               3   NO OF FRAMES TO READ
#
#PERIPHERAL     TRO
#LOWER          NXWD,FRMCT,IMAGE(20)
TRCON           0/#20,0,80,0/IMAGE.0
FSWD            0/IMAGE.0
ERBIT           #04000000
#PROGRAM
TPRD  OBEY      (1)
#
      LDX   7   (3)
      LDX   6   FRMCT
      BZE   7   BLOK
      ON    4   1
      ALLOT     TRO
RDNUL PERI  0   TRCON
      SUSBY     TRO
      LDX   2   FSWD
      LDCT  6   40
      LDX   4   TRCON+1
      ANDX  4   ERBIT
      BNZ   4   ERRET
#
LKNUL STO   2   NXWD
      LDCH  4   (2)
      BCHX  2   *+1
      LDCH  5   (2)
      BCHX  2   *+1
      SLL   4   6
      ORX   4   5
      BNZ   4   BLOK
      BUX   6   LKNUL
      BRN       RDNUL
#
BLOK  OBEY      1(1)
      LDLA  4   3
      OBEY      2(1)
      LDX   2   0(3)
      LDCT  3   0(2)
      ORX   3   4
```

```
        LDX    2  NXWD
#
NXFRM   LDCH   4  (2)
        BCHX   2  *+1
        LDCH   5  (2)
        BCHX   2  *+1
        SLL    4  6
        ORX    4  5
        STO    4  (3)
        BUX    6  FRLP
        PERI   0  TRCON
        LDX    2  FSWD
        LDCT   6  40
        SUSBY     TRO
        LDX    4  TRCON+1
        ANDX   4  ERBIT
        BNZ    4  ERRET
FRLP    BUX    3  NXFRM
#
        STO    6  FRMCT
        STO    2  NXWD
        EXIT   1  2
#
ERRET   LDN    4  999
        OBEY      (1)
        STO    4  (3)
        EXIT   1  2
#END
```

```
        LIST
        WORK(ED,ICLF-DEFAULT)
        LIBRARY(SUBGROUPFSCE)
        DUMP ON (PROGRAM DUMP)
        LIBRARY (COMMON FILEA)
        LIBRARY (SUBGROUPS-RS)
        PROGRAM (SORT)
        INPUT 2=CRO
        OUTPUT 3=LPO
      → INPUT 5=MT1/FORMATTED(ECCRAIN(26))/2502
      → CREATE 4=MTO/FORMATTED(ECCRAIN(29,4095))/2502
        COMPACT
        COMPRESS INTEGER AND LOGICAL
        TRACE 0
        END
```

```
        MASTER SORT
        INTEGER ERR,A,TM,AREF,BREF,TMO
        DIMENSION A(23),DIMENSION INPT(10),DIMENSION N(20),
        DIMENSION TMO(5)
C
C  COPY PREVIOUS ECCRAIN MT
C
     5  READ (5,900)TM,(N(J),J=1,20),ERR,AREF,BREF,NULLS
   900  FORMAT(25A4)
        IF(TM.EQ.999999) GO TO 6
        WRITE(4,900)TM,(N(J),J=1,20),ERR,AREF,BREF,NULLS
        GO TO 5
     6  CONTINUE
```

```
C
C  INITIALISE VARIABLES
C
      DATA A/34,3,36,5,6,39,40,9,10,43,12,45,46,15,48,17,18,51,20,
     153,23,33,63/
     →NOTAPE=27
      WRITE(3,1001)NOTAPE
 1001 FORMAT(1H1,//////' TAPE NUMBER',I4,//)
      DO 50 K=1,20
      N(K)=0
   50 CONTINUE
      MREC=0
      NREC=0
      NERREC=0
     → TM=85179
      LFTM=TM
      ERR=0
      AREF=0
      BREF=0
      NULLS=0
      IFST=-1
C
C  READ AND COMPUTE NEW DATA FROM PT
C
   10 CALL TPRD(IFST,INPT(1),10)
      IFST=0
      DO 120 J=1,10
      IF(INPT(J).NE.0)GO TO 40
  120 CONTINUE
      GO TO 300
   40 I=1
   20 DO 30 K=1,20
      IF(INPT(I).EQ.A(K))GO TO 170
   30 CONTINUE
      IF(INPT(I).EQ.A(23))GO TO 100
      IF(INPT(I).EQ.A(22))GO TO 130
      IF(INPT(I).EQ.A(21))GO TO 150
      IF(INPT(I).EQ.0)GO TO 190
      ERR=ERR+1
      GO TO 70
  130 BREF=BREF+1
      GO TO 70
  150 AREF=AREF+1
      GO TO 70
  190 NULLS=NULLS+1
      GO TO 70
  100 TM=TM+1
      WRITE(4,1040)TM,(N(K),K=1,20),ERR,AREF,BREF,NULLS
 1040 FORMAT(25A4)
      ISUM=0
      DO 200 J=1,20
      ISUM=ISUM+N(J)
  200 CONTINUE
      IF(ISUM.LT.7) GO TO 210
      MREC=MREC+1
  210 CONTINUE
      NREC=NREC+1
      NERSUM=ERR+AREF+BREF+NULLS
      IF(NERSUM.EQ.0) GO TO 105
      NERREC=NERREC+1
      IF (NERREC.NE.1) GO TO 104
```

```
C
C  OUTPUT RESULTS
C
      WRITE(3,1015)
 1015 FORMAT(' RECORDS CONTAINING ERRORS',//)
      WRITE(3,1020)
 1020 FORMAT(1X,4HTIME,7X,79H   1   2   3   4   5   6   7   8   9
     110  11  12  13  14  15  16  17  18  19  20,4X,6HERRORS,2X,
     24HAREF,2X,4HBREF,1X,5HNULLS,//)
  104 WRITE(3,1005)TM,(N(K),K=1,20),ERR,AREF,BREF,NULLS
 1005 FORMAT(1X,I6,4X,20I4,4X,4I6,/)
  105 DO 110 K=1,20
      N(K)=0
  110 CONTINUE
      ERR=0
      AREF=0
      BREF=0
      NULLS=0
      GO TO 70
  170 N(K)=N(K)+1
   70 I=I+1
      IF(11-I)10,10,20
C
C  OUTPUT SUMMARY AND WRITE TERMINATOR ON MT
C
  300 WRITE(3,1030)MREC
 1030 FORMAT(//,' TOTAL MINUTES OF DATA:',I6,//)
      WRITE(3,1031)NERREC
 1031 FORMAT(/,' TOTAL MINUTES WITH ERRORS:',I6,/)
      WRITE(3,1050)NREC
 1050 FORMAT(//,' TOTAL MINUTES ON TAPE:',I6,//)
      TM=NREC+LFTM
      TM=999999
      WRITE(4,1040)TM,(N(K),K=1,20),ERR,AREF,BREF,NULLS
      STOP
      END
      FINISH
****
```

TAPE NUMBER 14

RECORDS CONTAINING ERRORS

TIME	1	2	3	4	5	6	7	8	9	10	11	12	13	14	15	16	17	18	19	20	ERRORS	AREF	BREF	NULLS
39335	24	15	8	1	0	0	1	0	0	0	0	0	0	0	0	0	0	0	0	0	0	0	0	1
39336	10	1	4	0	1	0	1	1	0	0	0	0	0	0	0	0	0	0	0	0	0	0	0	1

TOTAL MINUTES OF DATA: 502

TOTAL MINUTES WITH ERRORS: 2

TOTAL MINUTES ON TAPE: 1007

Example of line printer output - RAINDROPS

Program Listing - RAINSPECTRA

```
JOB RAINSPECTRA,074006CF,ECCLESTON
PFORTPLUS DROP,1
PRUN DROP,,,,5000
****
      LIST
      WORK(ED,ICLF-DEFAULT)
      DUMP ON (PROGRAM DUMP)
      PROGRAM (DROP)
      INPUT 2=CRO
      OUTPUT 3=LPO
→     INPUT 4=MTO/FORMATTED(ECCRAIN(37))/2502
→     CREATE 5=MT1/FORMATTED(ECCSPECT(8,4095))/2302
      COMPRESS INTEGER AND LOGICAL
      TRACE 0
      END


      MASTER DROP
      INTEGER ERR,AREF,BREF,TMO,TM
      DIMENSION NQ(20),DIMENSION N(20),DIMENSION R(20)
      DIMENSION TMO(5)
      WRITE(3,2000)
 2000 FORMAT(1H1,111H TIME  0.3  0.4  0.5  0.6  0.7  0.8  1.0  1.2
     11.6  1.8  2.1  2.4  2.7  3.0  3.3  3.7  4.1  4.5  5.0  RAIN,/)
      WRITE(3,2001)
 2001 FORMAT(112H       0.4  0.5  0.6  0.7  0.8  1.0  1.2  1.4  1.6
     2 1.8  2.1  2.4  2.7  3.0  3.3  3.7  4.1  4.5  5.0  MM/HR,//)
C
C  READ DATA FROM ECCRAIN MT AND CALL SUBROUTINE SPECR AS REQUIRED
C
   25 READ(4,5000)TM,(N(J),J=1,20),ERR,AREF,BREF,NULLS
 5000 FORMAT(25A4)
      IF (TM.EQ.999999) GO TO 2400
      ISUM=0
      DO 210 J=1,20
      ISUM=N(J)+ISUM
  210 CONTINUE
      IF(ISUM.LT.7) GO TO 2100
  215 MFLAG=ERR+AREF+BREF+NULLS
      IF(MFLAG.EQ.0) GO TO 220
      IFLAG=1
      GO TO 230
  220 IFLAG=0
  230 CALL SPECR(TM,N,IFLAG)
      GO TO 25
 2100 NORAIN=0
 2110 NORAIN=NORAIN+1
      IF(NORAIN.GT.5) GO TO 2200
      READ(4,5000)TM,(N(J),J=1,20),ERR,AREF,BREF,NULLS
      IF (TM.EQ.999999) GO TO 2400
      ISUM=0
      DO 240 J=1,20
      ISUM=N(J)+ISUM
  240 CONTINUE
      IF(ISUM.LT.7) GO TO 2110
      TMO(1)=TM-NORAIN
```

→ These statements marked by an arrow are altered on each run.

```
      TMO(2)=TM-NORAIN+1
      TMO(3)=TM-NORAIN+2
      TMO(4)=TM-NORAIN+3
      TMO(5)=TM-NORAIN+4
      RAIN=0
      IFLAG=0
      DO 250 J=1,NORAIN
      WRITE(3,1050)TMO(J)
 1050 FORMAT(1X,I6,2X,7HNO RAIN,/)
  250 CONTINUE
      GO TO 215
 2200 READ(4,5000)TM,(N(J),J=1,20),ERR,AREF,BREF,NULLS
      IF (TM.EQ.999999) GO TO 2400
      ISUM=0
      DO 260 J=1,20
      ISUM=ISUM+N(J)
  260 CONTINUE
      IF(ISUM.LT.7) GO TO 2300
      WRITE(3,1060)NORAIN
 1060 FORMAT(/,10X,11HNO RAIN FOR,I5,8H MINUTES,//)
      GO TO 215
 2300 NORAIN=NORAIN+1
      GO TO 2200
C
C  END OF DATA - WRITE TERMINATOR ON MT
C
 2400 WRITE(3,4000)
 4000 FORMAT(//'  END OF DATA')
      TM=888888
      WRITE(5,4040)TM,(N(J),J=1,20),ERR,IFLAG)
 4040 FORMAT(23A4)
      STOP
      END


      SUBROUTINE SPECR(TM,N,IFLAG)
      INTEGER TM
      DIMENSION N(20),DIMENSION X(20),DIMENSION D(21),
      DIMENSION IQ(20),DIMENSION R(20),DIMENSION V(20),
      DIMENSION Q(20)
C
C  COMPUTE SPECTRUM AND WRITE TO ECCSPECT MT
C
      DATA V/1.4,1.84,2.26,2.67,3.07,3.65,4.33,4.90,5.41,5.87,6.4,6.
     198,7.48,7.88,8.21,8.50,8.77,8.95,9.05,9.12/
      DATA X/0.1,0.1,0.1,0.1,0.1,0.2,0.2,0.2,0.2,0.2,0.3,0.3,0.3,0.3
     1,0.3,0.4,0.4,0.4,0.5,0.4/
      DATA D/0.3,0.4,0.5,0.6,0.7,0.8,1.0,1.2,1.4,1.6,1.8,2.1,2.4,2.7
     1,3.0,3.3,3.7,4.1,4.5,5.0,5.4/
      RAIN=0
      DO 100 J=1,20
      R(J)=0
      IQ(J)=0
      Q(J)=0
  100 CONTINUE
      DO 290 J=1,20
      Q(J)=N(J)/(0.005*V(J)*60*X(J))
      R(J)=N(J)*(D(J)**3+D(J+1)**3)
      RAIN=RAIN+R(J)
  290 CONTINUE
      RAIN=RAIN*0.0031416
```

```
      IRAIN=1000*RAIN
      DO 295 J=1,20
      IF(Q(J).EQ.0) GO TO 295
      IQ(J)=1000*ALOG10(Q(J))
  295 CONTINUE
      WRITE (5,3040)TM,(IQ(J),J=1,20),IRAIN,IFLAG
 3040 FORMAT(23A4)
      DO 291 J=1,20
      IF(Q(J).EQ.0) GO TO 291
      Q(J)=ALOG10(Q(J))
  291 CONTINUE
      WRITE(3,3000)TM,(Q(J),J=1,20),RAIN,IFLAG
 3000 FORMAT(1X,I6,20F5.2,2X,F7.3,2X,I1,/)
      RETURN
      END
      FINISH
****
```

Minute No.	← Computed spectrum (20 log N_D values) →																					R ($mm\ hr^{-1}$)	Error flag
43960	3.76	3.52	3.55	2.92	2.31	2.53	2.19	1.61	0.97	0.75	0.84	0.00	0.00	0.00	0.00	0.00	0.00	0.00	0.00	0.00	0.00	1.890	0
43961	3.43	3.31	3.23	2.66	2.66	2.52	2.13	1.53	1.33	0.45	0.24	0.00	0.00	0.00	0.00	0.00	0.00	0.00	0.00	0.00	0.00	1.421	0
43962	3.50	3.34	3.20	2.75	2.68	2.43	2.09	1.43	0.97	0.75	0.54	0.00	0.00	0.00	0.00	0.00	0.00	0.00	0.00	0.00	0.00	1.328	0
43963	3.28	3.12	3.04	2.42	2.60	2.19	1.70	1.01	0.49	0.00	0.00	0.00	0.00	0.00	0.00	0.00	0.00	0.00	0.00	0.00	0.00	0.619	0
43964	3.23	3.12	2.96	2.53	2.64	2.24	1.82	1.43	1.09	0.45	0.24	0.00	0.00	0.00	0.00	0.00	0.00	0.00	0.00	0.00	0.00	0.887	0
43965	3.00	2.66	2.75	2.33	2.36	1.96	1.76	1.31	0.79	0.00	0.00	0.00	0.00	0.00	0.00	0.00	0.00	0.00	0.00	0.00	0.00	0.505	0
43966	2.55	2.26	2.37	1.80	1.31	1.66	1.36	1.43	0.79	1.06	0.24	0.00	0.00	0.00	0.00	0.00	0.00	0.00	0.00	0.00	0.00	0.479	0
43967	2.55	2.37	2.14	1.80	2.15	1.56	1.36	1.13	0.49	0.00	0.24	0.00	0.00	0.00	0.00	0.00	0.00	0.00	0.00	0.00	0.00	0.280	0
43968	2.68	2.46	2.58	1.57	1.88	1.26	1.06	0.00	0.00	0.00	0.00	0.00	0.00	0.00	0.00	0.00	0.00	0.00	0.00	0.00	0.00	0.112	0
43969	2.46	2.10	2.21	1.10	1.34	0.60	0.00	0.00	0.00	0.00	0.00	0.00	0.00	0.00	0.00	0.00	0.00	0.00	0.00	0.00	0.00	0.026	0
43970	2.08	1.86	1.77	0.00	1.04	0.00	0.00	0.00	0.00	0.00	0.00	0.00	0.00	0.00	0.00	0.00	0.00	0.00	0.00	0.00	0.00	0.011	0
NO RAIN FOR 10 MINUTES																							
43981	2.08	1.74	1.47	0.00	0.00	0.00	0.00	0.00	0.00	0.00	0.00	0.00	0.00	0.00	0.00	0.00	0.00	0.00	0.00	0.00	0.00	0.005	0
43982	2.08	1.74	1.47	1.10	0.00	0.00	0.00	0.00	0.00	0.00	0.00	0.00	0.00	0.00	0.00	0.00	0.00	0.00	0.00	0.00	0.00	0.007	0
43983	1.98	1.74	1.17	0.00	0.00	0.00	0.00	0.00	0.00	0.00	0.00	0.00	0.00	0.00	0.00	0.00	0.00	0.00	0.00	0.00	0.00	0.004	0
43984	2.22	1.74	1.17	0.00	1.14	0.00	0.00	0.00	0.00	0.00	0.00	0.00	0.00	0.00	0.00	0.00	0.00	0.00	0.00	0.00	0.00	0.008	0
43985	NO RAIN																						
43986	NO RAIN																						
43987	2.22	0.00	1.47	0.00	0.10	0.00	0.00	0.00	0.00	0.00	0.00	0.00	0.00	0.00	0.00	0.00	0.00	0.00	0.00	0.00	0.00	0.004	0
43988	1.68	1.56	1.47	1.10	0.00	0.66	0.00	0.00	0.00	0.00	0.00	0.00	0.00	0.00	0.00	0.00	0.00	0.00	0.00	0.00	0.00	0.010	0
43989	NO RAIN																						
43990	2.22	1.86	1.65	0.00	0.10	0.00	0.00	0.00	0.00	0.00	0.00	0.00	0.00	0.00	0.00	0.00	0.00	0.00	0.00	0.00	0.00	0.008	0
43991	2.21	2.41	2.07	0.00	0.00	0.00	0.00	0.01	0.00	0.00	0.00	0.00	0.00	0.00	0.00	0.00	0.00	0.00	0.00	0.00	0.00	0.016	0

Example of line printer output - RAINSPECTRA

Appendix IV

AVERAGE RAINDROP-SIZE DISTRIBUTIONS FROM SECOND DATA SET

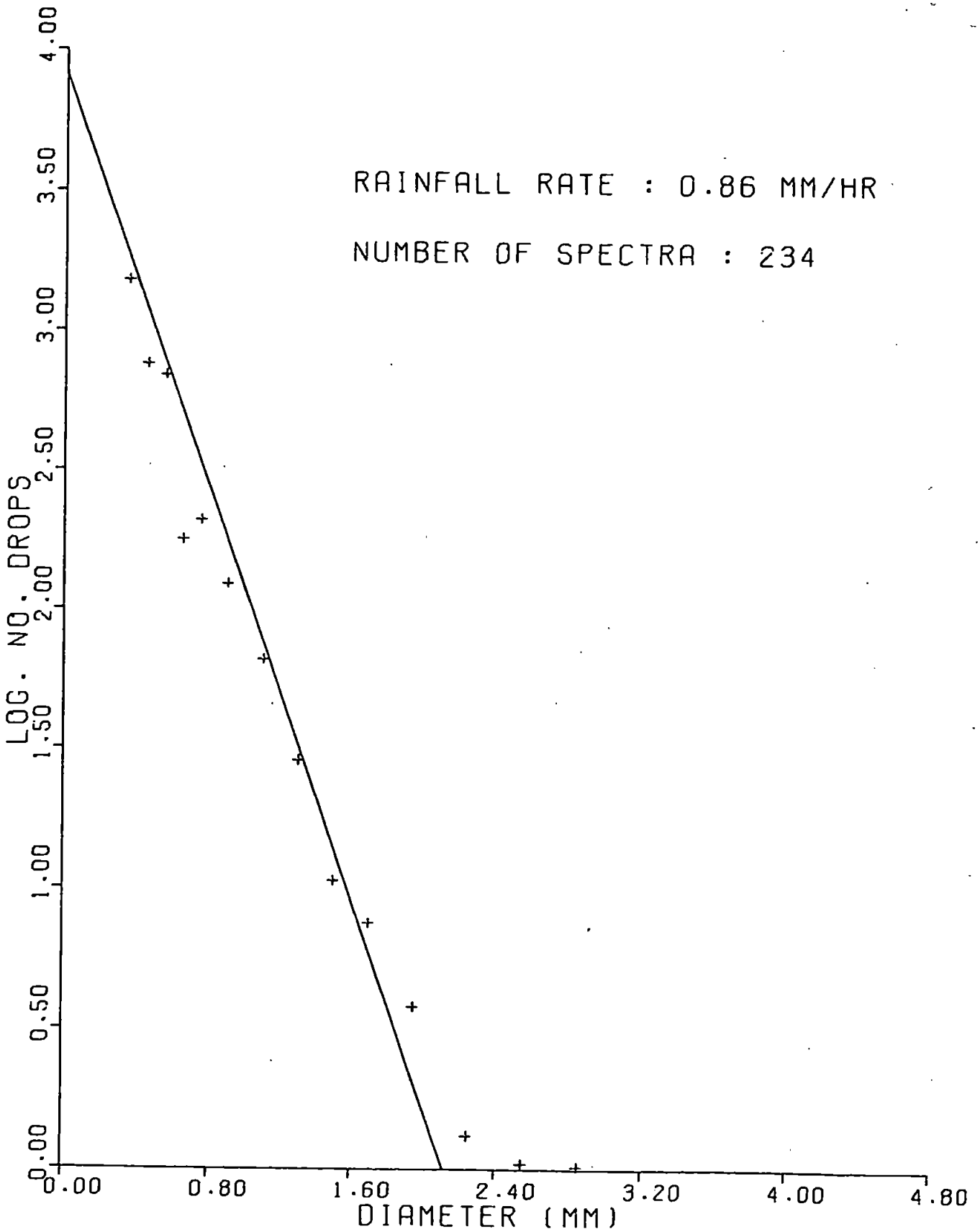

Average raindrop-size distribution (2ND DATA SET)
Rainfall rates about 1.0 mm hr^{-1}.

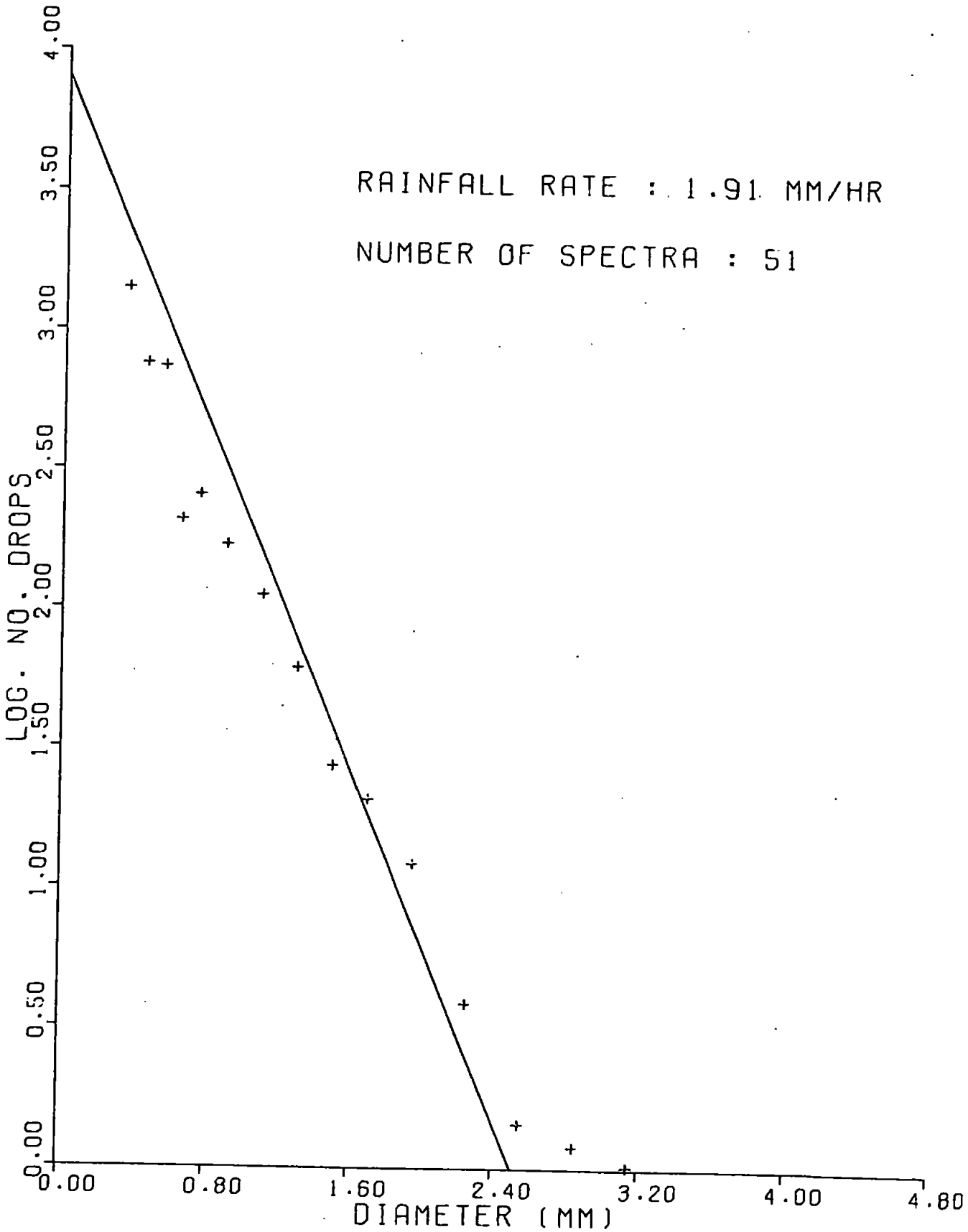

Average raindrop-size distribution (2ND DATA SET)
Rainfall rates about 2.0 mm hr^{-1}.

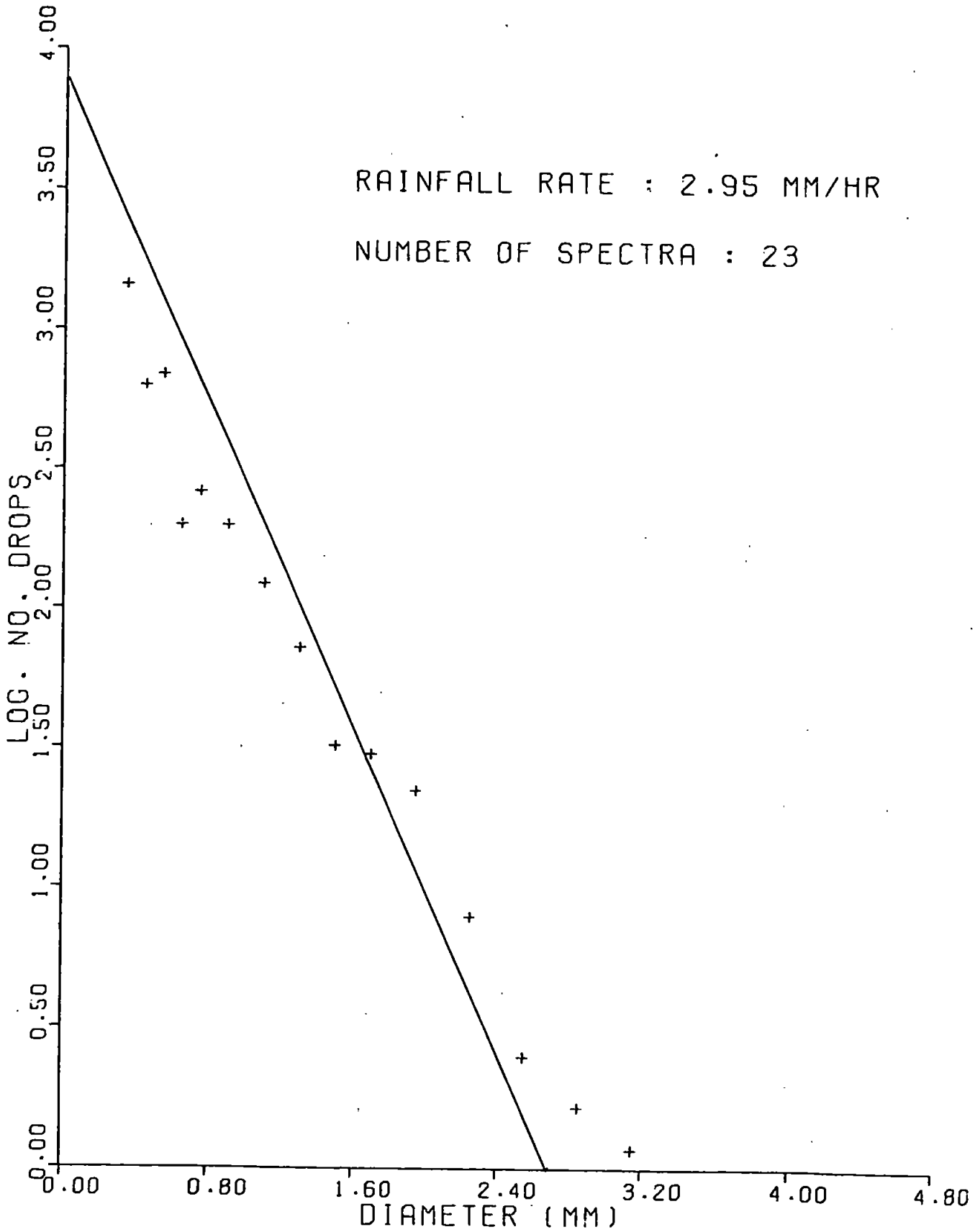

Average raindrop-size distribution (2ND DATA SET)
Rainfall rates about 3.0 mm hr^{-1}.

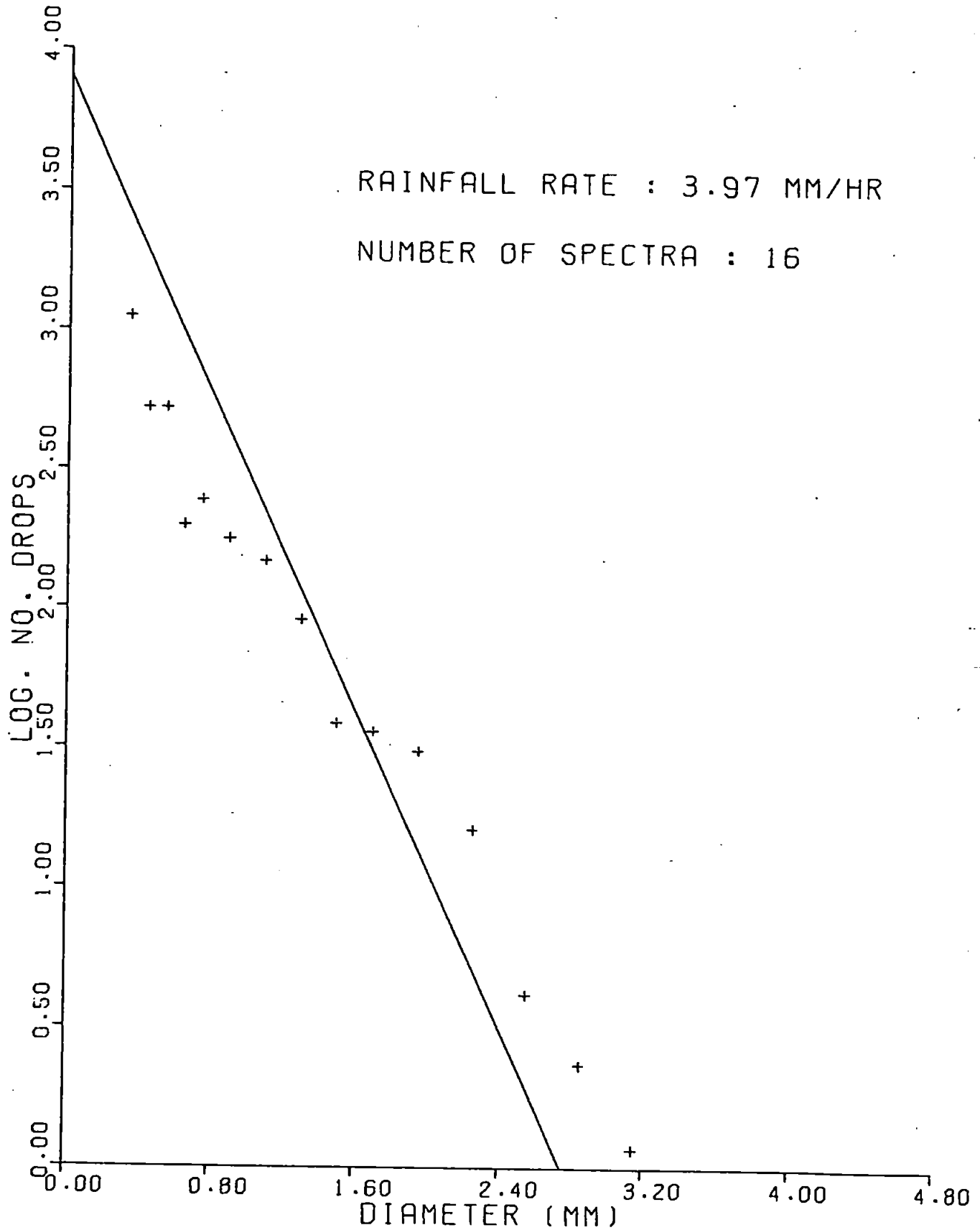

Average raindrop-size distribution (2ND DATA SET)
Rainfall rates about 4.0 mm hr^{-1}.

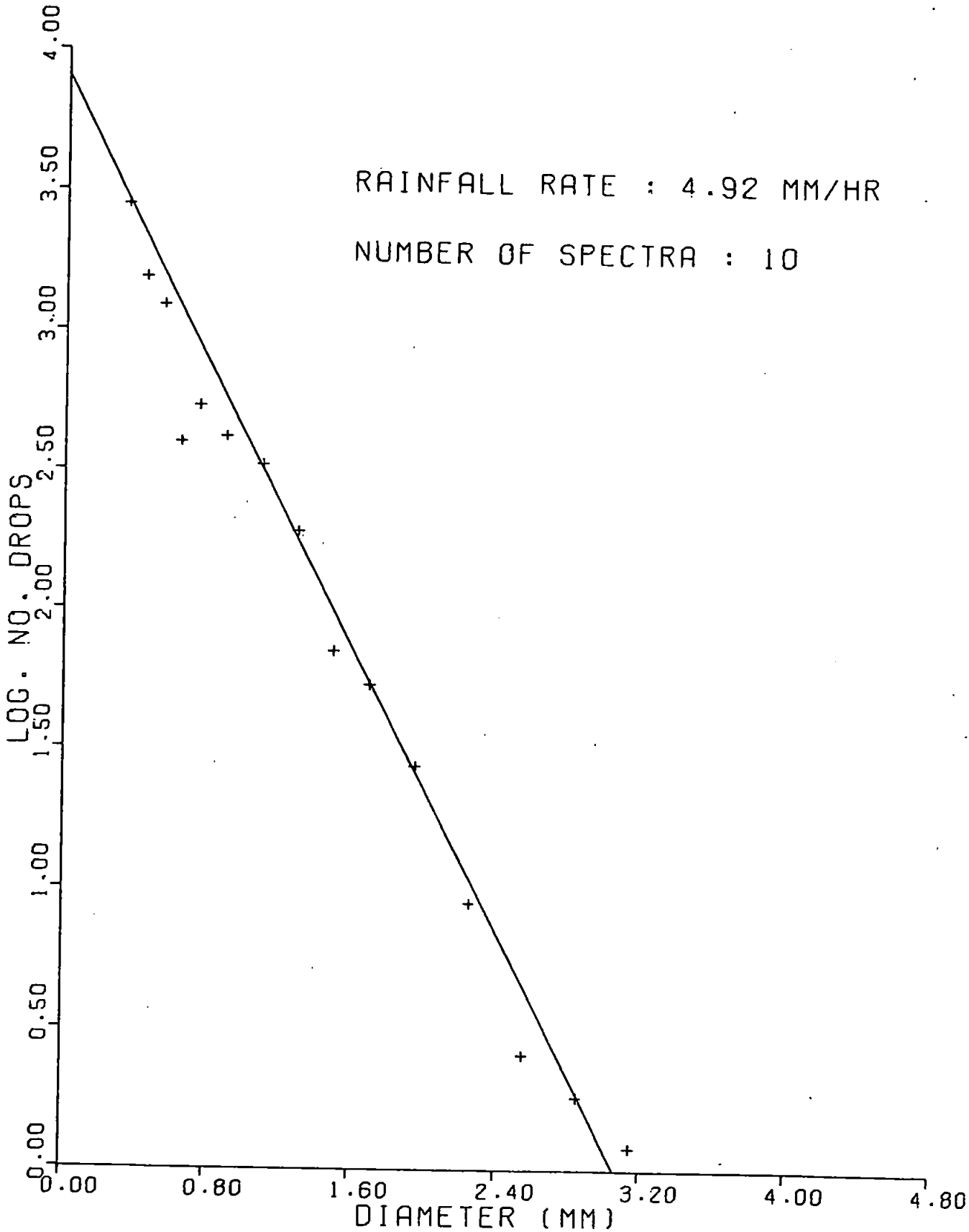

Average raindrop-size distribution (2ND DATA SET)
Rainfall rates about 5.0 mm hr^{-1}.

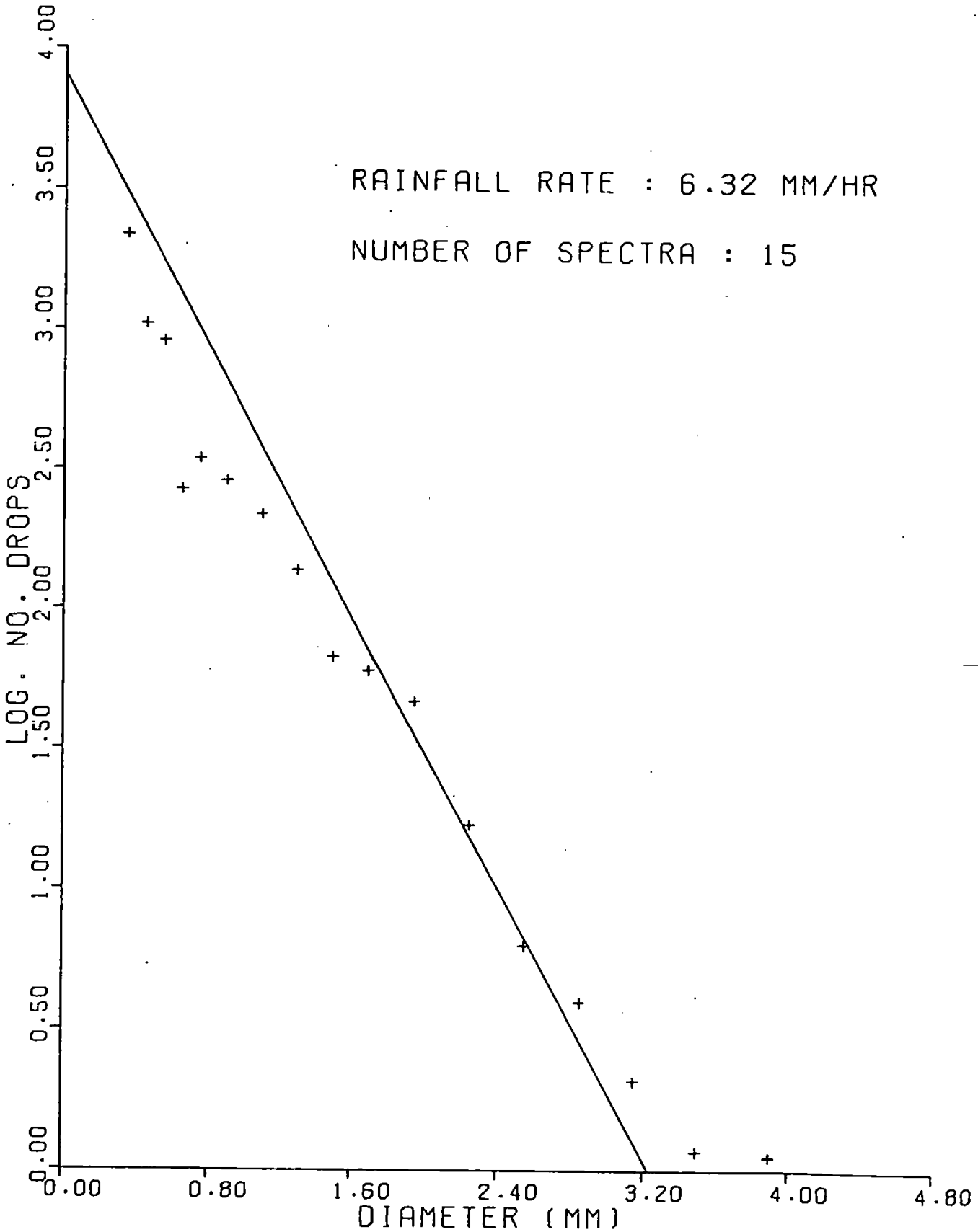

Average raindrop-size distribution (2ND DATA SET)
Rainfall rates about 6.5 mm hr^{-1}.

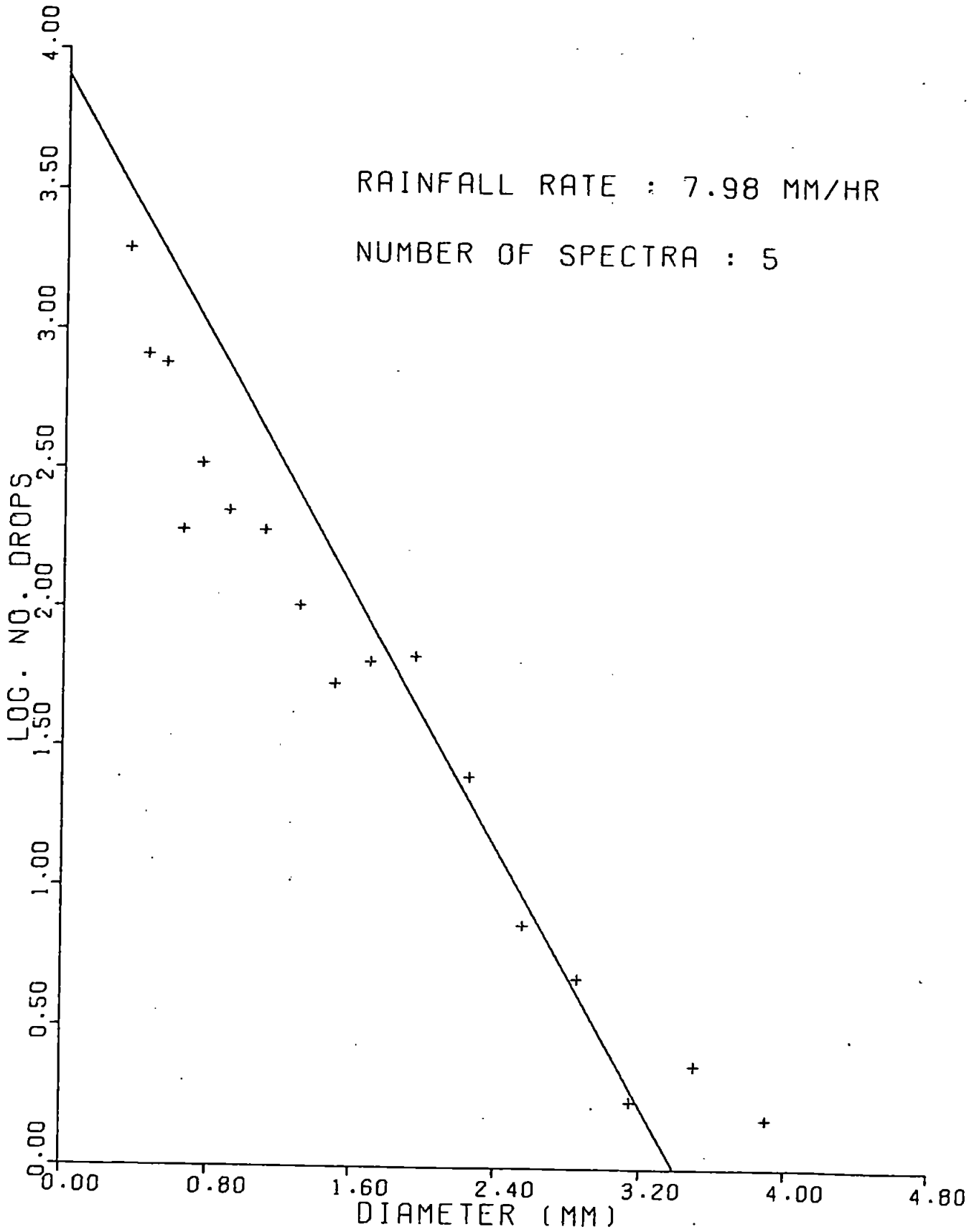

Average raindrop-size distribution (2ND DATA SET)
Rainfall rates about 8.5 mm hr^{-1}.

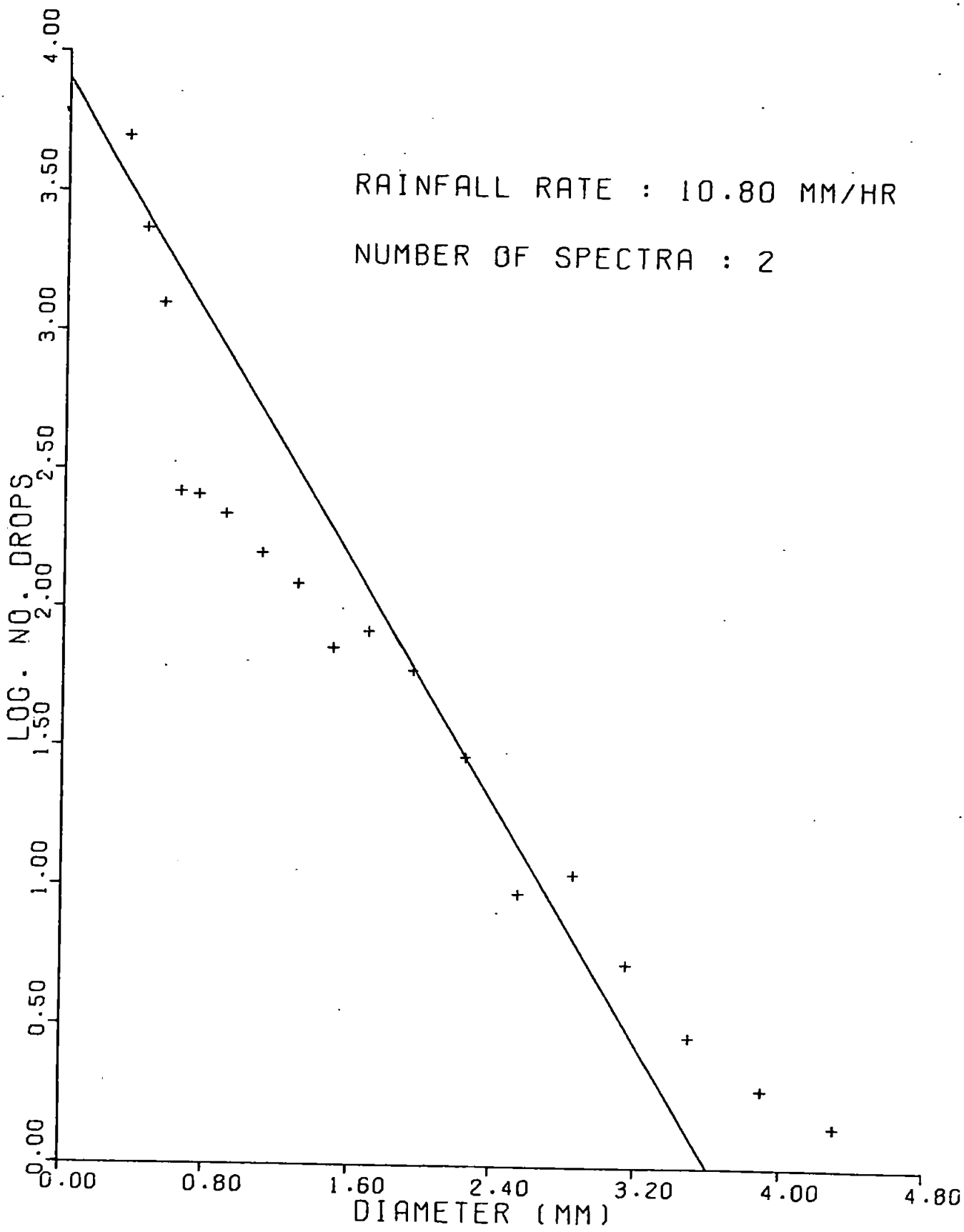

Average raindrop-size distribution (2ND DATA SET)
Rainfall rates about 10.5 mm hr^{-1}.

Appendix V

NOTES ON CALCULATIONS

Interpolation of Z values

The interpolation described in 4.3.3 was carried out by fitting a cubic to the logarithms of the data points using a third order Lagrangian interpolation. Each point is represented by a time (x_n) and a radar reflectivity factor value (f_n). A computer program subroutine accepted four consecutive pairs of values and output interpolated Z values between the second and third time mark, at intervals of one minute. The interval between the input time marks was generally five minutes.

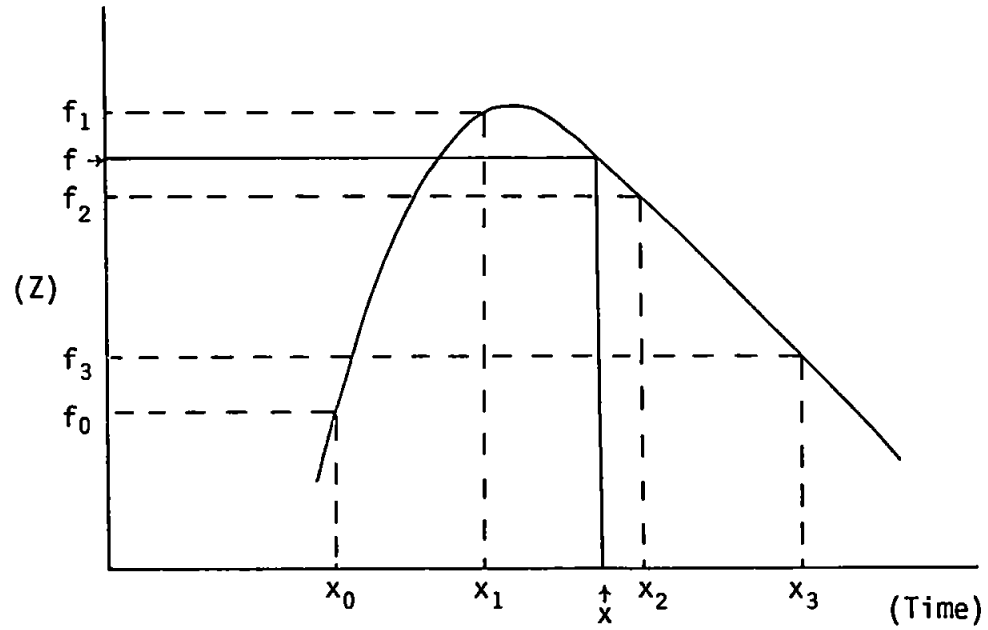

The value of f at time x is given by:

$$f = f_0 + a_1(x-x_0) + a_2(x-x_0)(x-x_1) + a_3(x-x_0)(x-x_1)(x-x_2)$$

where $a_1 = f_0/(x_0-x_1) + f_1/(x_1-x_0)$

$$a_2 = f_0/((x_0-x_1)(x_0-x_2)) + f_1/((x_1-x_0)(x_1-x_2)) + f_2/((x_2-x_0)(x_2-x_1))$$

$$a_3 = f_0/((x_0-x_1)(x_0-x_2)(x_0-x_3)) + f_1/((x_1-x_0)(x_1-x_2)(x_1-x_3)) + f_2/((x_2-x_0)(x_2-x_1)(x_2-x_3)) + f_3/((x_3-x_0)(x_3-x_1)(x_3-x_2))$$

Comparison of rainfall totals

Each pair of n rainfall totals is represented by (x_i, y_i) for values of i from 1 to n. Three measures were used for comparison as described in 5.1.5 and were computed using the following formulae:-

Mean percentage error (regardless of sign)

$$= \frac{1}{n} \left(\sum_{i=n}^{1} \left| \frac{x_i - y_i}{y_i} \times 100 \right| \right) \qquad (y_i > 0)$$

Root mean square error

$$= \sqrt{\frac{1}{n} \left(\sum_{i=n}^{1} (x_i - y_i)^2 \right)}$$

Root mean square cumulative error

$$= \sqrt{\frac{1}{n} \left(\sum_{i=n}^{1} \left(\sum_{i=i}^{1} (x_i - y_i) \right)^2 \right)}$$

Appendix VI

SYNOPTIC AND OBSERVATIONAL DATA

Synoptic and observational data relevant to the second data set, comprising a brief synopsis for St. Mawgan and a surface chart. The cloud amount, types and height are contained in the log abstract and the heights of the 0°C isotherm estimated from Camborne ascent data are given.

PT53 27.3.79 1100-1900 GMT

Unstable north westerly airstream with minor troughs associated with complex low pressure system over North Sea. Moderate rain showers from isolated cumulonimbus giving way to lighter, more widespread precipitation. Wind generally WNW 15 kts.

St. Mawgan log

TIME	Amount of low (oktas)	Form of low	Height of low (feet)	Form of medium	Form of high
1046	7	Cu Sc St	800	-	-
1146	7	Cu Sc	1000	-	-
1246	7	Cu Sc Cb	1000	-	-
1346	7	Cu Sc St	1000	-	-
1446	7	Cu Cb St	1000	-	-
1546	7	Cu Sc	1600	Ac As	-
1646	5	Cu Cb Sc	1600	-	-
1746	7	Cu St	600	-	-
1846	7	Cu	1100	-	-

Camborne ascent

TIME	Height of 0°C (m)
27/00	1067
27/12	917
28/00	634

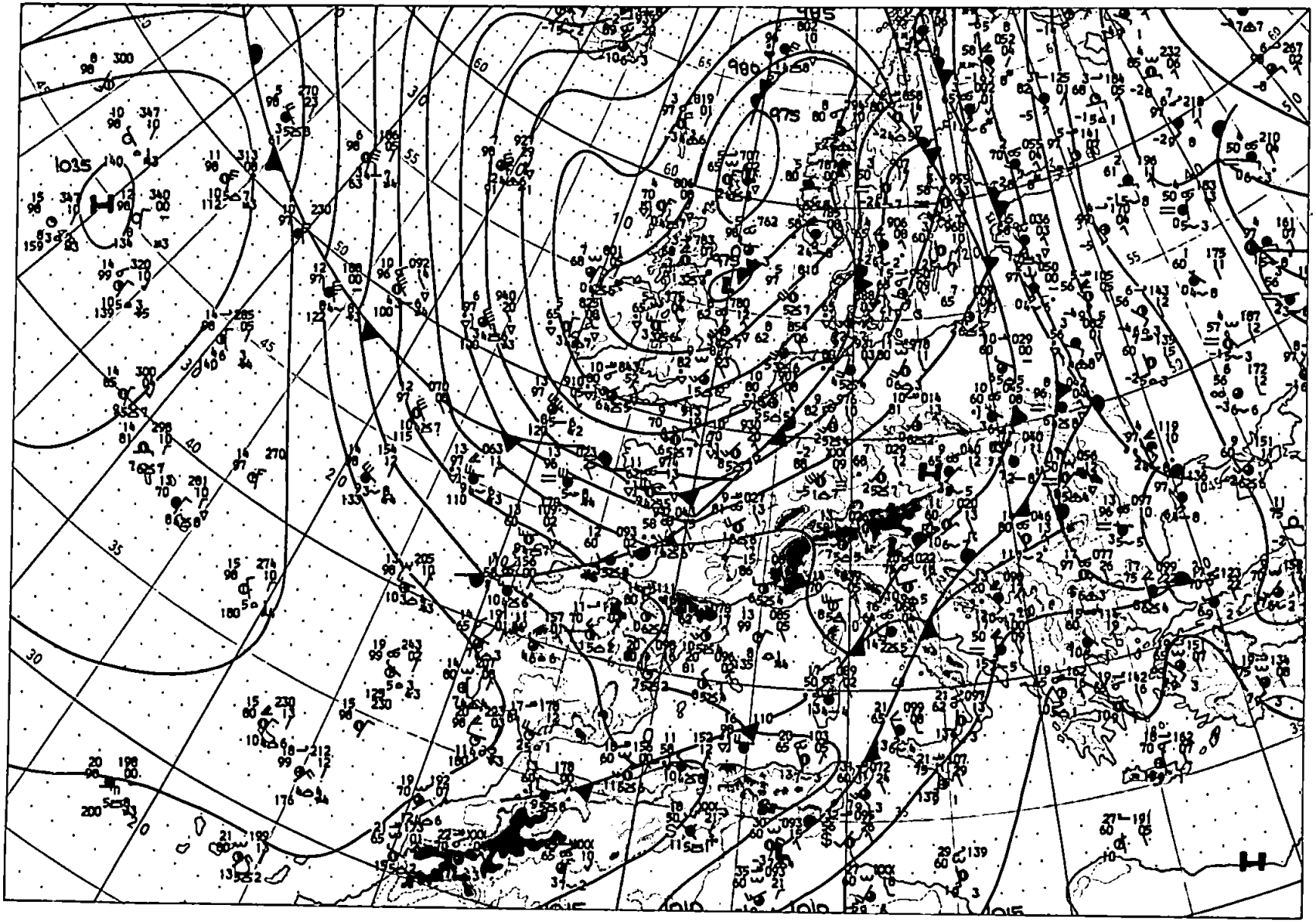

Surface Chart 1200 GMT 27.3.79

PT54 9.4.79 1300-2100 GMT

Complex low pressure system over western approaches and Spain with warm fronts pushing north. Continuous light/moderate rainfall from mainly stratiform cloud. Wind generally NNE 10 kts.

St. Mawgan log

TIME	Amount of low (oktas)	Form of low	Height of low (feet)	Form of medium	Form of high
1250	8	St Cu	800	As	-
1350	6	St Sc	800	As	-
1450	6	St Sc	800	As	-
1550	8	St	800	Ns	-
1650	8	St Sc	400	Ns	-
1750	8	St	100	-	-
1850	8	St	100	-	-
1950	8	St	0	-	-
2050	8	St	0	-	-

Camborne ascent

TIME	Height of 0°C (m)
9/12	709
10/00	1007

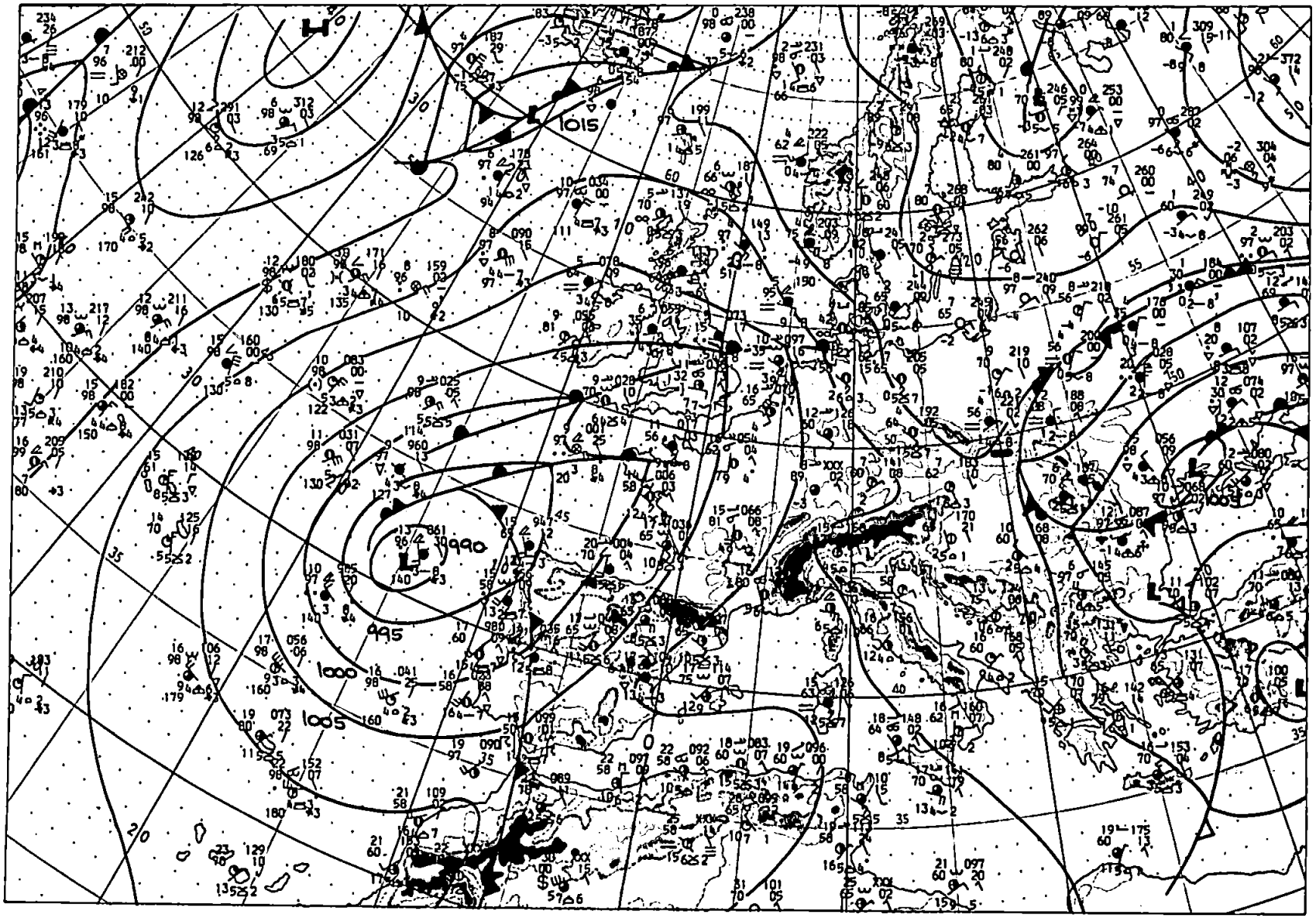

Surface Chart 1200 GMT 9.4.79

PT55 22.5.79 1600-2100 GMT

Minor trough embedded in low pressure system over SE Iceland.

Continuous light rain becoming heavy during passage of cumulonimbus.

Wind generally S 15 kts.

St. Mawgan log

TIME	Amount of low (oktas)	Form of low	Height of low (feet)	Form of medium	Form of high
1550	6	Cu Sc	1300	Ac Cs	Ci Cs
1650	6	St Cu Sc	900	Ac As	-
1750	7	St Cu Sc	800	As	-
1850	5	St Sc	500	Ns	-
1950	7	St Sc Cb	500	Ns	-
2050	5	Cu Sc	1400	As	-

Camborne ascent

TIME	Height of 0°C (m)
22/12	1188
23/00	1130

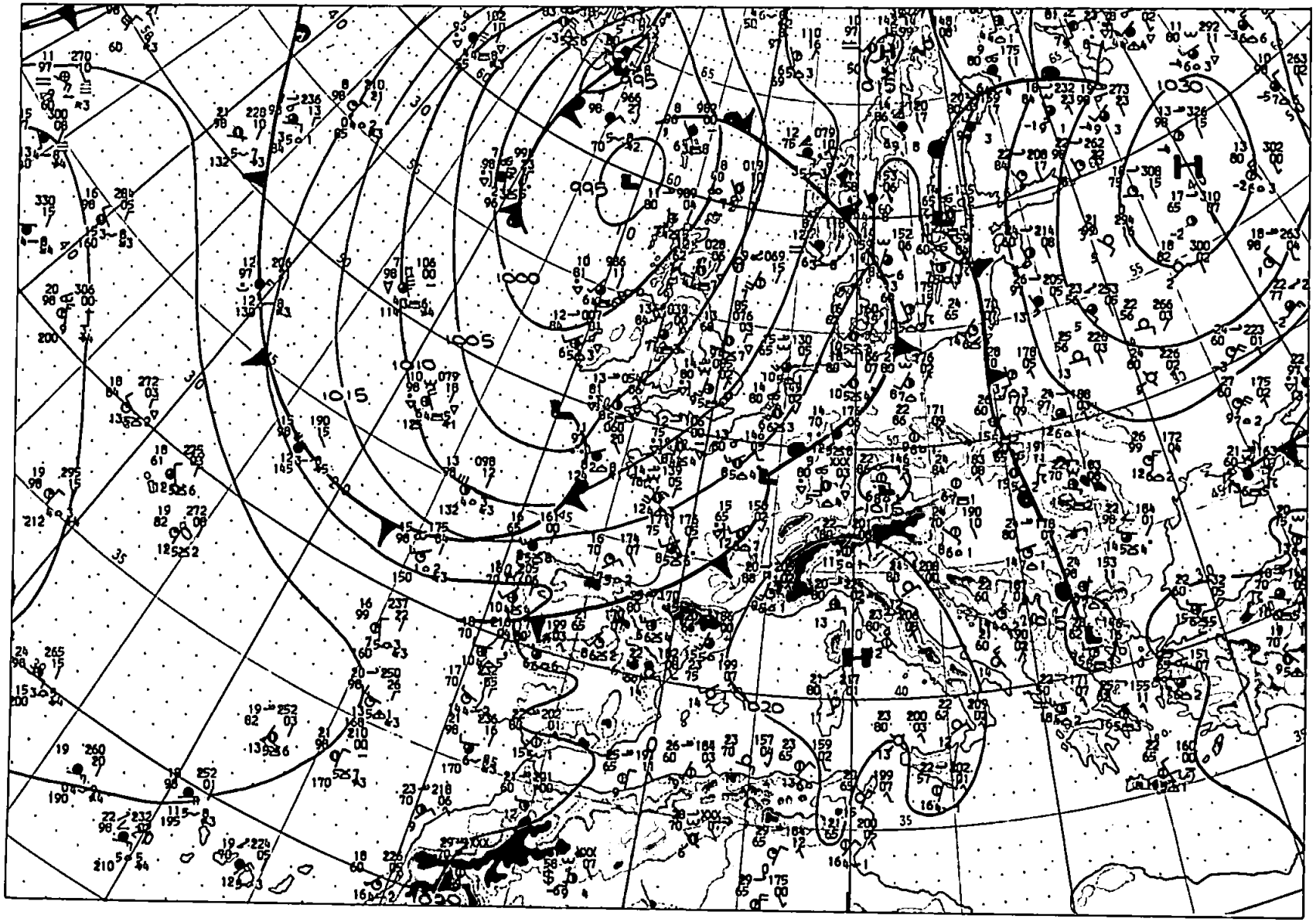

Surface Chart 1200 GMT 22.5.79

Appendix VII

TIME-HEIGHT RADAR PROFILES AND SURFACE DATA

Complete sets of time-height radar profiles and surface data for the 33 half hour periods detailed in Chapter 5.

Key to Figures

R_D - Distrometer surface rainfall rate (five-minute moving average)

R_Z - Radar rainfall rate at lowest elevation (interpolated values - method 4, Table 5.3)

N_o - Distrometer surface measurement (five-minute moving average)

In the second set of figures*, showing only modified surface data, R_D and N_o are plotted as above but in the upper plot R_Z is derived from the modified radar data (method 8, Table 5.3) and in the lower plot R_Z is derived from these data after applying a variable Z-R relationship and the total is denoted R_{ZN} (method 9, Table 5.3).

* p. A 72 - A 102

Radar Reflectivity

Contours (dBz)

(1) 530028 - 057

1200-29 : 27.3.79

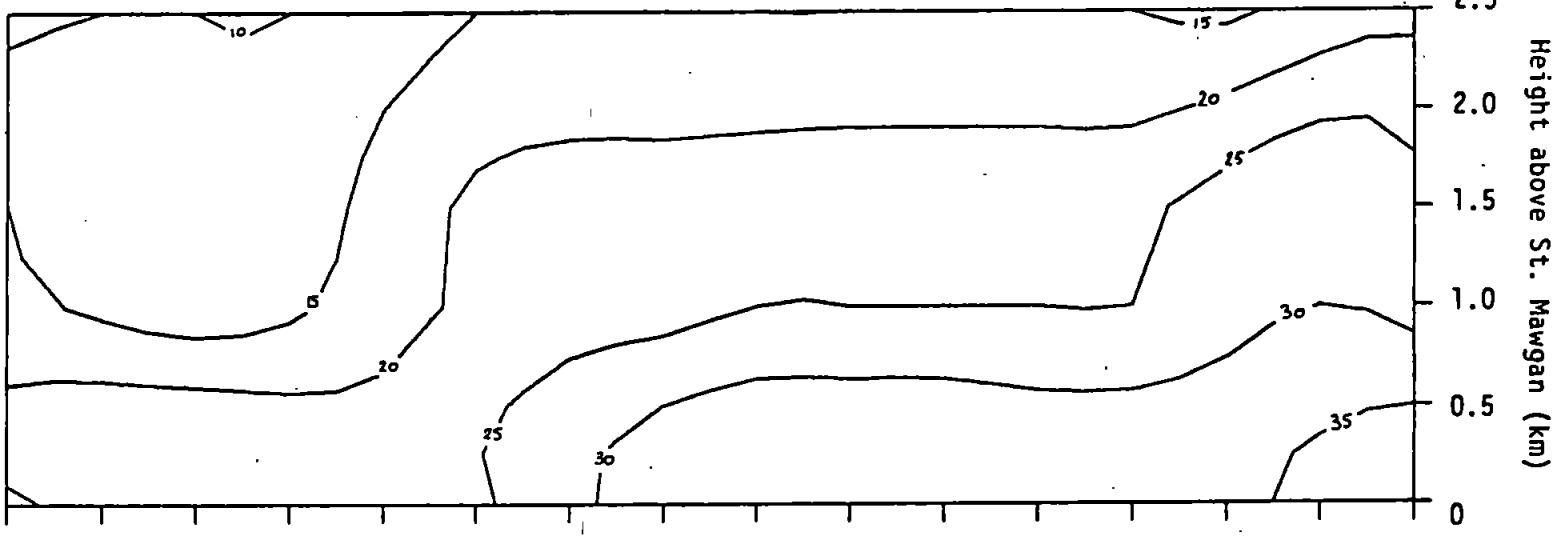

Totals:

R_G : 1.6 mm

R_D : 1.00 mm

R_Z : 1.50 mm

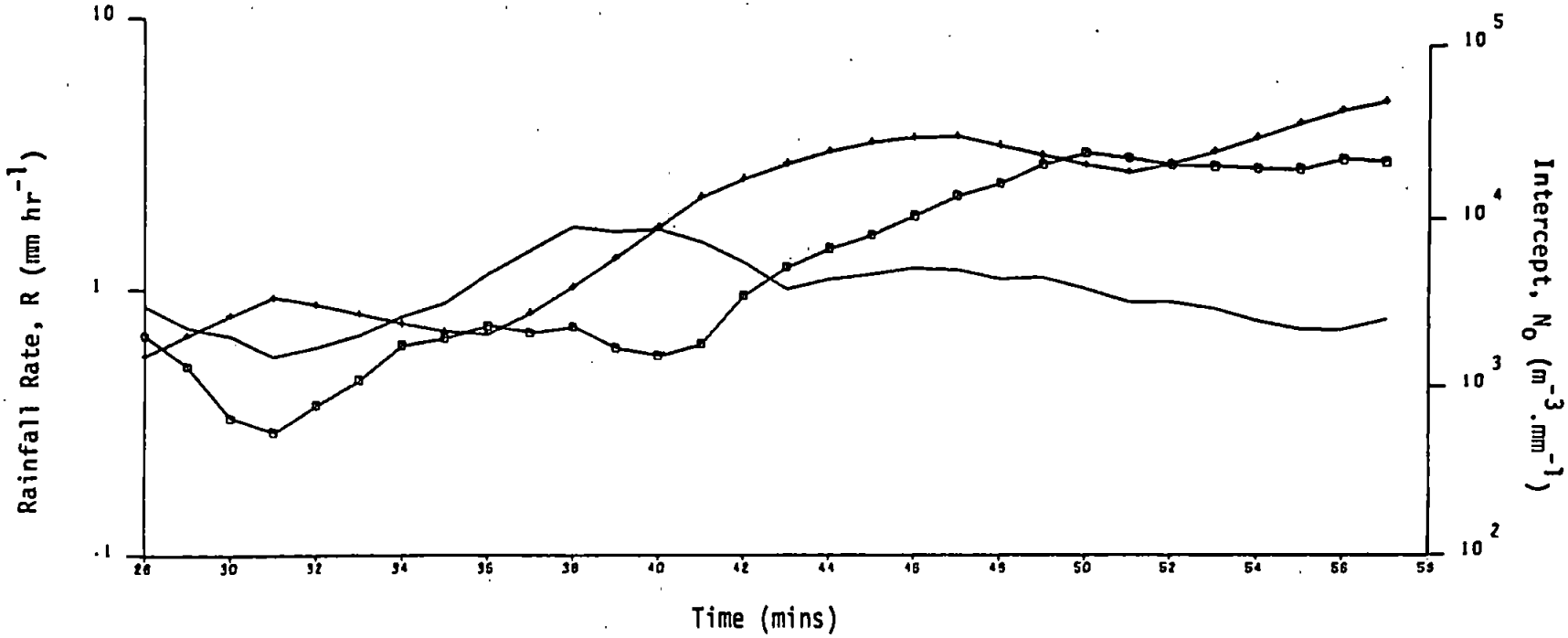

Radar Reflectivity

Contours (dBz)

(2) 530058 - 087

1230-59 : 27.3.79

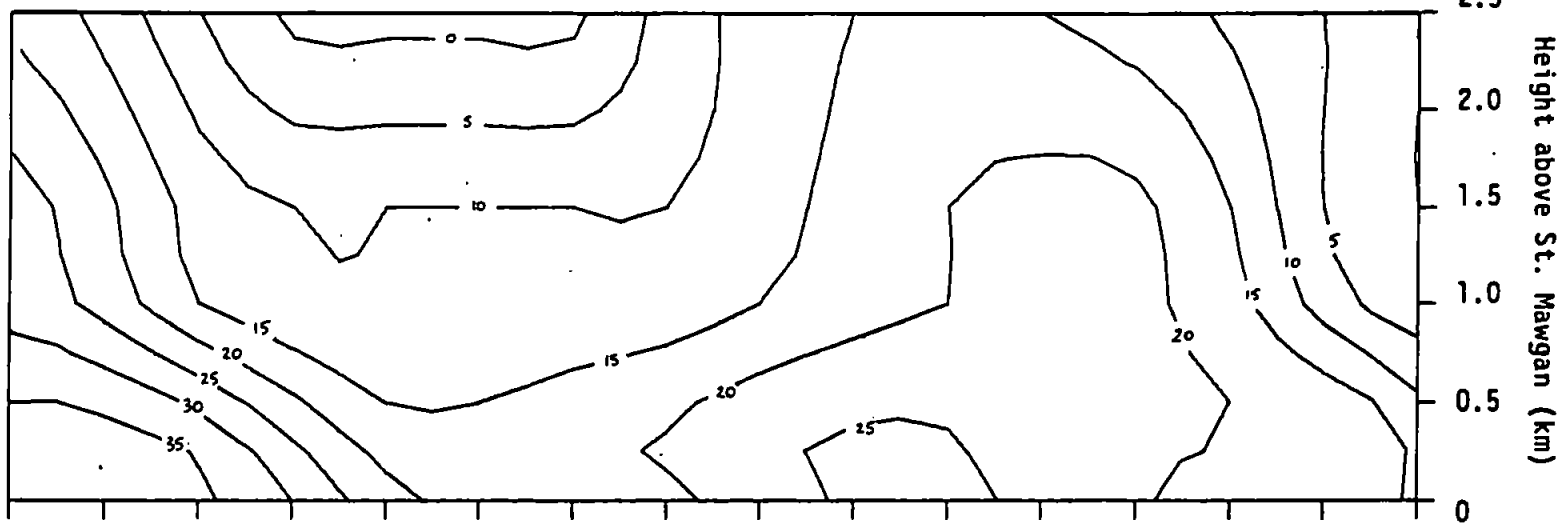

Totals:

R_G : 0.8 mm

R_D : 0.77 mm

R_Z : 0.63 mm

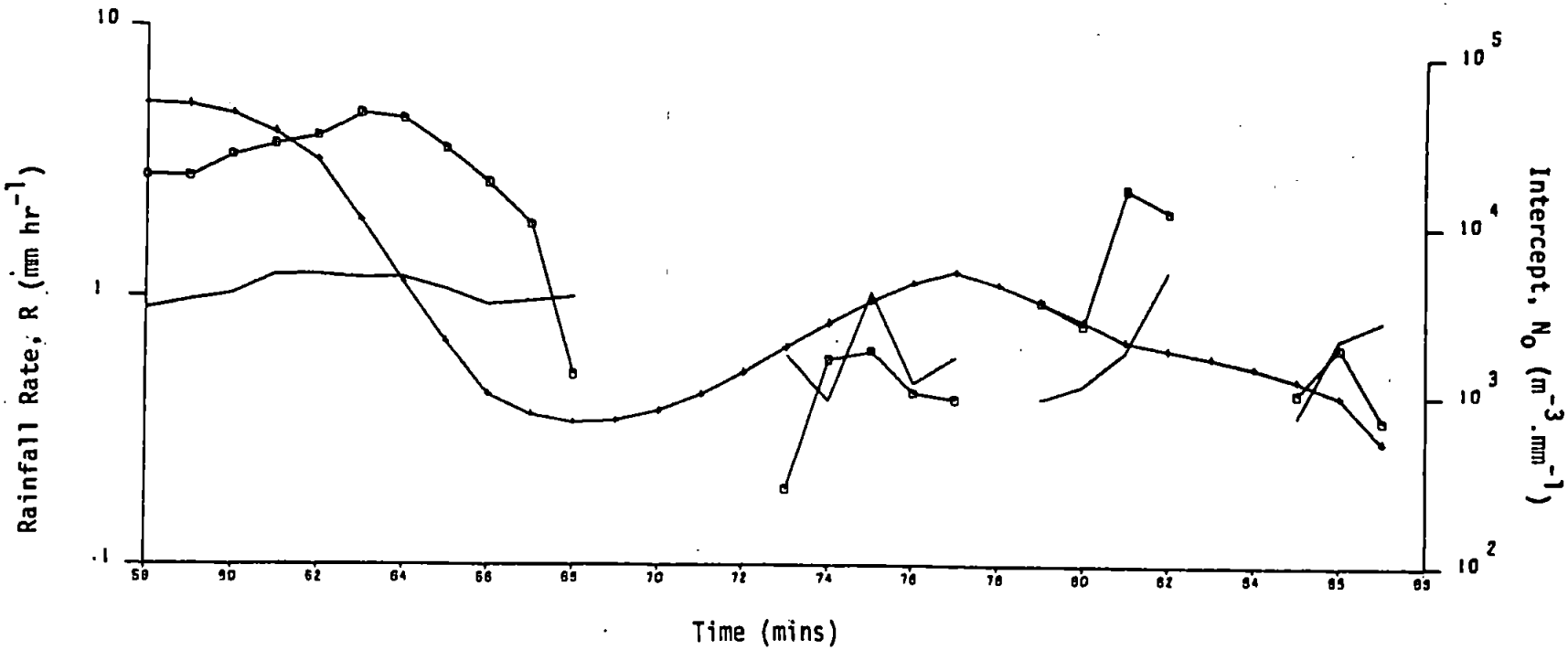

A 42

Radar Reflectivity

Contours (dBz)

(3) 530088 - 117

1300-29 : 27.3.79

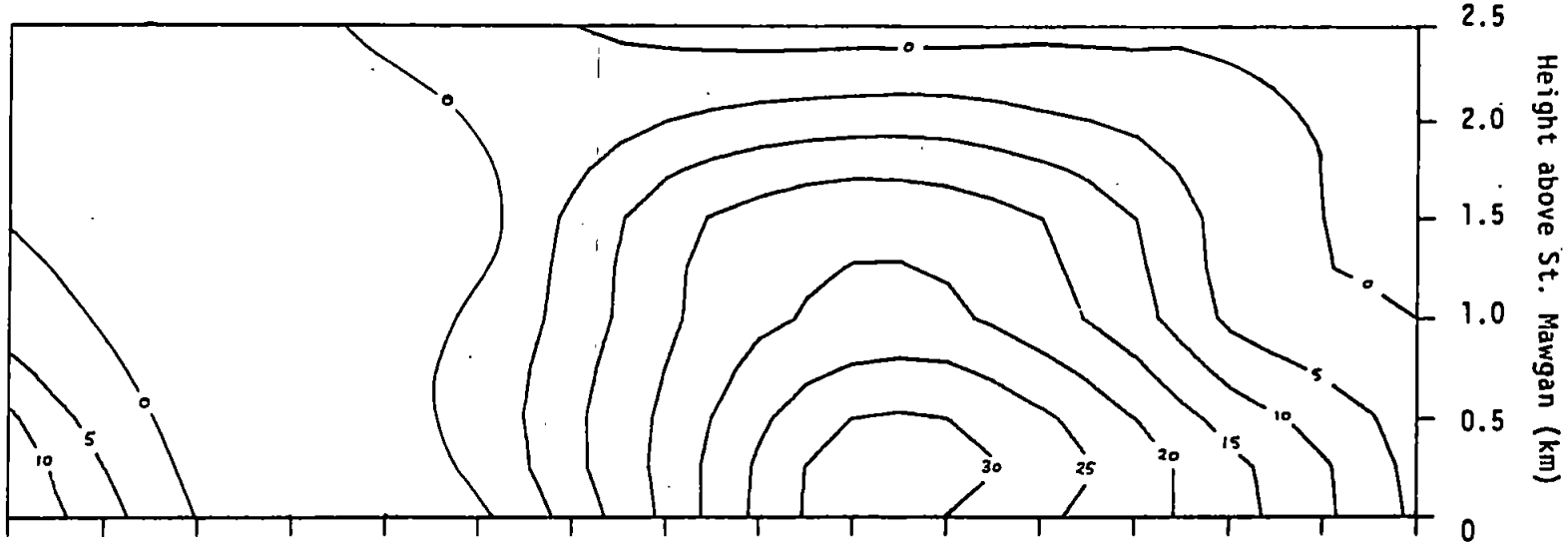

Totals:

R_G : 0.5 mm

R_D : 0.35 mm

R_Z : 0.40 mm

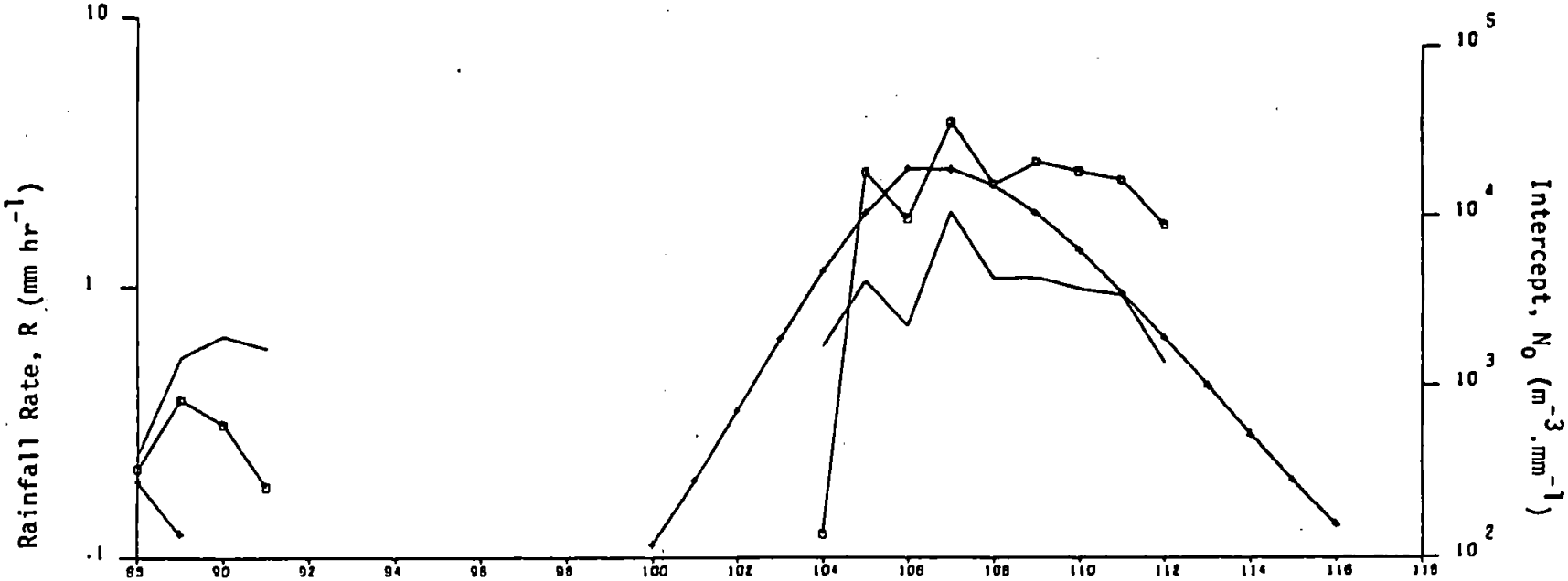

Radar Reflectivity

Contours (dBz)

(4) 530118 - 147

1330-59 : 27.3.79

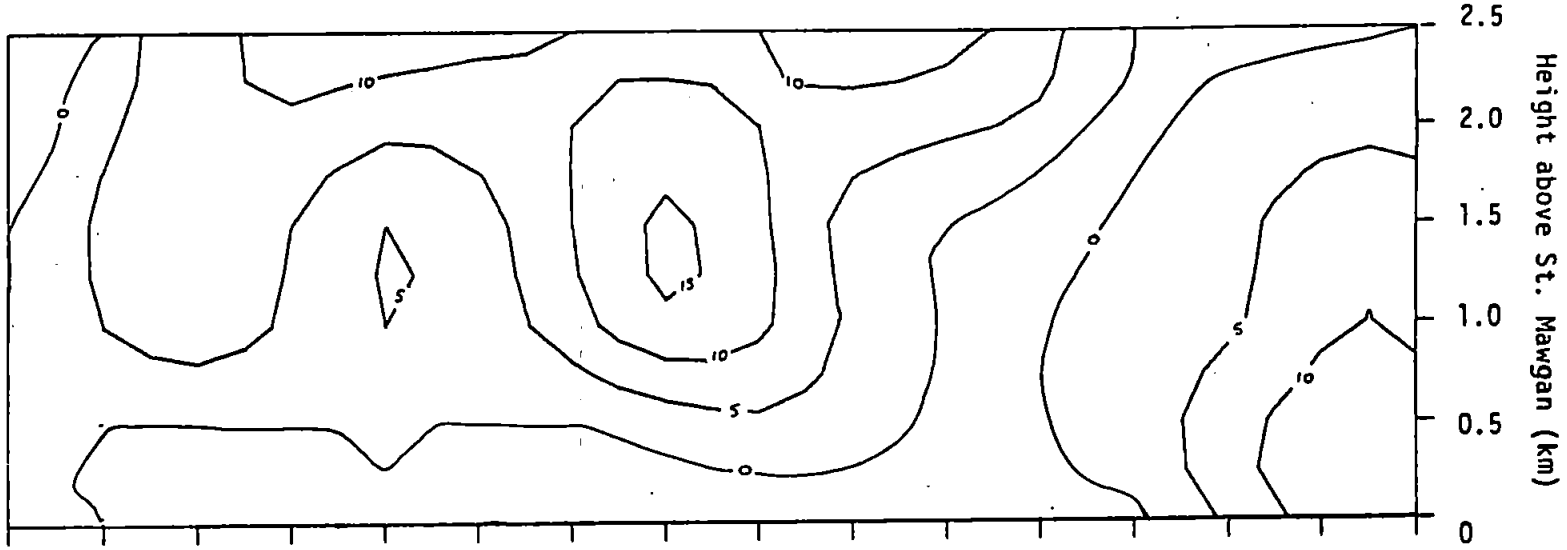

Totals:

R_G : 0 mm

R_D : 0.01 mm

R_Z : 0.02 mm

A 44

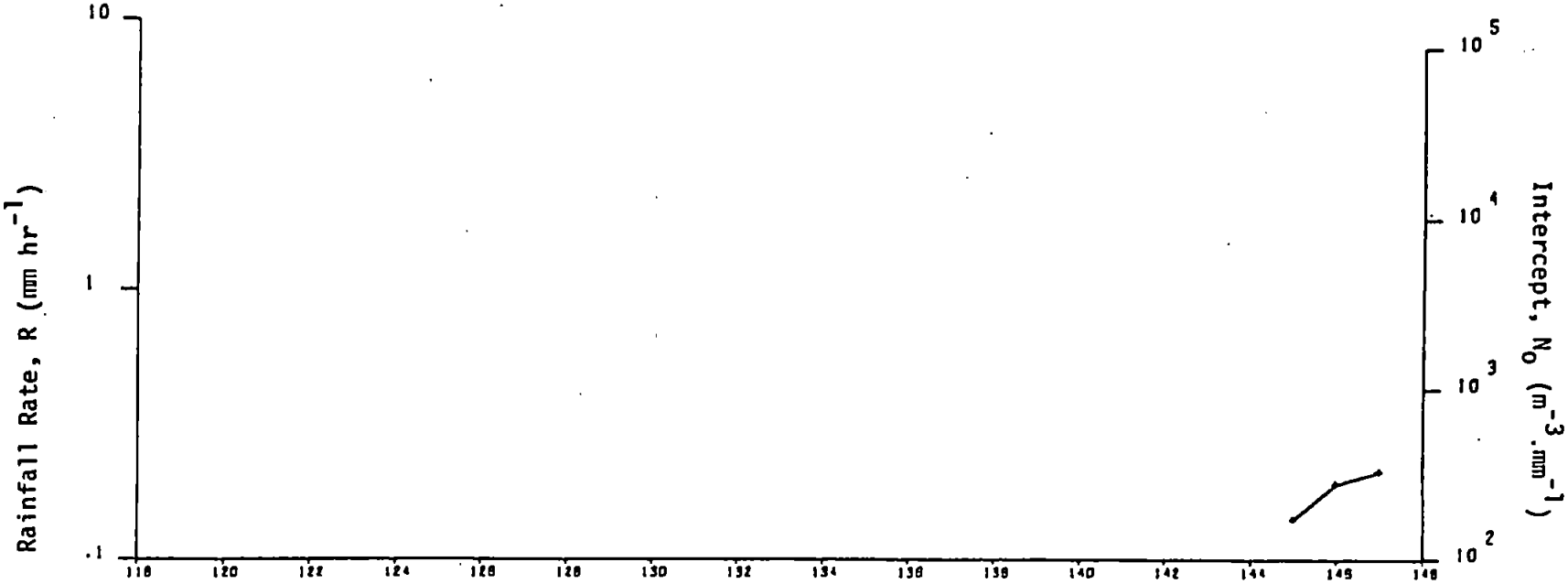

Radar Reflectivity

Contours (dBz)

(5) 530148 - 177

1400-29 : 27.3.79

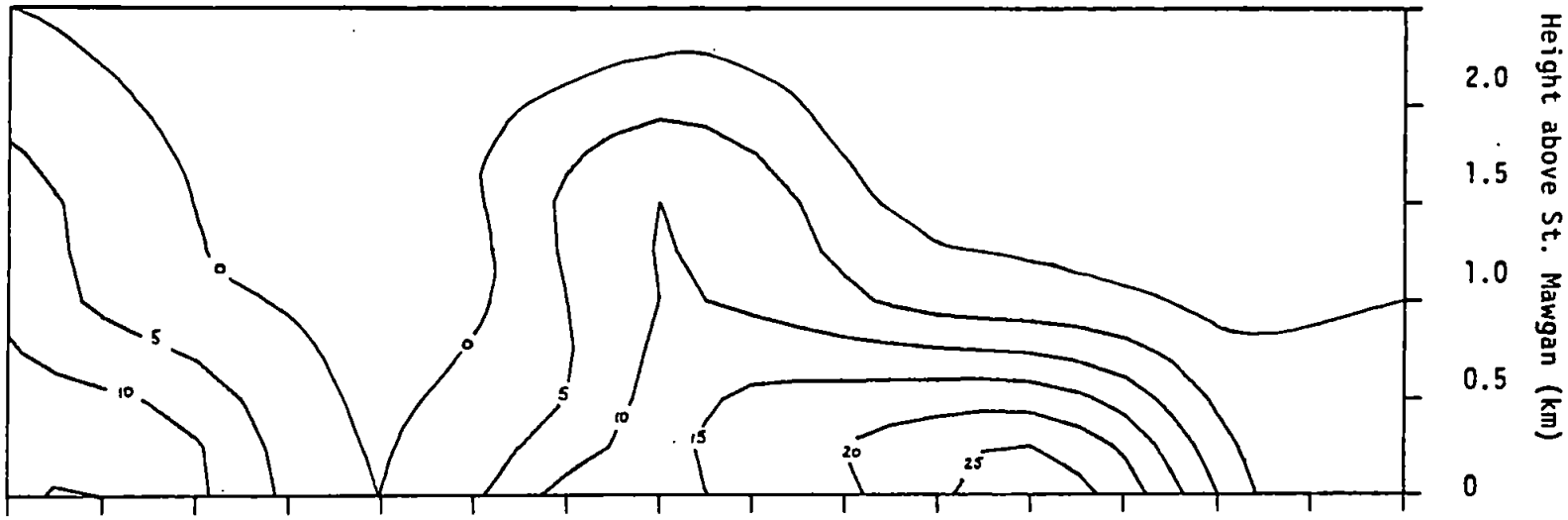

Totals:

R_G : 0 mm

R_D : 0.10 mm

R_Z : 0.14 mm

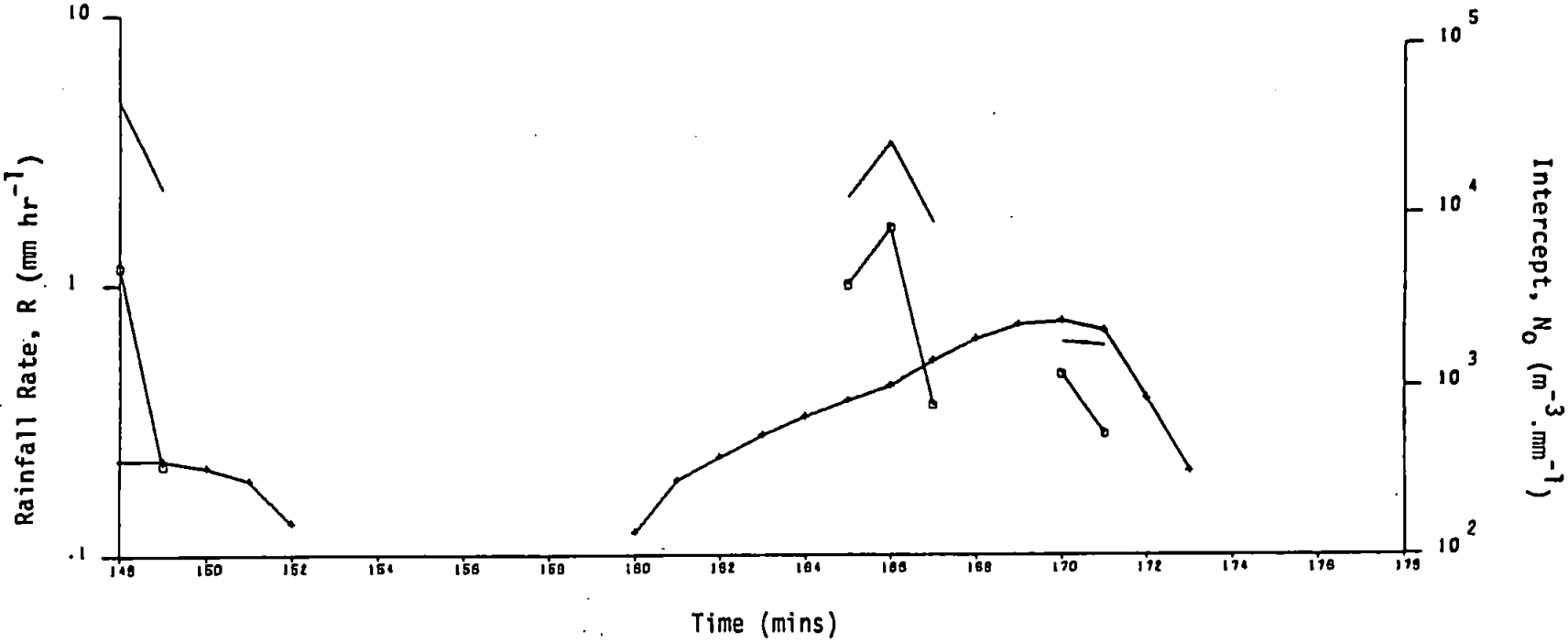

A 45

Radar Reflectivity

Contours (dBz)

(6) 530178 - 207

1430-59 : 27.3.79

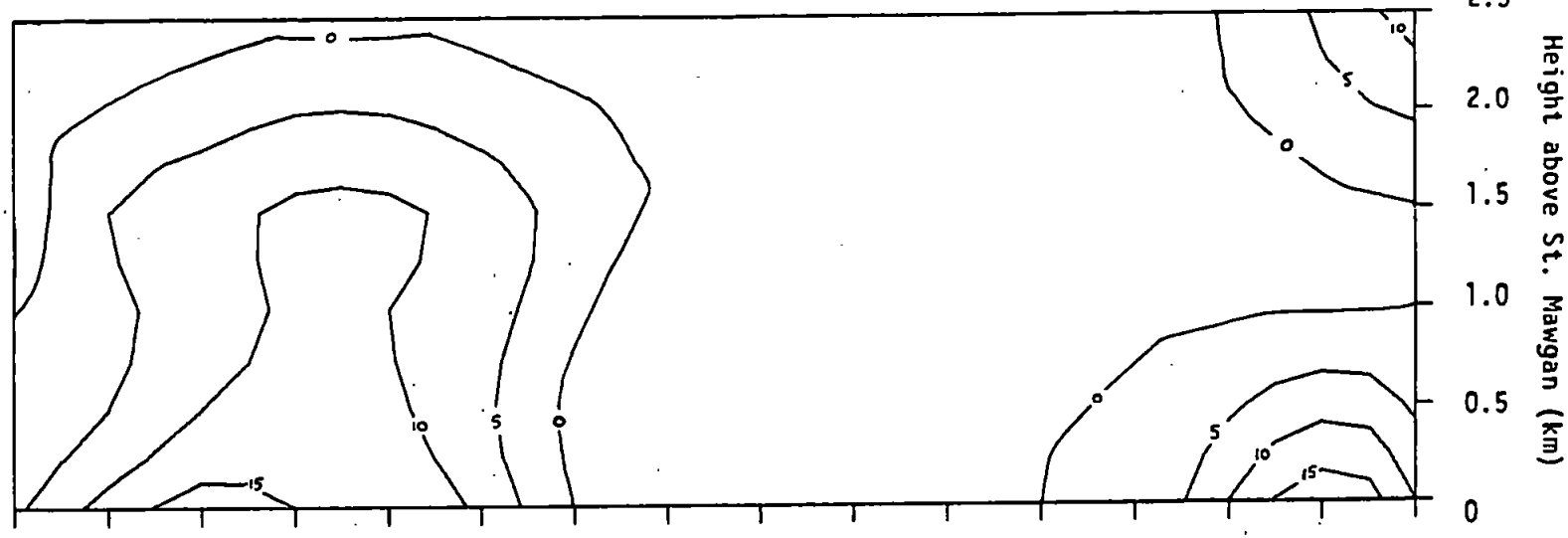

Totals:

R_G : 0 mm

R_D : 0 mm

R_Z : 0.05 mm

A 96

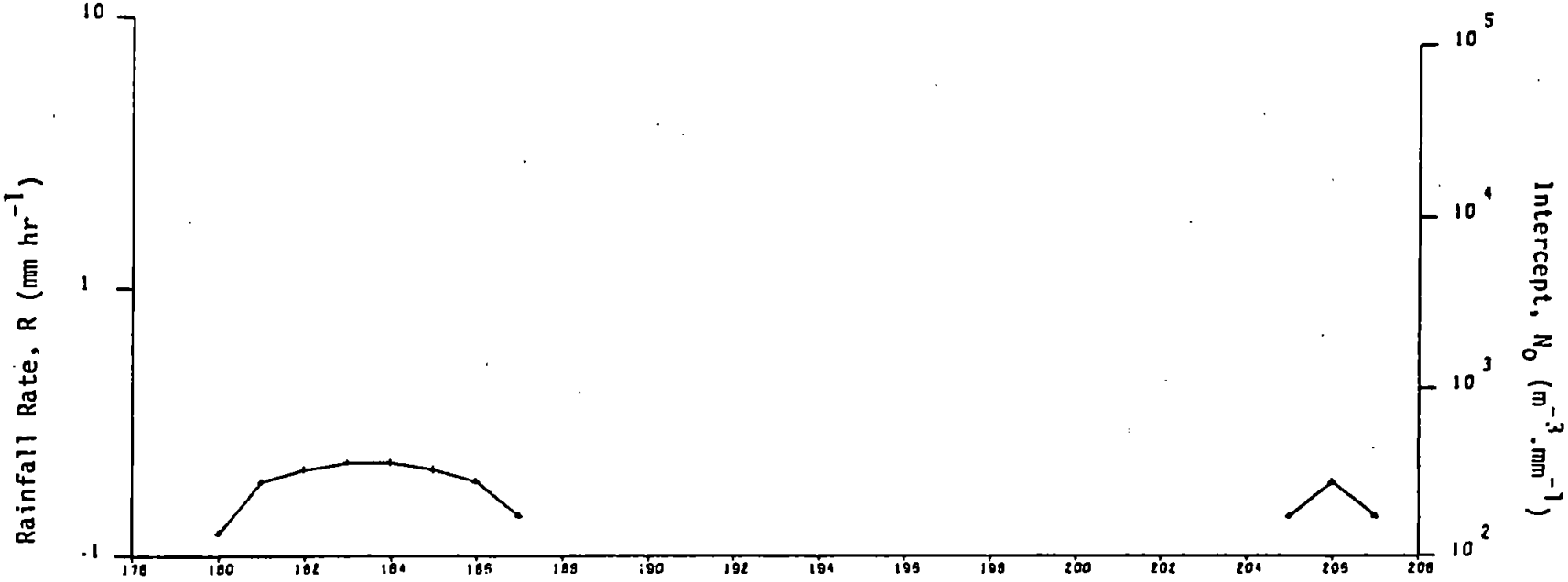

Radar Reflectivity

Contours (dBz)

(7) 530208 - 237

1500-29 : 27.3.79

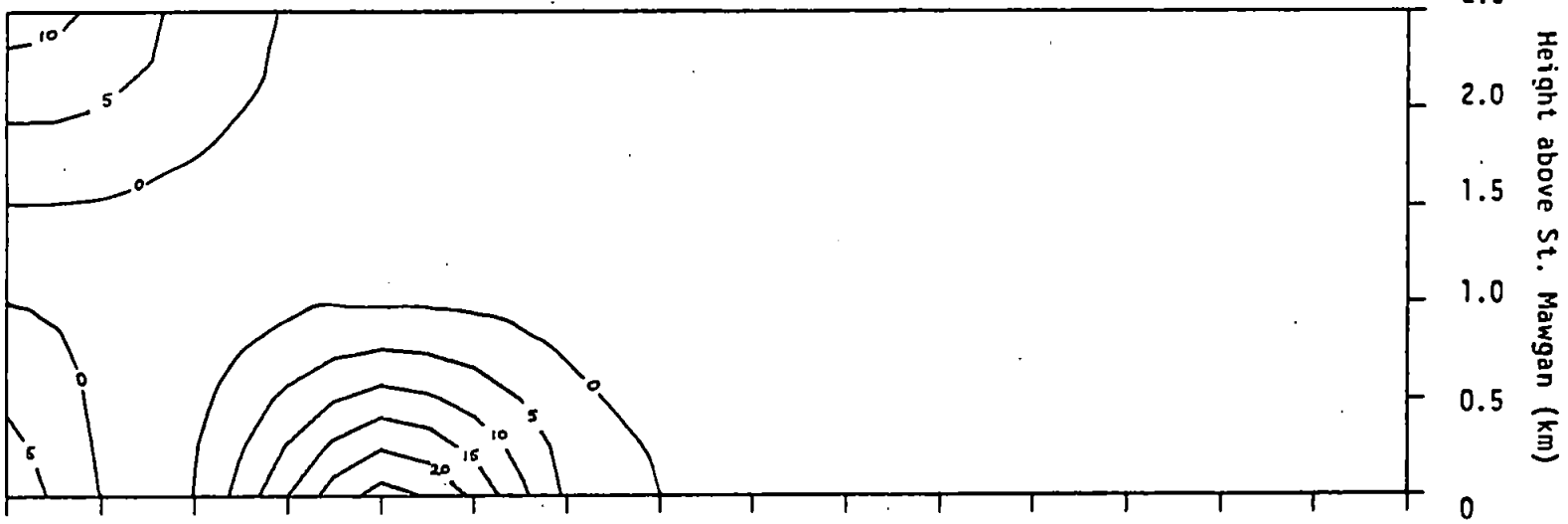

Totals:

R_G : 0 mm

R_D : 0 mm

R_Z : 0.04 mm

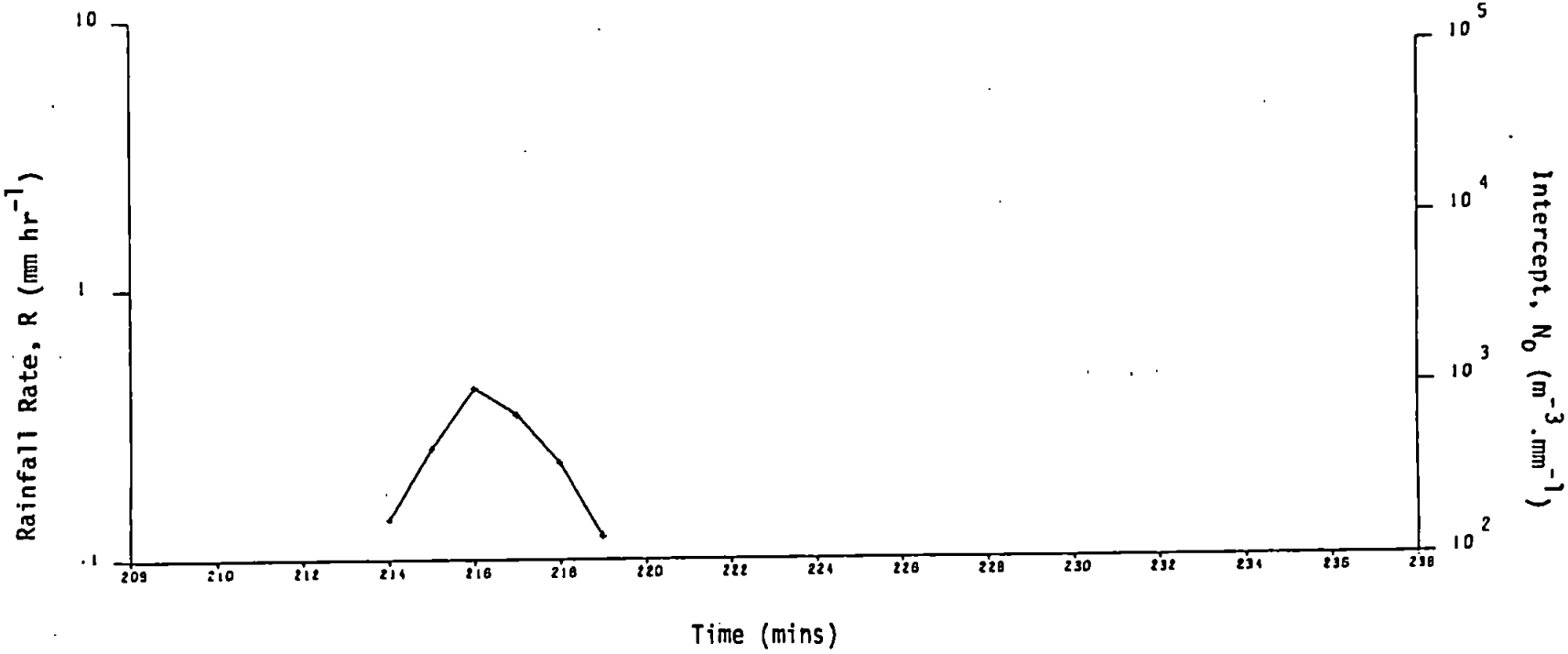

Radar Reflectivity

Contours (dBz)

(8) 530238 - 267

1530-59 : 27.3.79

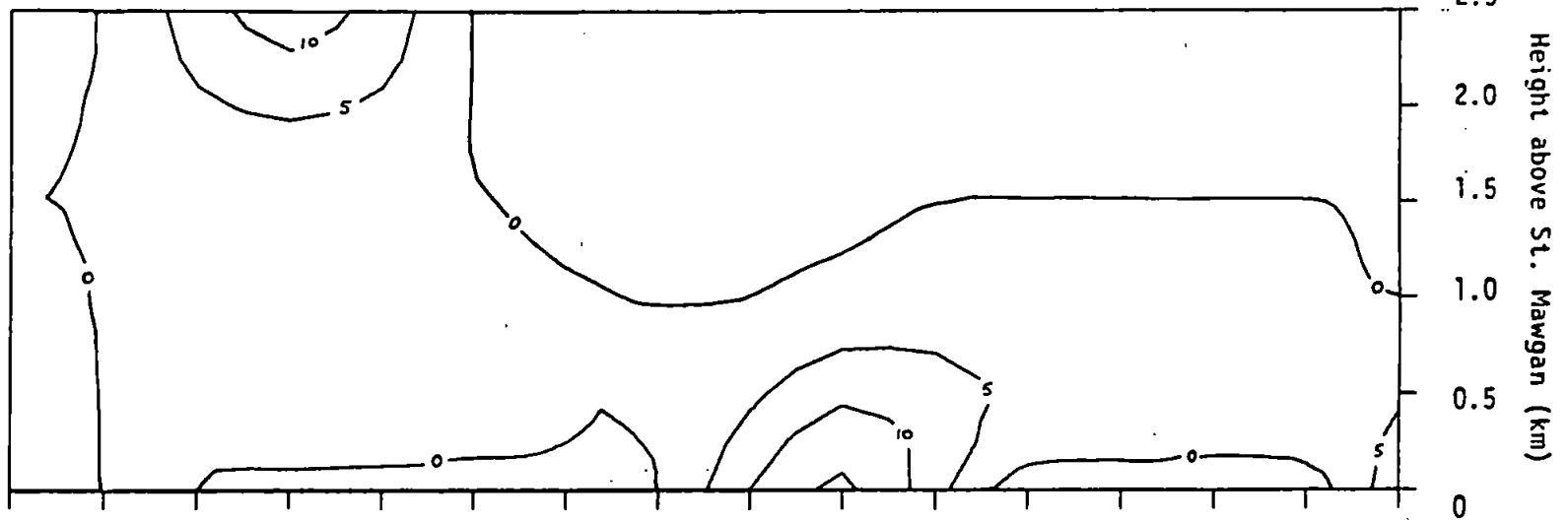

Totals:

R_G : 0 mm

R_D : 0 mm

R_Z : 0.02 mm

A 48

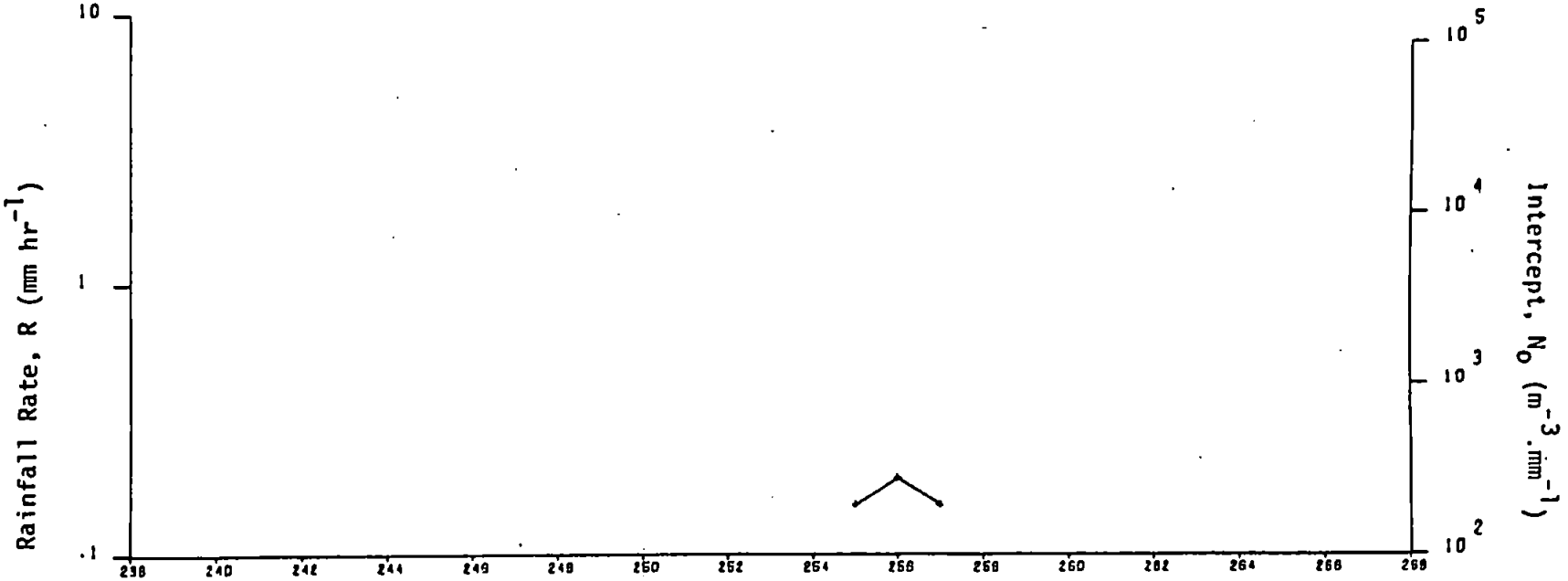

Radar Reflectivity

Contours (dBz)

(9) 530268 - 297

1600-29 : 27.3.79

Totals:

R_G : 0.1 mm

R_D : 0.07 mm

R_Z : 0.03 mm

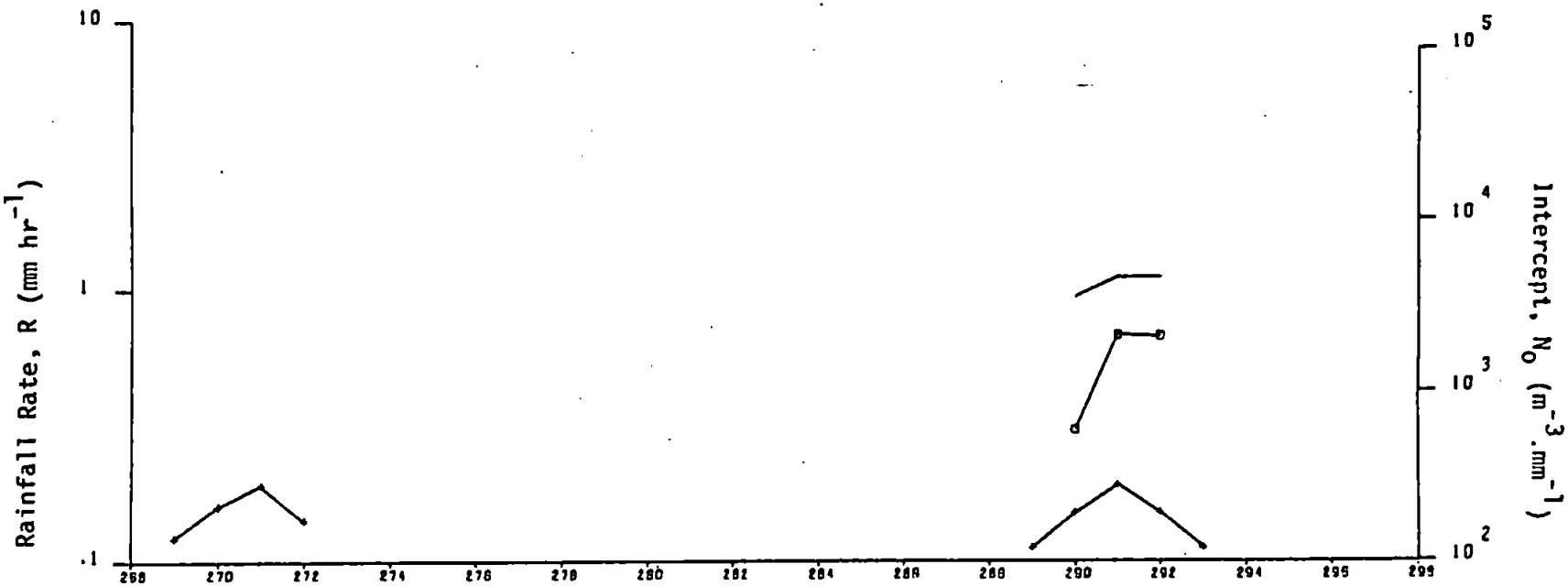

Radar Reflectivity

Contours (dBz)

(10) 530298 - 327

1630-59 : 27.3.79

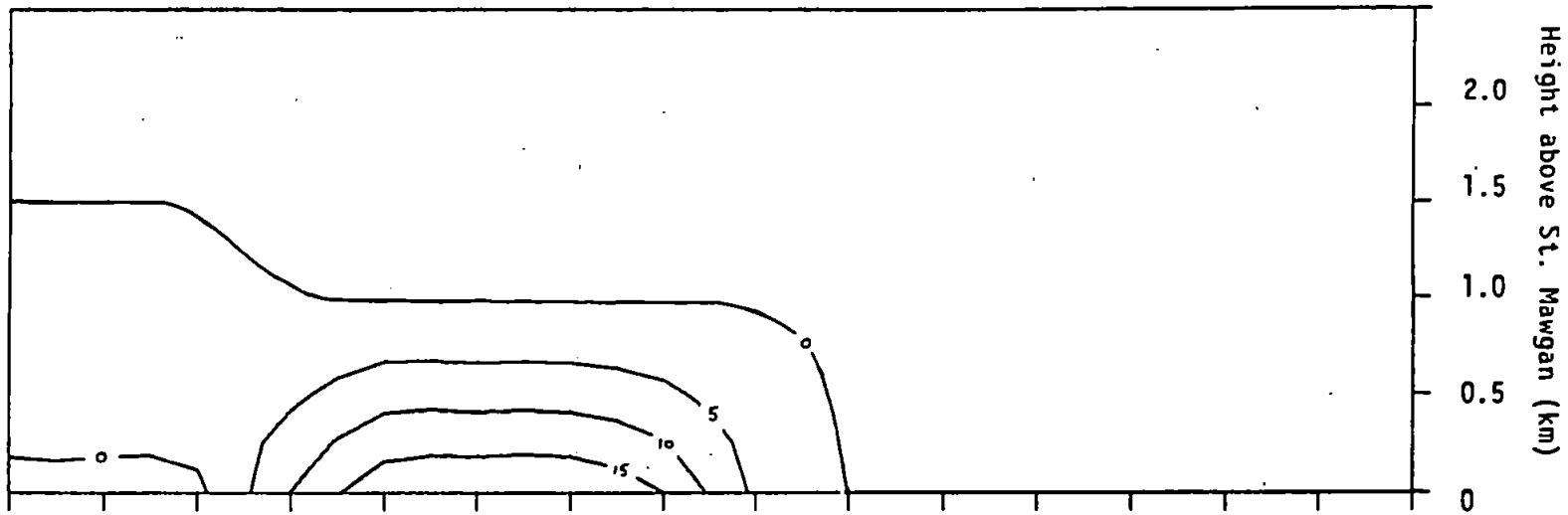

Totals:

R_G : 0 mm

R_D : 0 mm

R_Z : 0.03 mm

A 50

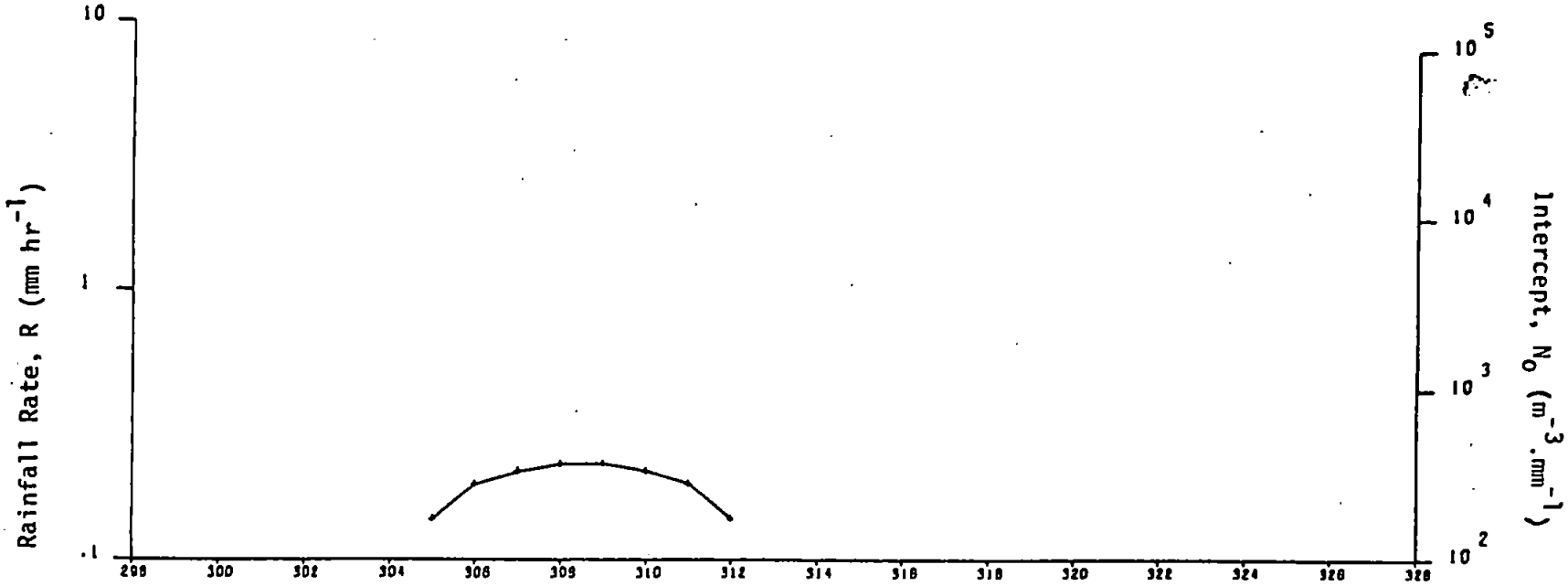

Radar Reflectivity

Contours (dBz)

(12) 530358 - 387

1730-59 : 27.3.79

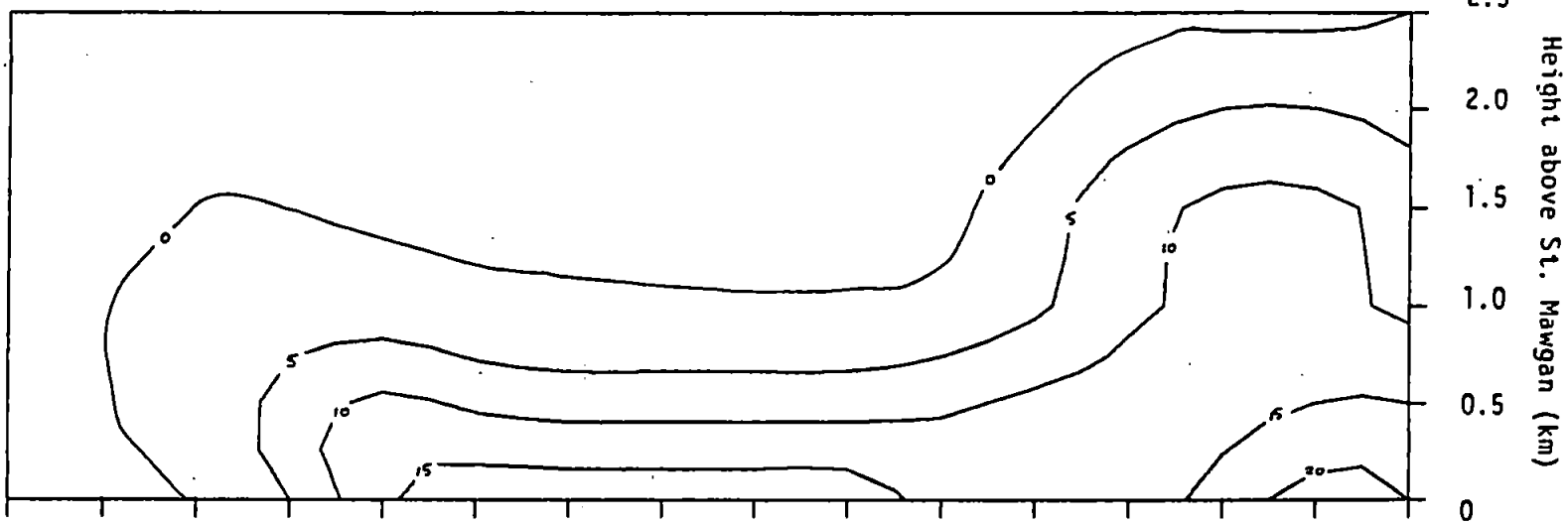

Totals:

R_G : 0.1 mm

R_D : 0.11 mm

R_Z : 0.11 mm

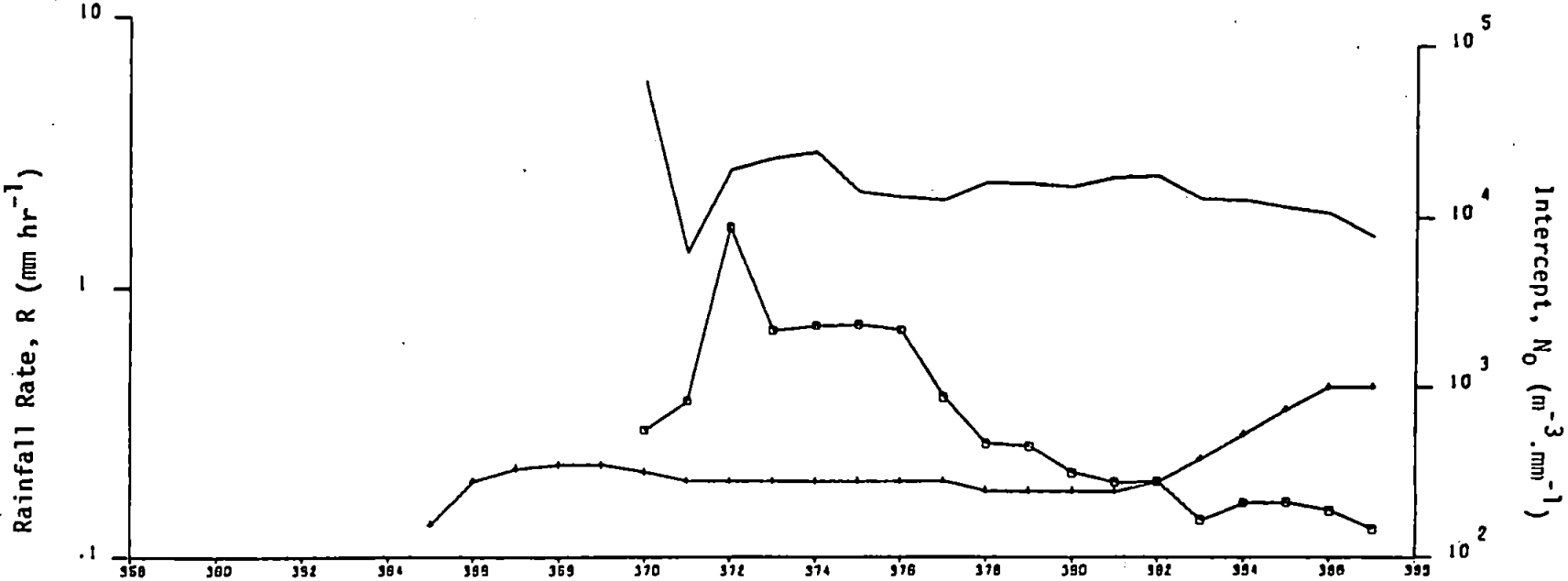

A 51

Radar Reflectivity

Contours (dBz)

(13) 530388 - 417

1800-29 : 27.3.79

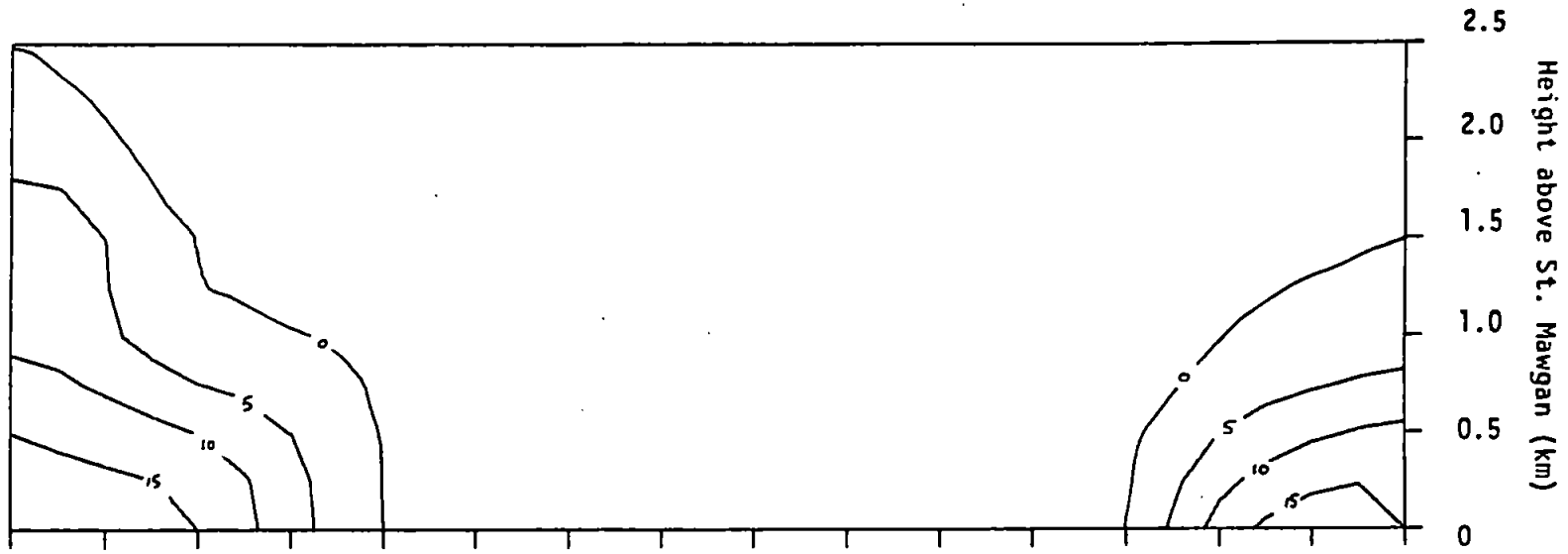

Totàls:

R_G : 0.1 mm

R_D : 0.03 mm

R_Z : 0.03 mm

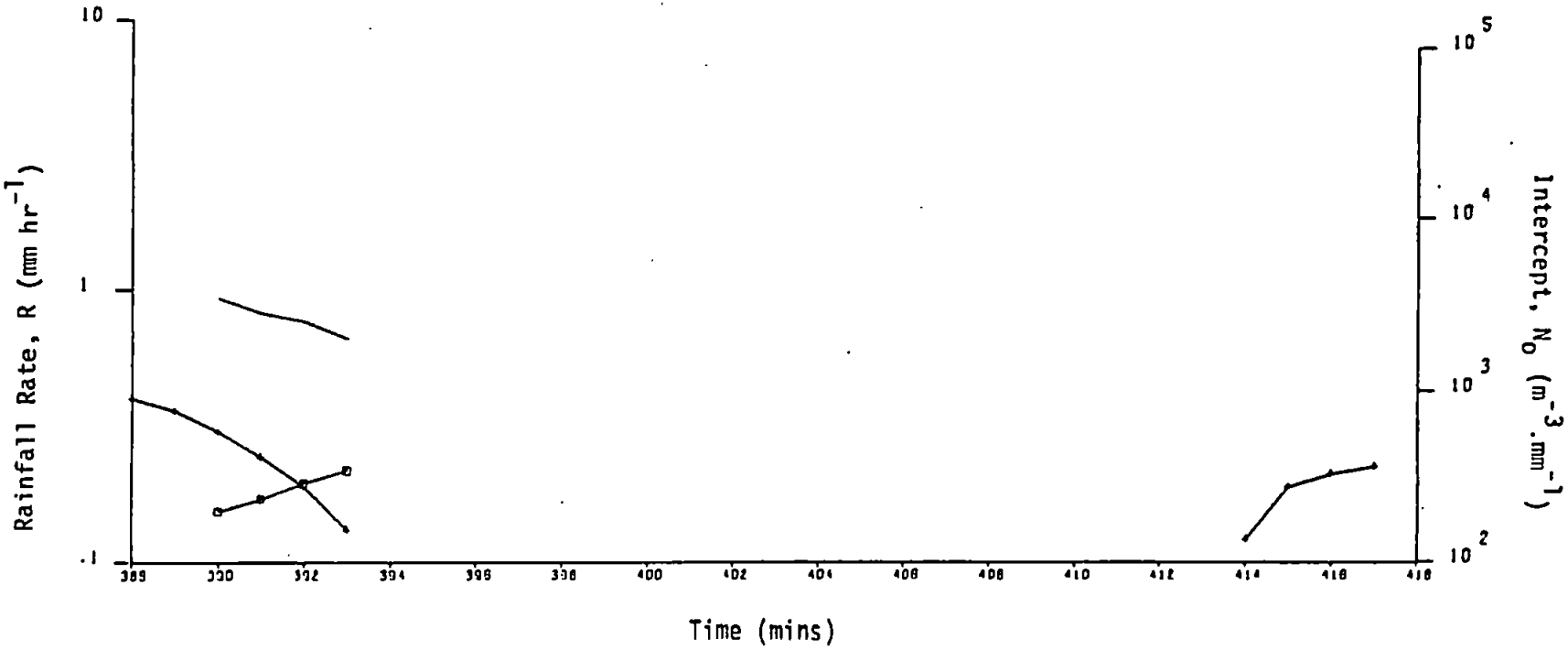

A 52

Radar Reflectivity

Contours (dBz)

(14) 540030 - 059

1330-59 : 9.4.79

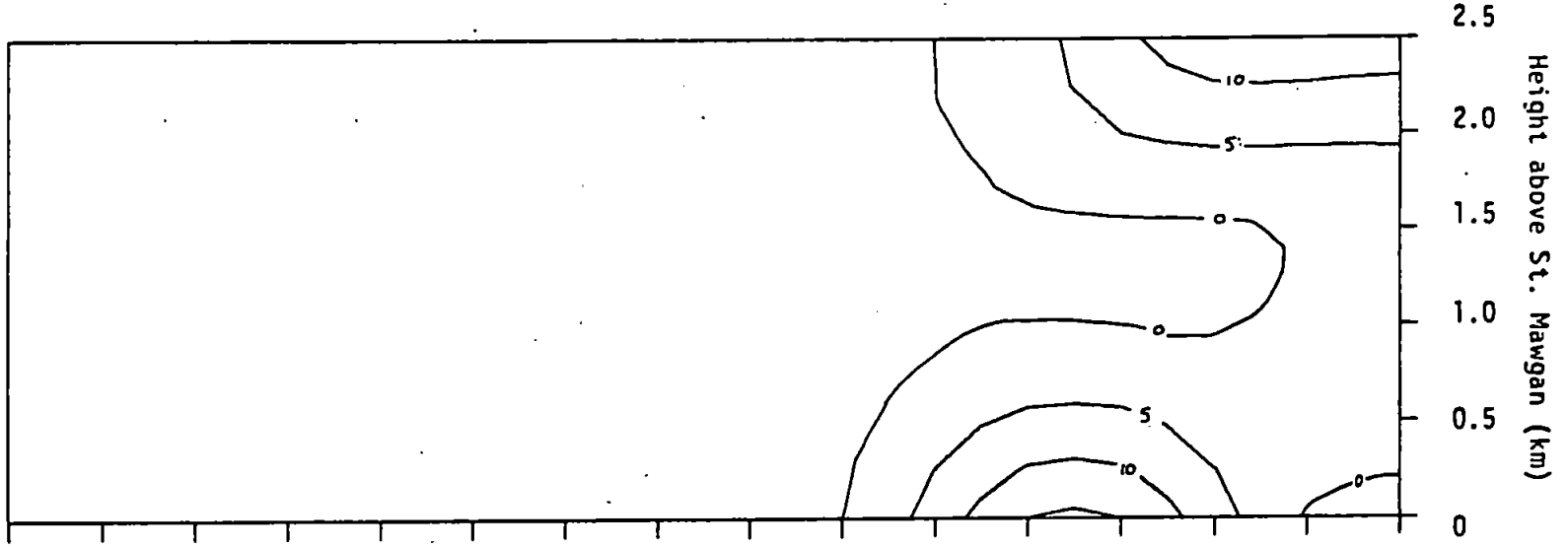

Totals:

R_G : 0 mm

R_D : 0 mm

R_Z : 0.02 mm

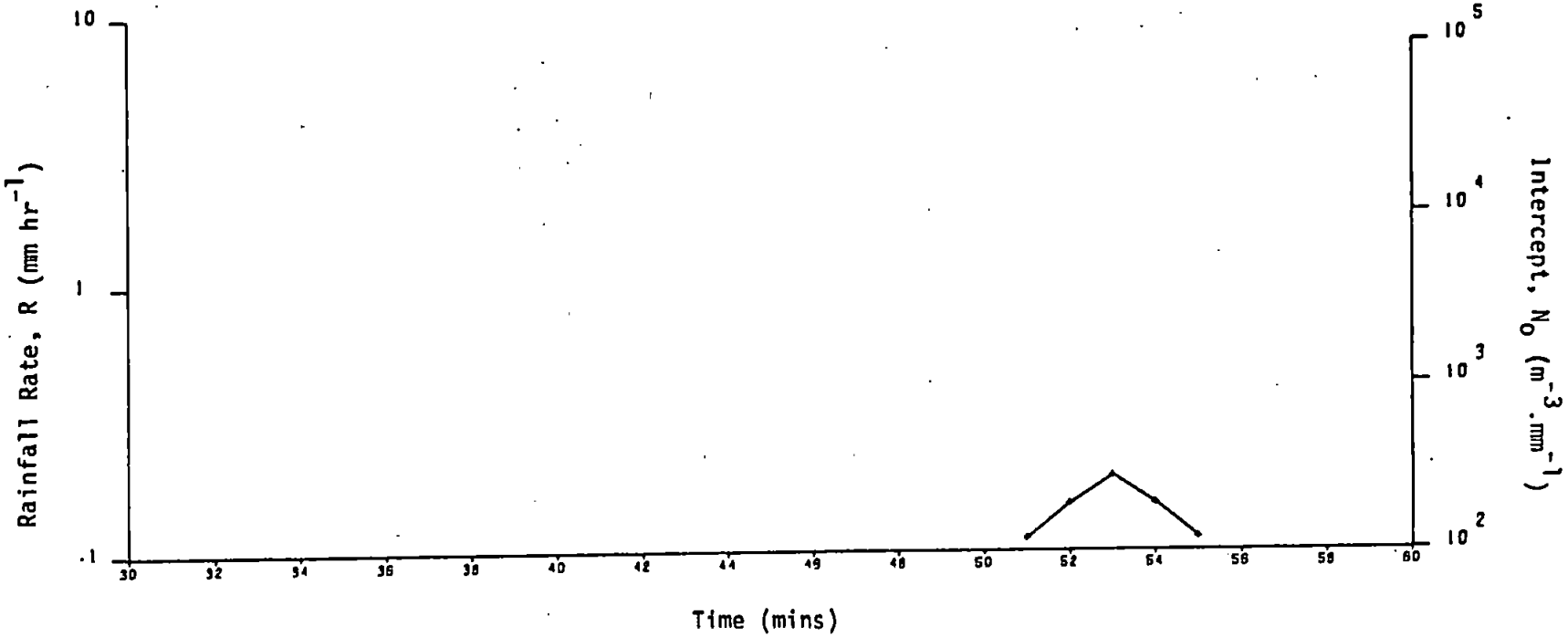

Radar Reflectivity

Contours (dBz)

(15) 540060 - 089

1400-29 : 9.4.79

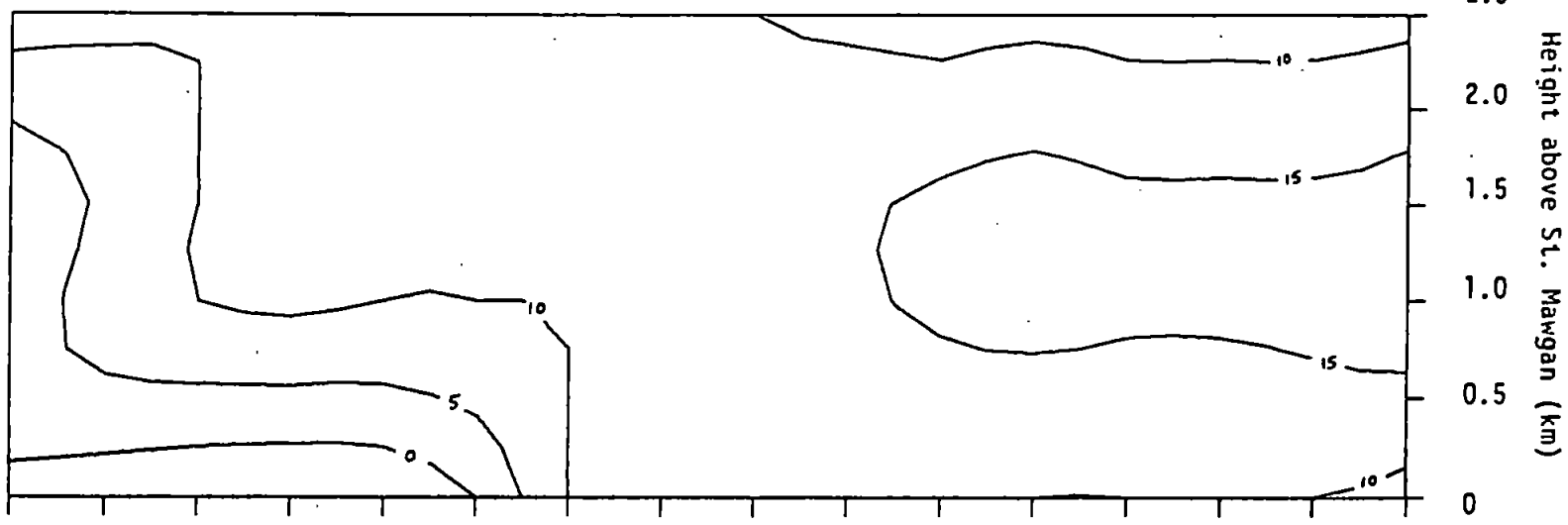

Totals:

R_G : 0 mm

R_D : 0.03 mm

R_Z : 0.07 mm

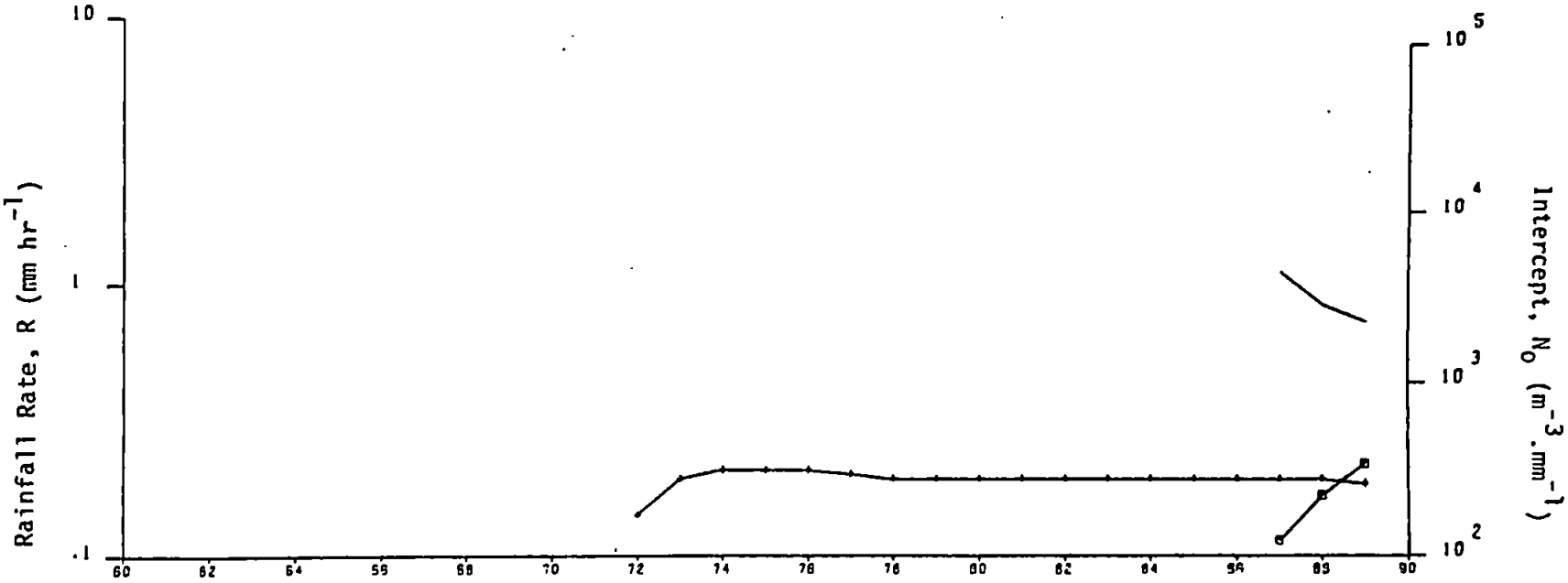

Radar Reflectivity

Contours (dBz)

(16) 540090 - 119

1430-59 : 9.4.79

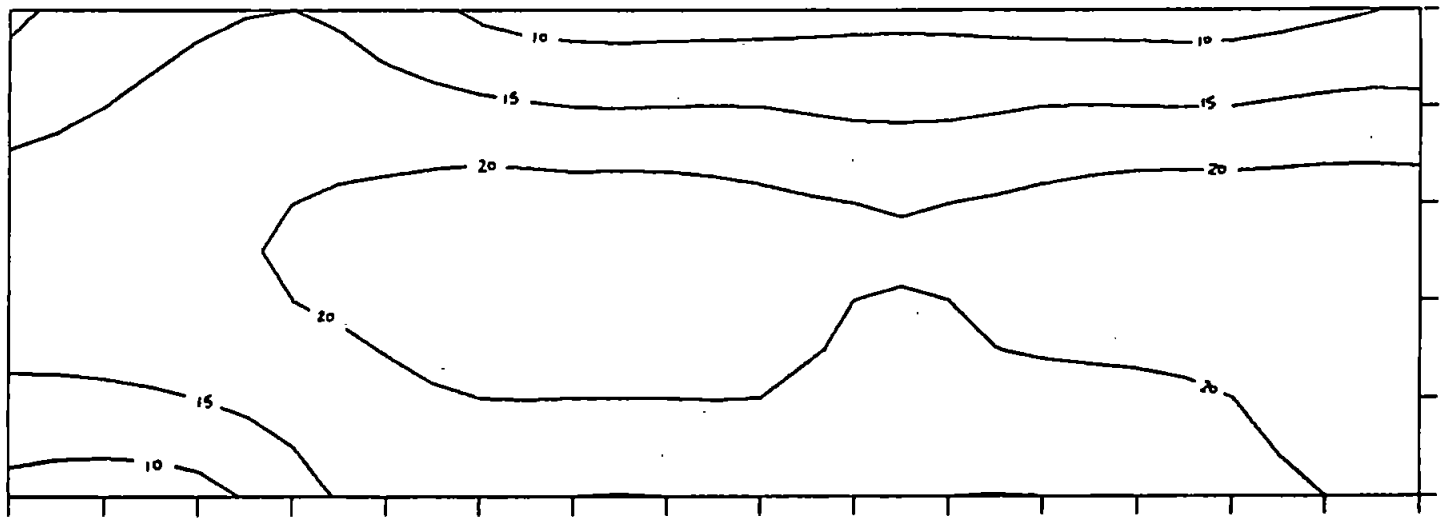

Totals:

R_G : 0.3 mm

R_D : 0.29 mm

R_Z : 0.24 mm

A 55

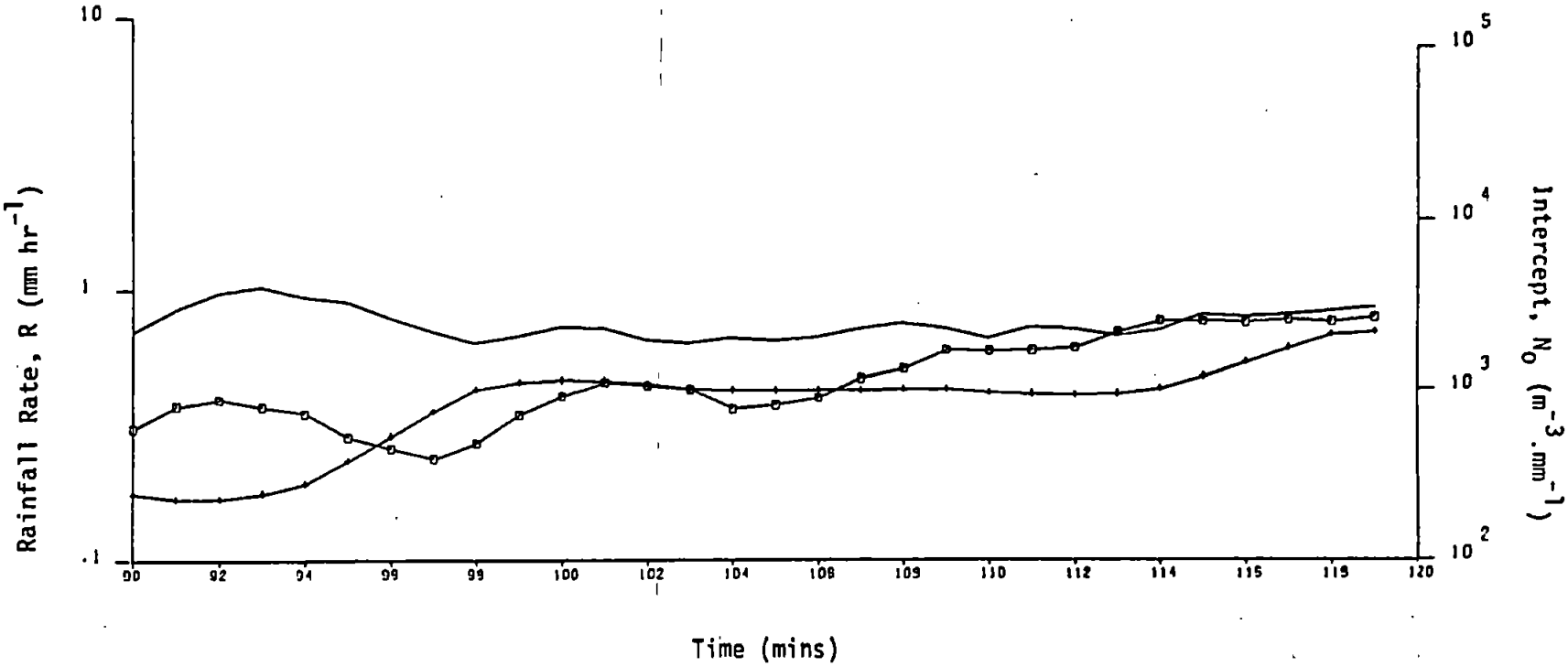

Radar Reflectivity

Contours (dBz)

(17) 540120 - 149

1500-29 : 9.4.79

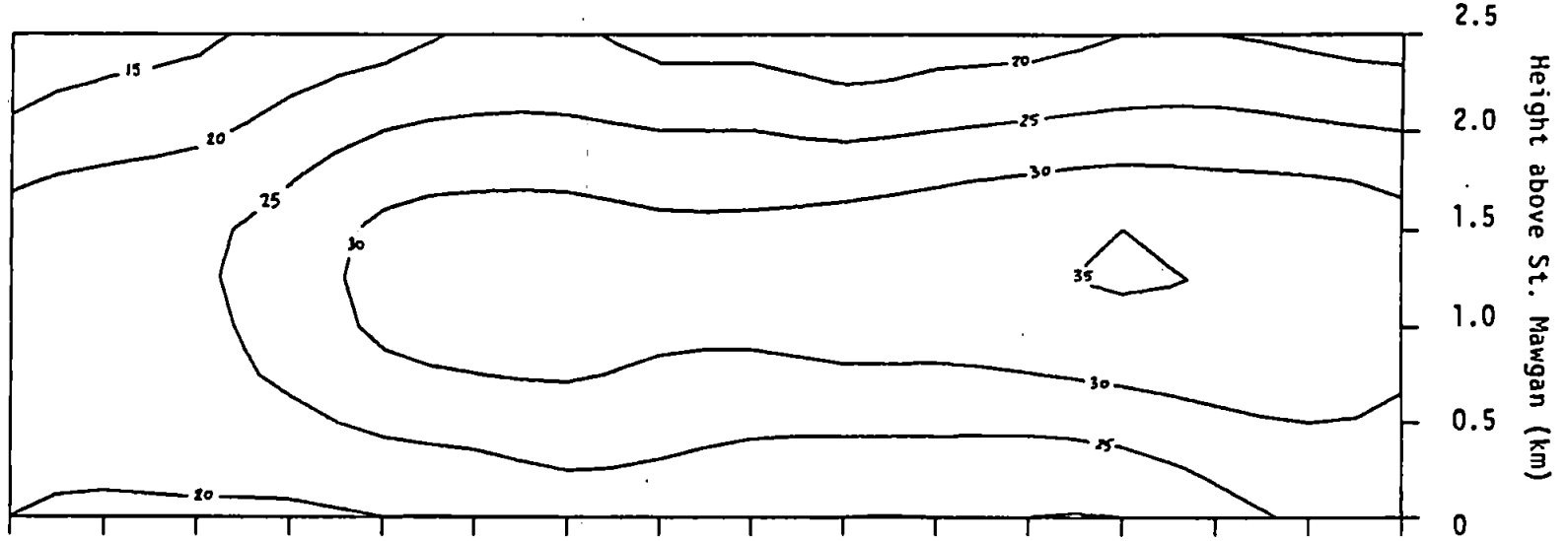

Totals:

R_G : 0.7 mm

R_D : 0.71 mm

R_Z : 0.61 mm

A 56

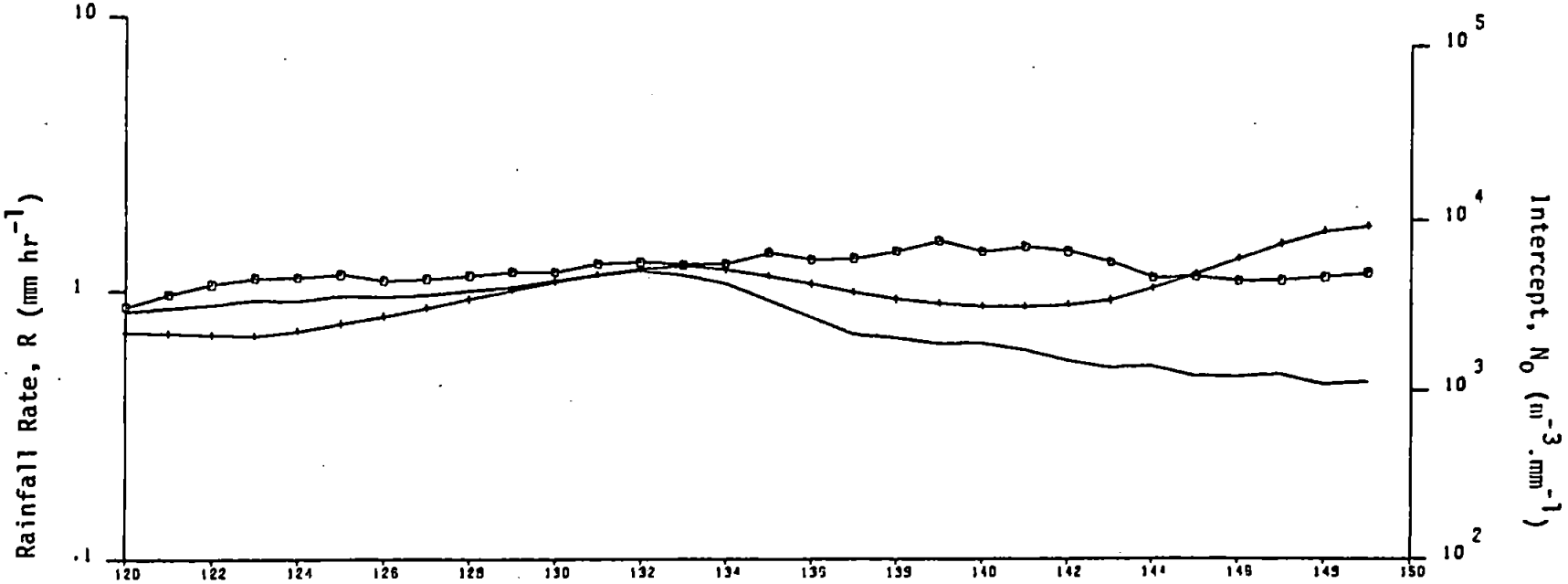

Radar Reflectivity

Contours (dBz)

(18) 540150 - 179

1530-59 : 9.4.79

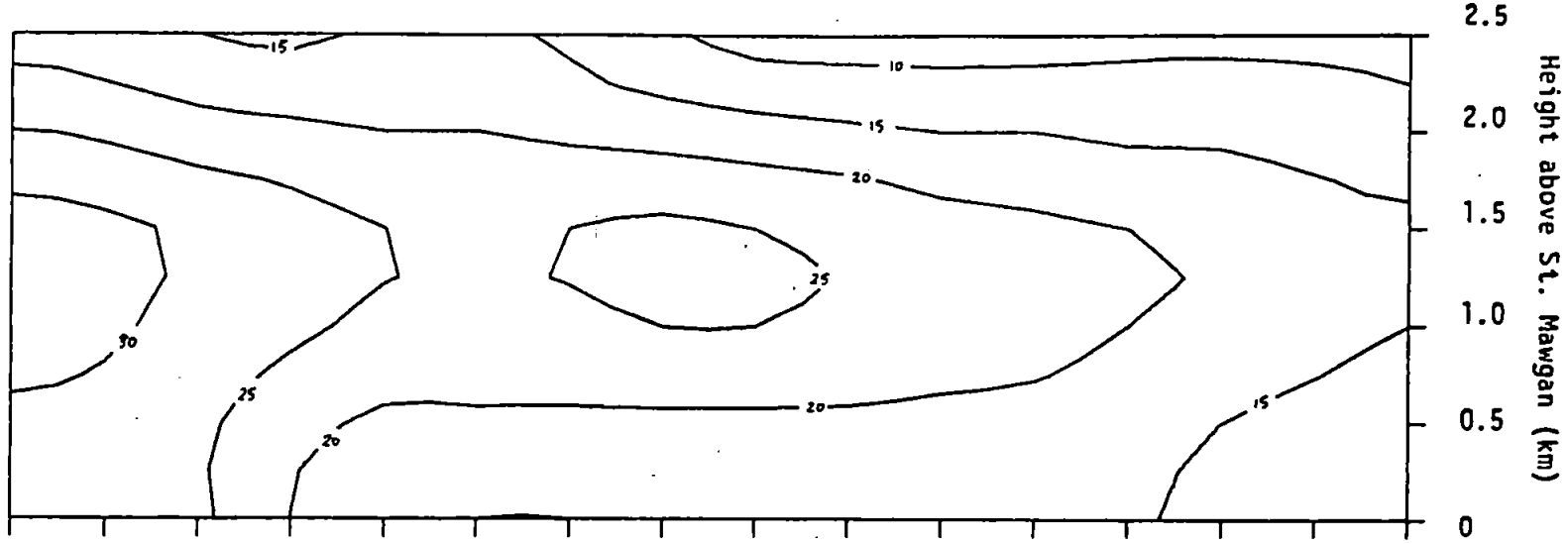

Totals:

R_G : 0.6 mm

R_D : 0.52 mm

R_Z : 0.29 mm

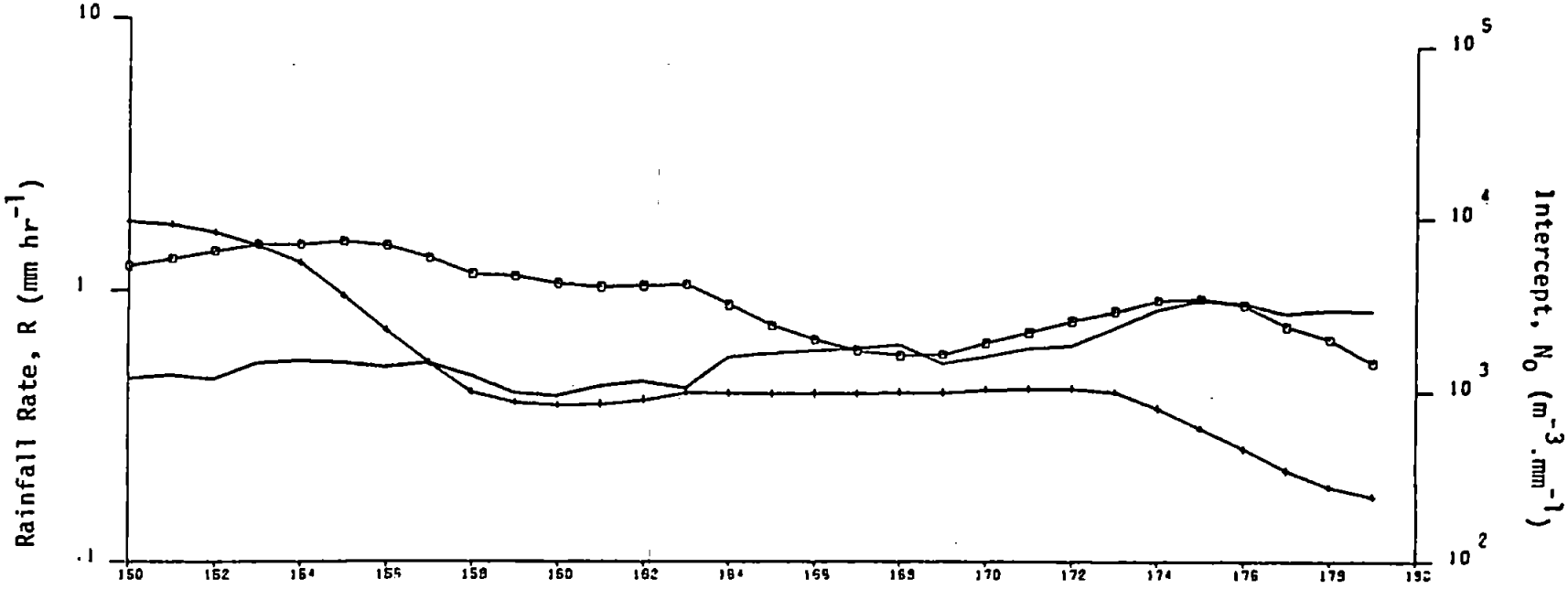

A 57

Radar Reflectivity

Contours (dBz)

(19) 540180 - 209

1600-29 : 9.4.79

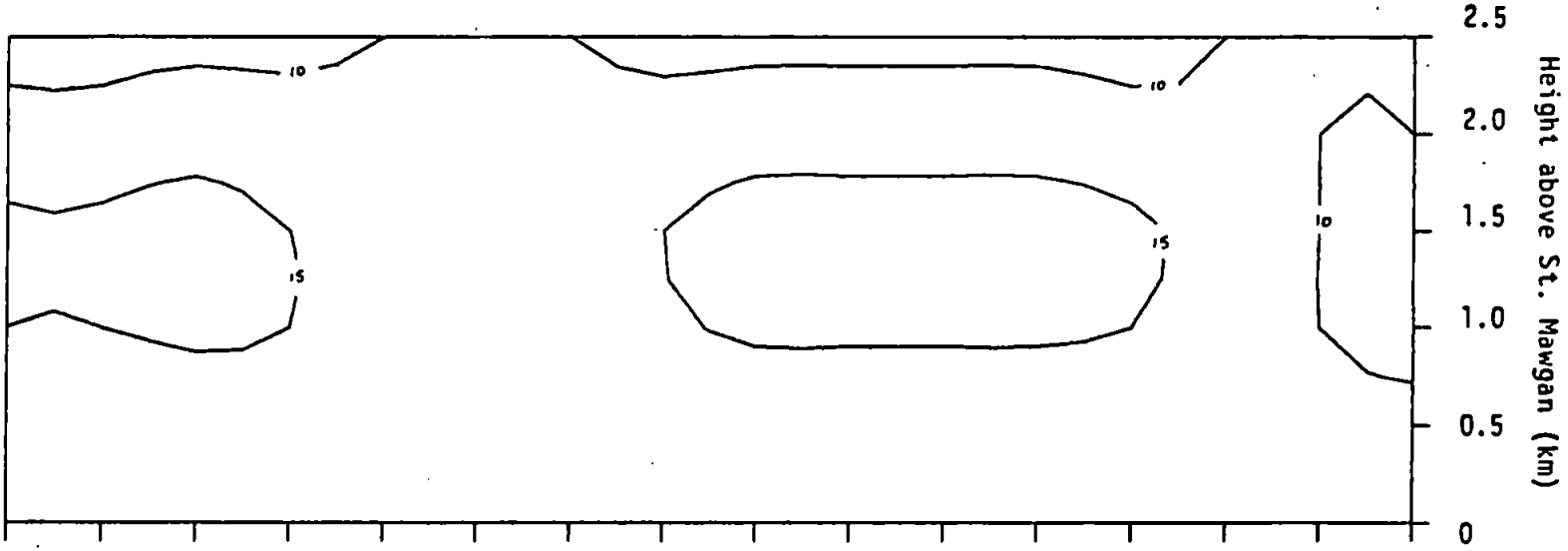

Totals:

R_G : 0.2 mm

R_D : 0.22 mm

R_Z : 0.10 mm

A 58

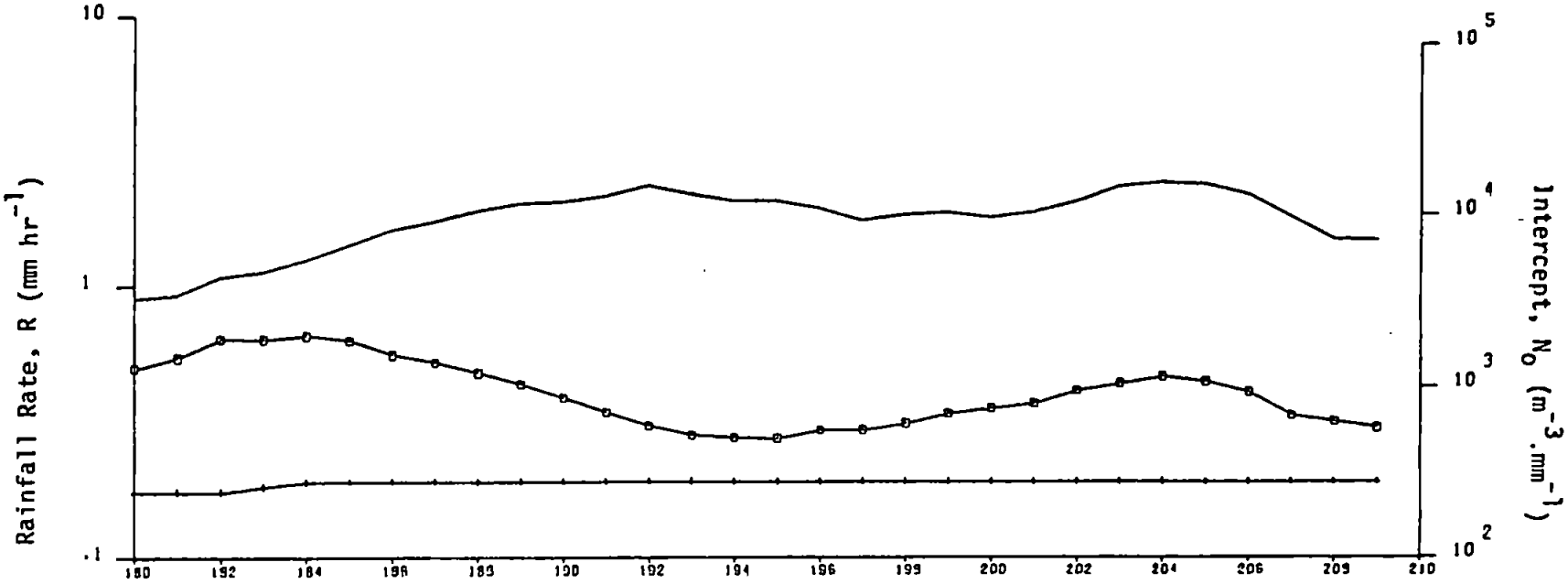

Radar Reflectivity

Contours (dBz)

(20) 540210 - 239

1630-59 : 9.4.79

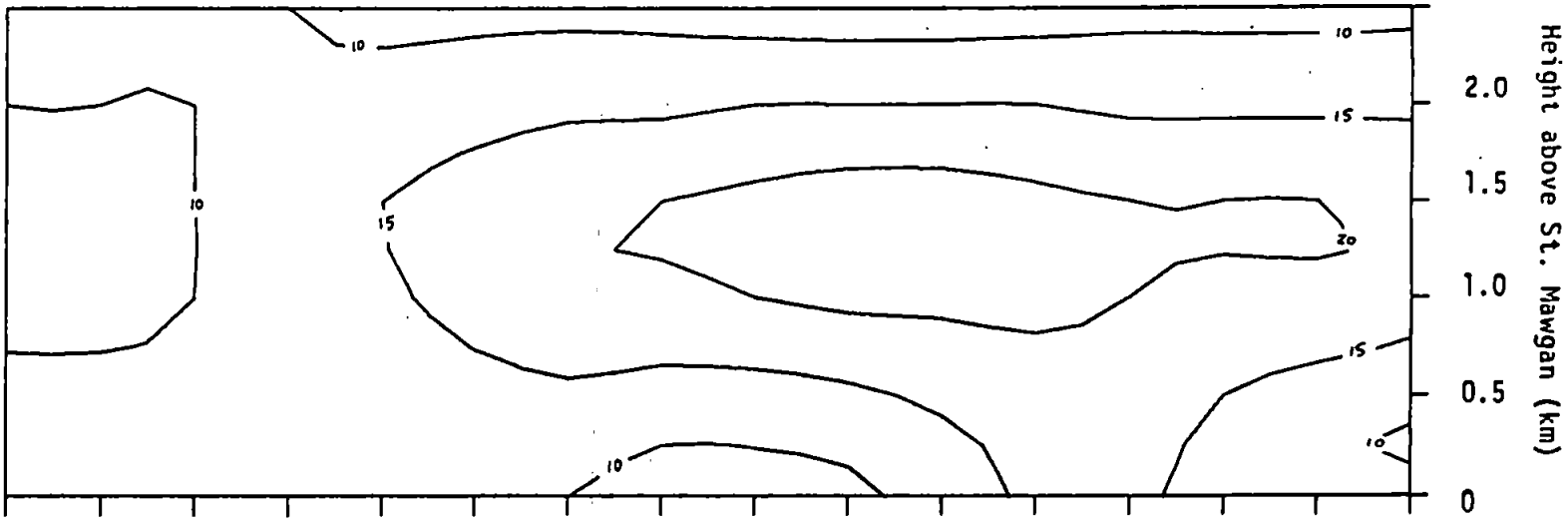

Totals:

R_G : 0.3 mm

R_D : 0.27 mm

R_Z : 0.12 mm

A 59

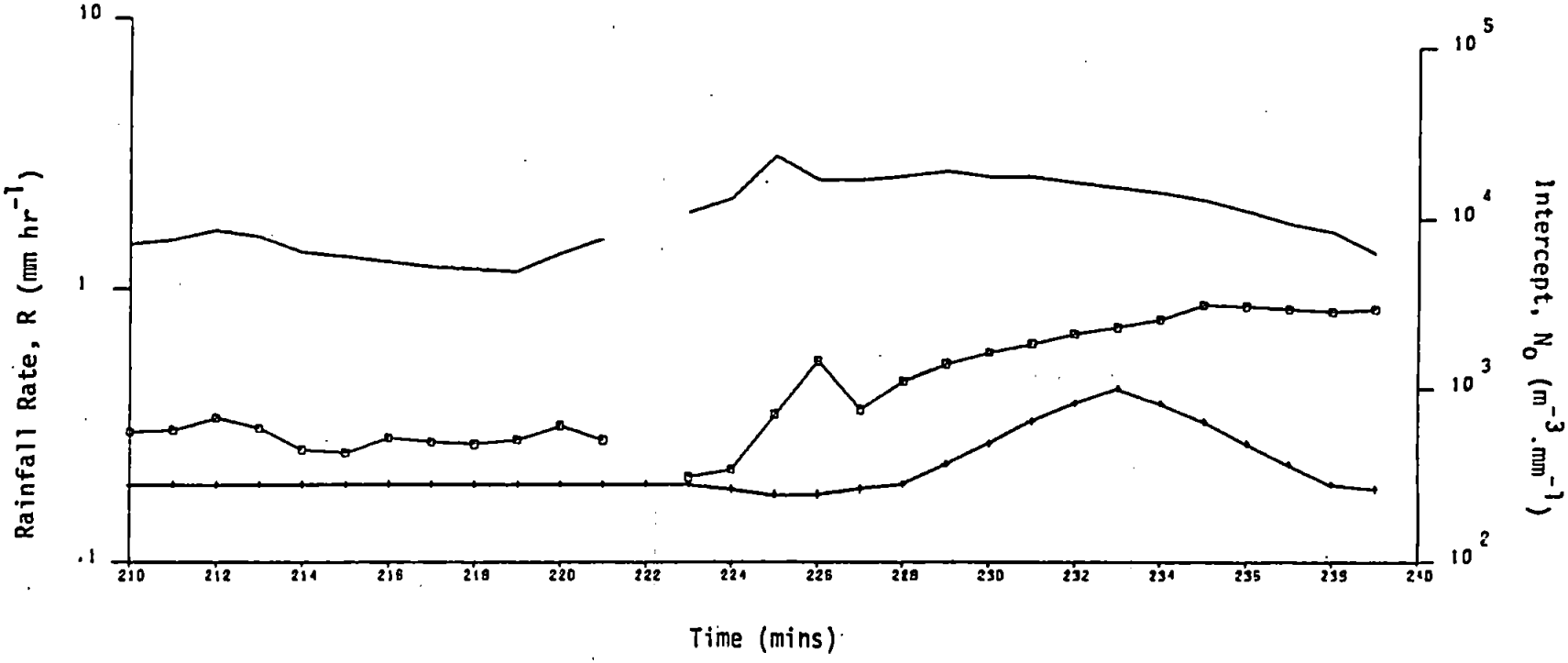

Radar Reflectivity

Contours (dBz)

(21) 540240 - 269

1700-29 : 9.4.79

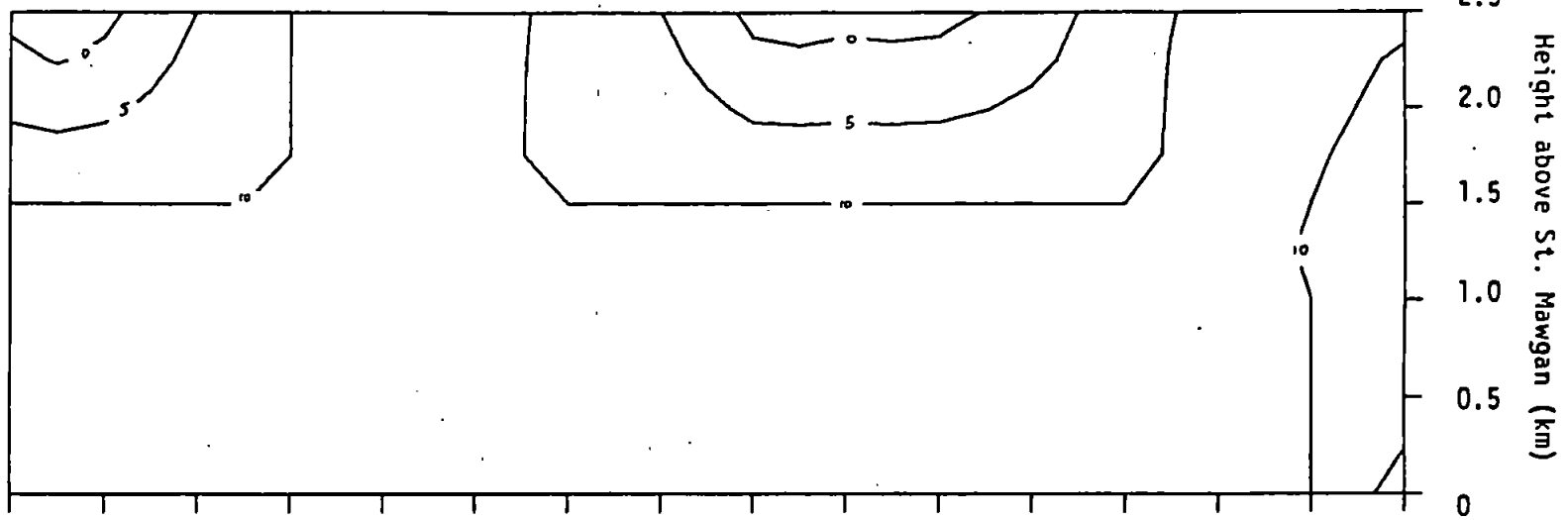

Totals:

R_G : 0.4 mm

R_D : 0.35 mm

R_Z : 0.10 mm

A 60

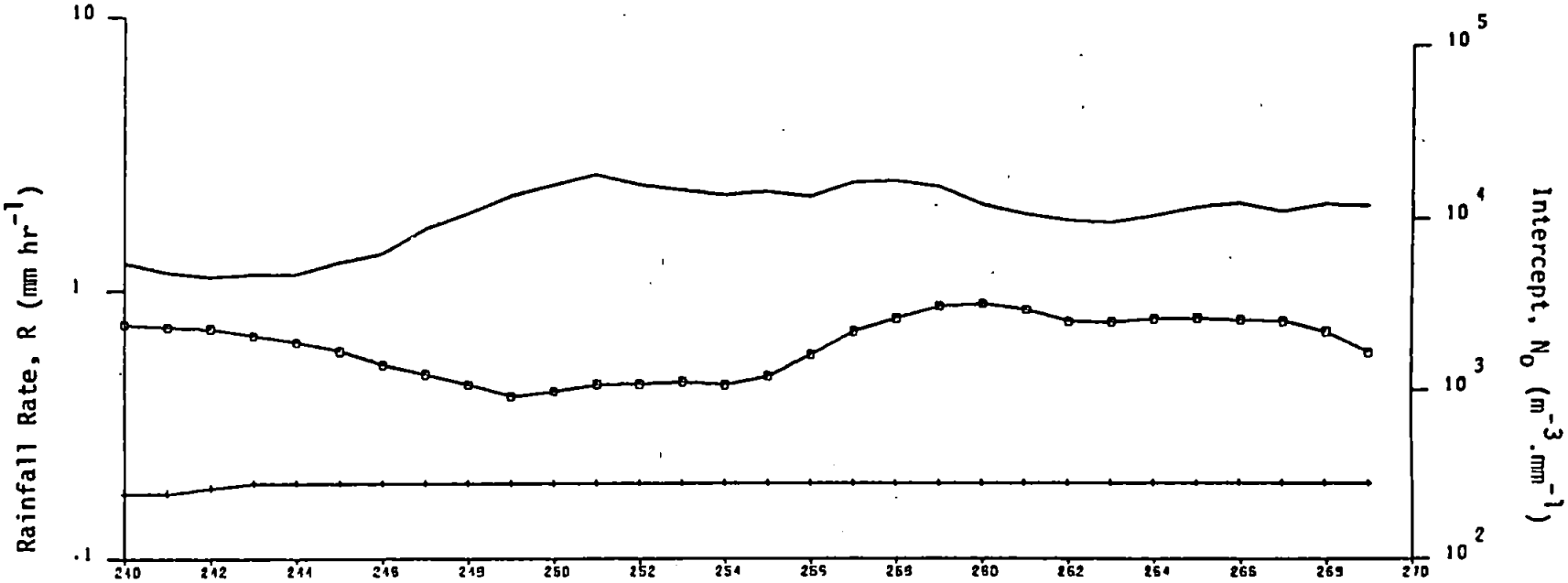

Radar Reflectivity

Contours (dBz)

(22) 540270 - 299

1730-59 : 9.4.79

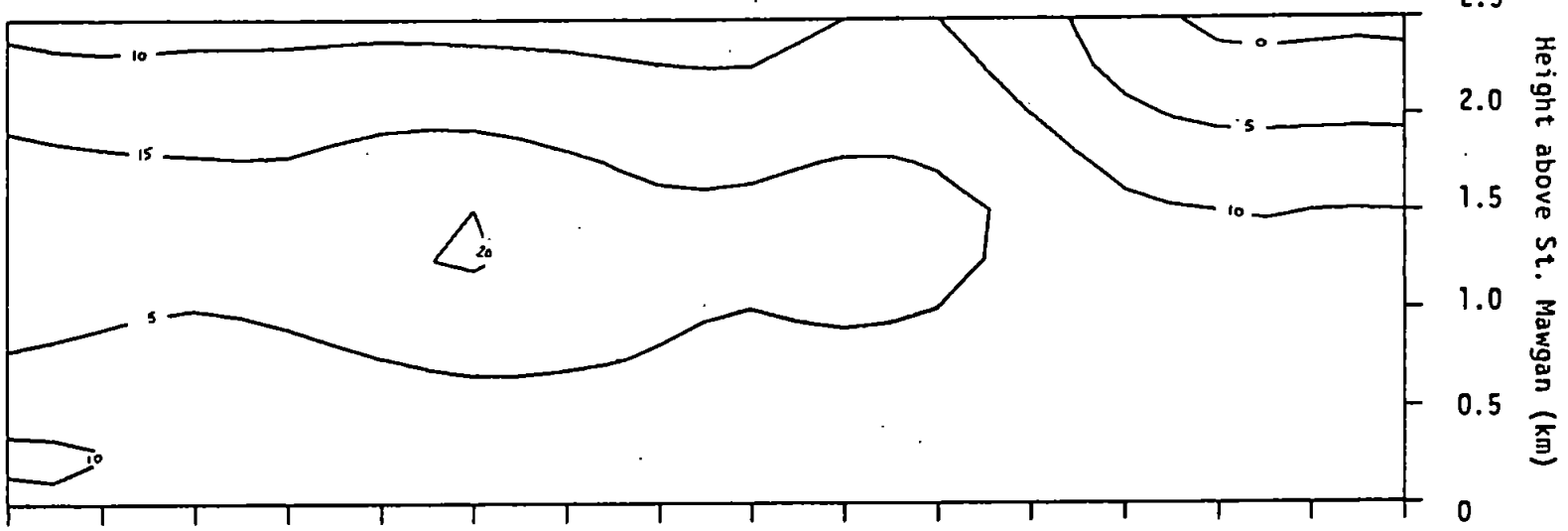

Totals:

R_G : 0.1 mm

R_D : 0.07 mm

R_Z : 0.10 mm

A 61

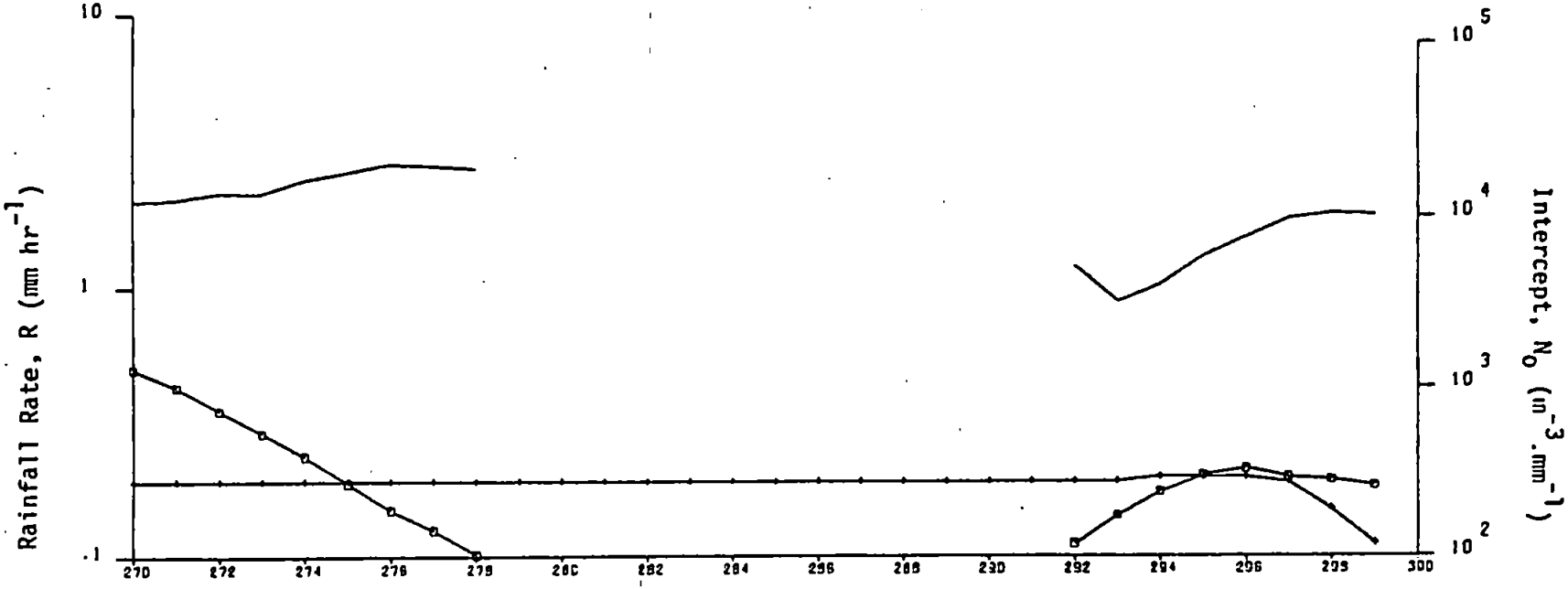

Radar Reflectivity

Contours (dBz)

(23) 540300 - 329

1800-29 : 9.4.79

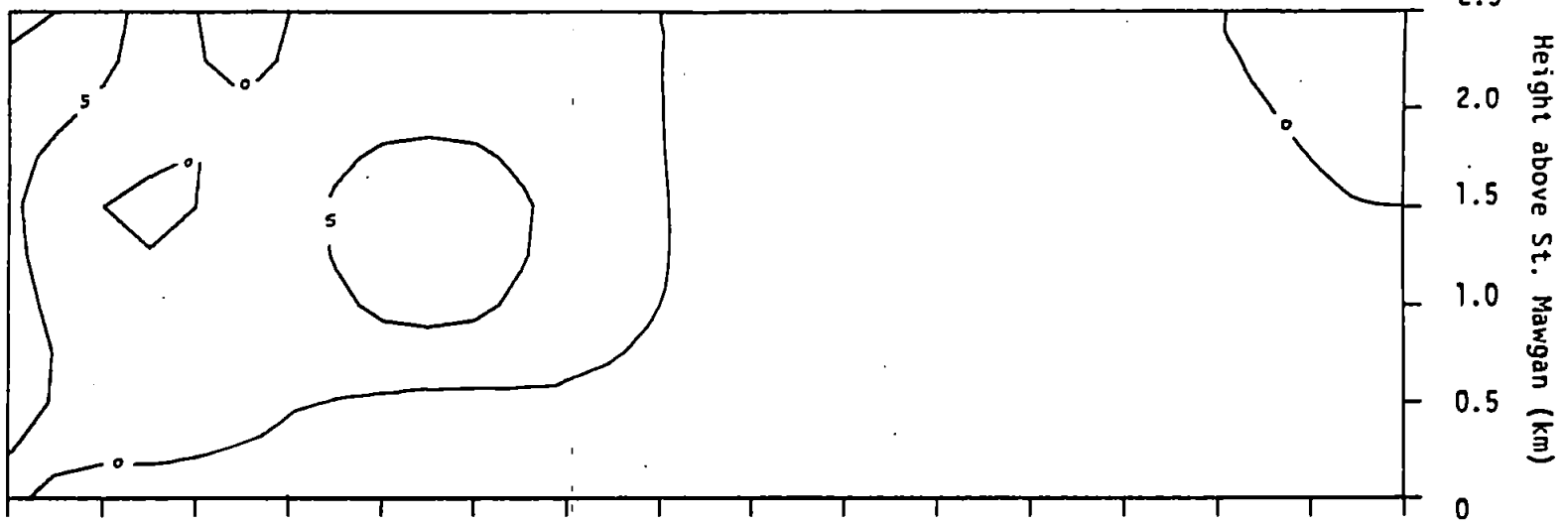

Totals:

R_G : 0 mm

R_D : 0.01 mm

R_Z : 0 mm

A 62

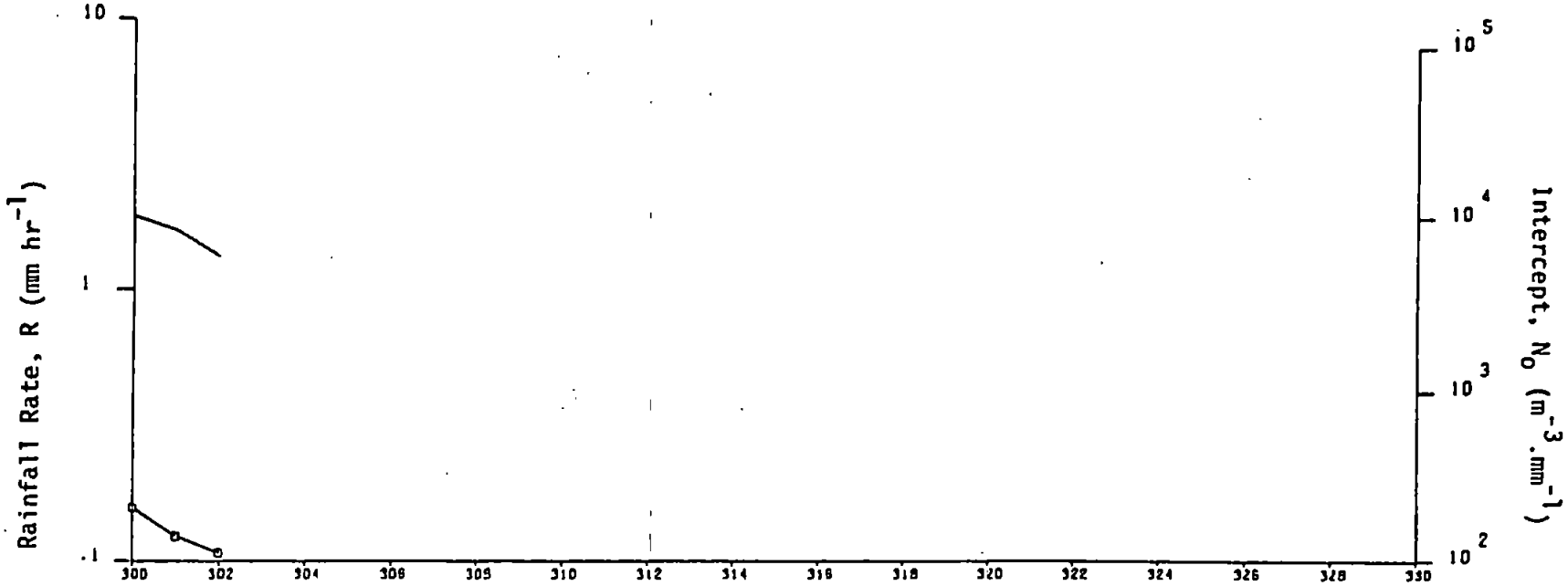

Radar Reflectivity

Contours (dBz)

(24) 540330 - 359

1830-59 : 9.4.79

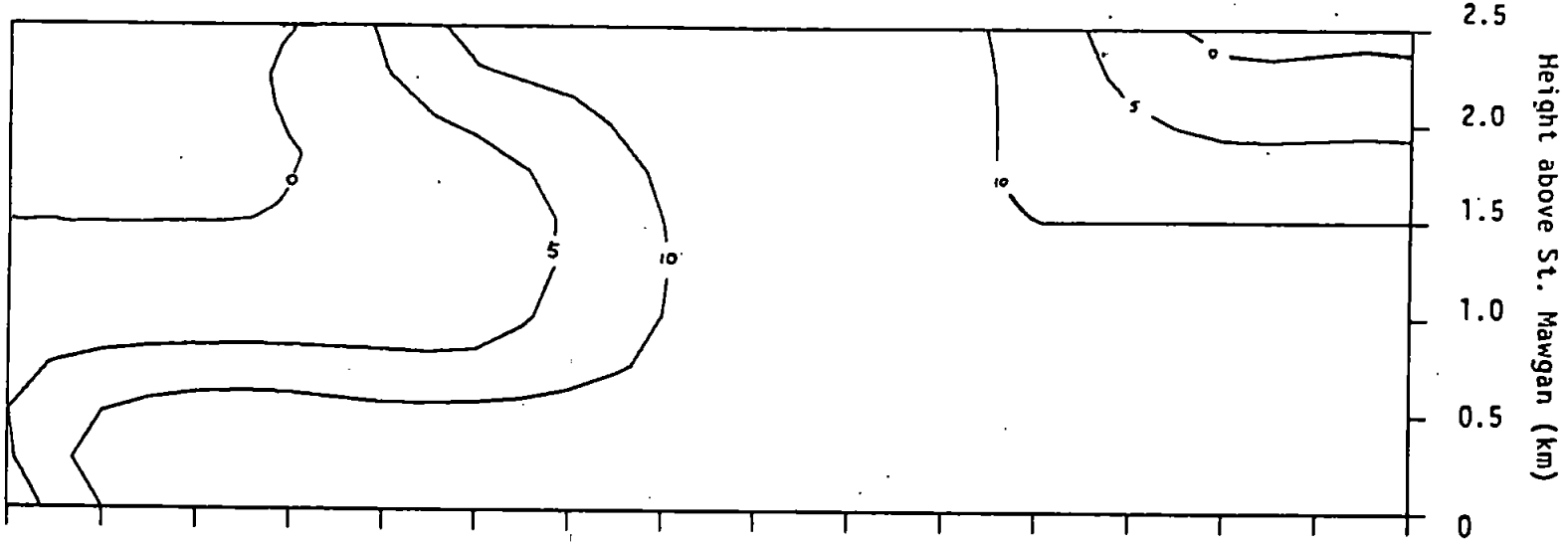

Totals:

R_G : 0.2 mm

R_D : 0.10 mm

R_Z : 0.10 mm

A 63

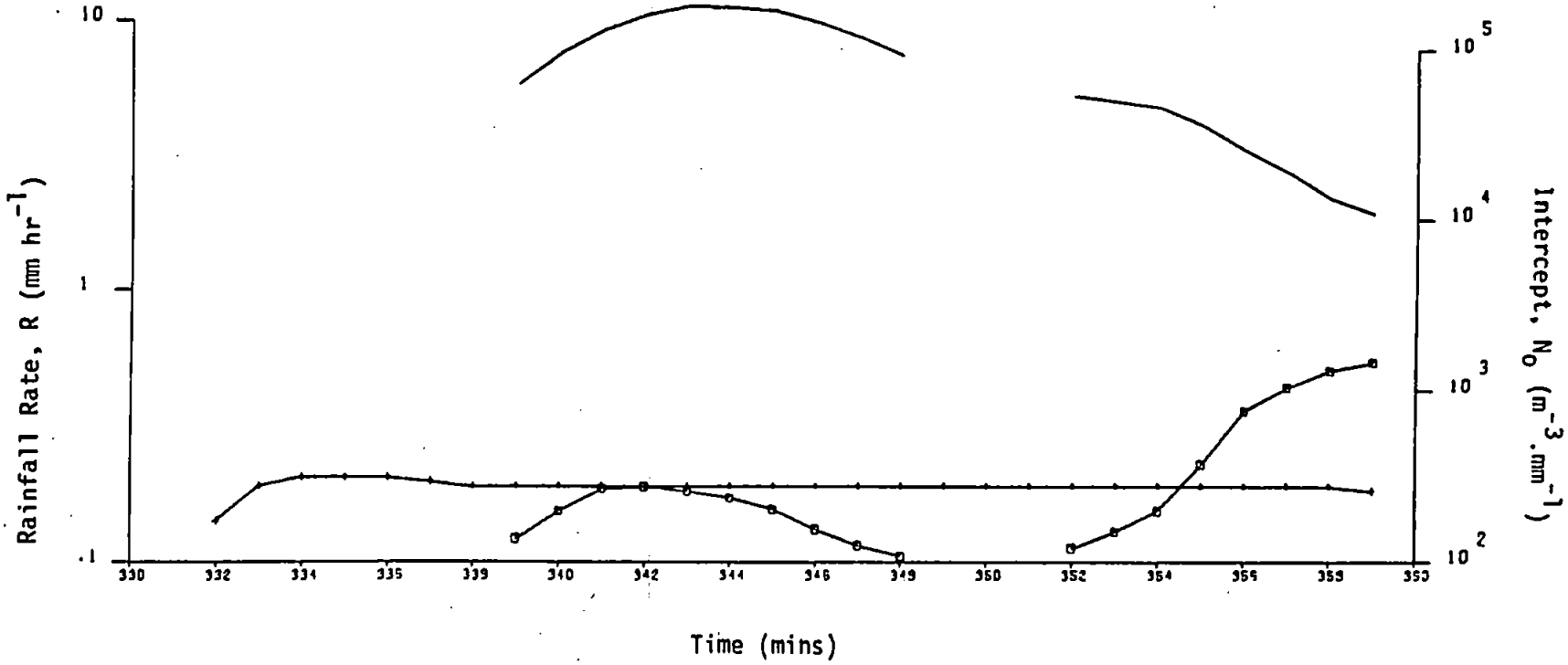

Radar Reflectivity

Contours (dBz)

(25) 540360 - 389

1900-29 : 9.4.79

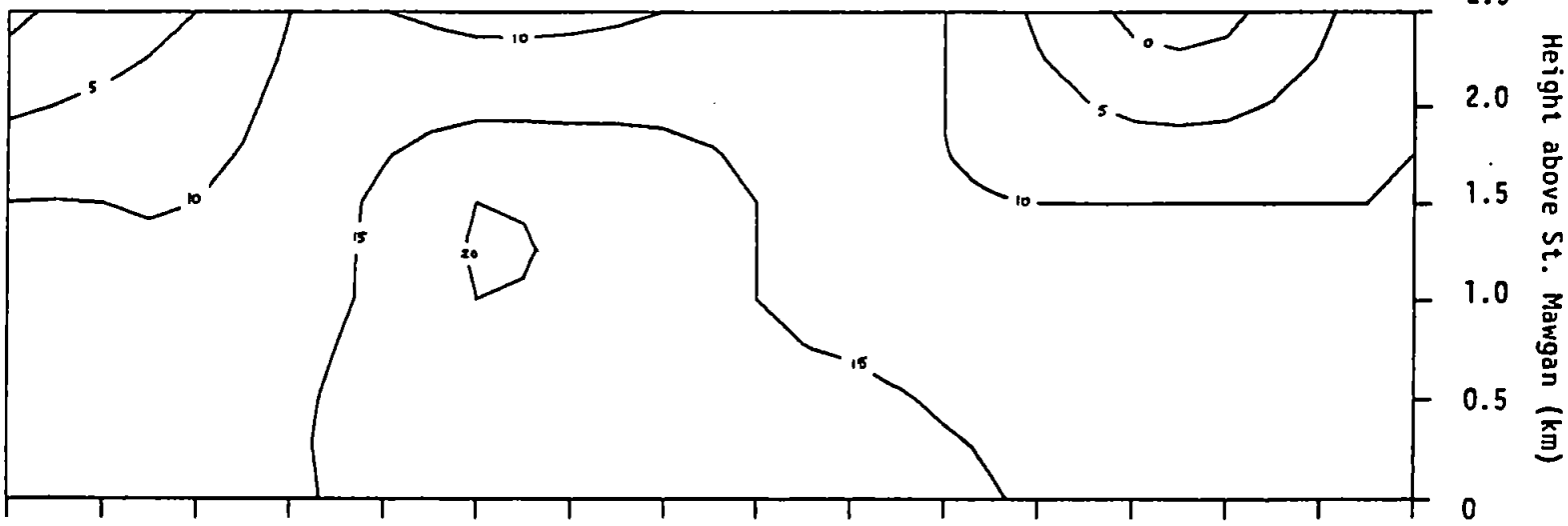

Totàls:

R_G : 0.5 mm

R_D : 0.33 mm

R_Z : 0.17 mm

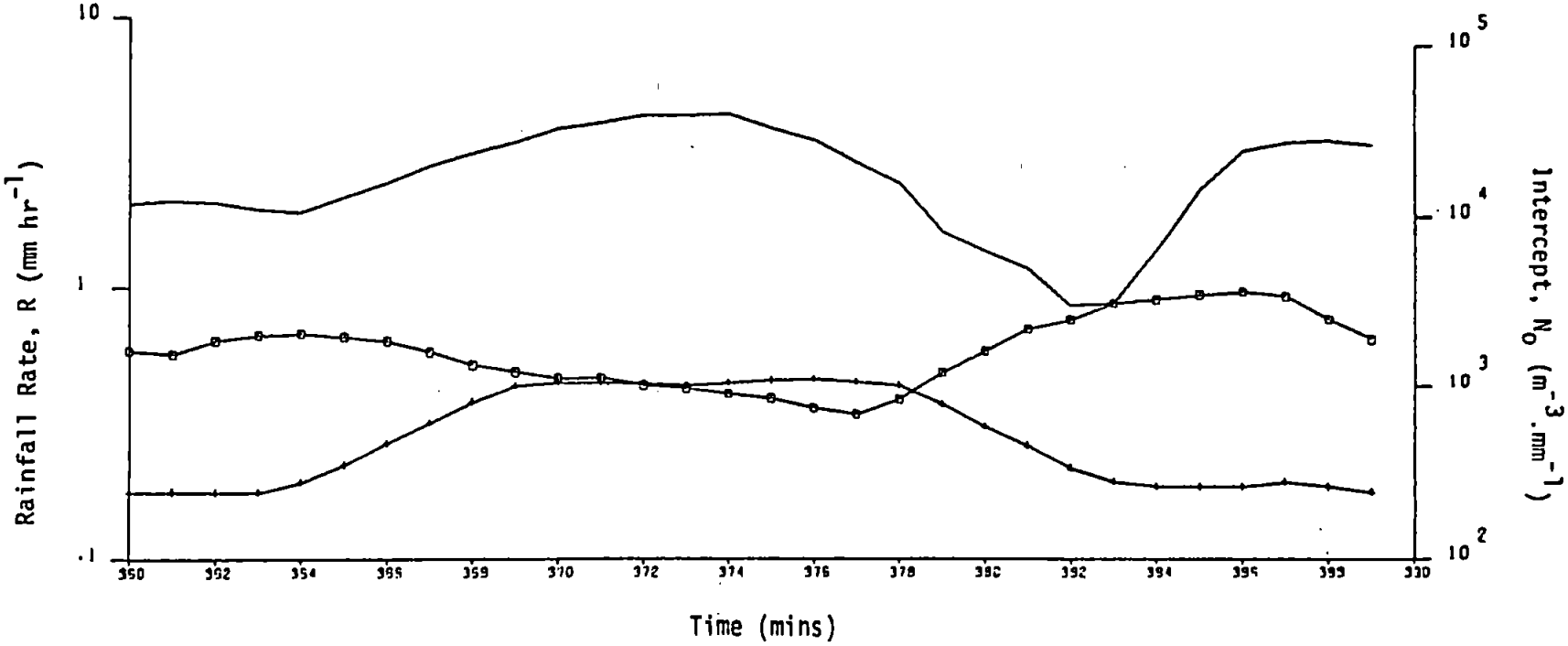

A 64

Radar Reflectivity

Contours (dBz)

(26) 540390 - 419

1930-59 : 9.4.79

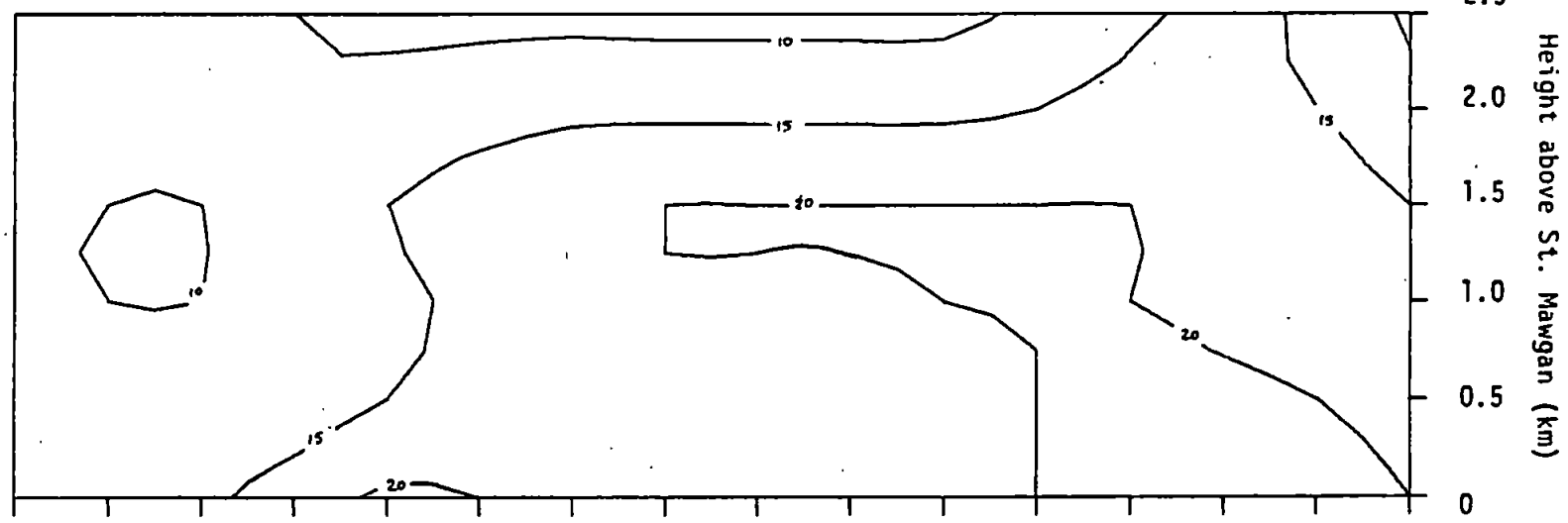

Totals:

R_G : 0.8 mm

R_D : 0.41 mm

R_Z : 0.26 mm

A 65

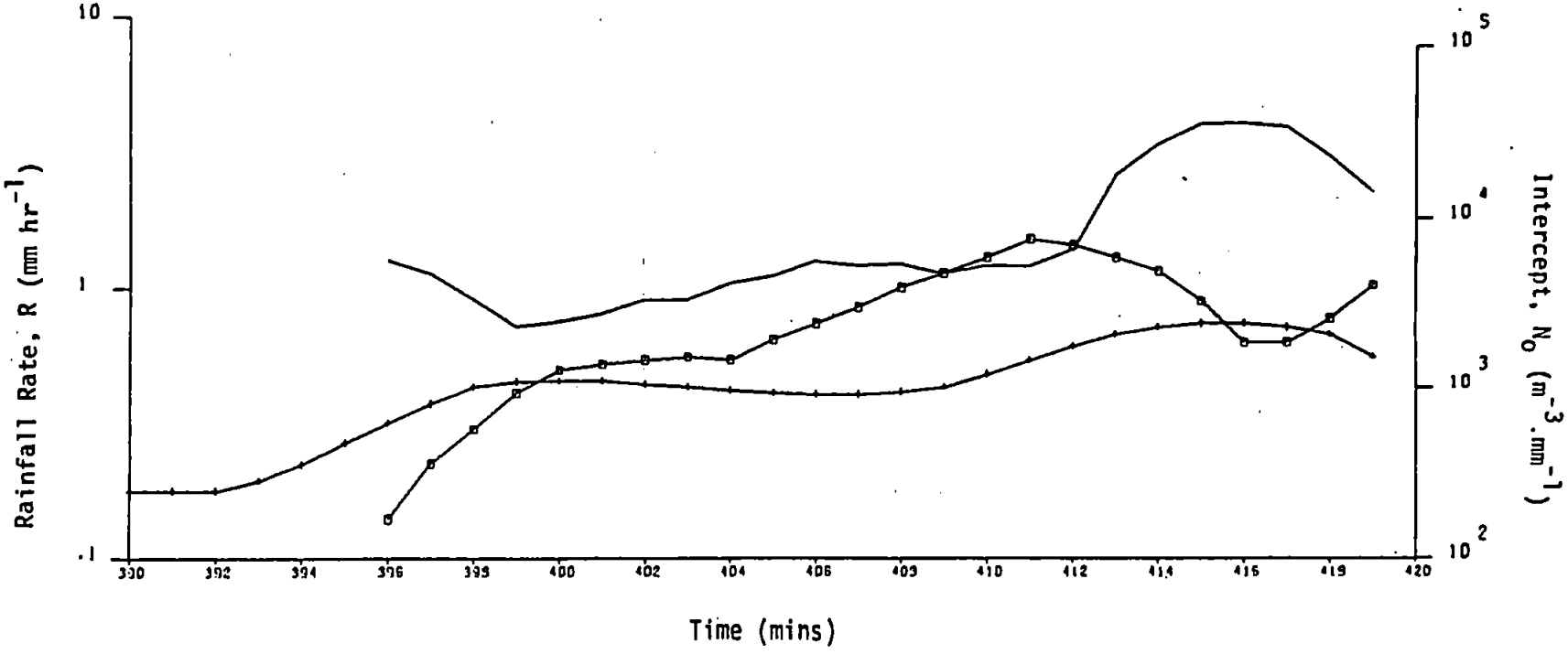

Radar Reflectivity

Contours (dBz)

(27) 540420 - 449

2000-29 : 9.4.79

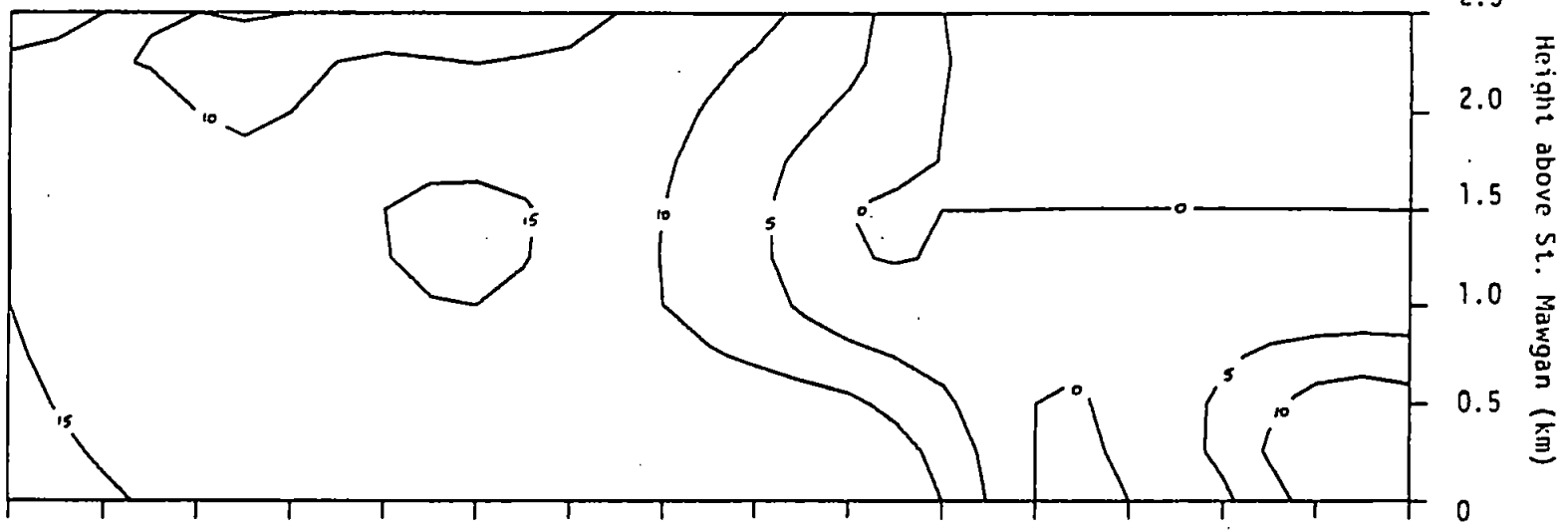

Totals:

R_G : 0.4 mm

R_D : 0.36 mm

R_Z : 0.08 mm

A 66

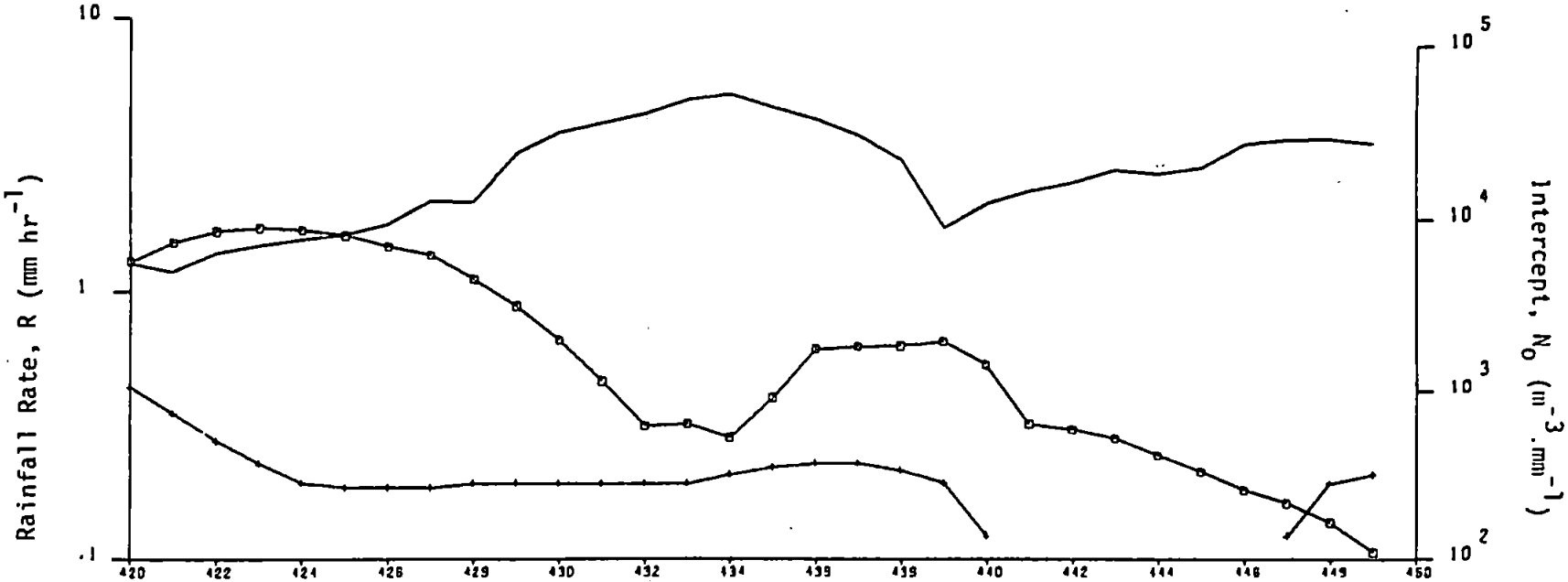

Radar Reflectivity

Contours (dBz)

(28) 550090 - 119

1730-59 : 22.5.79

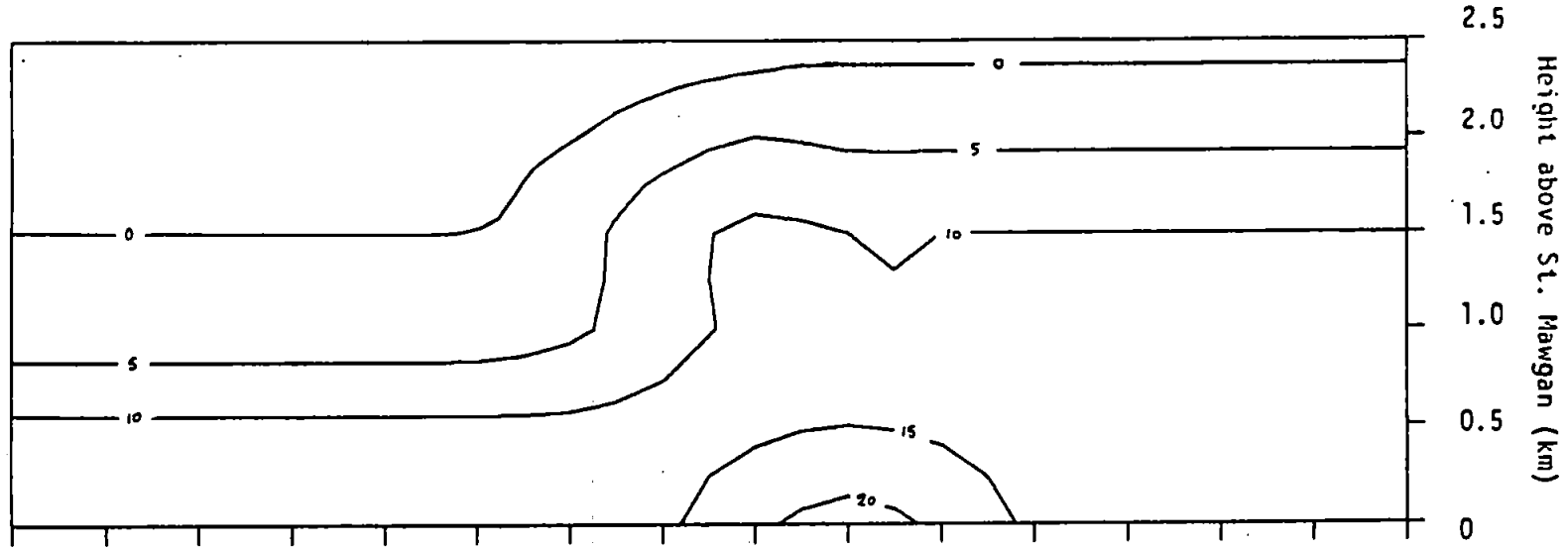

Totals:

R_G : 0.2 mm

R_D : 0.19 mm

R_Z : 0.12 mm

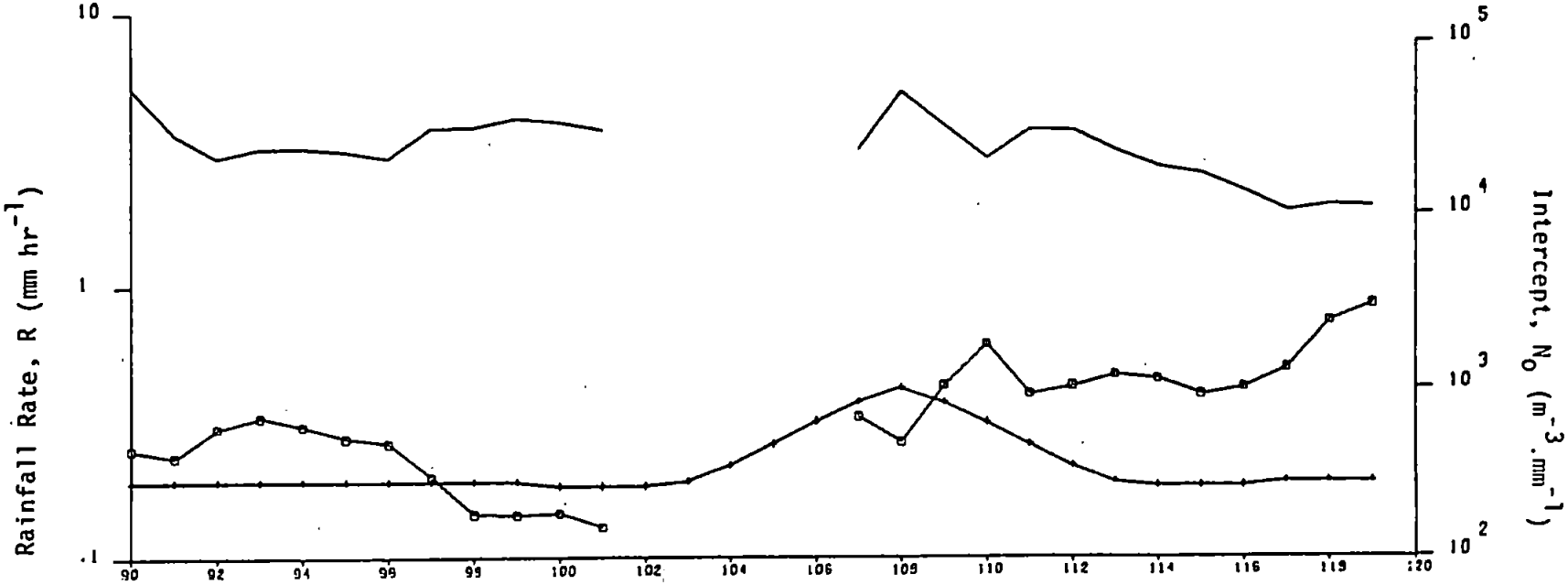

Radar Reflectivity

Contours (dBz)

(29) 550120 - 149

1800-29 : 22.5.79

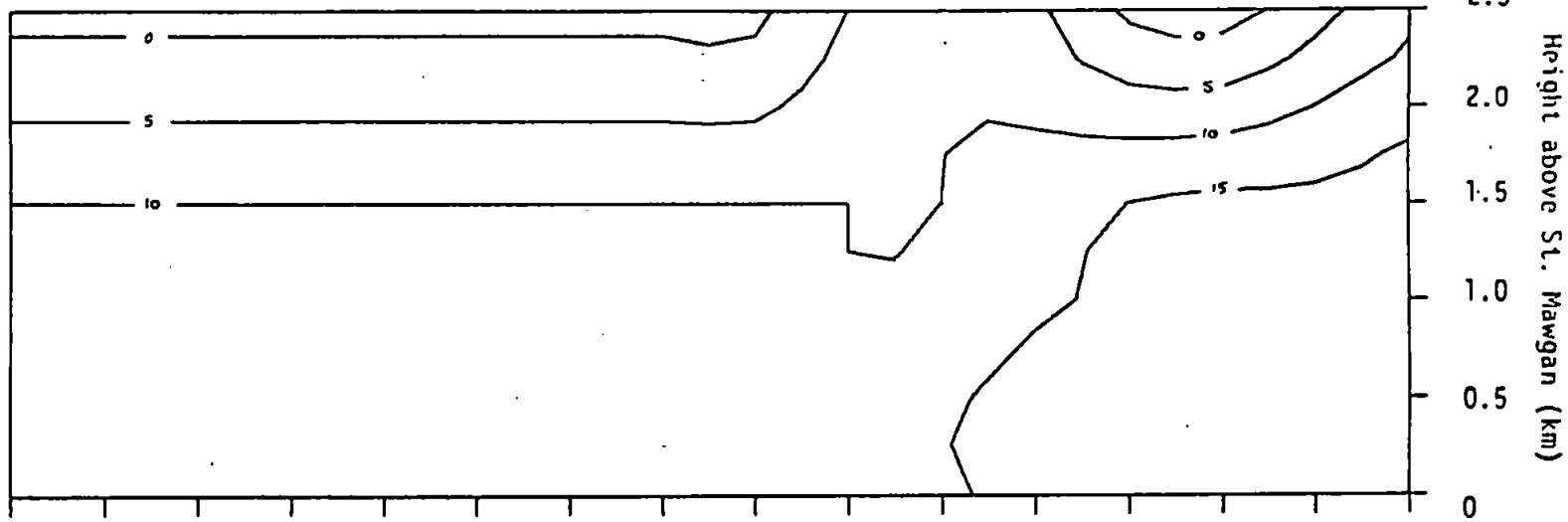

Totals:

R_G : 0.3 mm

R_D : 0.22 mm

R_Z : 0.15 mm

A 68

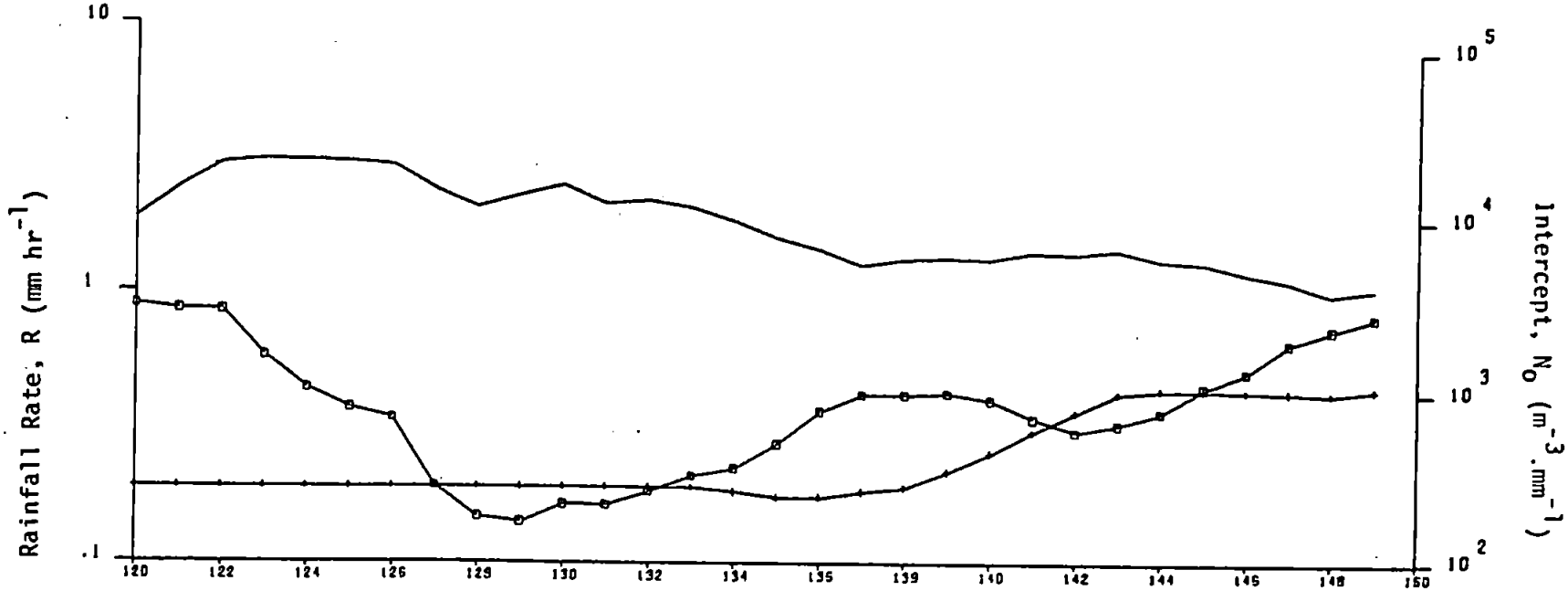

Radar Reflectivity

Contours (dBz)

(30) 550150 - 179

1830-59 : 22.5.79

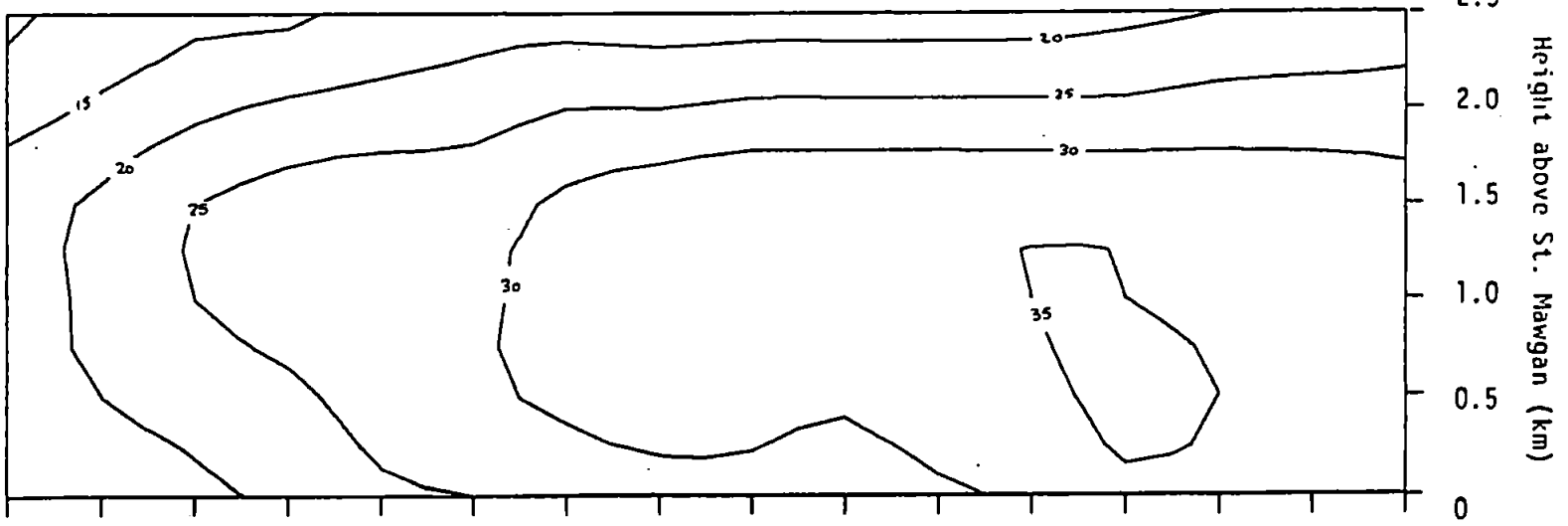

Totals:

R_G : 1.1 mm

R_D : 1.62 mm

R_Z : 1.42 mm

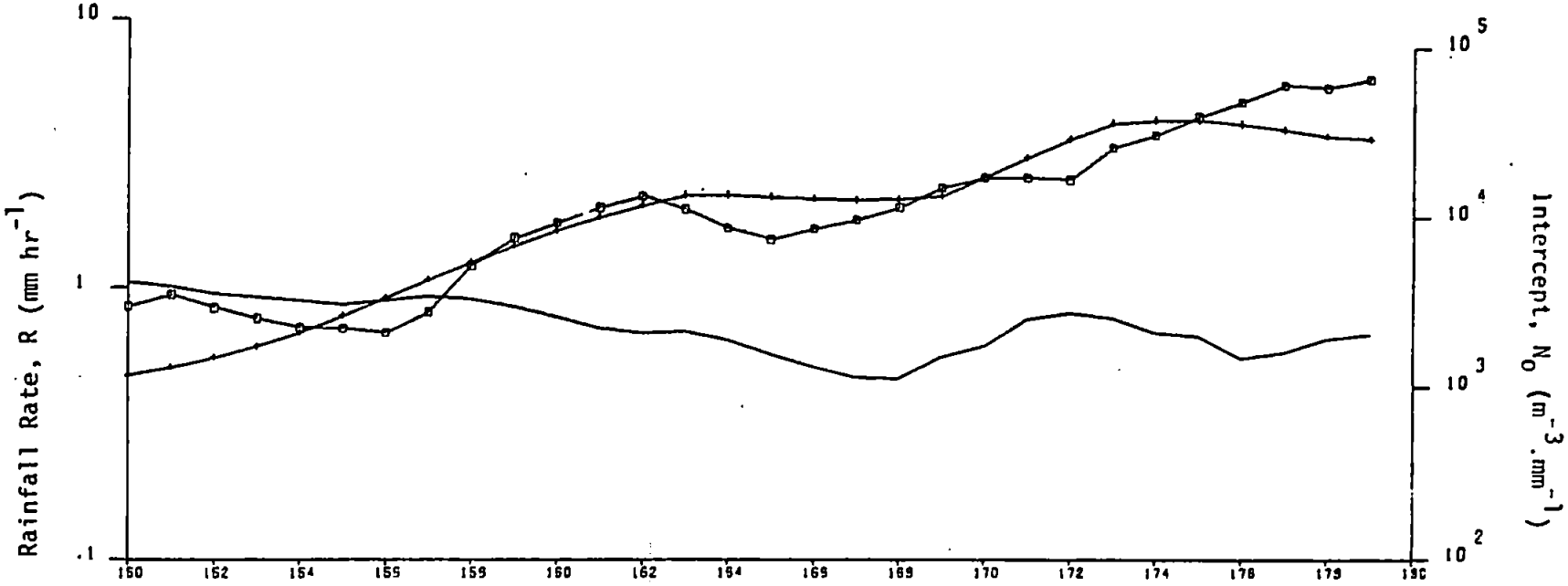

A 69

Radar Reflectivity

Contours (dBz)

(31) 550180 - 209

1900-29 : 22.5.79

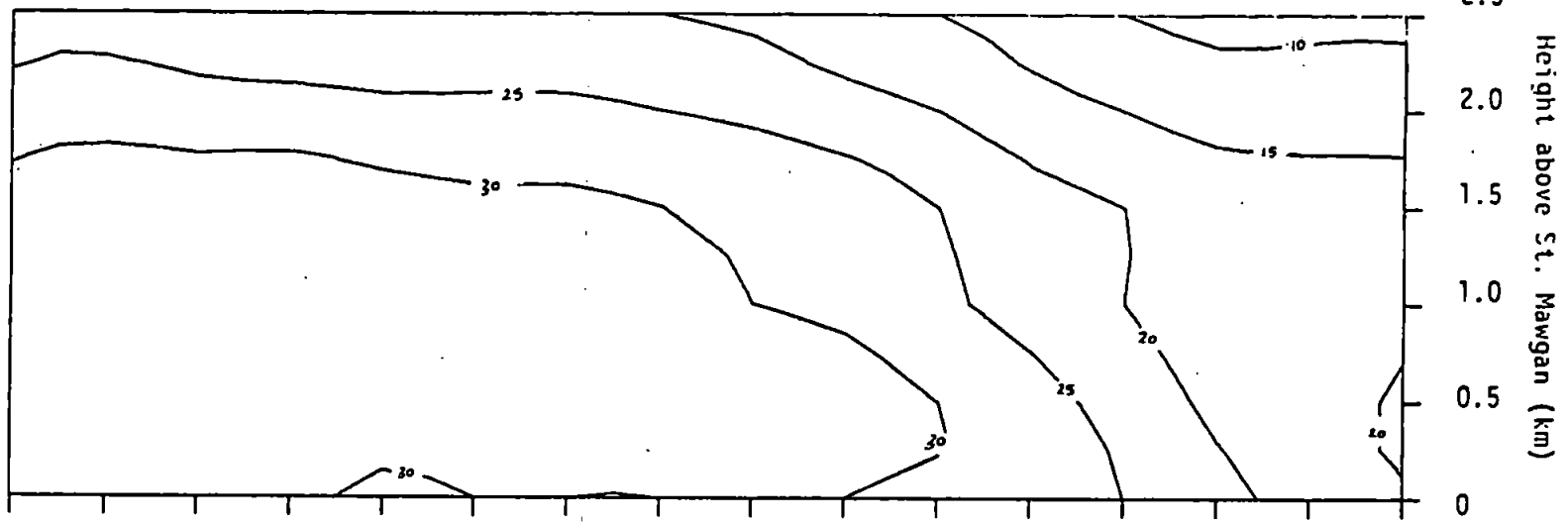

Totals:

R_G : 3.2 mm

R_D : 2.59 mm

R_Z : 1.31 mm

A 70

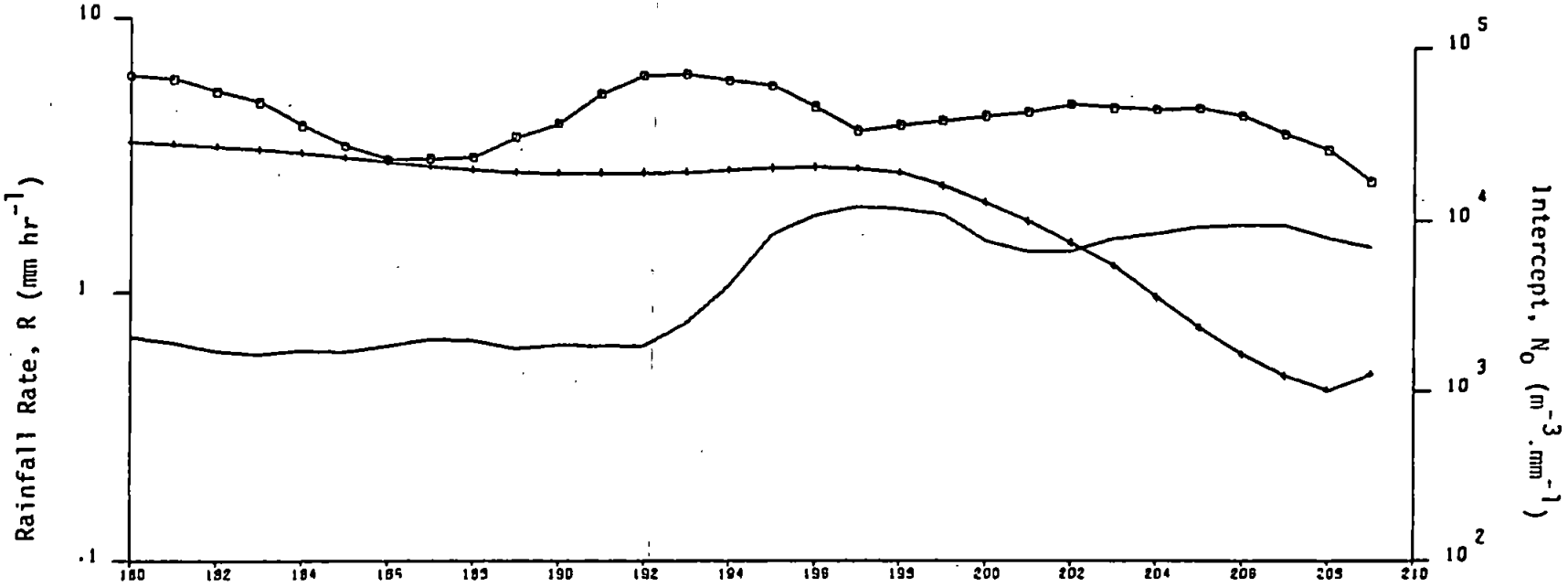

Radar Reflectivity

Contours (dBz)

(32) 550210 - 239

1930-59 : 22.5.79

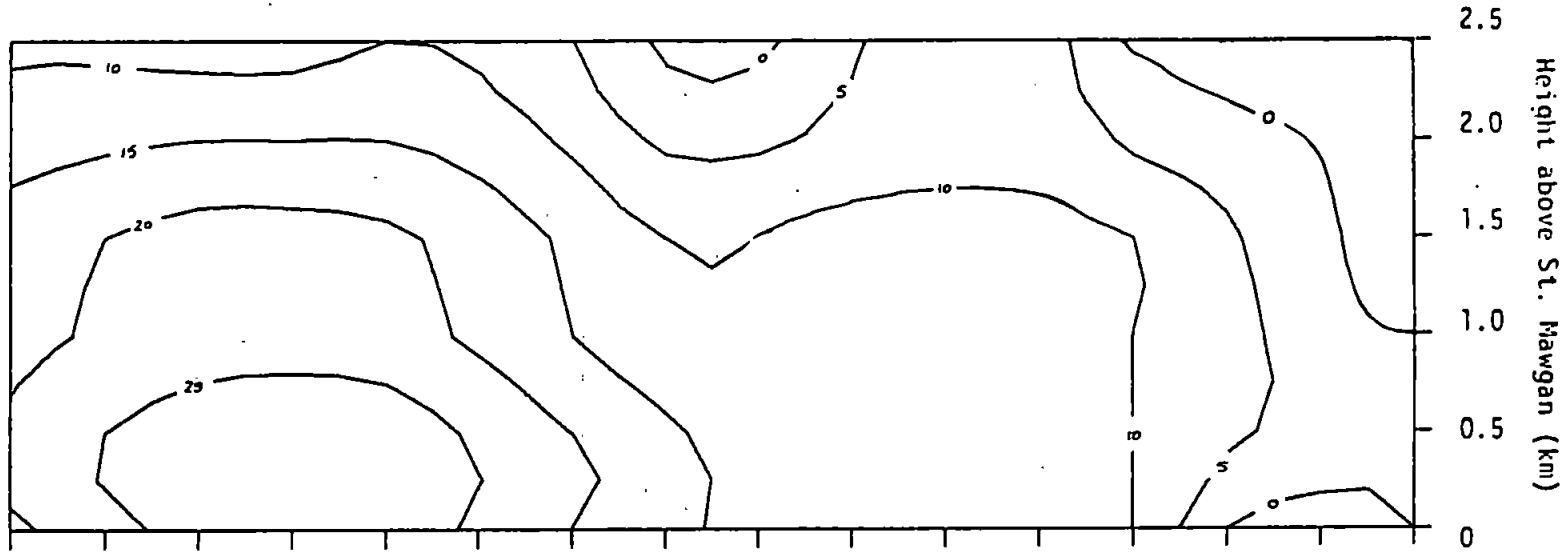

Totals:

R_G : 0.6 mm

R_D : 0.42 mm

R_Z : 0.36 mm

A 71

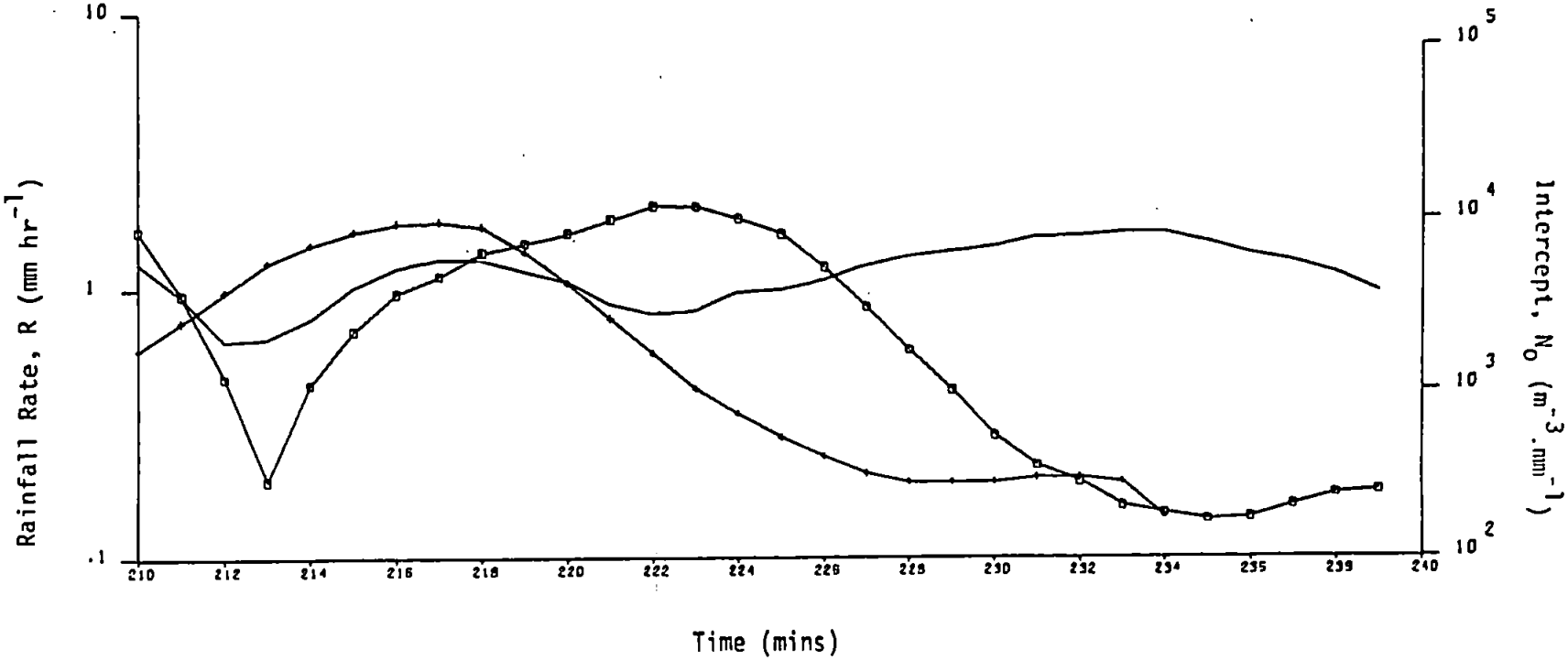

(1)
1200-29
27.3.79

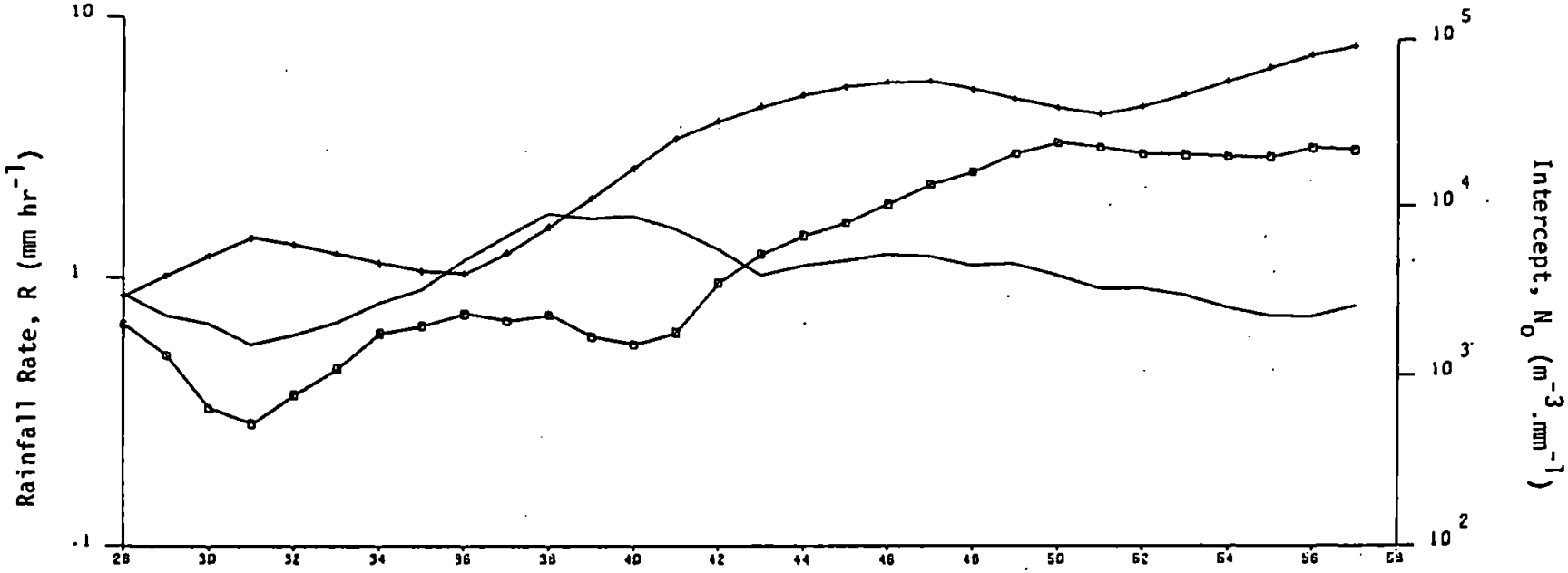

Totals:

R_G : 1.6 mm

R_D : 1.00 mm

R_Z : 2.14 mm

R_{ZN}: 1.71 mm

A 72

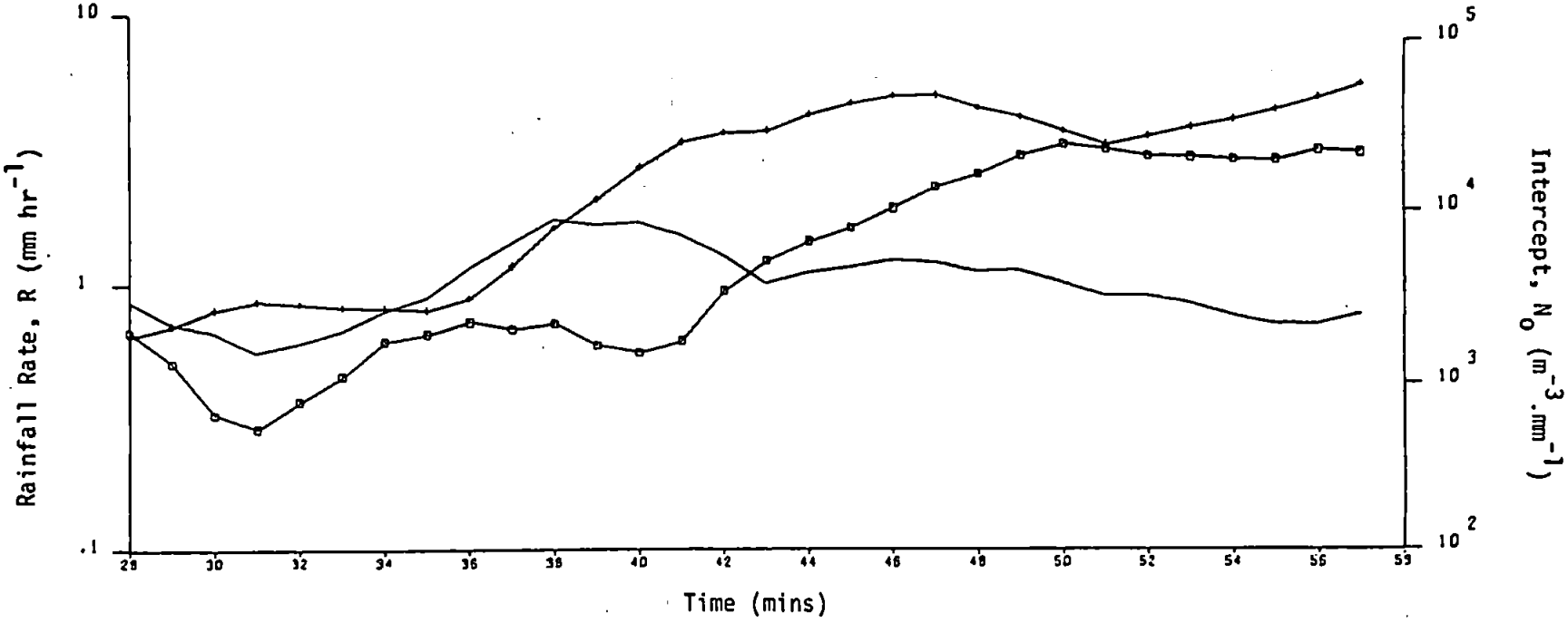

(2)
1230-59
27.3.79

Totals:

R_G : 0.8 mm

R_D : 0.77 mm

R_Z : 1.22 mm

R_{ZN}: 0.97 mm

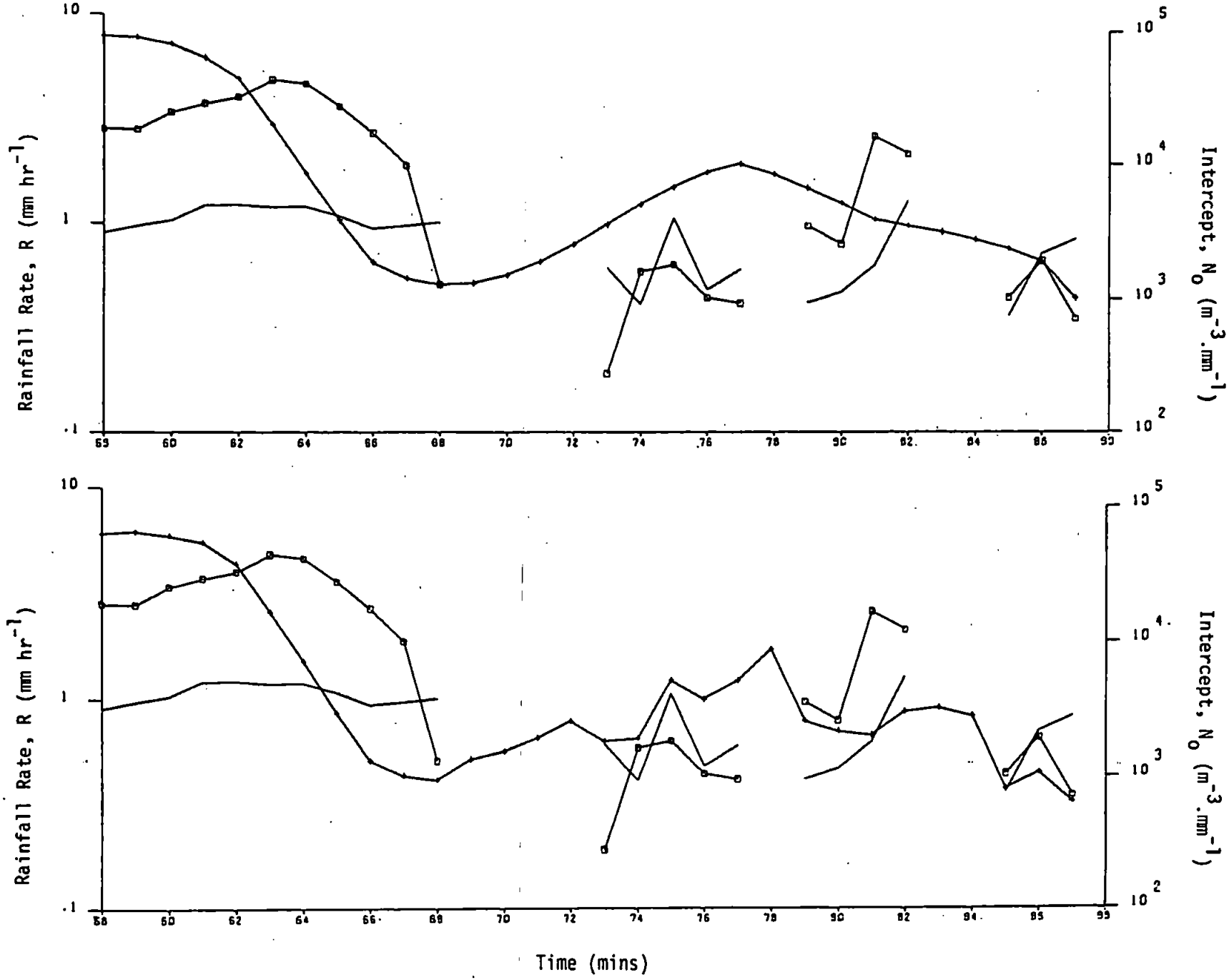

(3)
1300-29
27.3.79

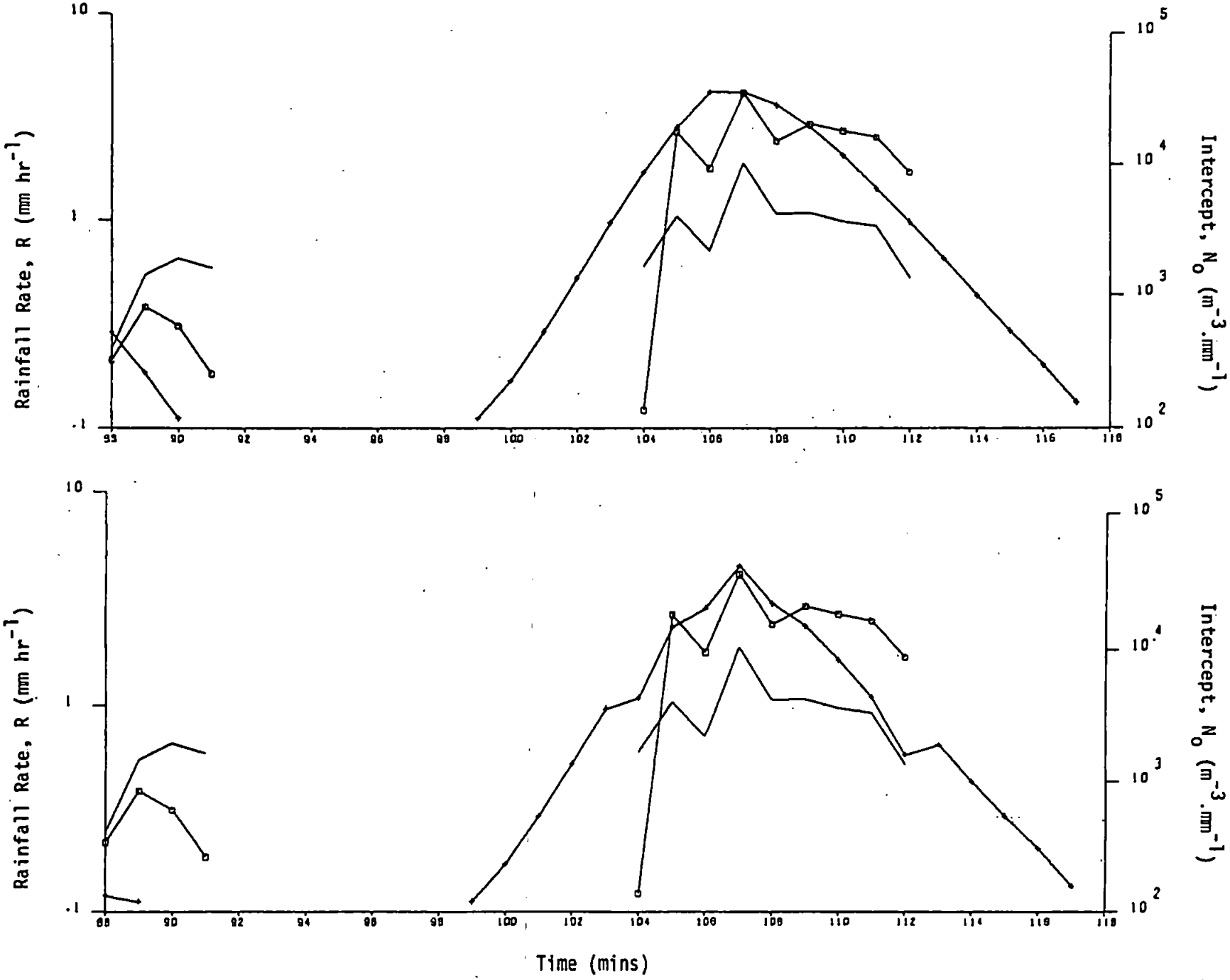

Totals:

R_G : 0.5 mm

R_D : 0.35 mm

R_Z : 0.55 mm

R_{ZN}: 0.46 mm

A 74

(4)
1330-59
27.3.79

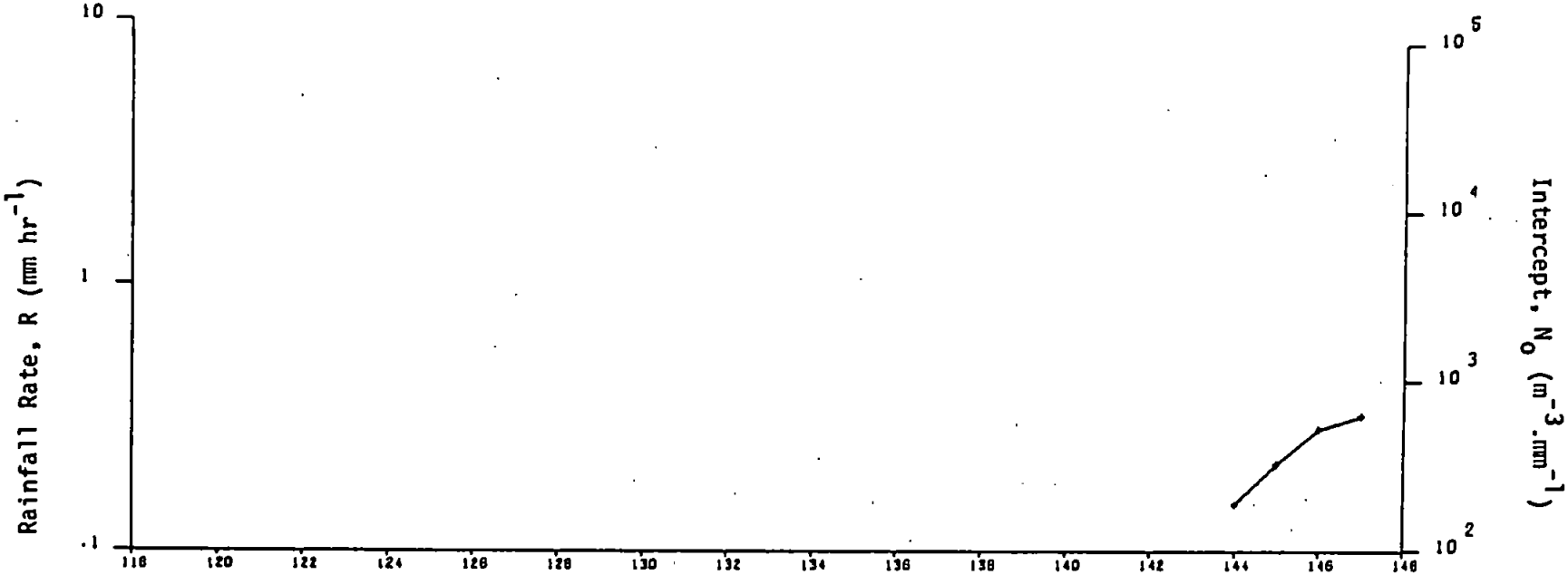

Totals:

R_G : 0 mm

R_D : 0.01 mm

R_Z : 0.02 mm

R_{ZN}: 0.02 mm

A 75

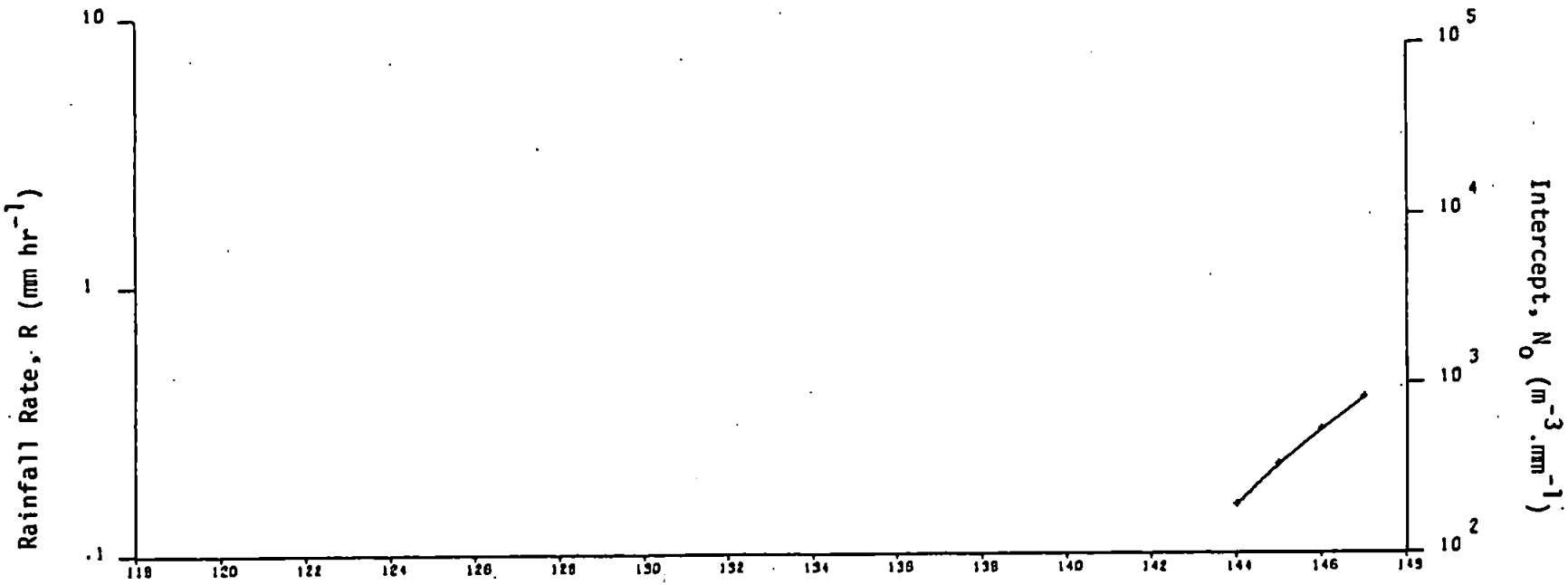

(5)
1400-29
27.3.79

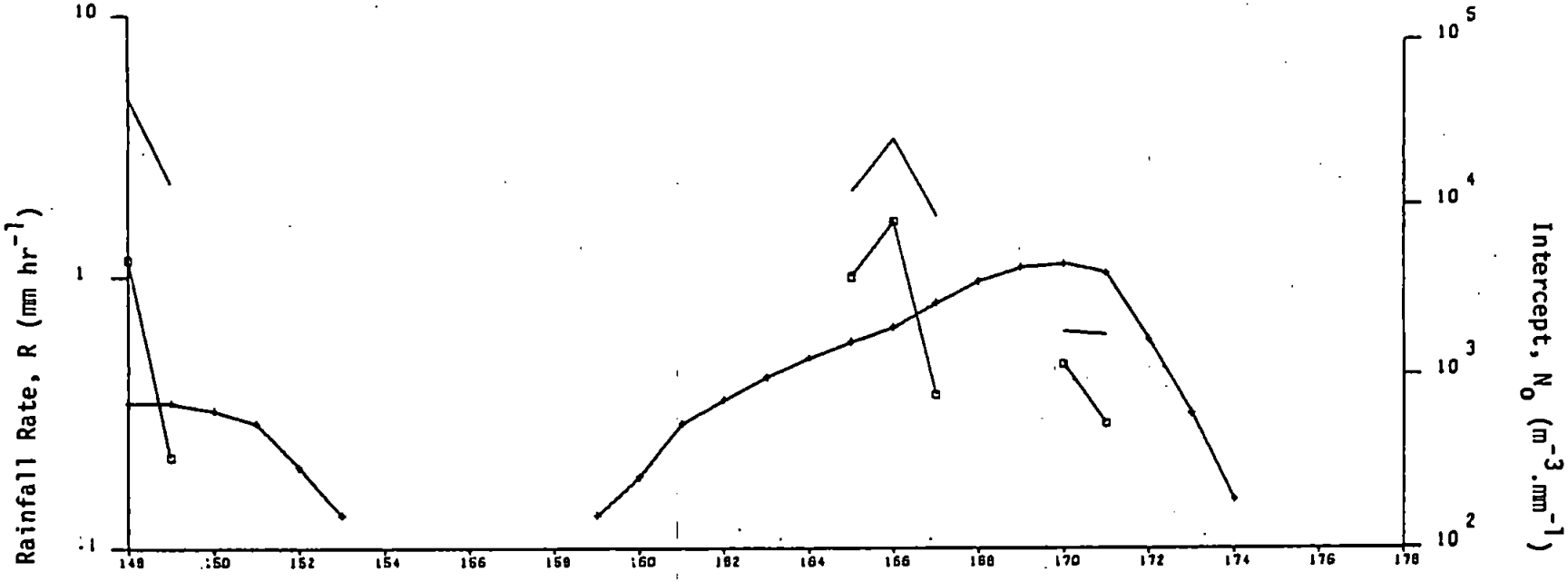

Totals:

R_G : 0 mm

R_D : 0.10 mm

R_Z : 0.20 mm

R_{ZN}: 0.18 mm

A 76

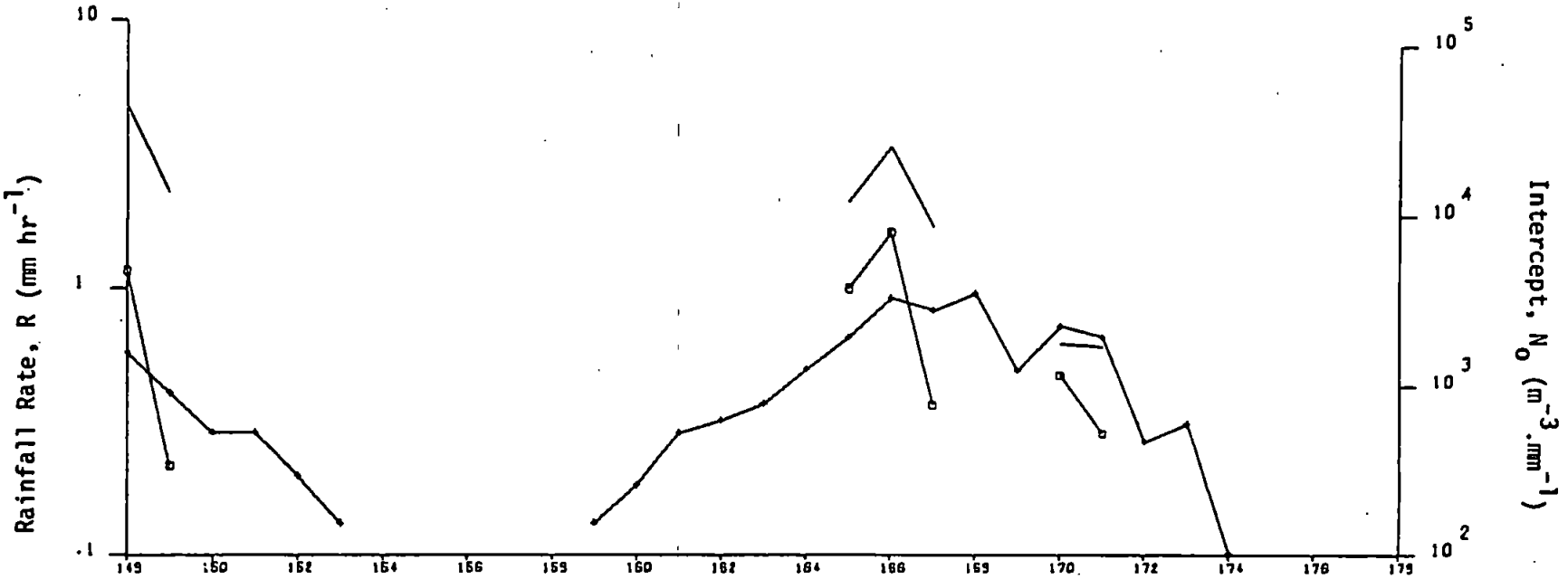

6
1430-59
27.3.79

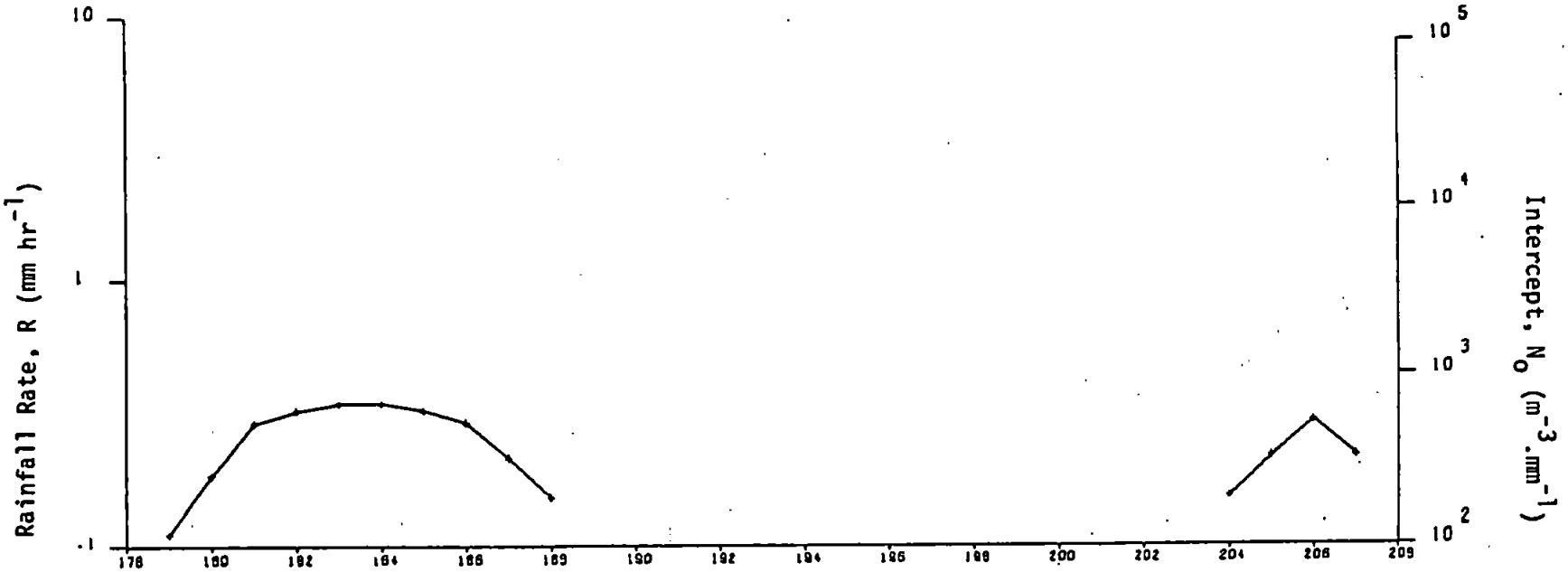

Totals:

R_G : 0 mm

R_D : 0 mm

R_Z : 0.06 mm

R_{ZN}: 0.06 mm

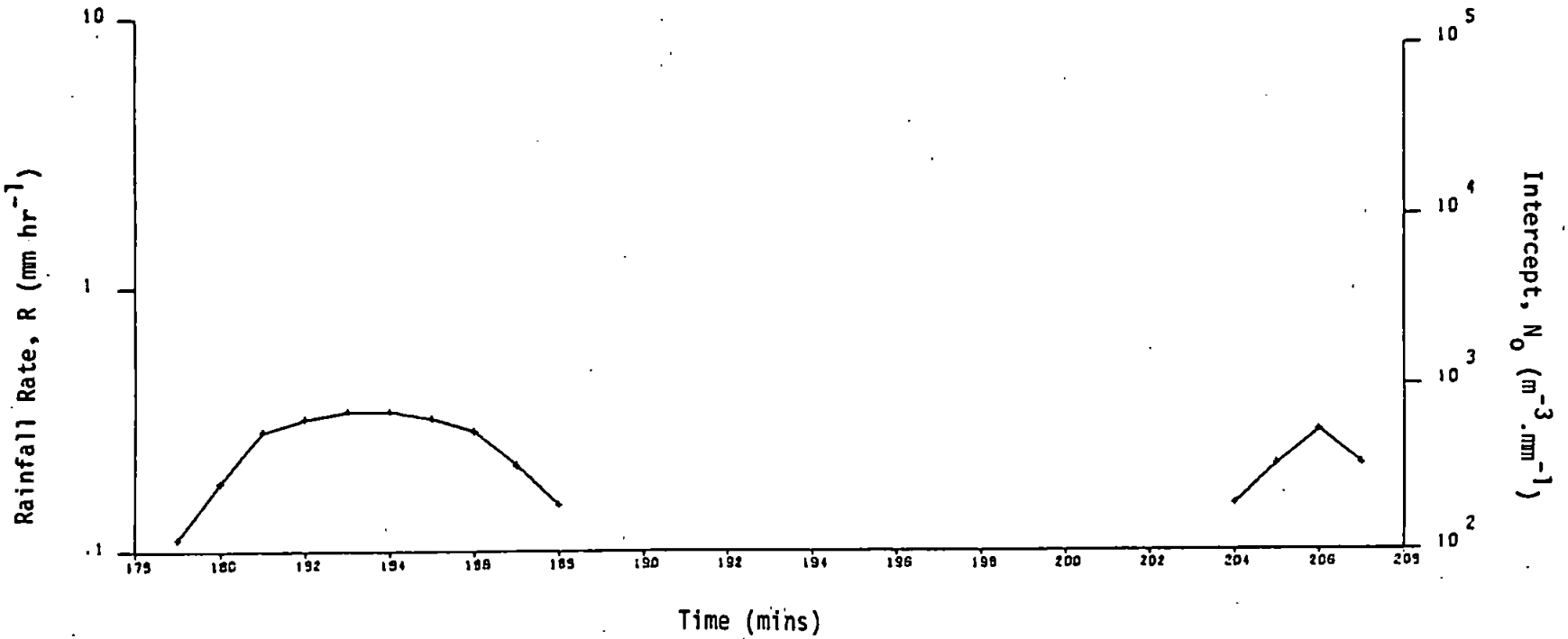

A 77

7

1500-29

27.3.79

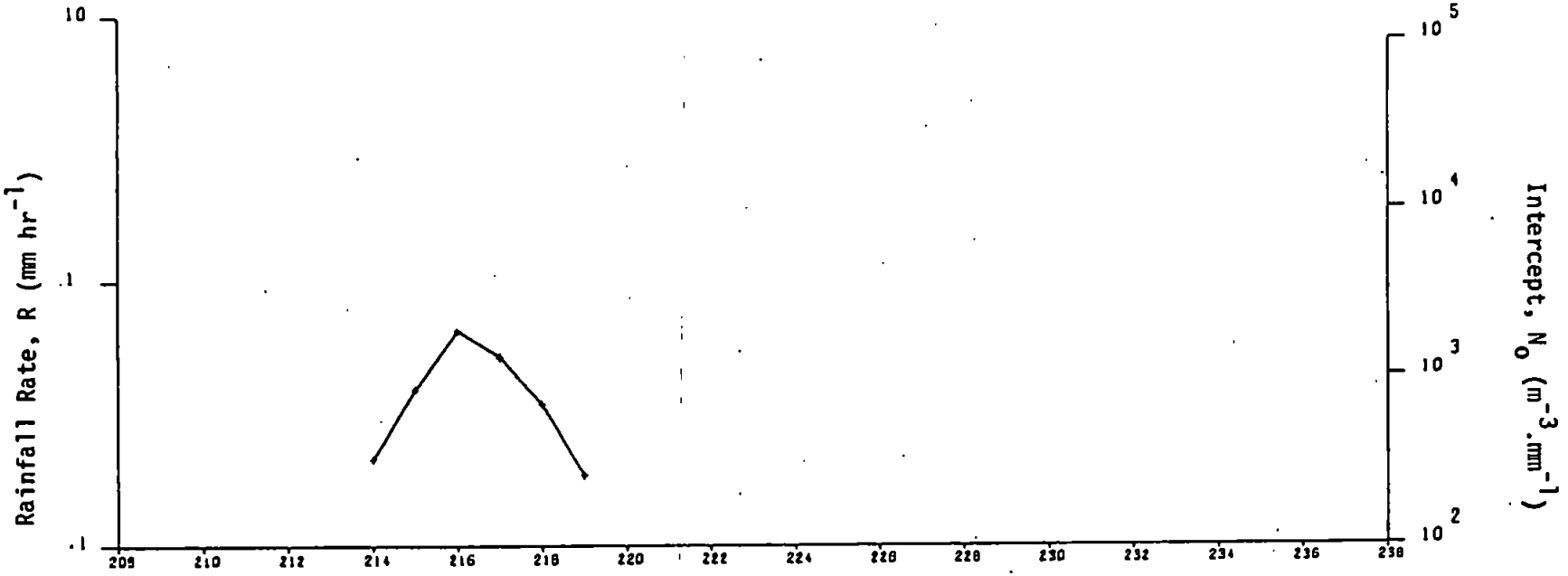

Totals:

R_G : 0 mm

R_D : 0 mm

R_Z : 0.05 mm

R_{ZN}: 0.05 mm

A 78

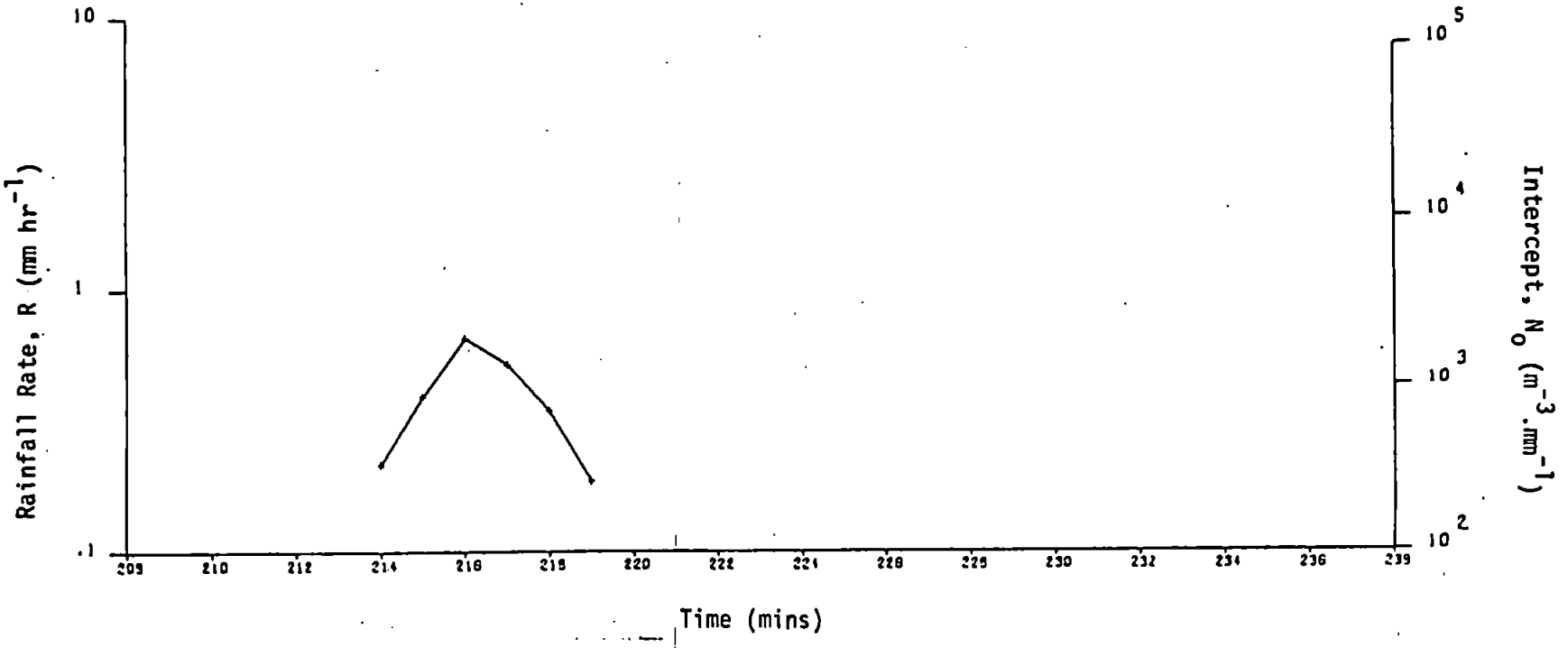

(8)
1530-59
27.3.79

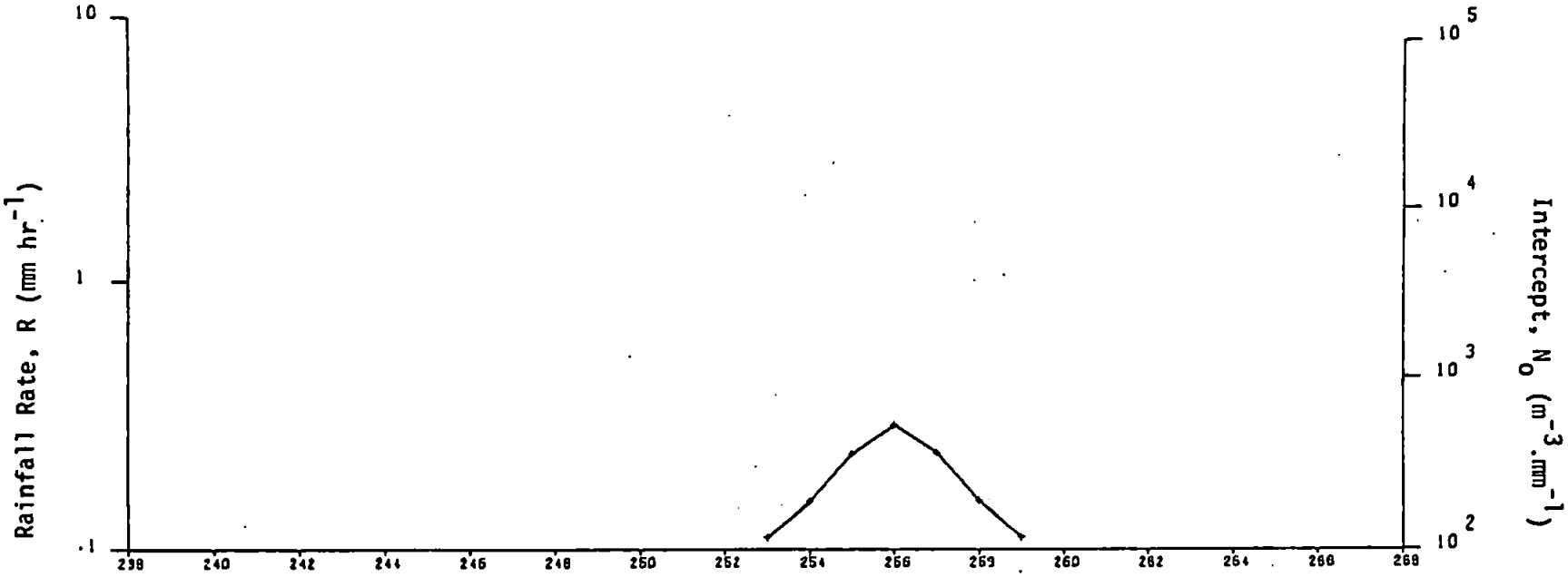

Totals:

R_G : 0 mm

R_D : 0 mm

R_Z : 0.02 mm

R_{ZN}: 0.02 mm

A 79

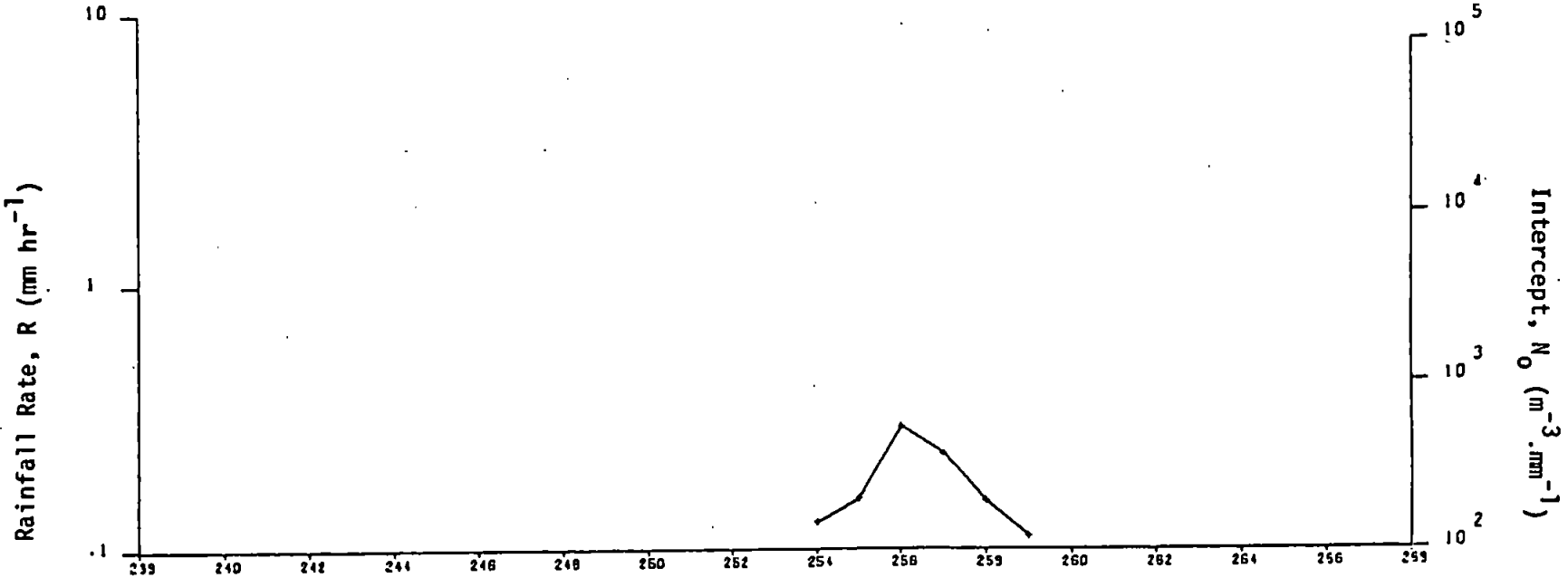

Time (mins)

(9)
1600-29
27.3.79

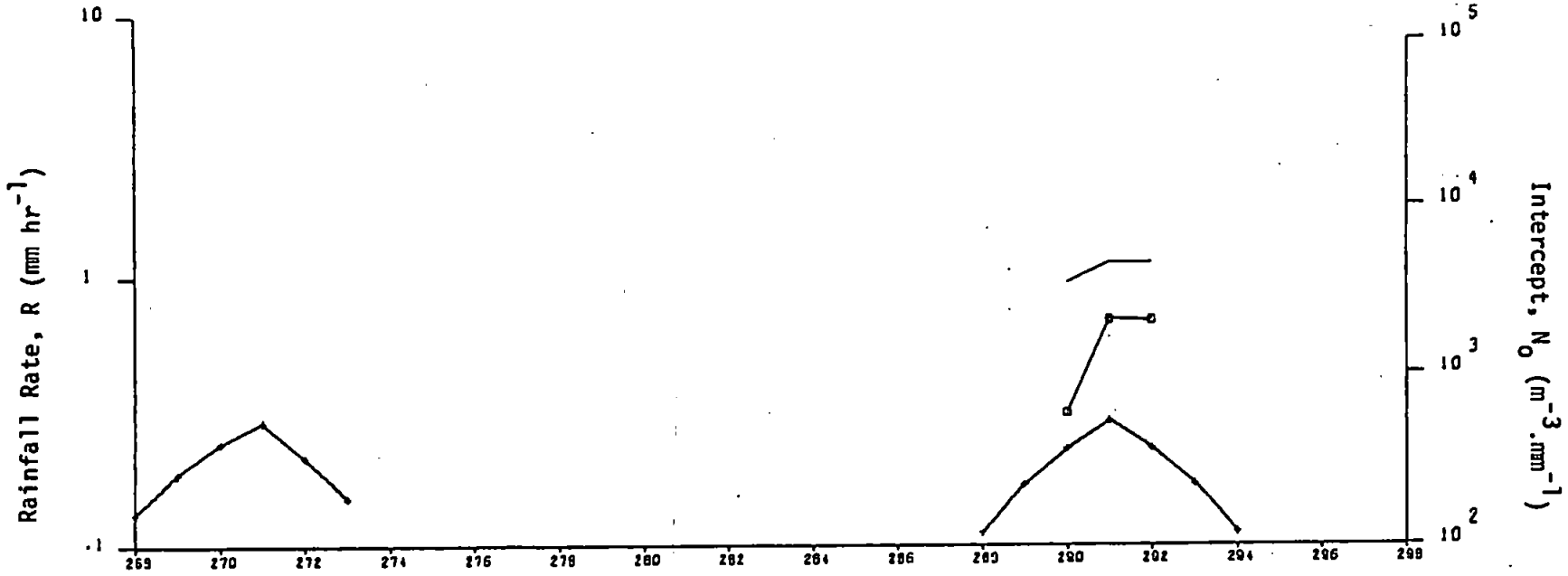

Totals:

R_G : 0.1 mm

R_D : 0.07 mm

R_Z : 0.04 mm

R_{ZN}: 0.04 mm

A 80

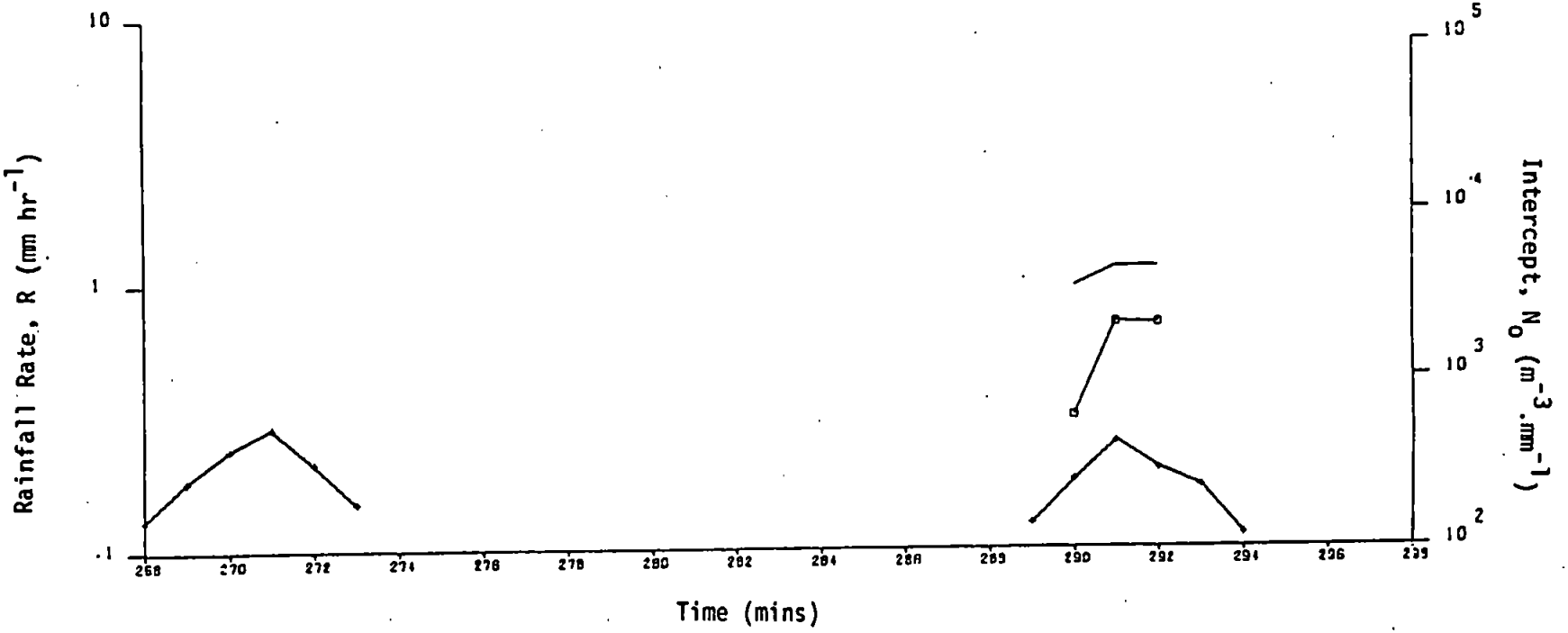

(10)
1630-59
27.3.79

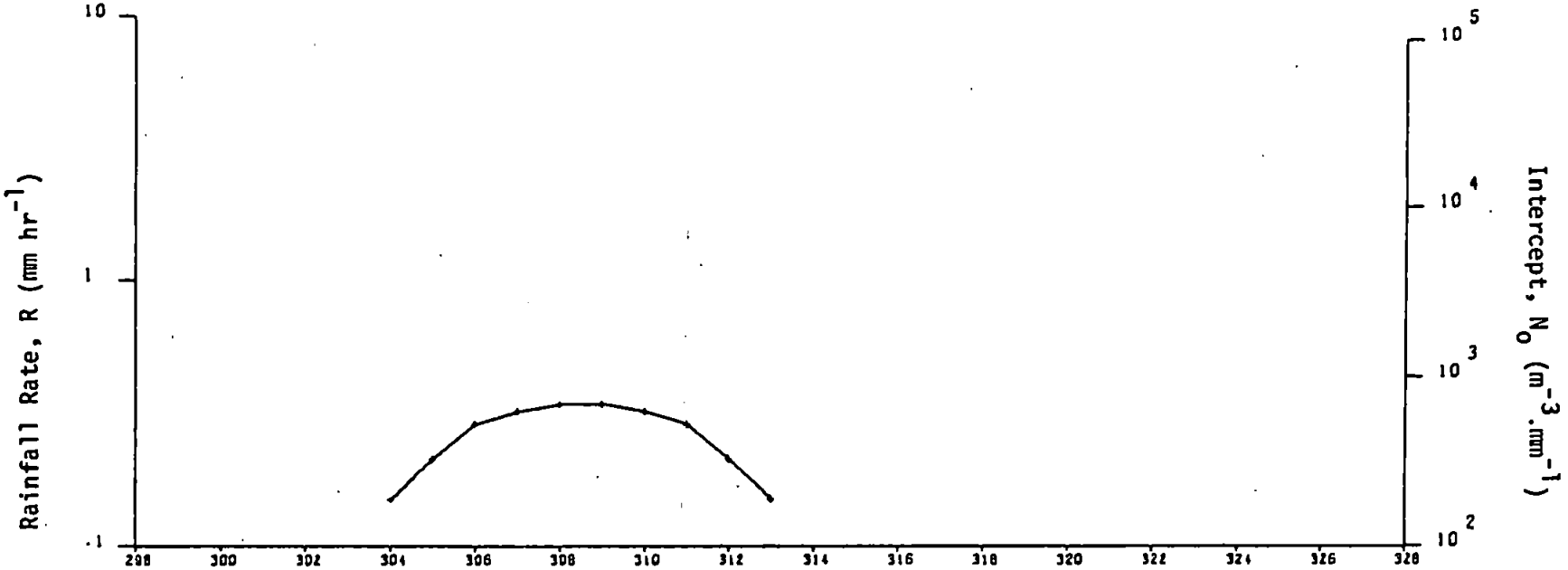

Totals:

R_G : 0 mm

R_D : 0 mm

R_Z : 0.05 mm

R_{ZN}: 0.05 mm

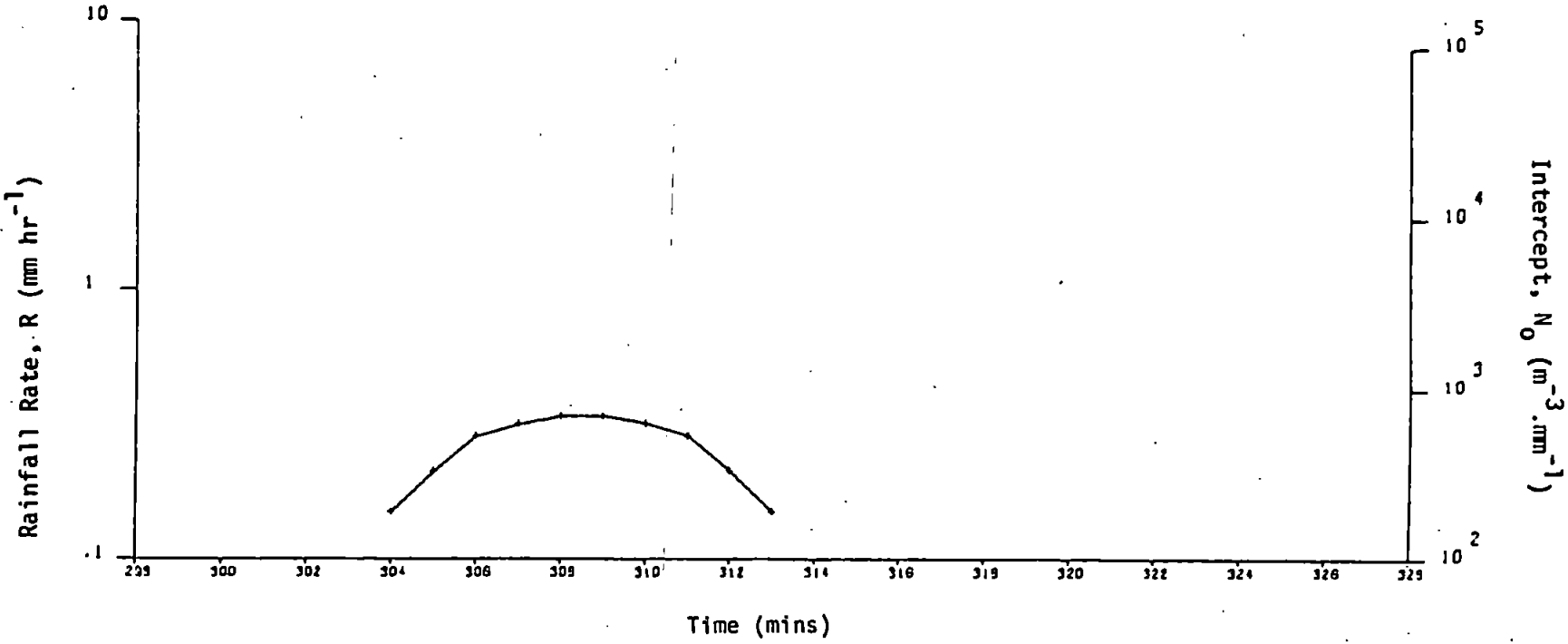

A 81

(12)
1730-59
27.3.79

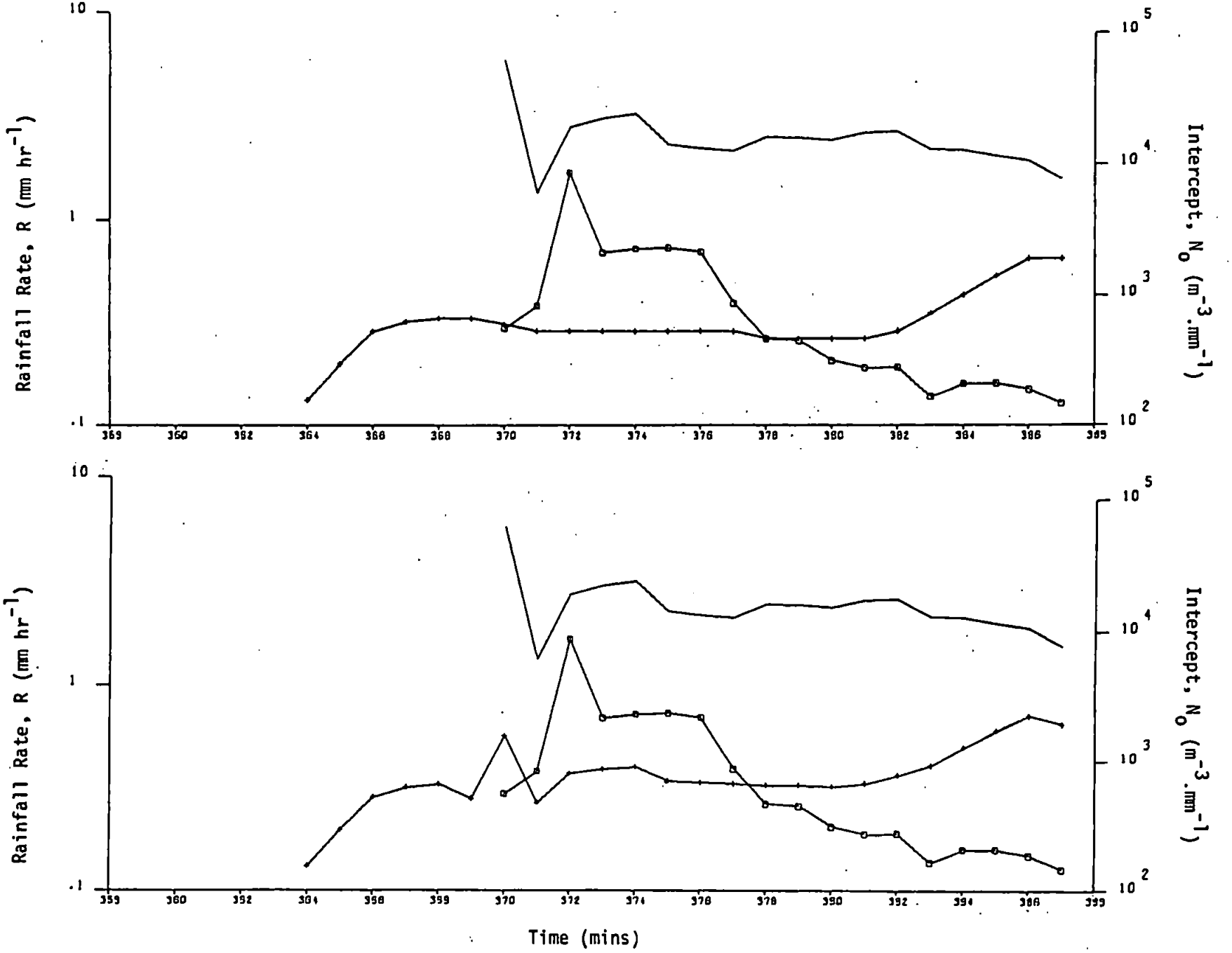

Totals:

R_G : 0.1 mm

R_D : 0.11 mm

R_Z : 0.14 mm

R_{ZN}: 0.16 mm

A 82

(13)
1800-29
27.3.79

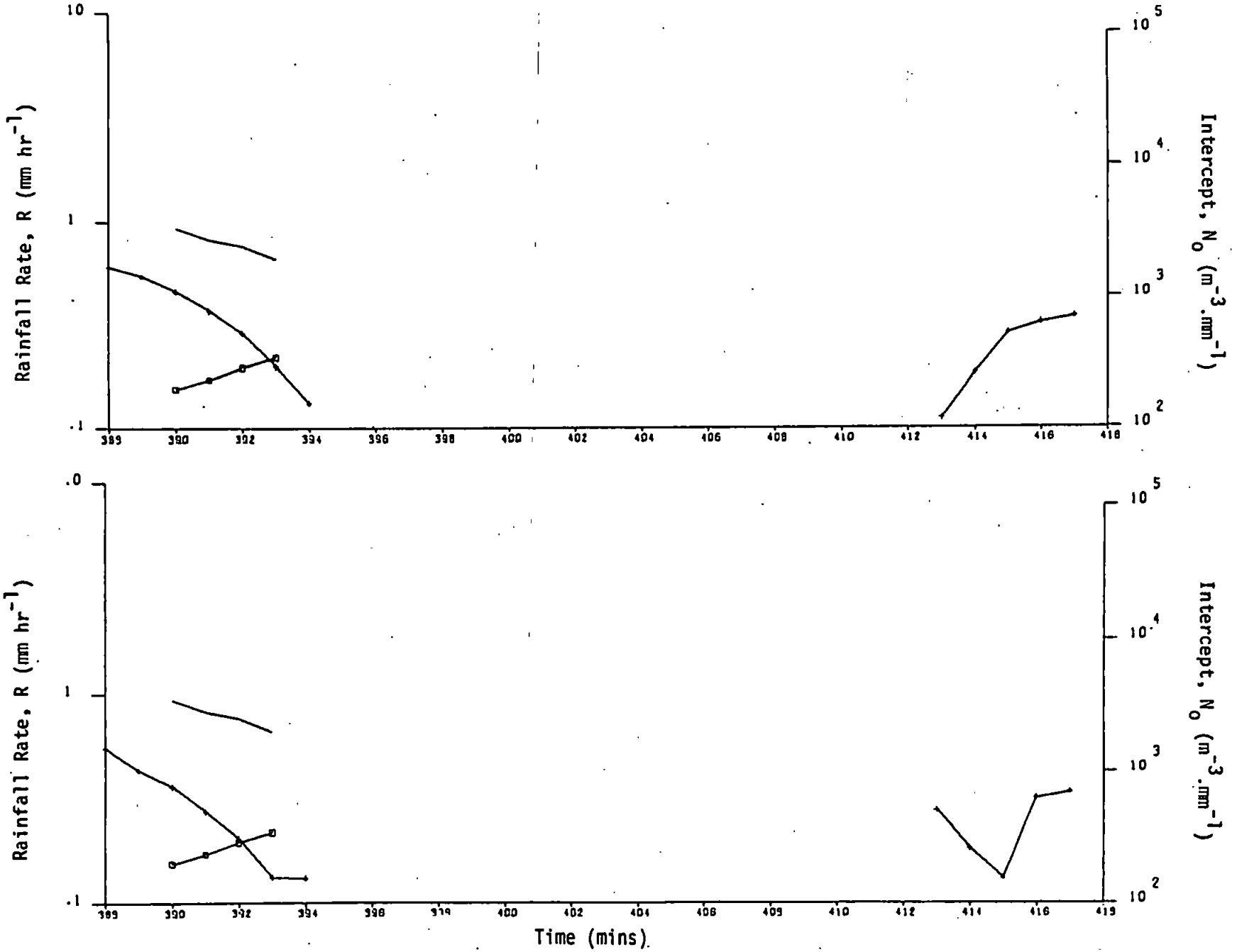

Totals:

R_G : 0.1 mm

R_D : 0.03 mm

R_Z : 0.07 mm

R_{ZN}: 0.06 mm

(14)
1330-59
9.4.79

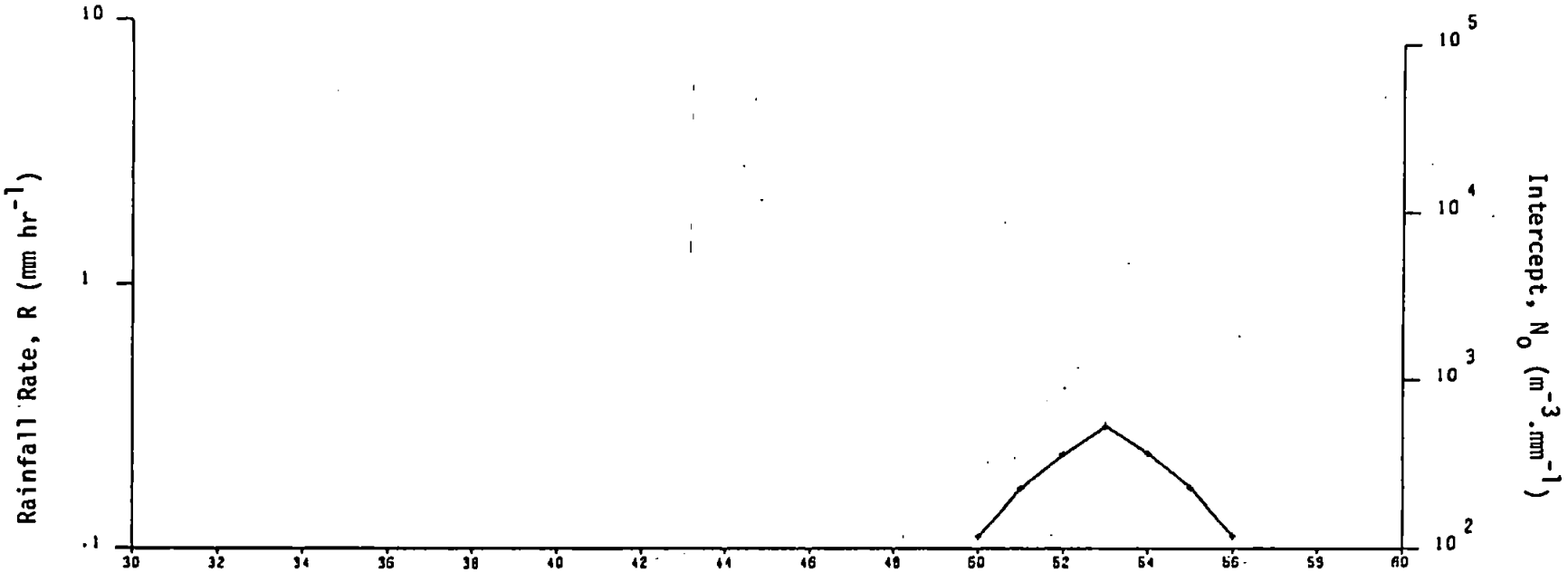

Totals:

R_G : 0 mm

R_D : 0 mm

R_Z : 0.02 mm

R_{ZN}: 0.02 mm

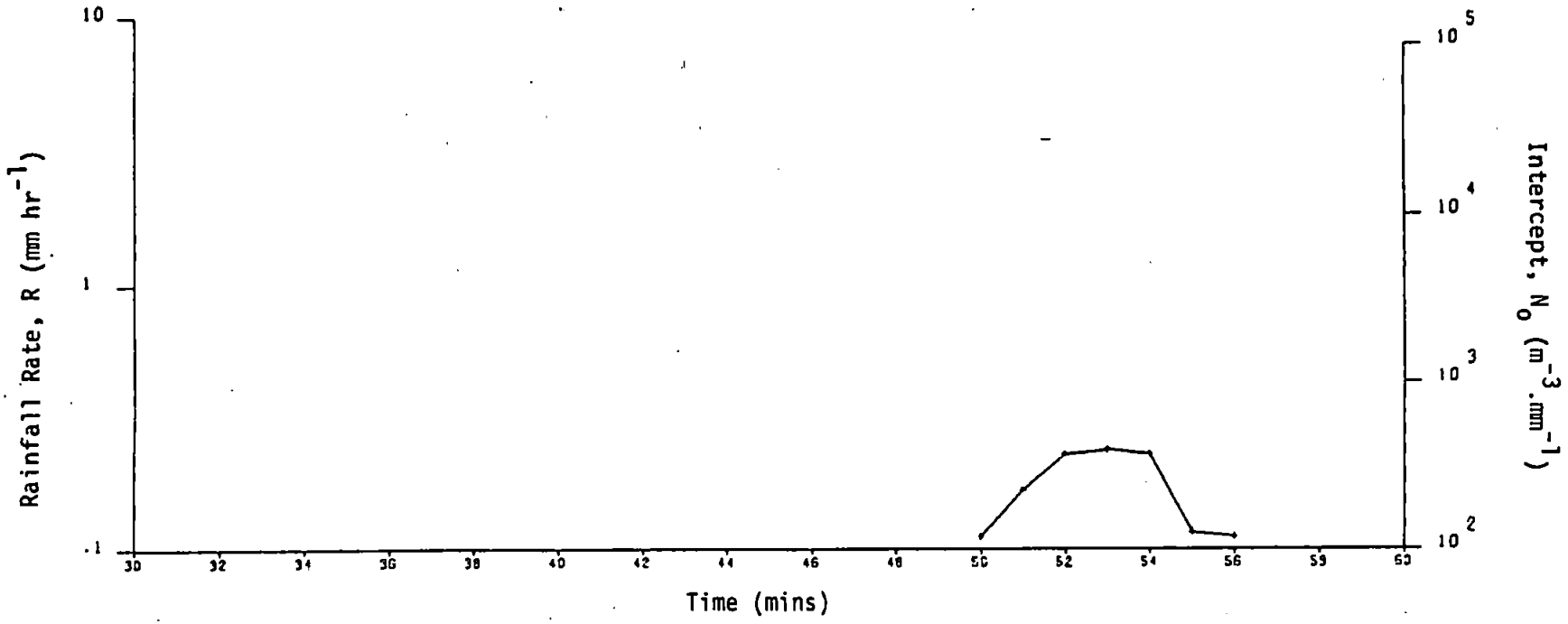

A 84

15
1400-29
9.4.79

Totals:

R_G : 0 mm

R_D : 0.03 mm

R_Z : 0.10 mm

R_{ZN}: 0.08 mm

A 85

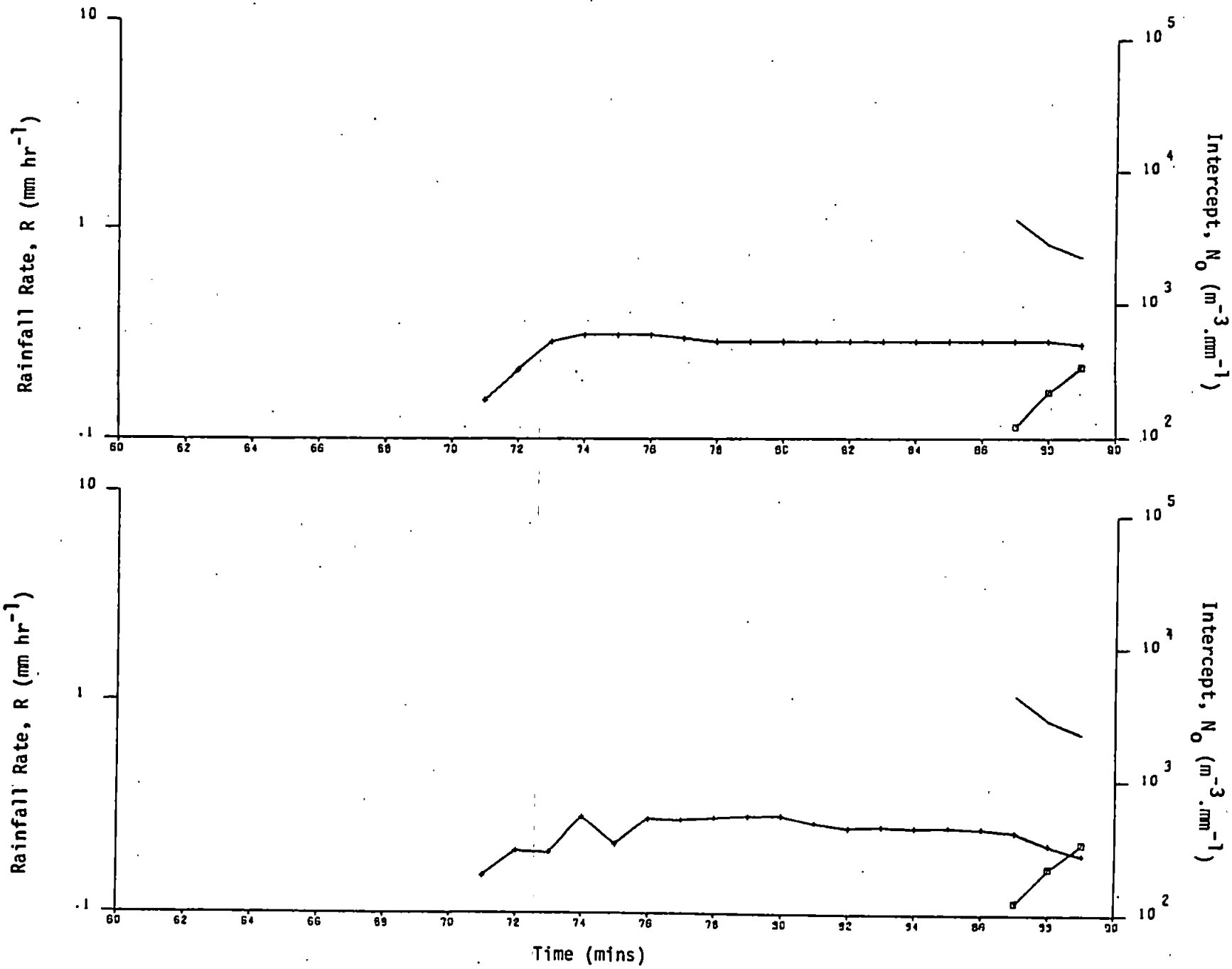

(16)
1430-59
9.4.79

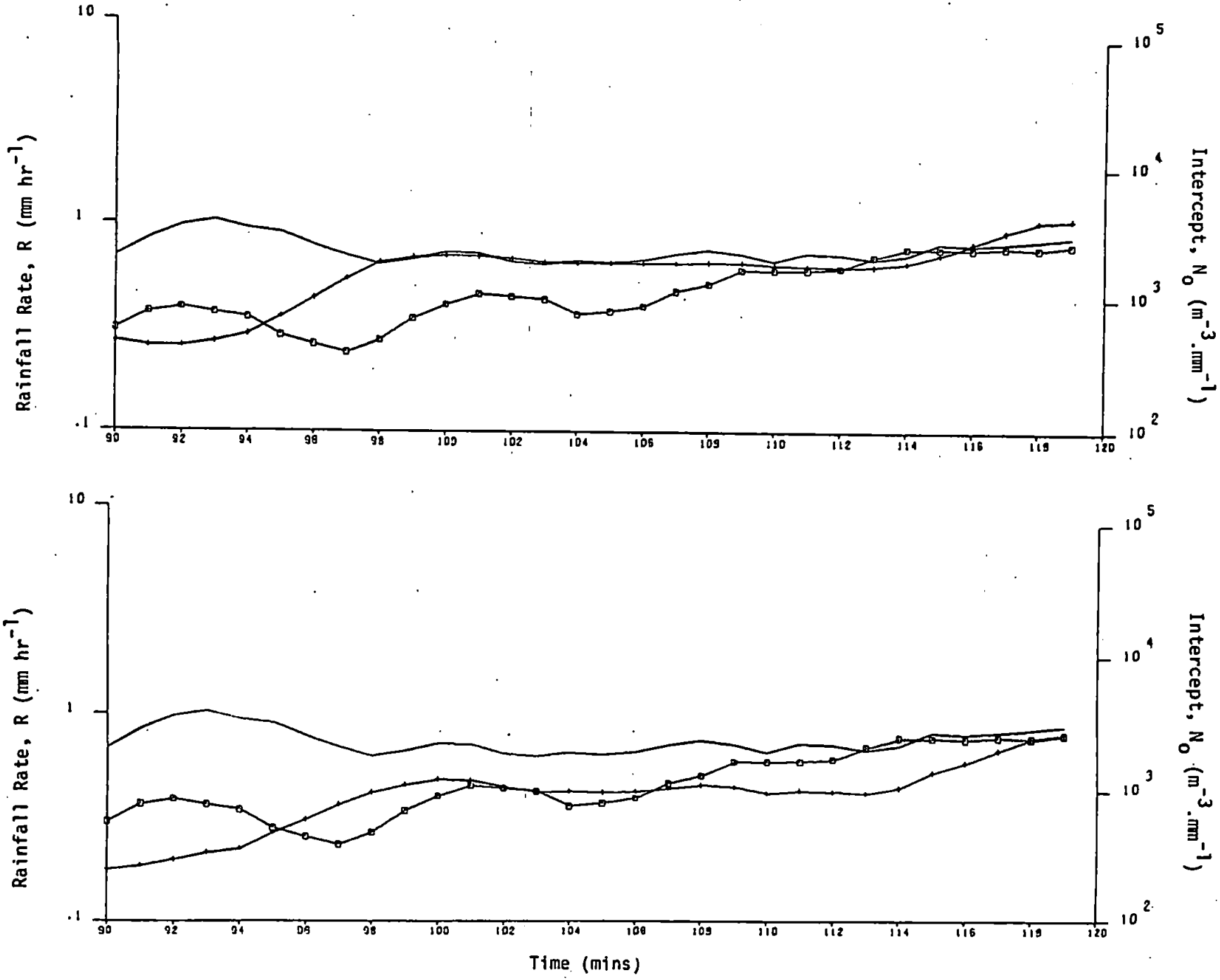

Totals:

R_G : 0.3 mm

R_D : 0.29 mm

R_Z : 0.34 mm

R_{ZN}: 0.23 mm

A 86

(17)
1500-29
9.4.79

Totals:

R_G : 0.7 mm

R_D : 0.71 mm

R_Z : 0.90 mm

R_{ZN}: 0.63 mm

A 87

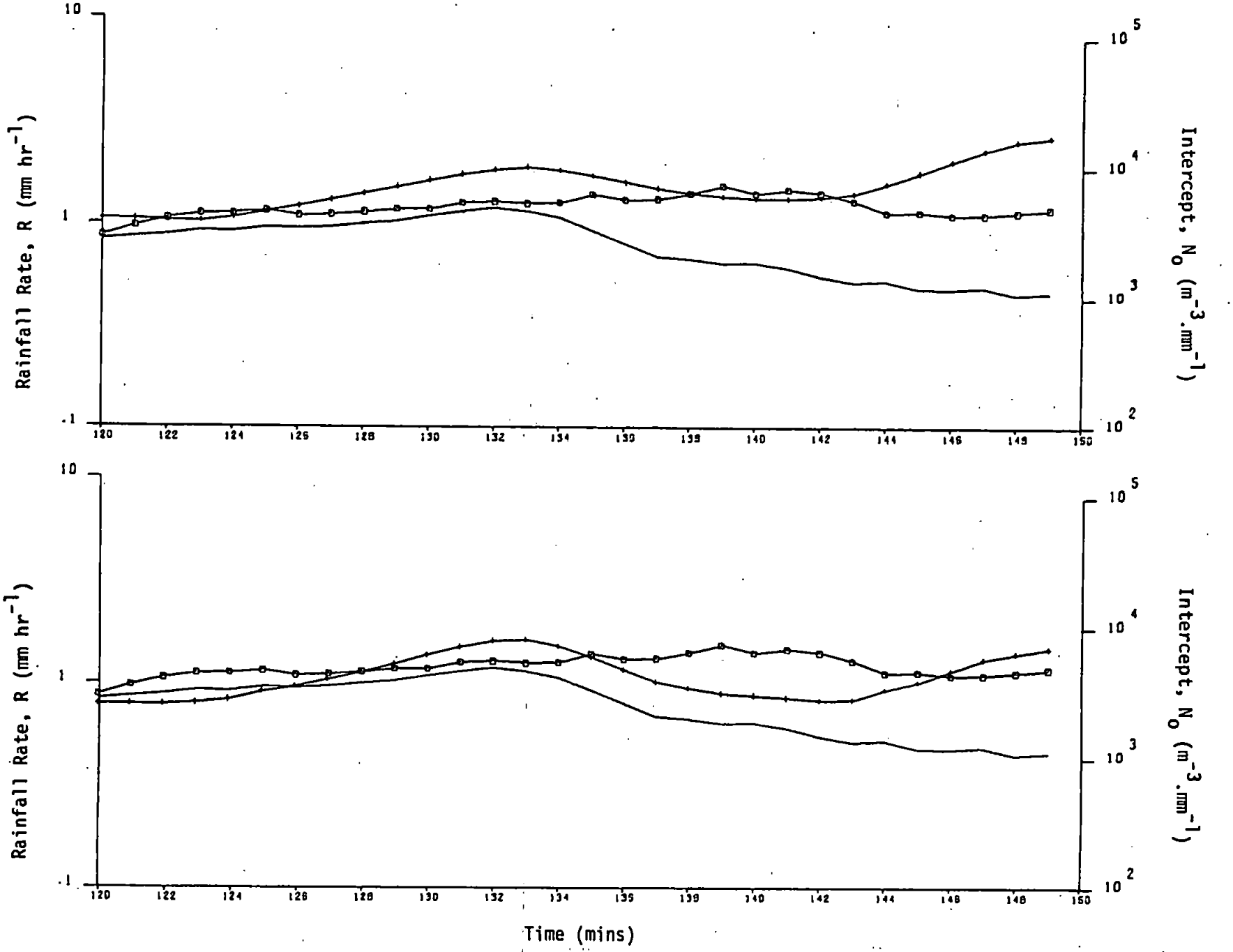

(18)
1530-59
9.4.79

Totals:

R_G : 0.6 mm

R_D : 0.52 mm

R_Z : 0.52 mm

R_{ZN}: 0.31 mm

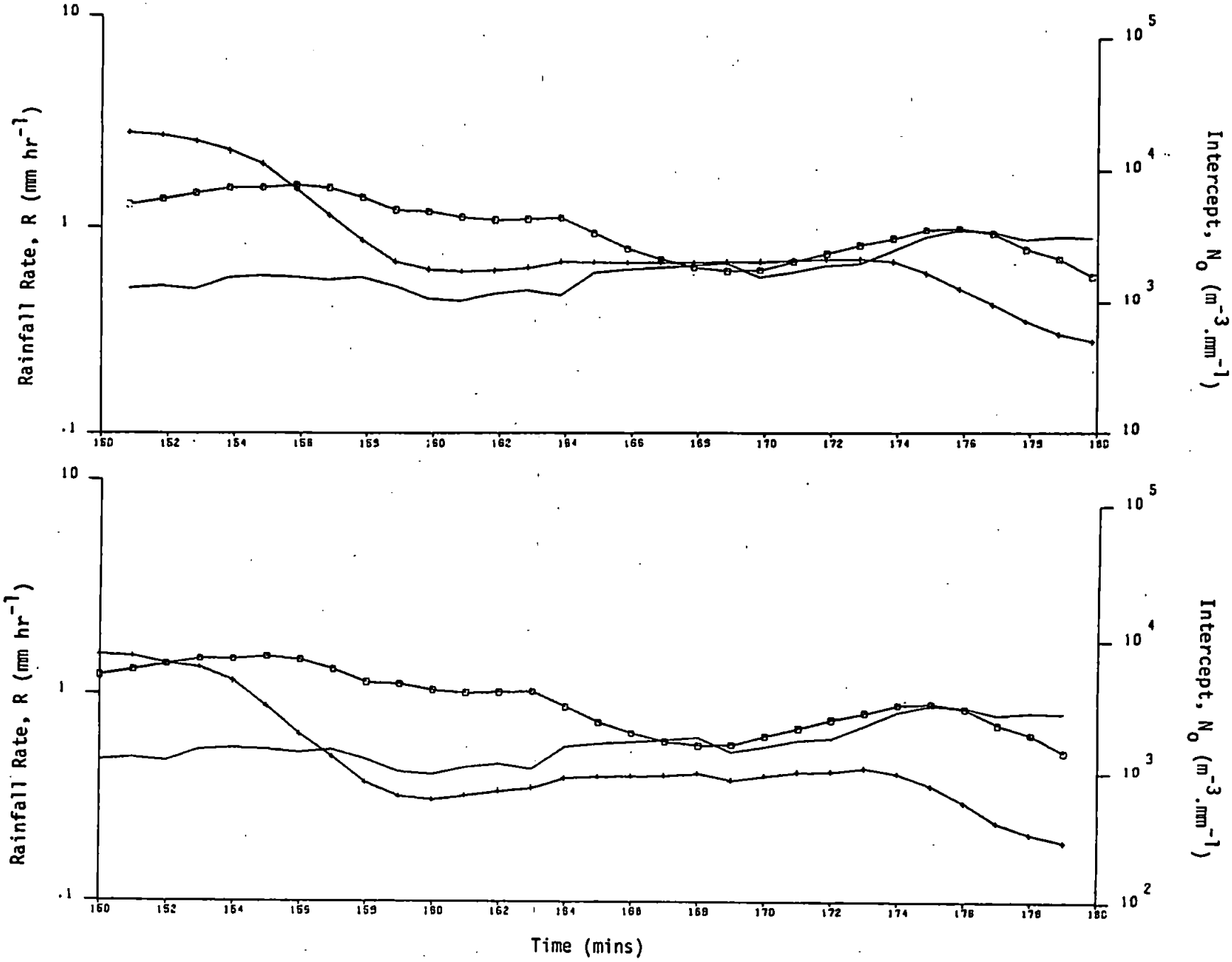

(19)
1600-29
9.4.79

Totals:

R_G : 0.2 mm

R_D : 0.22 mm

R_Z : 0.15 mm

R_{ZN}: 0.16 mm

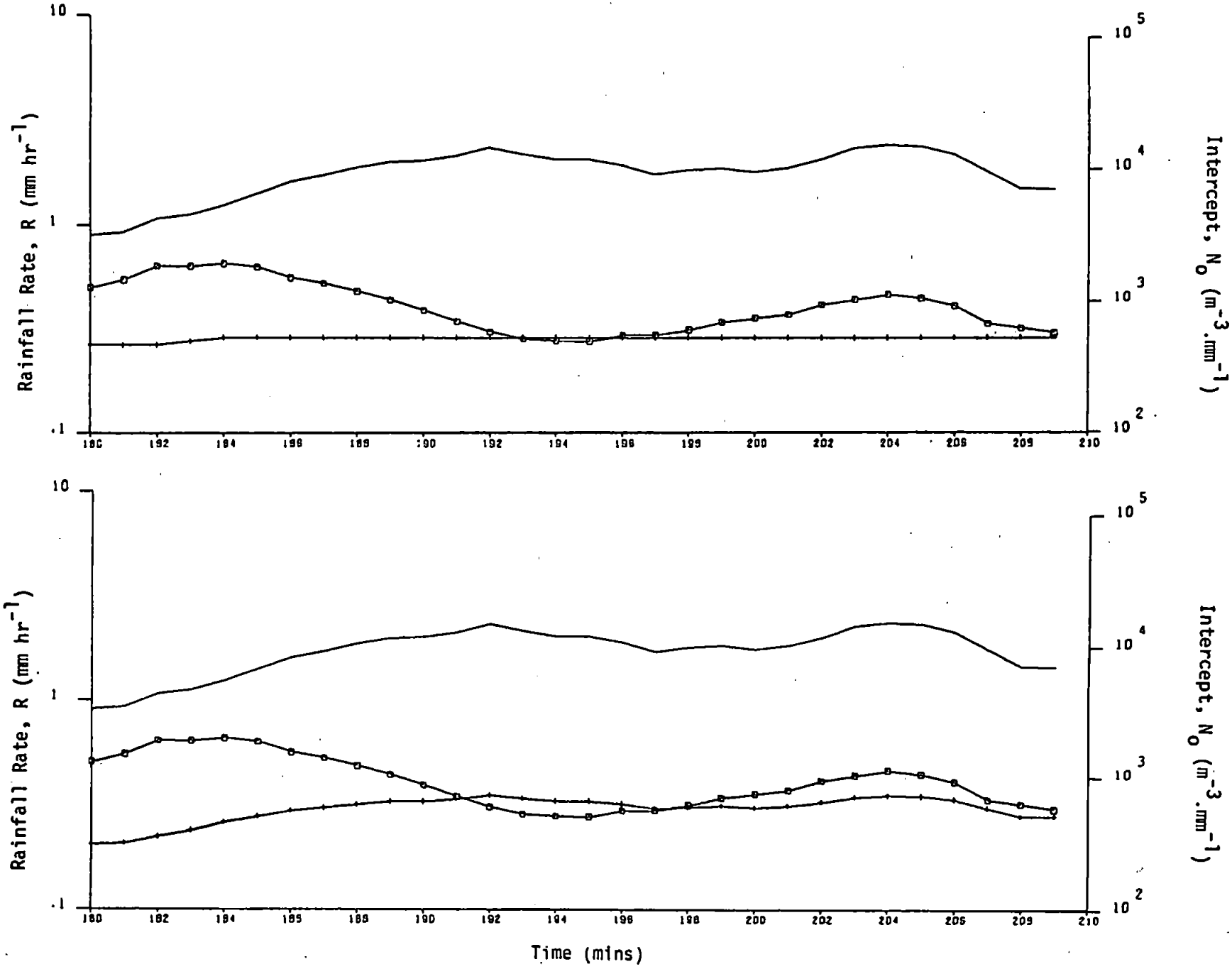

(20)
1630-59
9.4.79

Totals:

R_G : 0.3 mm

R_D : 0.27 mm

R_Z : 0.18 mm

R_{ZN}: 0.20 mm

A 90

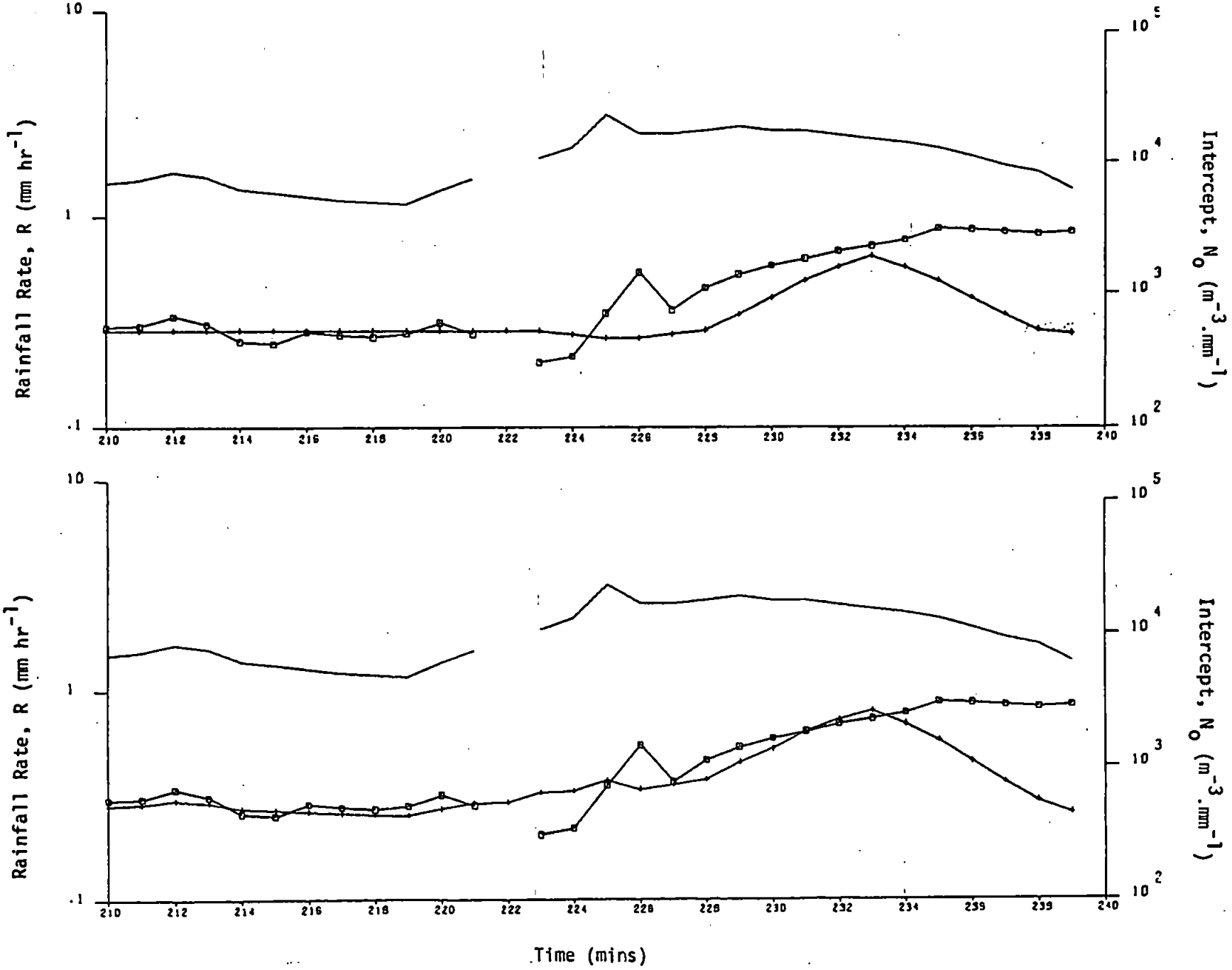

(21)
1700-29
9.4.79

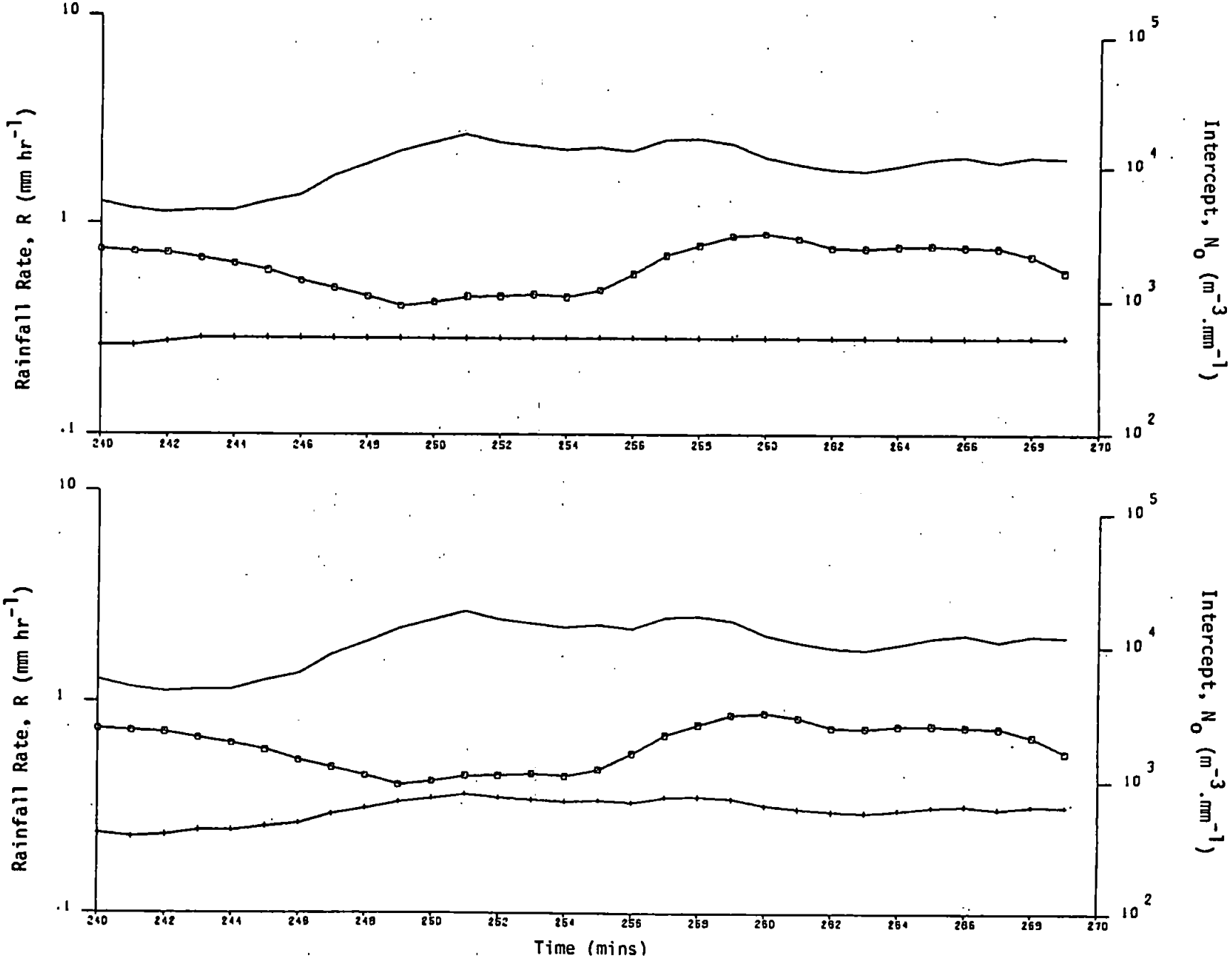

Totals:

R_G : 0.4 mm

R_D : 0.35 mm

R_Z : 0.15 mm

R_{ZN}: 0.17 mm

A 91

(22)
1730-59
9.4.79

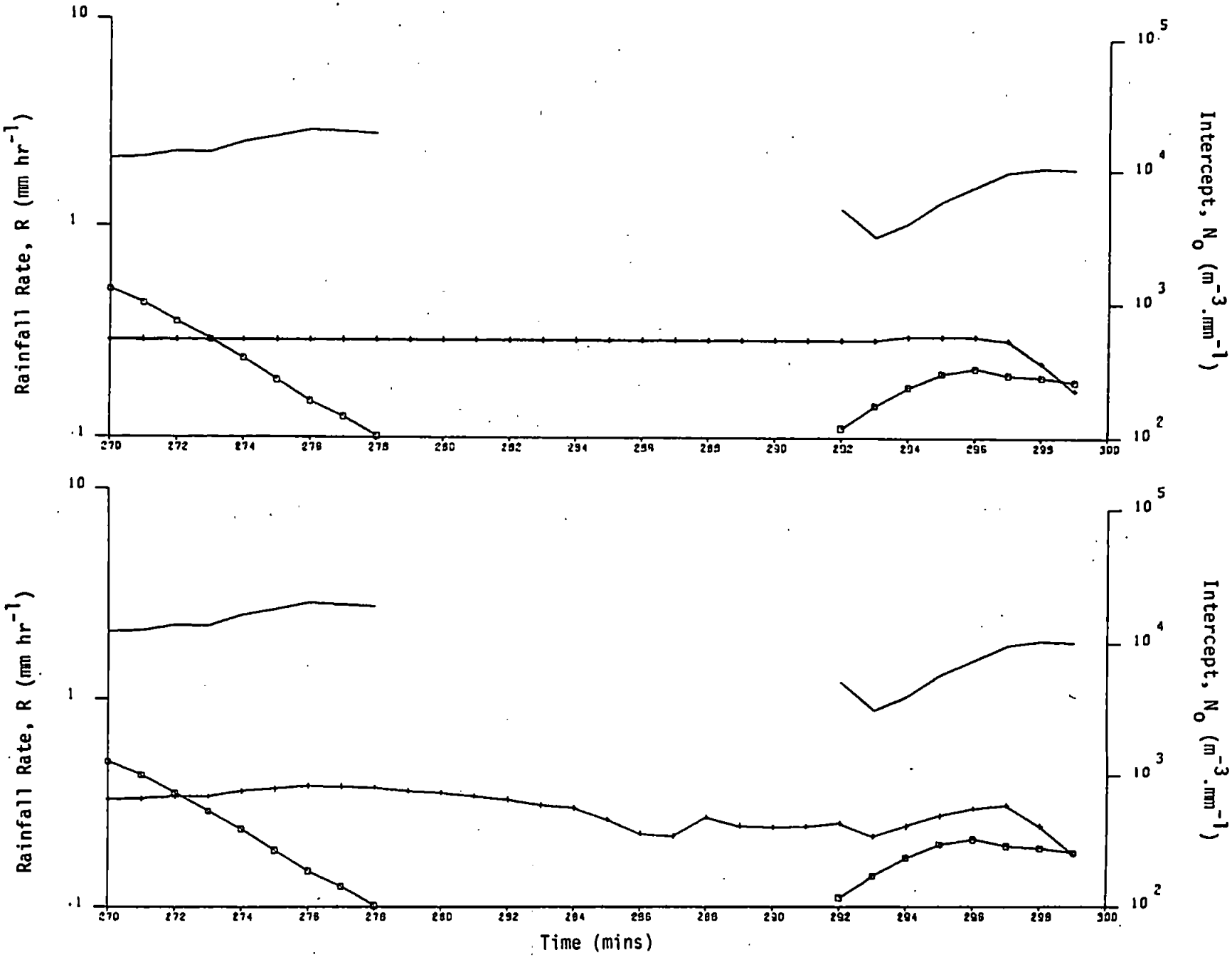

Totals:

R_G : 0.1 mm

R_D : 0.07 mm

R_Z : 0.15 mm

R_{ZN}: 0.16 mm

A 92

(23)
1800-29
9.4.79

Totals:

R_G : 0 mm

R_D : 0.01 mm

R_Z : 0 mm

R_{ZN}: 0 mm

A 93

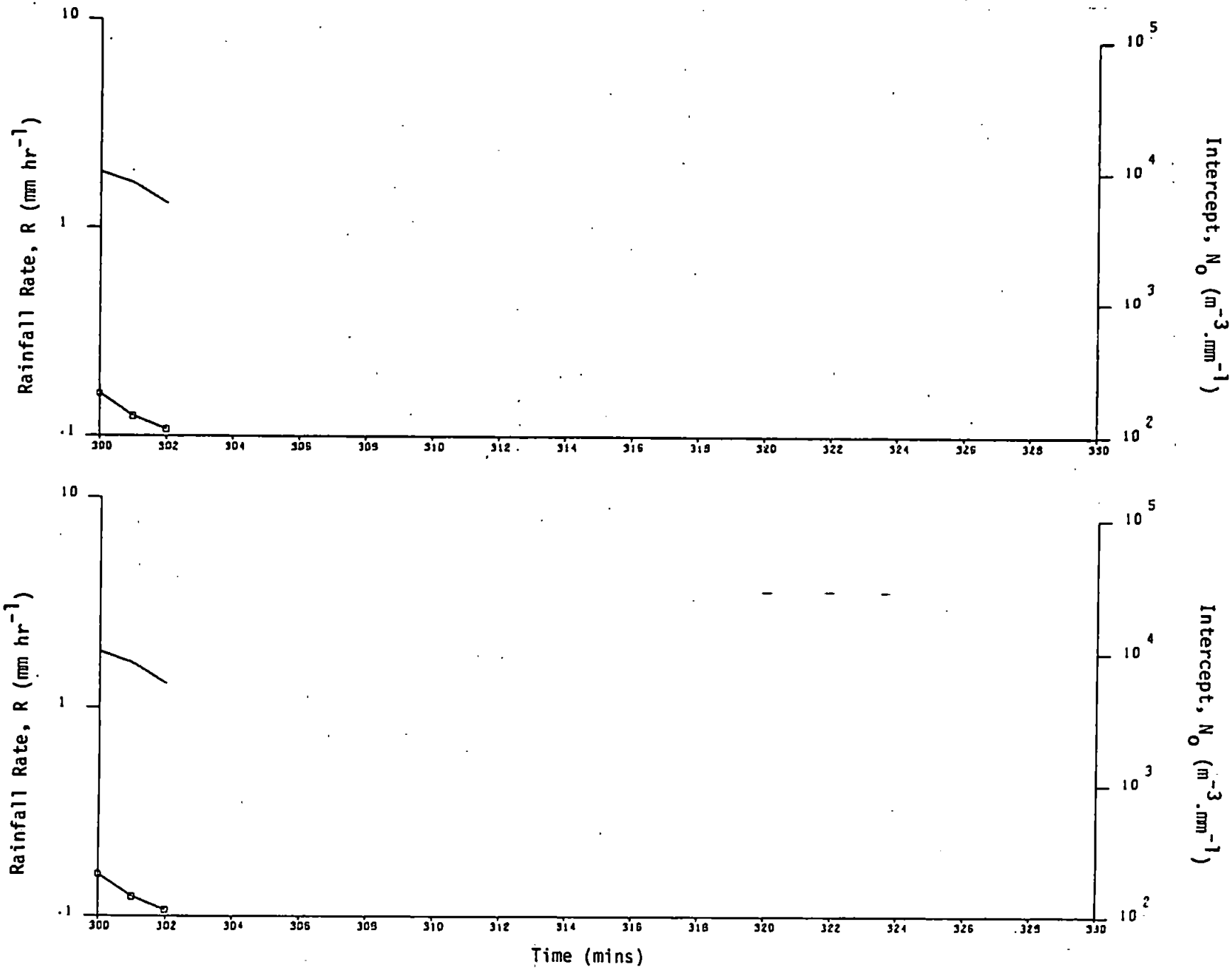

(24)
1830-59
9.4.79

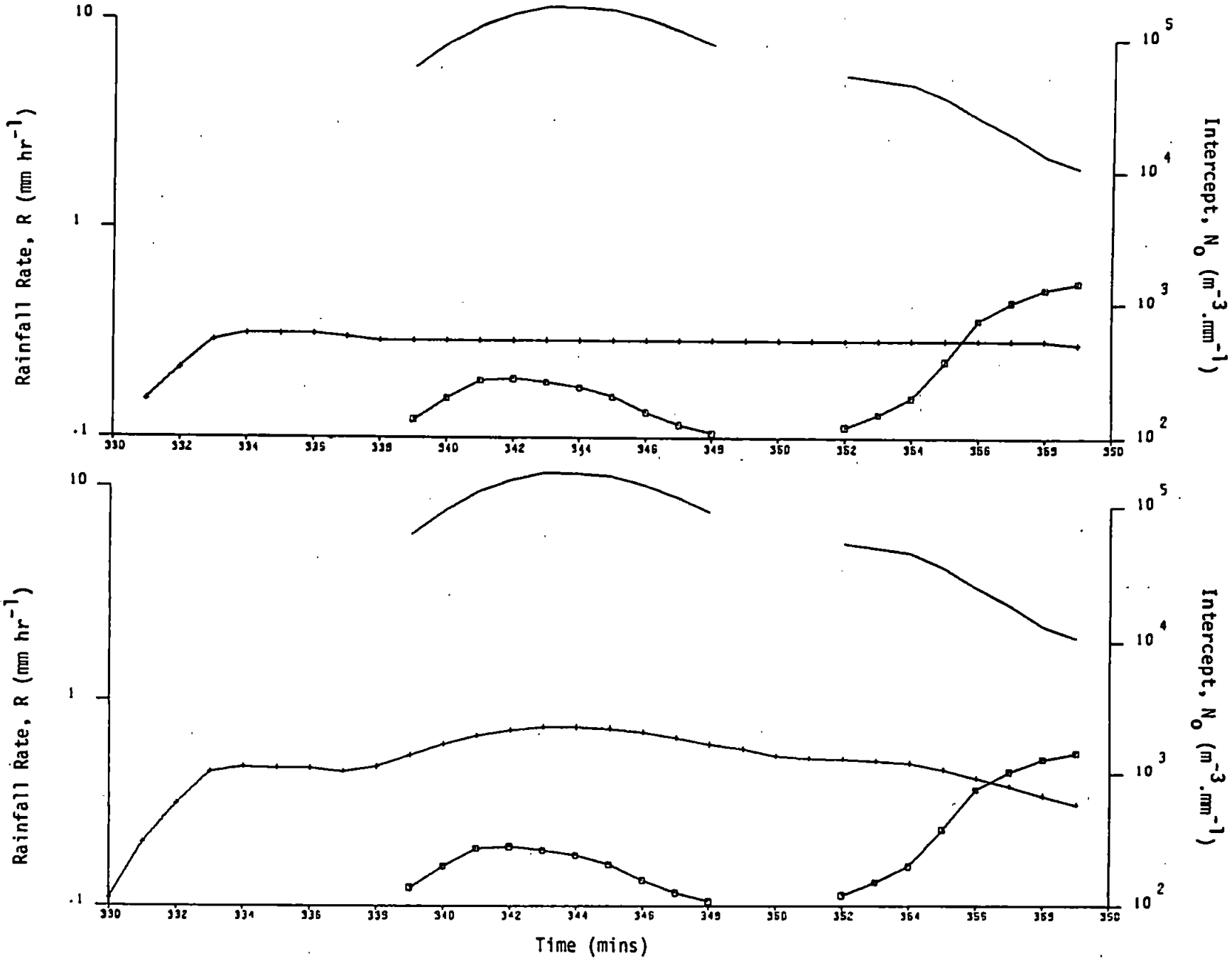

Totals:

R_G : 0.2 mm

R_D : 0.10 mm

R_Z : 0.15 mm

R_{ZN}: 0.27 mm

A 94

(25)
1900-29
9.4.79

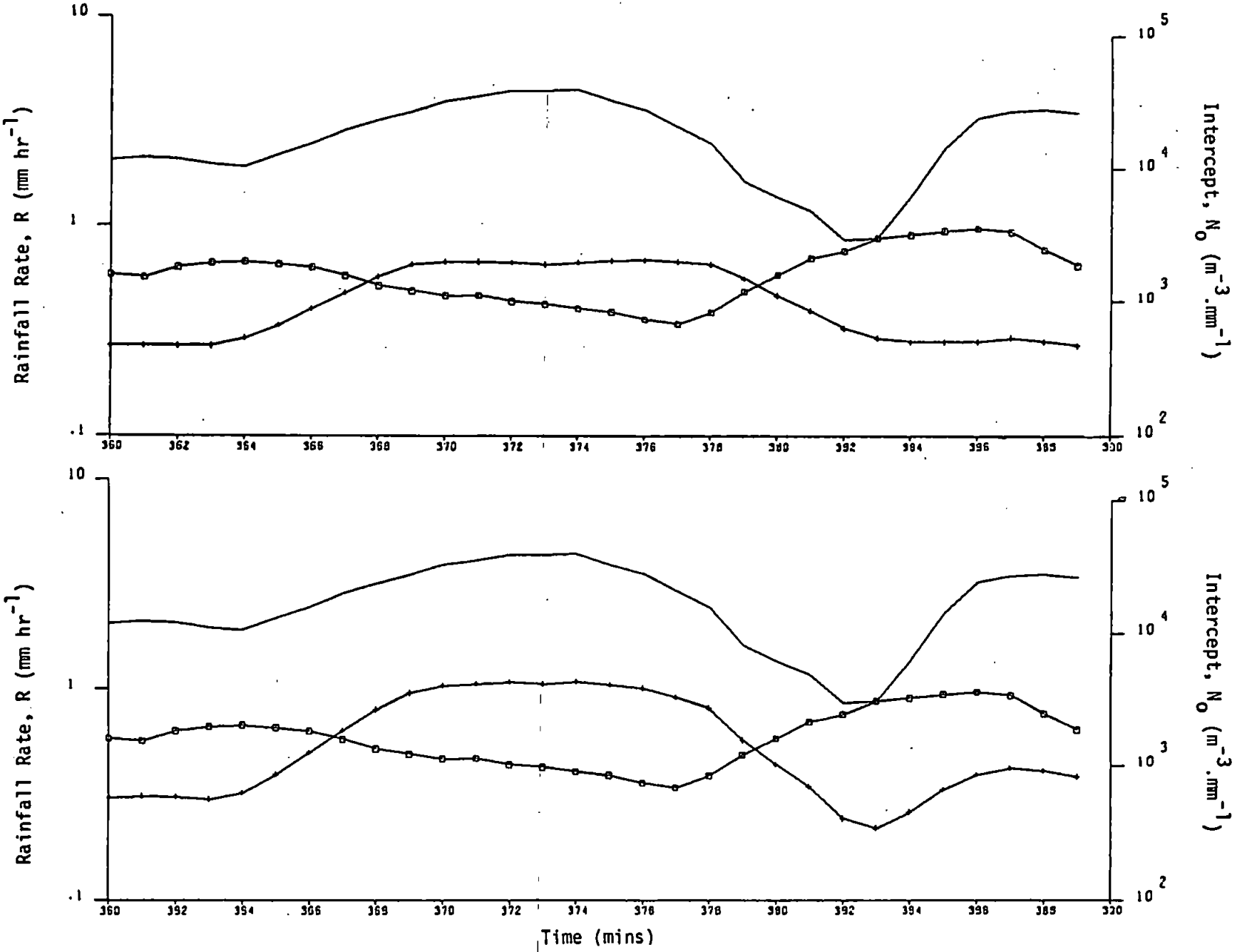

Totals:

R_G : 0.5 mm

R_D : 0.33 mm

R_Z : 0.24 mm

R_{ZN}: 0.33 mm

A 95

(26)
1930-59
9.4.79

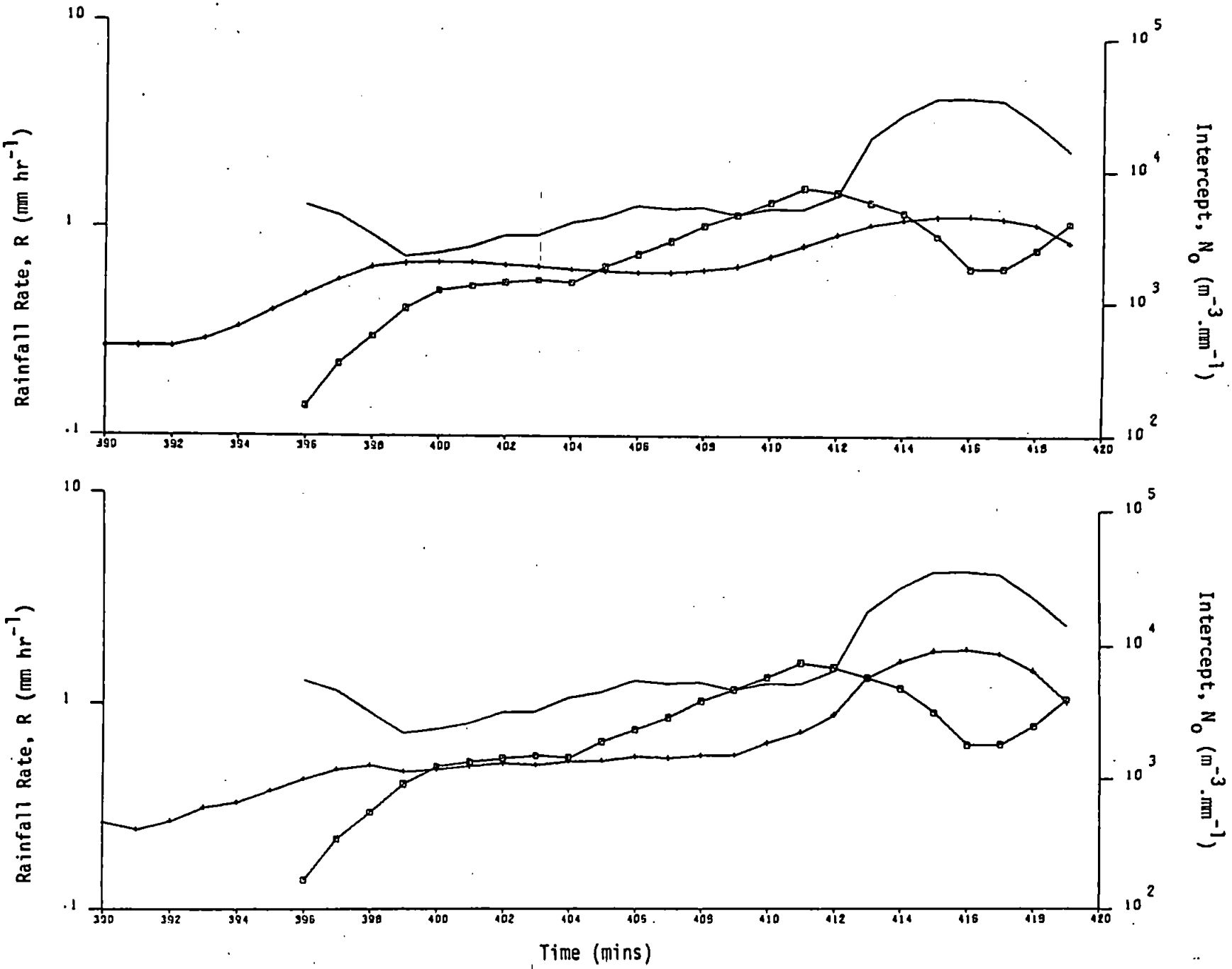

Totals:

R_G : 0.8 mm

R_D : 0.41 mm

R_Z : 0.38 mm

R_{ZN}: 0.41 mm

A 96

(27)
2000-29
9.4.79

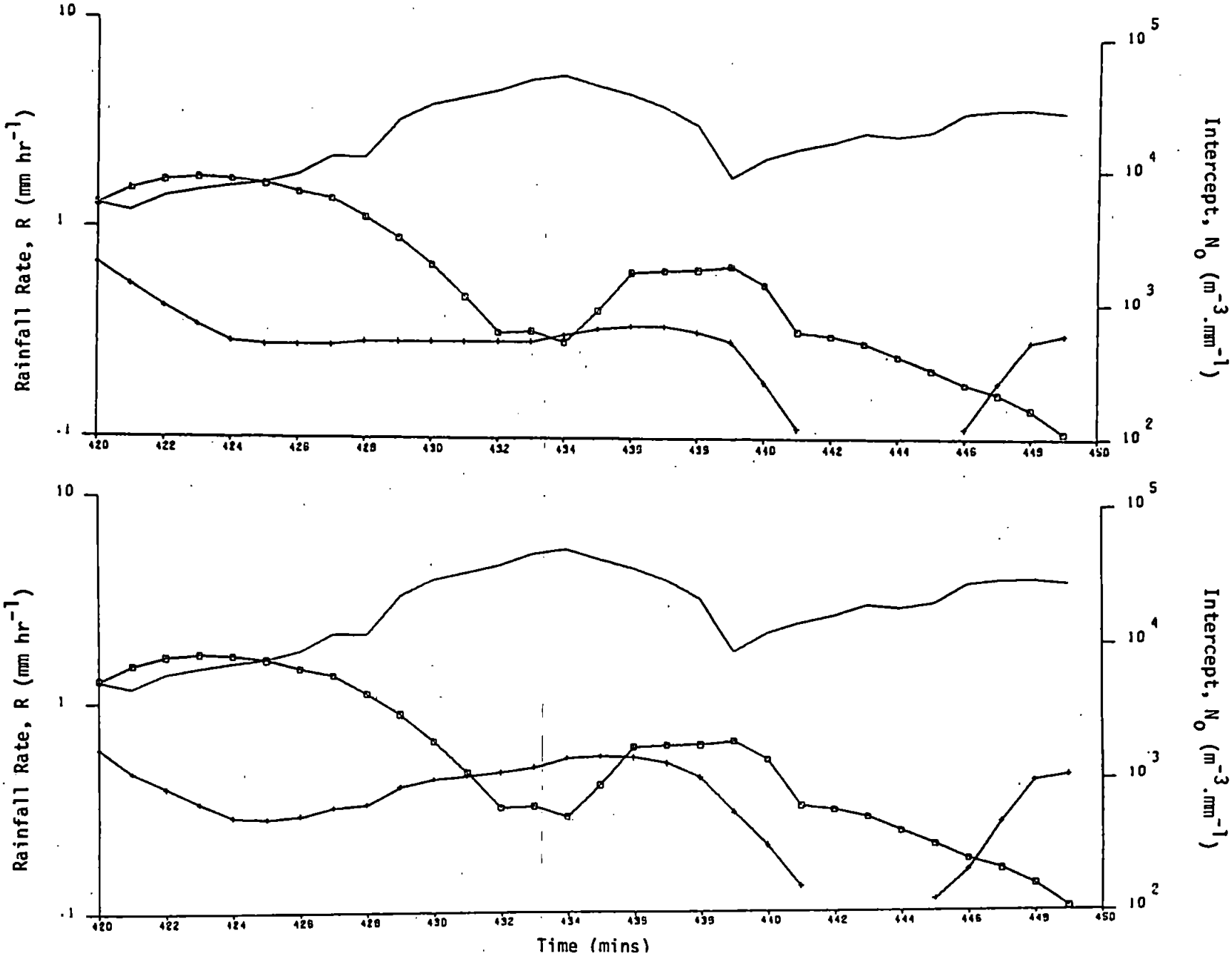

Totals:

R_G : 0.4 mm

R_D : 0.36 mm

R_Z : 0.14 mm

R_{ZN}: 0.18 mm

A 97

(28)
1730-59
22.5.79

Totals:

R_G : 0.2 mm

R_D : 0.19 mm

R_Z : 0.18 mm

R_{ZN}: 0.25 mm

A 98

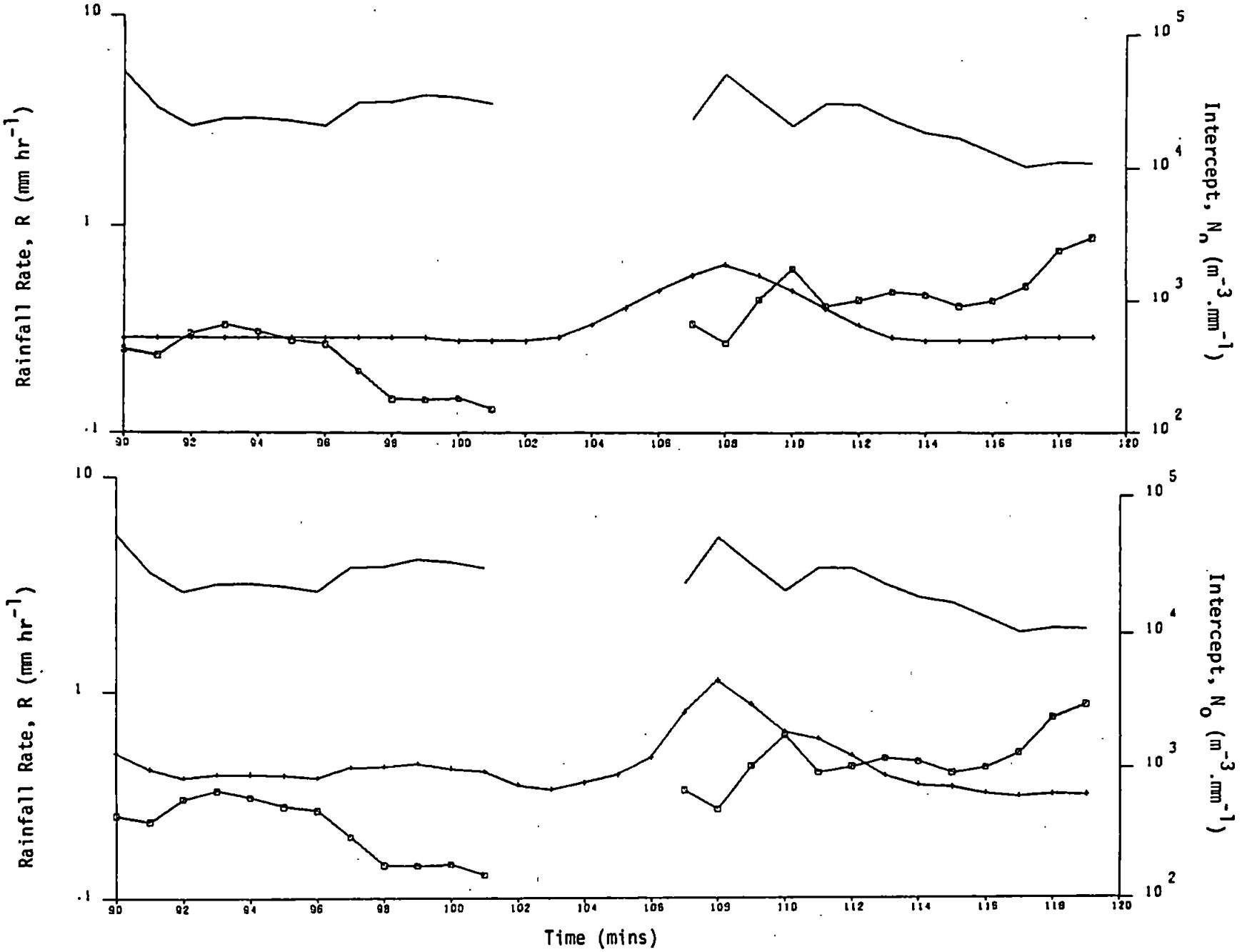

29
1800-29
22.5.79

Totals:

R_G : 0.3 mm

R_D : 0.22 mm

R_Z : 0.21 mm

R_{ZN}: 0.22 mm

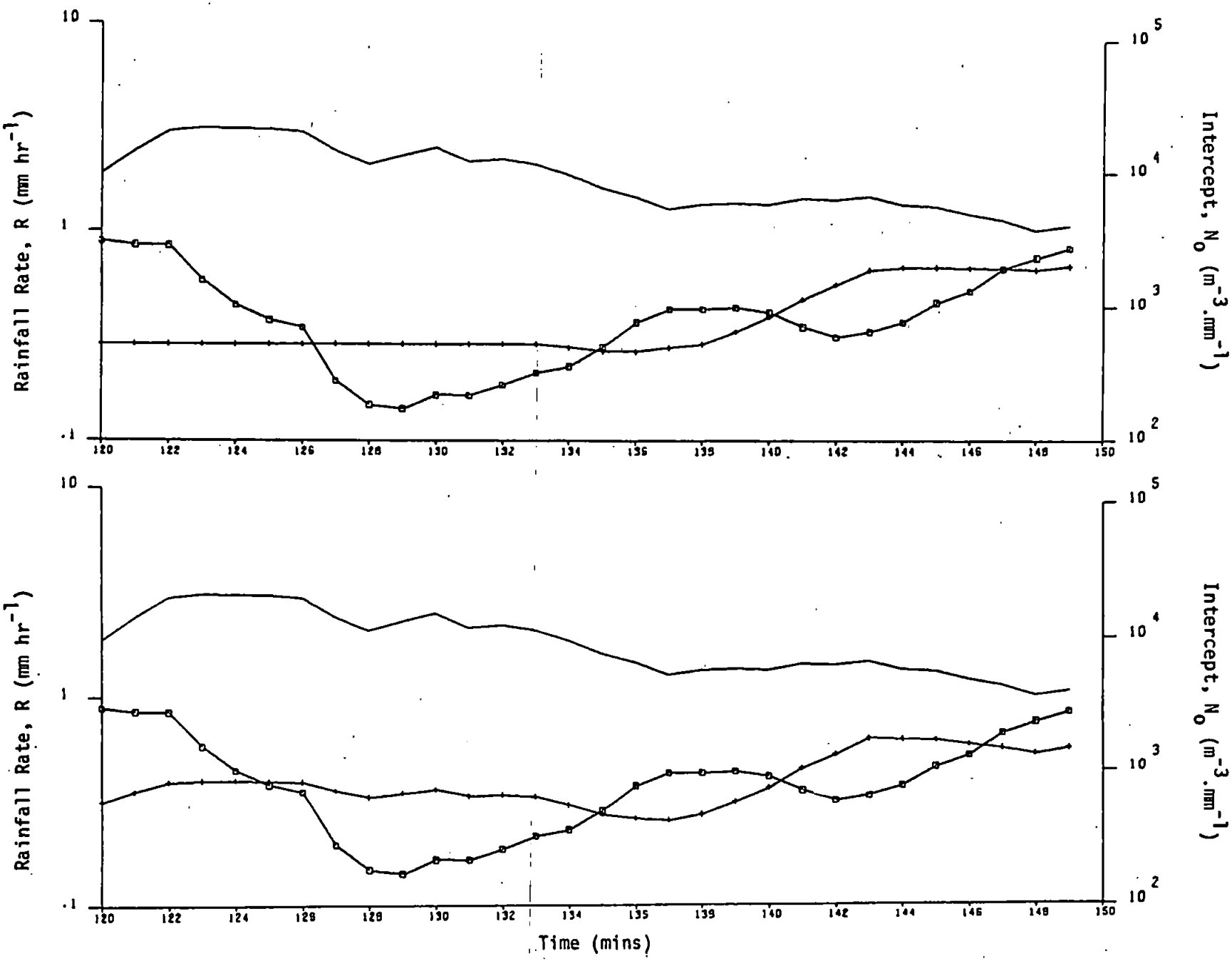

30

1830-59

22.5.79

Totals:

R_G : 1.1 mm

R_D : 1.62 mm

R_Z : 2.04 mm

R_{ZN}: 1.34 mm

A 100

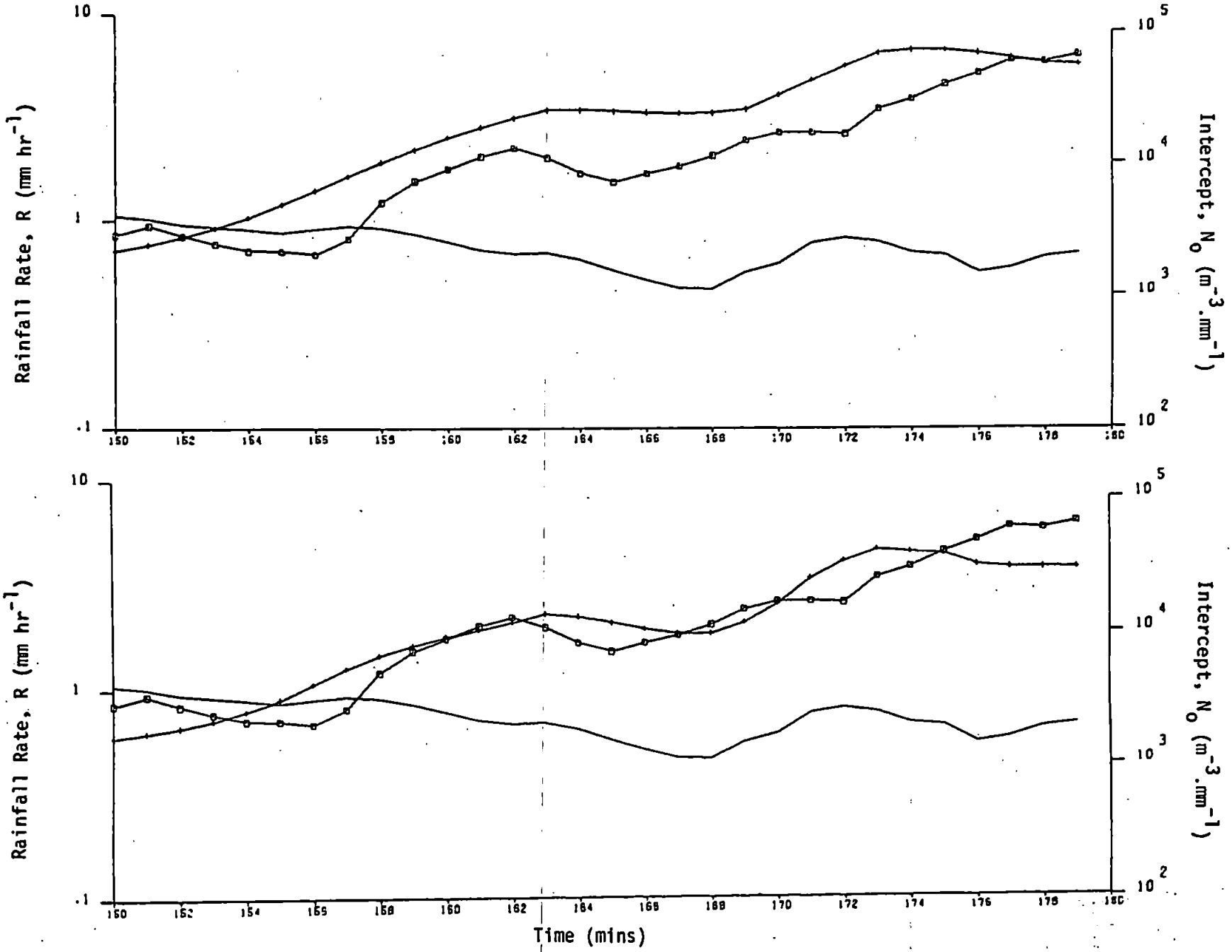

(31)
1900-29
22.5.79

Totals:

R_G : 3.2 mm

R_D : 2.59 mm

R_Z : 2.13 mm

R_{ZN}: 1.69 mm

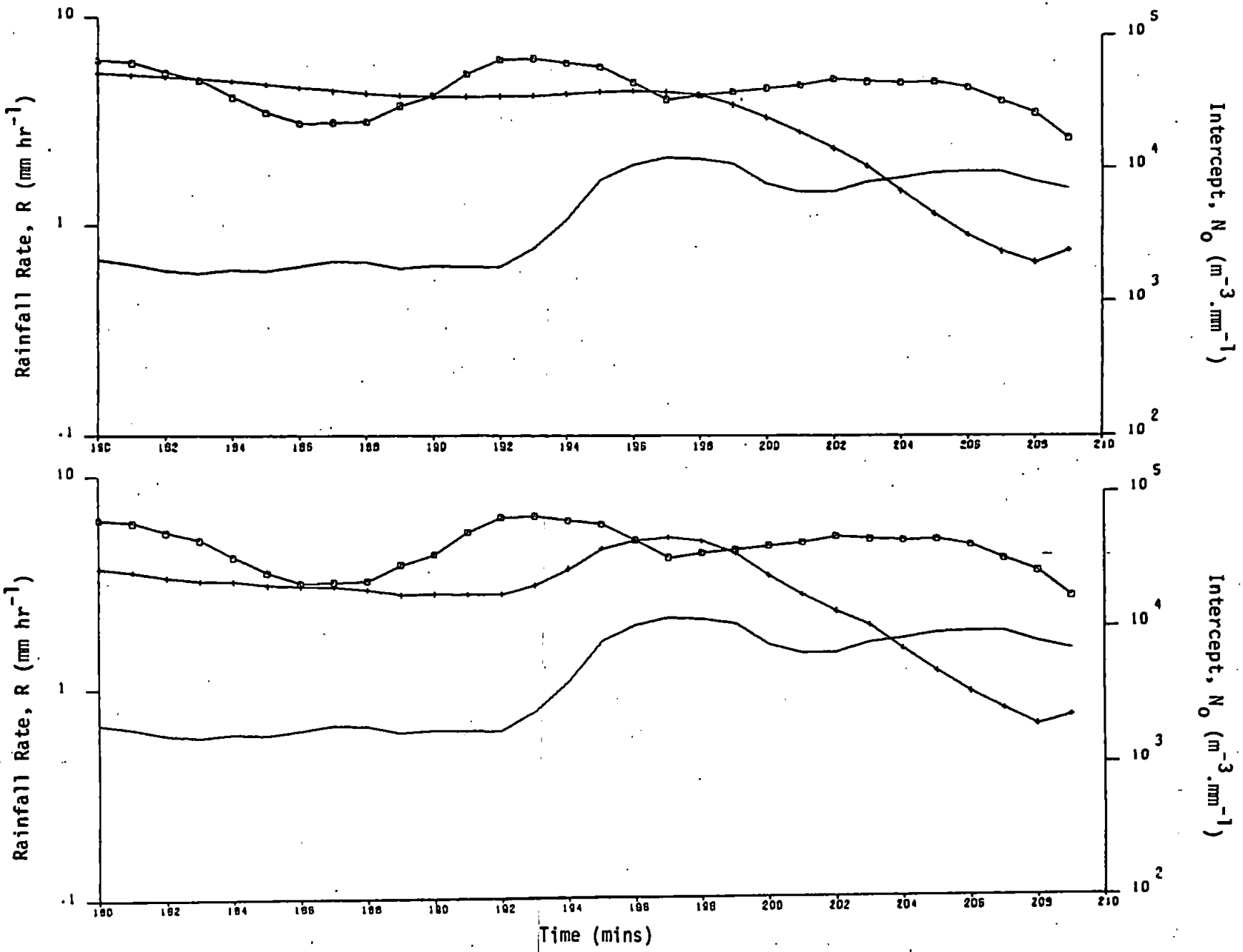

(32)
1930-59
22.5.79

Totals:

R_G : 0.6 mm

R_D : 0.42 mm

R_Z : 0.54 mm

R_{ZN}: 0.44 mm

A 102

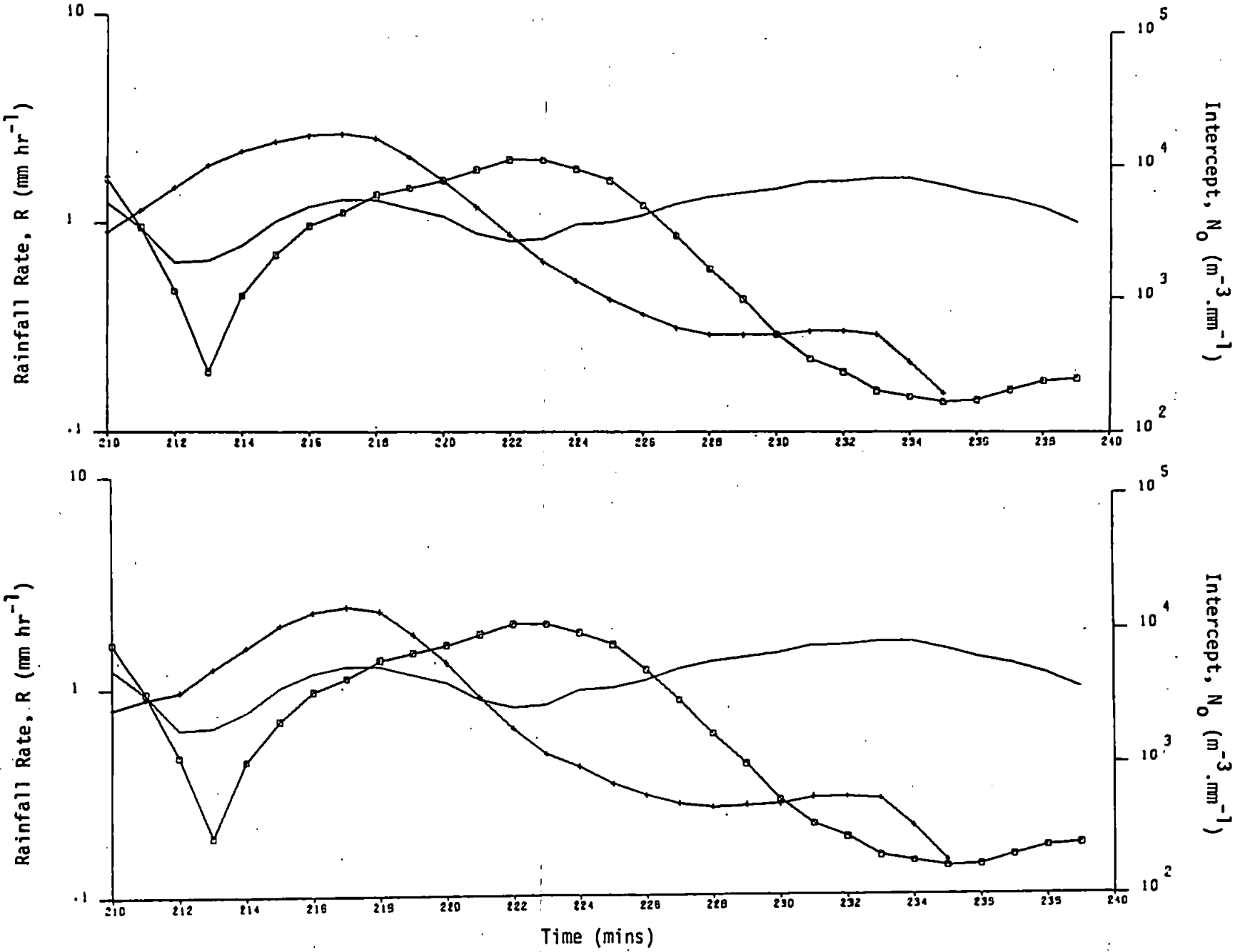

Appendix VIII

REFERENCE 54

Personal communication from JOSS

ntrale meteorologica Svizzera
Osservatorio Ticinese

CH- 6605 Locarno-Monti, 25 May 1979 WOL 332Joss/for

Mr. Andrew Eccleston
Research Assistant
PLIMOUTH POLYTECHNIC
Drake Circus
PLYMOUTH DEVON PL4 8AA
(England)

Dear Mr. Eccleston

It is a pleasure to receive your paper, which I also forwarded to A.Waldvogel (LAPETH Zürich). We are expecially pleased to see your comparison and the good agreement with the rain gauge. Here is our comment:

1. Your investigations in respect to wind influence on the measurement of drop size indicate no systematic error due to wind speed below 20 knots (hourly average). We hoped, that this result would be true, and are glad to have it confirmed by your experiments. Do you have an explanation for the tendency to overread in the northerly quadrant? Instrumental set-up? Is the tendency statistically significant?
2. We do not understand the last paragraphe of page 3 (see annex 1).
3. Page 5 ... 17655 one-minute ... We would like to know something more about your distributions, e.g. minimum number of drop in a single distribution, minimum amount of rain; total amount of rain $\int_0^{17665} R(t)dt$?
4. Page 5, middle, sounds as if we should find the M-P yardstick. On the other hand on page 8 bottom you mention, that small samples deviate from exponential, corresponding to our experience (see also annex 2).
5. Page 10 and 11: Your experimentally determined N_o-A relation agrees very well with Waldvogels findings on a theoretical base (annex 3).
6. Page 13. Obviously it would be most interesting, if you could verify your proposal by measuring the drop size distributions in various places and scanning simultaneously the reflectivity profiles over them. The correlation of the results will demonstrate to what extent the idea (to deduce A-values from the radar-reflectivity profiles) is operationally feasible or whether it is easier to obtain the desired Z-R-relation directly from the ground-based measurements. Furthermore the question is still open to what extent drop size measurements made in one location are representative for an area. A lot of work however is involved in solving these questions, and personally I will not be able to help answering them in the near future as I am involved at present in more operational projects. Therefore we are loooking forward to see more of your results!

./..

Annex 4 gives a description of our operational radars. When your read the short error analyses on page 17, you must keep in mind, the the radar horizon and ground clutter are much more restricting in a mountanous country like Switzerland as compared to a flat country. In view of that, errors due to Z-R-variations are treated only very briefly in annex 4.

Yours sincerely

Jürg Joss

Copy to A.Waldvogel and T.Gutermann

Annex:

1. Page 3 of manuscript
2. Shapes of Raindrop Size Distribution
3. A Comment on "The N_oJump of Raindrop Spectra"; Reply; The N_oJump of Raindrop Spectra
4. Meteorological Office Translation: Translation No. 1389 + Working Report SMI No. 79